Towards the rational use of antibiotics: Utilising pharmacometric approaches to improve meropenem and piperacillin treatment in critically ill patients

Inaugural-Dissertation

to obtain the academic degree

Doctor rerum naturalium (Dr. rer. nat)

submitted to the Department of Biology, Chemistry, Pharmacy

of Freie Universität Berlin

by

Ferdinand Anton Weinelt

from Ellwangen (Jagst)

2022

The present thesis was conducted from 2018 to 2022 under the supervision of Prof. Dr. Charlotte Kloft at the Institute of Pharmacy, Freie Universität Berlin.

1. Reviewer: Prof. Dr. Charlotte Kloft
2. Reviewer: Prof. Dr. Sebastian Wicha

Date of disputation: 09.12.2022

To my parents for unconditional and limitless support

Hierdurch versichere ich, dass ich meine Dissertation selbstständig verfasst
und keine anderen als die von mir angegeben Quellen und Hilfsmittel verwendet habe. Die Dissertation ist in keinem früheren Promotionsverfahren angenommen oder abgelehnt worden.

Abstract

In 1909 the discovery of the antibiotic arsphenamin marked the beginning of a new era in treating potentially deadly bacterial infections. In the following decades, the discovery of various new antibiotic drugs substantially contributed to a rise in life expectancy from 47.0 to 78.8 years in the United States of America. Despite this considerable progress in treating infectious diseases, bacterial infections remain a major threat to public health. Especially vulnerable patient populations, like critically ill patients, continued to suffer under mortality rates up to 60%. Worryingly, the described achievements are threatened by two alarming developments: While no truly novel antibiotic classes have been discovered and developed in the last three decades, the emergence and spread of antimicrobial resistance -accelerated by the inappropriate use of antibiotic drugs - steadily reduces the efficacy of currently available drugs. As a response to this new challenge, several national and international action plans call not only for a determined search for new antimicrobial drugs, but also for a more rational use of existing antibiotics. One vital component of rational antibiotic drug therapy is an adequate drug exposure at the site of infection, facilitated by the selection of suitable antibiotic drug(s) in combination with an appropriate dosing regimen. The antibiotic drug administered to the patient should be selected based on its efficacy against the pathogen causing the infection. Unfortunately, the pathogen causing the infection is often unknown at the start of antibiotic therapy. As a consequence, broad spectrum antibiotics – like meropenem and piperacillin/tazobactam - are frequently administered to increase the likelihood of an effective therapy. The selection of an appropriate dosing regimen can be complicated and is especially challenging in critically ill patients: The broad range of pathophysiological changes observed in this patient population leads to high pharmacokinetic (PK) variability, which results in substantial differences in drug exposures between patients receiving the same antibiotic drug and dosing regimen. Under the concept of model-informed precision dosing (MIPD), population pharmacokinetic/pharmacodynamic models and patient-specific data (e.g. patient characteristics, drug measurement(s)) can be leveraged to inform and improve dosing decisions in this vulnerable patient population.

The objective of the presented thesis was the development, implementation and evaluation of MIPD tools for antibiotic drugs in critically ill patients. To enable the successful integration of MIPD into clinical practice an *iterative*, *integrative* and *translational* approach was followed. The initial and central question ’Is the current antibiotic dosing appropriate?’, was *iteratively* addressed *integrating* expertise from a diverse interprofessional team of healthcare professionals and can be segmented into four intermediate steps, all vital to the main objective. First, and as a prerequisite both for model development/evaluation and dosing adaptation, the establishment of a reliable and frequent antibiotic concentration measurement program was required. Second, the collected data was analysed employing pharmacometric and statistical methodology to characterise population

PK/pharmacodynamics (PD) and local factors influencing antibiotic therapy (e.g. local pathogen susceptibility). Third, the gained scientific knowledge was *translated* into easy-to-use, model-informed dosing tools and comprehensive dosing strategies optimised for clinical practice. And fourth, the developed model-informed dosing tools were implemented into clinical routine and subsequently evaluated and optimised. This thesis focused on meropenem and the fixed drug combination piperacillin/tazobactam and addressed individual or multiple of these four steps in three different projects.

In Project I, a possible adsorption of the antibiotic meropenem at the cytokine adsorber CytoSorb®, its effect on meropenem exposure and possible consequences for an adequate meropenem dosing were investigated. Despite the absence of clear evidence for a beneficial effect on patients outcomes, the CytoSorb® filter is increasingly used to reduce circulating cytokines in patients experiencing sepsis. Due to its unspecific binding and therefore elimination of molecules up to a molar mass of 55 kDa, concerns have been raised that the CytoSorb® filter unintentionally adsorbs various drugs including meropenem. To investigate if meropenem dosing needs to be increased during CytoSorb® treatment, a nonlinear mixed-effects (NLME) modelling and simulation approach was employed: A population pharmacokinetic model was developed and three distinct approaches to assess if meropenem clearance differed without or during CytoSorb® treatment were applied: (i) quantification of a possible proportional increase in clearance during CytoSorb® treatment (ii) investigation of (non)saturable adsorption at the CytoSorb® filter using different adsorption submodels and (iii) model parameter re-estimation excluding samples collected during CytoSorb® treatment and evaluating the predictive performance for meropenem concentrations during CytoSorb® treatment. In contrast to the expectation of meropenem being adsorped at the CytoSorb® filter, no significant ($p<0.05$) or relevant effect of CytoSorb® treatment on meropenem exposure was observed. Consequently, neither additional dosing nor a more frequent drug concentration monitoring of meropenem is necessary during the application of CytoSorb® therapy.

Project II focused on improving meropenem and piperacillin/tazobactam treatment for critically ill patients at the Charité-Universitätsmedizin Berlin. For this purpose, a 3-staged clinical study was initiated as a coordinated intervention. In *stage I*, a frequent and reliable concentrations measurement program was implemented to evaluate the current antibiotic therapy. The assessment of the current antibiotic therapy provided insights about local pathogen susceptibility, while highlighting the need for dose individualisation based on patient characteristics: The majority (>90%) of observed pathogens were susceptible to the two administered antibiotic drugs, but target range attainment (minimum antibiotic drug concentrations between 1 and 5 times minimum inhibitory concentration (MIC) of the pathogen) was low for the observed drug concentrations (meropenem: 35.7%, piperacillin: 50.5%) and highly variable between patients with different renal functions. To improve initial meropenem dosing (i.e. prior to the first concentration measurement) and to exploit the newly

gained information about the local pathogen susceptibility, a tabular model-informed dosing tool was developed and implemented in *stage II* of the study. For the development of the tool, an appropriate meropenem PK model was selected from literature and successfully evaluated using the local clinical data. The PK model was then used to conduct stochastic simulations investigating clinically relevant dosing regimens, possible clinical scenarios and the probability of the dosing regimens to achieve adequate drug exposures. To inform dosing prior to pathogen identification, the local pathogen-independent mean fraction of response (LPIFR) was introduced: The LPIFR characterises the probability of a dosing regimen to reach a defined target, e.g. time above the MIC, if only the underlying MIC distribution at a hospital and not the individual MIC of the pathogen causing the infection is known. To inform dosing after MIC value determination, probability of target attainment analyses (PTA) were performed. Dosing recommendations achieving PTA>90% or LPIFR>90% for patients with different creatinine clearances (10.0-300 mL/min) were derived and summarised in one concise and clear table. To assess the potential of the newly developed model-informed dosing tool prior to implementation, the total daily dose of the dosing regimens recommended by the dosing tool for the local study population was compared to the total daily dose of the actually administered dosing regimens. For 77% of the patients with meropenem concentrations outside the target range, the dosing tool suggested a change in daily dose, highlighting the potential of the tool to optimise dosing regimens. To integrate patient individual antibiotic drug measurements and allow for more user flexibility, an interactive model-informed dosing software termed 'DoseCalculator' was developed for *stage III* of the study. In addition to the meropenem PK model already evaluated for *stage II* of the study, different piperacillin/tazobactam models were extracted from literature, evaluated using the local clinical data collected in *stage I* of the study and the best performing model implemented into the tool. Based on available knowledge about the infection, three possibilities to calculate the probability of a dosing regimen to reach adequate antibiotic exposures were integrated into the tool: (i) the LPIFR if neither the pathogen nor the MIC is available, (ii) the cumulative fraction of response (CFR) based on the MIC distribution of a specific pathogen if the pathogen is available and (iii) the PTA if the MIC is available. Furthermore, employing a maximum a-posterior (MAP) estimation approach the observed antibiotic drug measurement(s) of a patient can be used in the DoseCalculator to derive patient individual parameter estimates. If drug measurement(s) of a patient are supplied, all analyses and the resulting recommended dosing regimen are based on the individual parameter estimates of the patient. Compared to the observed dosing in *stage I*, the recommendations of the DoseCalculator led to a substantial relative increase in predicted target attainment (322% meropenem, 505% piperacillin) while reducing the daily dose (median reduction: 77.8% meropenem, 83.4% piperacillin).

In Project III the MeroRisk Calculator, an easy-to-use Excel tool to determine the risk of meropenem target non-attainment after standard dosing previously developed at our department, was evaluated using clinical routine data. Since the direct evaluation of the MeroRisk Calculator was not feasible

with the available retrospective clinical dataset, a two-step data- and model-based evaluation was conducted: In step one, a meropenem PK model was successfully evaluated using the clinical data. In step two, the evaluated PK model was used as a benchmark for the drug concentration and risk predictions of the MeroRisk Calculator. Compared to the successfully evaluated compartmental PK model, the MeroRisk Calculator provided an equally good and reliable risk assessment (Lin's concordance correlation coefficient = 0.99) for patients with maintained renal function (creatinine clearance $\geq$ 50 mL/min). However, for patients with creatinine clearances below 50 mL/min significant deviations were observed. As a consequence, the MeroRisk Calculator should not be used in patients with (severe) renal impairment. In addition to the successful evaluation, the functionality of the MeroRisk Calculator was extended. Based on CFR analysis and EUCAST reported MIC value distributions, risk of target non-attainment can now be assessed depending on the infecting pathogen informing dosing decisions prior to MIC value determination.

To conclude, the presented thesis contributed to an individualised and more rational antibiotic drug therapy in critically ill patients. While PK modelling was employed in Project I to exclude a clinically relevant adsorption of meropenem at the CytoSorb® filter, Project II and Project III represent a successful example on development, implementation and evaluation of MIPD tools. As a next step, both the tabular model-informed dosing tool and the DoseCalculator should be prospectively evaluated at Charité-Universitätsmedizin Berlin. The results from this evaluation in particular and this thesis demonstrate the potential of MIPD using comprehensive examples on how to develop, implement and evaluate model-informed dosing tools and contribute to the accelerating implementation of MIPD into clinical practice.

Zusammenfassung

Die Entdeckung des Antibiotikums Arsphenamin im Jahr 1909 markierte den Beginn einer neuen Ära in der Behandlung potenziell tödlicher bakterieller Infektionen. In den folgenden Jahrzehnten trug die Entdeckung verschiedener neuer Antibiotika wesentlich zu einem Anstieg der Lebenserwartung in den Vereinigten Staaten von Amerika von 47,0 auf 78,8 Jahre bei. Trotz dieser beträchtlichen Fortschritte bei der Behandlung von Infektionskrankheiten stellen bakterielle Infektionen nach wie vor eine große Gefahr für die öffentliche Gesundheit dar. Besonders gefährdete Patientengruppen, wie z. B. Intensivpatienten, leiden weiterhin unter Sterblichkeitsraten von bis zu 60%. Besorgniserregend ist, dass die beschriebenen Fortschritte in der Behandlung von Infektionskrankheiten durch zwei alarmierende Entwicklungen gefährdet sind: Während in den letzten drei Jahrzehnten keine neuen Antibiotikaklassen entdeckt und entwickelt wurden, verringert die Entstehung und Ausbreitung antimikrobieller Resistenzen, unter anderem beschleunigt durch den unsachgemäßen Einsatz von Antibiotika, die Wirksamkeit der derzeit verfügbaren Medikamente. Als Reaktion auf diese neue Herausforderung wird in nationalen und internationalen Aktionsplänen nicht nur eine entschlossene Suche nach neuen antimikrobiellen Medikamenten, sondern auch ein rationalerer Einsatz der vorhandenen Antibiotika gefordert. Ein wesentlicher Bestandteil einer rationalen Antibiotikatherapie ist eine angemessene Medikamentenexposition am Ort der Infektion, die durch die Auswahl eines geeigneten Antibiotikums in Kombination mit einem geeigneten Dosierungsschema erreicht wird. Das dem Patienten verabreichte Antibiotikum sollte auf der Grundlage seiner Wirksamkeit gegen den Erreger der Infektion ausgewählt werden. Leider ist der Erreger der Infektion zu Beginn der Antibiotikatherapie oft nicht bekannt. Daher werden häufig Breitbandantibiotika - wie Meropenem und Piperacillin/Tazobactam - verabreicht, um die Wahrscheinlichkeit einer wirksamen Therapie zu erhöhen. Die Auswahl eines geeigneten Dosierungsschemas kann kompliziert sein und ist besonders bei schwerkranken Patienten eine Herausforderung. Das breite Spektrum an pathophysiologischen Veränderungen, das bei dieser Patientenpopulation zu beobachten ist, führt zu einer hohen pharmakokinetischen (PK) Variabilität. Diese Variabilität führt wiederum zu erheblichen Unterschieden in der Arzneimittelexposition zwischen Patienten, die das gleiche Dosierungsschema erhalten. Im Rahmen des Konzepts der modellgestützten Präzisionsdosierung (model-informed precision dosing, MIPD) können populationspharmakokinetische Modelle und patientenspezifische Daten (z. B. Patientencharakteristika, Konzentrationsmessung(en)) genutzt werden, um Dosierungsentscheidungen in dieser vulnerablen Patientengruppe zu verbessern.

Das Ziel der vorliegenden Arbeit war die Entwicklung, Implementierung und Evaluierung von MIPD Tools um die Antibiotikatherapie bei kritisch kranken Patienten zu verbessern. Um die erfolgreiche Integration von MIPD in die klinische Praxis zu ermöglichen, wurde ein *iterativer*, *integrativer* und

translationaler Ansatz verfolgt. Die anfängliche und zentrale Frage "Ist die derzeitige Antibiotikadosierung angemessen?" wurde *iterativ* unter *Integration* des Fachwissens eines vielfältigen interprofessionellen Teams adressiert und kann in vier Zwischenschritte unterteilt werden: Erstens, die Einrichtung eines zuverlässigen und regelmäßigen Konzentrationsmessprogramms als Voraussetzung für die Modellentwicklung/-bewertung und die Dosisanpassung während der Therapie. Zweitens, die Analyse der gesammelten Daten mit Hilfe pharmakometrischer und statistischer Methoden. Fokus hierbei war es die PK/Pharmakodynamik (PD) der Population und lokale Faktoren, die die Antibiotikatherapie beeinflussen (z. B. Empfindlichkeit der Erreger gegenüber einzelner Antibiotika) zu charakterisieren. Drittens, die Anwendung der gewonnenen wissenschaftlichen Erkenntnisse durch einfache, modellgestützte Dosierungsinstrumente und umfassende, für die klinische Praxis optimierte Dosierungsstrategien. Und viertens die Implementierung, Evaluierung und Optimierung der entwickelten modellgestützten Dosierungsinstrumente. Die vorgelegte Arbeit konzentrierte sich auf Meropenem und die Wirkstoffkombination Piperacillin/Tazobactam und behandelte einzelne oder mehrere dieser vier Schritte in drei verschiedenen Projekten.

In Projekt I wurde eine mögliche Adsorption des Antibiotikums Meropenem an den Zytokinadsorber CytoSorb® und die daraus folgenden Konsequenzen auf die Meropenemexposition und adequate Dosierungsschemata untersucht. Obwohl es bis heute keine verlässlichen Belege für eine positive Auswirkung auf den Krankheitsverlauf gibt, wird der CytoSorb®-Filter häufig zur Reduzierung der zirkulierenden Zytokine bei Patienten mit Sepsis eingesetzt. Da der CytoSorb®-Filter Moleküle bis zu einer molaren Masse von 55 kDa unspezifisch bindet und eliminiert, könnte der CytoSorb®-Filter unbeabsichtigt auch verschiedene Arzneimittel, darunter Meropenem, adsorbieren. Um zu untersuchen, ob die Meropenem-Dosierung während der CytoSorb®-Behandlung erhöht werden muss, wurde ein NLME-Modellierungs- und Simulationsansatz verwendet: Bei der Entwicklung des populationspharmakokinetisches Modells wurden drei verschiedene Ansätze angewandt, um festzustellen, ob sich die Meropenem-Clearance während der CytoSorb®-Behandlung verändert: (i) Quantifizierung eines möglichen proportionalen Anstiegs der Clearance während der CytoSorb®-Behandlung, (ii) Untersuchung der (nicht) sättigbaren Adsorption am CytoSorb®-Filter unter Verwendung verschiedener Adsorptions-Submodelle und (iii) erneute Schätzung der Modellparameter unter Ausschluss der während der CytoSorb®-Behandlung gesammelten Proben und Bewertung der Vorhersageleistung für die Konzentrationen während der CytoSorb®-Behandlung. Es wurde jedoch kein signifikanter ($p<0,05$) oder relevanter Effekt der CytoSorb®-Behandlung auf die Meropenem-Exposition festgestellt. Folglich ist während der Anwendung der CytoSorb®-Therapie weder eine zusätzliche Dosierung noch eine häufigere Überwachung der Meropenem-Konzentration erforderlich.

Projekt II konzentrierte sich auf die Verbesserung der Meropenem- und Piperacillin/Tazobactam-Behandlung von kritisch kranken Patienten an der Charité-Universitätsmedizin Berlin. Zu diesem Zweck wurde eine 3-stufige klinische Studie initiiert. In Stufe 1 wurde ein Programm zur regelmäßigen und zuverlässigen Konzentrationsmessung von Antibiotika eingeführt und die aktuelle Antibiotikatherapie bewertet. Die Bewertung der aktuellen Antibiotikatherapie lieferte Erkenntnisse über die Empfindlichkeit der lokalen Erreger und machte gleichzeitig deutlich, dass die Dosierung auf der Grundlage individueller Patientenmerkmale angepasst werden sollte: Die Mehrheit (>90 %) der beobachteten Erreger war empfindlich gegenüber den beiden verabreichten Antibiotika, gleichzeitig wurde der Zielbereich bei den beobachteten Wirkstoffkonzentrationen nur selten erreicht (Meropenem: 35,7 %, Piperacillin: 50,5 %). Der Anteil der Konzentrationsmessungen im Zielbereich variierte stark zwischen Patienten mit unterschiedlichen Nierenfunktionen. Um die Meropenemdosierung bei Therapiestart und damit vor der ersten Konzentrationsmessung zu verbessern und um neu gewonnenen Informationen über die lokale Erregerempfindlichkeit zu nutzen, wurde ein tabellarisches, modellgestütztes Dosierungstool entwickelt und in Stufe 2 der Studie eingesetzt. Für dieses Tool wurde ein Meropenem PK-Modell aus der Literatur ausgewählt und mit Hilfe der lokalen klinischen Daten von Stufe 1 erfolgreich evaluiert. Im nächsten Schritt wurde das PK-Modell verwendet, um mit Hilfe von stochastischen Simulationen klinisch relevante Dosierungsschemata, Szenarien und die Wahrscheinlichkeit adäquate Antibiotikakonzentrationen zu erreichen zu untersuchen. Um die beste Dosierung vor der Identifizierung des Erregers auszuwählen, wurde die “local pathogen-independent mean fraction of response“ (LPIFR) eingeführt. Die LPIFR beschreibt die Wahrscheinlichkeit eines Dosierungsschemas, ein definiertes Ziel z. B. eine Zeit oberhalb der MIC, zu erreichen wenn nur die zugrunde liegende MIC-Verteilung in einem Krankenhaus und nicht die individuelle MIC des Erregers bekannt ist. Für den Fall, dass die MIC des Erregers bekannt ist, wurden „proabiltiy of target attainment“ Analysen (PTA) durchgeführt. Dosierungen die eine PTA oder LPIFR >90% erreichten, wurden geordnet nach Kreatinin-Clearance (10,0-300 ml/min) in einer prägnanten und übersichtlichen Tabelle zusammengefasst. Um das Potenzial der neu entwickelten modellgestützten Dosierungstabellen zu bewerten, wurde die tägliche Gesamtdosis der von den Dosierungstabellen empfohlenen Dosierungsschemata mit der täglichen Gesamtdosis der tatsächlich verabreichten Dosierungsschemata für die lokale Studienpopulation verglichen. Bei 77% der Patienten mit Proben außerhalb des Zielbereichs schlug das Dosierungstool eine Änderung der Tagesdosis vor. Dieses Ergebnis unterstreicht das Potenzial des Tools zur Optimierung der Dosierungsschemata. Um individuelle Konzentrationsnmessungen der Patienten zu integrieren und dem Benutzer mehr Flexibilität zu bieten, wurde für Stufe 3 der Studie eine interaktive, modellgestützte Dosierungsanwendung, der 'DoseCalculator', entwickelt. Zusätzlich zu dem bereits in Stufe 2 der Studie evaluierten Meropenem PK Modell, wurden verschiedene Piperacillin/Tazobactam-Modelle in der Literatur identifiziert, anhand der lokalen klinischen Daten evaluiert und das Modell mit der besten Leistung in das Tool implementiert. Abhängig von den

verfügbaren Informationen über den Pathogen der die Infektion verursacht, wurden drei Möglichkeiten zur Berechnung der Wahrscheinlichkeit, mit der ein Dosierungsschema das pharmakokinetische/pharmakodynamische Ziel erreicht, in das Tool integriert: (i) die LPIFR, wenn weder der Erreger noch die MIC verfügbar sind, (ii) die "cummulative fraction of response" (CFR), wenn der Erreger verfügbar ist und (iii) die PTA, wenn die MIC verfügbar ist. Darüber hinaus können die beobachteten Antibiotikamessungen eines Patienten im DoseCalculator unter Verwendung eines MAP-Ansatzes (Maximum a-posterior estimation) verwendet werden, um patientenindividuelle Parameterschätzwerte abzuleiten. Wenn die Medikamentenmessung(en) eines Patienten vorliegt/vorliegen, basieren alle Analysen und die daraus resultierenden empfohlenen Dosierungsschemata auf den individuellen Parameterschätzungen des Patienten. Im Vergleich zur beobachteten Dosierung in Stufe 1 führten die Empfehlungen des DoseCalculators zu einer erheblichen Erhöhung der vorhergesagten Zielerreichung (222% Meropenem, 405% Piperacillin) bei gleichzeitiger Reduzierung der Tagesdosis (mediane Reduzierung: 77,8% Meropenem, 83,4% Piperacillin).

In Projekt III wurde der MeroRisk Calculator, ein einfach zu bedienendes Excel-Tool zur Risikobestimmung für eine zu niedrige Meropenemkonzentration nach Standarddosierung, anhand klinischer Routinedaten evaluiert. Da die direkte Bewertung des MeroRisk Calculators mit dem verfügbaren retrospektiven klinischen Datensatz nicht möglich war, wurde eine zweistufige daten- und modellbasierte Evaluierung durchgeführt. In der ersten Stufe wurde ein Meropenem PK Modell mit den klinischen Daten erfolgreich evaluiert. Im zweiten Schritt wurde das evaluierte PK Modell als Vergleichsstandard für die Medikamentenkonzentration- und Risikovorhersagen des MeroRisk Calculators verwendet. Im Vergleich zum erfolgreich evaluierten kompartimentellen PK Modell lieferte der MeroRisk Calculator eine ebenso gute und zuverlässige Risikobewertung (Lin's Konkordanzkorrelationskoeffizient = 0,99) für Patienten mit erhaltener Nierenfunktion (Kreatinin-Clearance > 50 mL/min). Bei Patienten mit einer Kreatinin-Clearance unter 50 mL/min wurden jedoch erhebliche Abweichungen beobachtet. Folglich sollte der MeroRisk Calculator nicht bei Patienten mit (schwerer) Nierenfunktionseinschränkung eingesetzt werden. Zusätzlich zur erfolgreichen Evaluation wurde die Funktionalität des MeroRisk Calculators erweitert. Basierend auf der CFR-Analyse und den von EUCAST gemeldeten MIC Verteilungen kann nun das Risiko einer Zielverfehlung in Abhängigkeit vom infektiösen Erreger abgeschätzt werden. Dies wird helfen Dosierungsentscheidungen vor der MIC Bestimmung zu treffen.

Zusammenfassend lässt sich sagen, dass die vorliegende Arbeit zu einer individualisierten und rationaleren Antibiotikatherapie bei kritisch kranken Patienten beigetragen hat. Während die PK-Modellierung in Projekt I zum Ausschluss einer klinisch relevanten Adsorption von Meropenem am CytoSorb®-Filter eingesetzt wurde, stellen Projekt II und Projekt III erfolgreiche Beispiele für die Entwicklung, Implementierung und Evaluierung von MIPD-Tools dar. In einem nächsten Schritt

werden sowohl das tabellarische modellgestützte Dosierungstool als auch der DoseCalculator an der Charité-Universitätsmedizin Berlin prospektiv evaluiert. Die Ergebnisse dieser Arbeit zeigen das Potential von MIPD anhand von umfassenden Beispielen zur Entwicklung, Implementierung und Evaluation von modellinformierten Dosierungswerkzeugen und tragen dazu bei, die Implementierung von MIPD in die klinische Praxis zu beschleunigen.

Acknowledgments

I would like to express my sincere gratitude to:

- first and foremost, my *supervisor Prof. Charlotte Kloft* for the opportunity to conduct my doctoral research under your supervision. Thank you for all the valuable discussions, your advice, feedback, support and trust – you provided the perfect conditions for me to enhance my scientific and personal development;
- the *Graduate Research Training Program PharMetrX* (Pharmacometrics and Computational Disease Modelling) for introducing me not only to exciting pharmacometric methods and techniques but also to a network of peers to discuss them with, for transdisciplinary co-/supervision and for funding during my doctoral studies;
- my *co-supervisor Prof. Wilhelm Huisinga* for your interest in my research, for adding your mathematical perspective and for stimulating scientific questions and discussions;
- *Prof. Hartmut Derendorf* for introducing me to and sparking my interest in pharmacometric research – without you there would not be this thesis;
- *Dr. Uwe Liebchen* for being a clinical collaboration partner and member of our AK, a mentor and a mentee, a medical doctor and a true scientist - we formed a great team making use of our different backgrounds and common love for science;
- my clinical collaboration partners *Dr. Miriam Stegemann, Anja Theloe, Dr. Frieder Pfäfflin* and *Stephan Achterberg* from the Charitè Berlin and *Dr. Michael Zoller, Dr. Johannes Zander, Dr. Uwe Liebchen* and *Dr. Christina Scharf* from the University Hospital Munich for sharing your clinical insight and experience in numerous productive discussions and meetings;
- all present and former members of the AK Kloft and the PharMetrX program for the experiences we shared. For scientific and not quite so scientific discussions, for sitting next to me in lecture and beer halls, for sharing code and food – I truly enjoyed my time in Berlin and you all have a great part in it! Thank you *Alix Demaris, Anna Mc Laughlin, Ayatallah Saleh, Francis Ojara, David Busse, Vicktoria Stachanow, Johanna Seeger, Josephine Schulz, Sebastian Franck, Luis Ilia, Yomna Nassar, Dr. Lisa Schmitt, Franziska Kluwe, Dr. Ana-Marija Gricis, Nicole Zimmermann, Antonia Thomas, Banafshe Pourshacheraghi, Franz Weber, Davide Bindellini, Felix Müller* and *Dr. Robin Michelet* for lunch and yoga breaks, for barbeques during summer and the Christmas party in winter, for filling the institute with life and laughter – the forced pause imposed by the COVID-19 pandemic emphasized how important such daily interactions are and foreshadowed how much I will miss you! Thank you *Franziska Kluwe* and *Dr. Lisa Schmitt* for introducing me into the AK and my first project as my mentors – you truly did an outstanding job and I always strived

to be as good a mentor to others as you have been to me! Thank you *Alix Demaris, David Busse, Luis Ilia, Dr. Felix Joost, Davide Bindellini, Felix Müller, Franz Weber* and *Dr. Robin Michelet* for all the hours we spend in calisthenics parks, Kraftklub and -1 – the (muscle-) pain the next day was always worth it!

Thank you *Alix Demaris, Anna Mc Laughlin, Franziska Kluwe, David Busse, Luis Ilia, Dr. Ana-Marija Grisic* and *Dr. Robin Michelet* for having an open ear and providing perspective in the face of (perceived) injustices, defeats and successes. Thank you *Franziska Kluwe, Dr. Ana-Marija Grisic* and *Dr. Felix Joost* for allowing me a peak behind the curtain of pharmaceutical industry and helping me to plan my post-PhD career.

A big thank you for to *Franz Weber, Marian Klose, Alix Demaris, David Busse, Davide Bindellini, Ayatallah Saleh, Yomna Nassar, Nicole Zimmermann* and *Dr. Uwe Liebchen* for reviewing parts of my doctoral thesis. Further I want to thank all my elective course students *Marian Klose, Lukas Dübel, Arabel Luscombe, Yvonne Deppisch* and *Beyzanur Yildiz* for supporting my projects through literature research, data collection and data analysis.

- My *friends* outside the scientific community for your interest in and the encouragement for my research, for all the interesting insights you share from your fields of expertise and for reminding me that there might be bigger problems then a model not converging.
- My *family* for unconditional and limitless support.

Table of content

Abbreviations

A	Amount
ABW	Adjusted body weight
AIC	Akaike information criterion
ALB	Serum albumin concentration (NONMEM® data item label)
AMS	Antimicrobial stewardship
APACHE	Acute physiology and chronic health evaluation
APE	Absolute prediction error
AUC	Area under the curve
BfArM	Federal Institute for Drugs and Medical Devices of Germany (‘Bundesinstitut für Arzneimittel und Medizinprodukte’)
BMI	Body mass index
C	Concentration
CCC	Lin’s concordance correlation coefficient
C(t)	Drug concentration over time
CFR	Cumulative fraction of response
CI	Confidence interval
CL	Clearance
CLCR	Creatinine clearance
CLCRCG	Creatinine clearance estimated according to Cockcroft and Gault
CLCRCG_INF	CLCRCG value serving as inflection point for meropenem CL in CLCRCG-CL relationship
Cmax	Maximum concentration
Cmin	Minimum concentration
CREA	Serum creatinine concentration (NONMEM® data item label)
CRRT	Continuous renal replacement therapy
CV	Coefficient of variation
CVVH	Continuous venovenous haemofiltration
CVVHD	Continuous veno-venous haemodialysis
CVVHDF	Continuous veno-venous haemodiafiltration
CWRES	Conditional weighted residuals

CXh	Concentration X h after start of infusion (e.g. C8h: Concentration 8 h after start of infusion)
DV	Dependent variable (NONMEM® data item label)
EBE	Empirical Bayes estimate
ECMO	Extracorporeal membrane oxygenation
EMA	European Medicines Agency
EUCAST	European Committee on Antimicrobial Susceptibility Testing
f	Unbound (‘free’)
*f*AUC/MIC	Area under the unbound drug concentration-time curve divided by MIC
*f*Cmax/MIC	Unbound maximum concentration divided by MIC
FOCE+I	First-order conditional expectation method including interaction
$fT_{>MIC}$	Time period that unbound drug concentration exceeds the MIC
fu	Fraction unbound
GOF	Goodness-of-fit
H	Sigmoidicity coefficient
HTC	Haematocrit
HT	Body height (NONMEM® data item label)
I	Category ‘susceptible at increased exposure’
ICU	Intensive care unit
i.v.	Intravenous
ID	Individual identifier (NONMEM® data item label)
IIV	Interindividual variability
IL-6	Interleukin 6
INF	Inflection point
INH	Intact nephron hypothesis
IOV	Interoccasion variability
IPRED	Individual prediction(s)
LMU	Ludwig-Maximilians-Universität
LPIFR	Local pathogen-independent mean fraction of response
log	Natural logarithm (=ln)
log10	Decadic logarithm
log2	Binary logarithm
LR	Likelihood ratio

LRT	Likelihood ratio test
MAP	Maximum *a-posteriori*
MC	Monte Carlo
MHK	Minimale Hemmkonzentration
MIC	Minimum inhibitory concentration
MIC_i	Instantaneous minimum inhibitory concentration
MIPD	Model-informed precision dosing
n	Number
NLME	Nonlinear mixed-effects
ODE	Ordinary differential equation
OFV	Objective function value
P0.025	2.5th percentile
P0.05	5th percentile
P0.5	50th percentile (=median)
P0.95	95th percentile
P0.975	97.5th percentile
PD	Pharmacodynamic(s)
PE	Prediction error
PI	Prediction interval
PK	Pharmacokinetic(s)
PRED	Population prediction(s)
PsN	Pearl speaks NONMEM
PTA	Probability of target attainment
Q	Intercompartmental clearance between CMT 1 and 2
R breakpoint	MIC breakpoint separating I and R category
R category	Category ‘resistant’
RF	Renal function
RI	Renal impairment
RPE	Relative prediction error
RRT	Renal replacement therapy
RSE	Relative standard error
RUV	Residual unexplained variability
S breakpoint	MIC breakpoint separating S and I category

S category	Category ‘susceptible at normal dosing’
SD	Standard deviation
SE	Standard error
SOFA	Sepsis-related organ failure assessment
t	Time
TA	Target attainment
TDM	Therapeutic drug monitoring
THR	Thrombocyte count
TID	‘Ter in die’ i.e. thrice daily
UREA	Serum urea concentration (NONMEM® data item label)
V	Volume of distribution
V1	Volume of distribution of central compartment
V2	Volume of distribution of peripheral compartment
V3	Volume of distribution of deep peripheral compartment
VM	Maximum elimination rate
VPC	Visual predictive check

Symbols

α	Level of significance
df	Degree of freedom
Δ	Difference
C_j	Observed concentration for the j^{th} sample of a patient
$\hat{C}_j$	Predicted concentration for the j^{th} sample of a patient
N	Normal (Gaussian) distribution
f	Function OR fraction
I	Fisher information matrix
p	Probability density function
$P_{orig,k}$	Original parameter estimate for the k^{th} fixed effects-parameter
$P_{bs,k}$	Median of the bootstrap parameter estimates of the k^{th} fixed effects-parameter
θ	Fixed-effects parameter: Typical parameter in population
Θ	Vector of fixed-effects parameters
θ_k	Typical parameter value of k^{th} parameter
$\theta_{k,EBE}$	Individual parameter value of the k^{th} parameter
$\theta_{k,pop}$	Population parameter value of the k^{th} parameter
θ_{ik}	Typical parameter value for the i^{th} individual and the k^{th} parameter
θ_{INF}	Typical parameter describing the inflection point of a piecewise-linear covariate-parameter relationship
θ_Z	Typical parameter describing the effect of the Z^{th} covariate
ϕ_i	Structural model parameters for the i^{th} individual
ϕ_{ik}	Structural model parameter for the i^{th} individual and the k^{th} parameter
ϕ_{ikq}	Structural model parameter of the i^{th} individual, at the q^{th} occasion and the k^{th} parameter
η	Random-effects parameter: Interindividual variability
η_k	Interindividual variability parameter values for the k^{th} parameter
η_{ik}	Interindividual variability parameter value for the i^{th} individual and the k^{th} parameter
η_Z	Interindividual variability parameter value for the Z^{th} covariate

ω_{κ}^2	Variance of η_k
$\omega_{1,1}^2$	Diagonal element (variance) of the first element of $\boldsymbol{\Omega}$
$\omega_{1,2}$	Off-diagonal element (covariance) of the first and second element of $\boldsymbol{\Omega}$
$\boldsymbol{\Omega}$	Omega matrix: Variance-covariance matrix of the interindividual variability
κ	Random-effects parameter: Interoccasion variability
κ_k	Interoccasion variability parameter values for the k^{th} parameter
κ_{ikq}	Interoccasion variability parameter value for the i^{th} individual, at the q^{th} occasion and the k^{th} parameter
π_k^2	Variance of κ_k
ε	Random-effects parameter: Residual unexplained variability
ε_{ij}	Residual variability parameter value for the i^{th} individual at the j^{th} observation
ε_{add}	Additive ε
ε_{prop}	Proportional ε
σ	Standard deviation of ε
σ^2	Variance of ε
${\sigma_{add}}^2$	Variance of ε_{add}
${\sigma_{prop}}^2$	Variance of ε_{prop}
${\hat{\sigma}_j}^2$	Variance of prediction variability
$\hat{\sigma}_{\varepsilon}^2$	Variance of residual variability
$\boldsymbol{\Sigma}$	Sigma matrix: Variance-covariance matrix of ε
OFV	Objective function value
OFV_{Bayes}	Bayes objective function value
OFV_{MAP}	MAP objective function value
Z_i	Observed covariate value(s) of the i^{th} individual
BZ_i	Observed baseline covariate value(s) of the i^{th} individual
Z_{median}	Median covariate value(s)
BZ_{median}	Median baseline covariate value(s)
Y	Matrix of observations
Y_i	Observations of the i^{th} individual
Y_{ij}	j^{th} observation of the i^{th} individual
$\hat{Y}_{ij}$	j^{th} prediction of the i^{th} individual

$\mathscr{L}$	Likelihood
$\mathscr{L}_i$	Contribution of the i^{th} individual to the likelihood
$\mathscr{LL}$	Log-likelihood
χ^2	Chi-square distribution
x_{ij}	Design variable of the i^{th} individual at the j^{th} observation

Relevant publications

Parts of the presented thesis have been published in the following original articles:

- **Project I: Characterising meropenem adsorption abilities at the cytokine adsorber CytoSorb®**

  U. Liebchen, C. Scharf, M. Zoller, **F. Weinelt***, C. Kloft*

  No clinically relevant removal of meropenem by cytokine adsorber CytoSorb® in critically ill patients with sepsis or septic shock

  Intensive Care Medicine 47, 1332–1333 (2021)

  DOI: 10.1007/s00134-021-06487-y

  *shared senior authorship

- **Project II: Utilising pharmacokinetic models to improve meropenem and piperacillin/tazobactam dosing**

  F. Weinelt, M. Stegemann, A. Theloe, F. Pfäfflin, S. Achterberg, F. Weber, L. Dübel, A. Mikolajewska, A. Uhrig, P. Kiesling, W. Husinga, R. Michelet, S. Hennig, C. Kloft

  Evaluation of a meropenem and piperacillin monitoring program in intensive care unit patients calls for the regular assessment of empirical targets and easy-to-use dosing decision tools.

  Antibiotics 11(6), 758 (2022)

  DOI: 10.3390/antibiotics11060758

  https://creativecommons.org/licenses/by/4.0/

  F. Weinelt, M. Stegemann, A. Theloe, F. Pfäfflin, S. Achterberg, L. Schmitt, W. Husinga, R. Michelet, S. Hennig, C. Kloft

  Development of a model-informed dosing tool to optimise initial antibiotic dosing - a translational example for intensive care units.

  Pharmaceutics 13(12), 2128 (2021)

  DOI: 10.3390/pharmaceutics13122128

  https://creativecommons.org/licenses/by/4.0/

- **Project III: Evaluation and extension of the MeroRisk Calculator**

  U. Liebchen, M. Klose, M. Paal, M. Vogeser, M. Zoller, I. Schroeder, L. Schmitt, W. Huisinga, R. Michelet, J. Zander, C. Scharf, **F. Weinelt***, C. Kloft*
  Evaluation of the MeroRisk Calculator, a user-friendly tool to predict the risk of meropenem target non-attainment in critically ill patients
  Antibiotics 10(4), 468 (2021).
  DOI: 10.3390/antibiotics10040468
  https://creativecommons.org/licenses/by/4.0/
  *shared senior authorship

Further original articles, as well as additional publications, are presented at the end of the thesis (see page 215).

1 Introduction

Since the dawn of time humankind has been plagued by infectious diseases [1]. Pathogens like *Yersinia pestis* regularly ravaged through the population killing hundreds of millions and for a long time a simple wound infection could be considered equivalent to a death sentence [2–4]. As recently as 1900, contagious diseases were the most common cause of death in the United States of America [5]. But in 1909 the discovery of arsphenamin during a systematic, large-scale screening process by Paul Ehrlich, Alfred Bertheim and Sahachiro Hata marked the beginning of the new antibiotic era and enabled the effective treatment of syphilis, a sexually transmitted disease caused by *Treponema palladium* [6,7]. In the following decades and especially during the 'golden age' of antibiotic drug discovery between 1950 and 1970, systematic investigations led to the discovery of various antibiotic drug classes [5,6,8]. It became possible to effectively treat a wide range of infectious diseases. As a consequence, non-contagious diseases replaced infections as the most common cause of death and the life expectancy rose from 47 to 78.8 years in the United States of America [9]. But even during the height of the antibiotic era bacterial infections remained a major threat to public health: vulnerable patient populations like critically ill patients suffering from severe infections still had mortality rates of up to 60% [10–13]. The 'golden age' of antibiotic drug discovery is long over: no truly novel antibiotic was found in the last three decades [14,15]. Furthermore, the emergence and spread of antimicrobial resistance, accelerated by the inappropriate use of antibiotic drugs, leads to a constant reduction in effective antibiotic drugs [16–18]. As a response to this new challenge, different international and national action plans call not only for a determined search of new antimicrobial drugs but also for a more rational use of existing antibiotic drugs [19,20].

1.1 The rational use of antibiotic drugs

The aim of a rational antibiotic drug therapy is to treat the bacterial infection with (i) the highest possible efficacy, (ii) the lowest possible rate of occurrence and severity of adverse events and (iii) the lowest possible risk for the emergence and spread of antimicrobial resistance. To achieve this aim, efficacious and safe drug exposures in each individual patient are needed [21]. Four vital components need to be considered to ensure adequate exposure during antibiotic drug therapy and form the basis of the rational use of antibiotics (Figure 1.1):

1. **Appropriate indication**: an evidence-based prescription of antibiotics should be the standard of care. Antibiotic drug therapy should only be initiated based on evidence or clear indication of bacterial infection [22–24].
2. **Appropriate choice of antibiotic**: the antibiotic drug administered to the patient should be selected based on its efficacy against the pathogen causing the infection. Prior knowledge about local epidemiological data and susceptibility pattern and microbiological diagnostics during treatment can support the selection of an appropriate antibiotic drug [22–24].
3. **Appropriate timing**: antibiotic drug therapy should be initiated as soon as possible after the diagnosis to increase the likelihood of an effective therapy [22–24]. In critically ill patients diagnosed with sepsis or septic shock each hour of delay was associated with an increased mortality [25–27].
4. **Appropriate dosing**: a suitable dosing regimen should be selected to achieve an adequate exposure at the site of infection in the patient [22,28]. Even if an appropriate antibiotic drug is administered early after diagnosis, an inappropriate dosing regimen disregarding influential drug-, patient- and infection-specific characteristics can lead to therapy failure.

While all four components are important for rational antibiotic drug therapy, the research presented in this thesis focused on the selection of an appropriate dosing regimen. In the subsequent chapters, drug- (see 1.2) and patient-specific (see 1.3) characteristics affecting the selection of such an appropriate dosing regimen will be introduced.

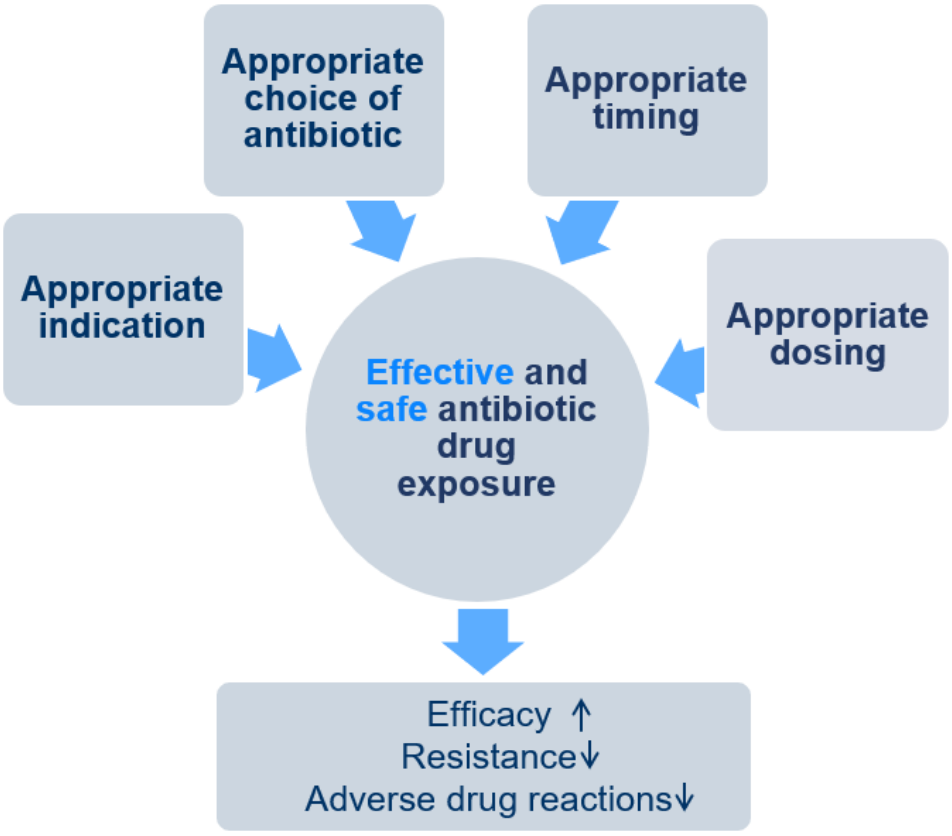

Figure 1.1: The four components needed to ensure effective and safe antibiotic exposure thereby increasing efficacy while reducing the rate of resistance and adverse drug reactions.

1.2 Antibiotic drugs

To achieve adequate drug exposure at the site of infection, drug-specific characteristics need to be considered. While the PK properties of the administered antibiotic drug in combination with patient-, disease- and pathogen-specific characteristics determine the drug exposure, the drug-specific PK/PD relationship determines the efficacy of the drug exposure. Before introducing the two investigated antibiotic drugs and their specific PK and PK/PD characteristics, the minimum inhibitory concentration (MIC, see 1.2.1) and common PK/PD indices such as the time period the unbound antibiotic drug concentration exceeds the MIC value (see 1.2.2) will be introduced.

1.2.1 The minimum inhibitory concentration

The MIC is a standard measure to quantify the antibacterial activity of a drug for a specific pathogen *in vitro* [29,30]. It determines the minimum drug concentration needed to inhibit visual bacterial growth in defined experimental conditions [31,32]. The more potent the antibiotic drug against the investigated pathogen, the lower the concentration to inhibit the visual growth and therefore the lower the measured MIC. The relatively simple and standardised determination of the MIC is both an advantage and disadvantage at the same time. It is an advantage because it (i) can easily be automated and integrated into clinical routine, (ii) enables the straightforward comparison between different drugs for a given specific bacterium and (iii) is easy to interpret for health care professionals. It is a disadvantage because – in contrast to static/dynamic time-kill curve experiments [33] - no information about the time-dependent growth-kill behaviour is included [34]. Furthermore, the commonly used two-fold dilution series to determine the MIC can lead to inaccurate measurements for high MIC values [29,35].

MIC determinations are still rare in clinical practice and, unfortunately, in many cases it is not possible to determine the pathogen causing the infection [36]. In addition, even if the pathogen is identified and the MIC successfully determined, the information usually becomes available to the healthcare personnel after therapy start [37]. Depending on the level of knowledge already available, healthcare professionals use information collected by organisations like the European Committee on Antimicrobial Susceptibility Testing (EUCAST). If no information about the pathogen causing the infection is available yet, non-species related and drug-specific PK/PD breakpoints can be used [38]. If the pathogen but not its individual MIC is known, species-specific MIC breakpoints based on the distribution of MIC values of a specific pathogen can be employed. In both cases, the breakpoints are separating three susceptibility categories: (i) susceptible at standard dosing (S), (ii) susceptible at increased exposure (I) and (iii) resistant (R) [38,39].

1.2.2 Pharmacokinetic/pharmacodynamic indices and their targets

Drug-specific PK/PD indices describe the relationship between PK measures of an antibiotic drug (e.g. the area under the curve (AUC), the maximum concentration (C_{max})) and a PD measure describing the susceptibility of a pathogen (e.g. the MIC value). Three major PK/PD indices have been derived based on *in vitro* and/or *in vivo* studies investigating the antibacterial activity of different antibiotic drugs (Figure 1.2) [40–43] PK/PD indices are usually determined for - and therefore apply to – unbound i.e. "free" drug concentrations:

1. ***f*T$_{>MIC}$:** The time period in precent the unbound antibiotic drug concentration exceeds the MIC value within 24 hours
2. ***f*C$_{max}$/MIC:** The ratio of the unbound maximum drug concentration and the MIC value
3. ***f*AUC/MIC:** The ratio of the area under the unbound concentration-time profile over 24 hours and the MIC value

The exposure in relation to the MIC needed (e.g. 100% *f*$T_{>MIC}$) to achieve bacterial eradication, clinical cure or survival is described by the PK/PD target and based on further *in vitro* and *in vivo* studies [40]. Those PK/PD targets often form the foundation to select the appropriate dosing regimen in clinical practice.

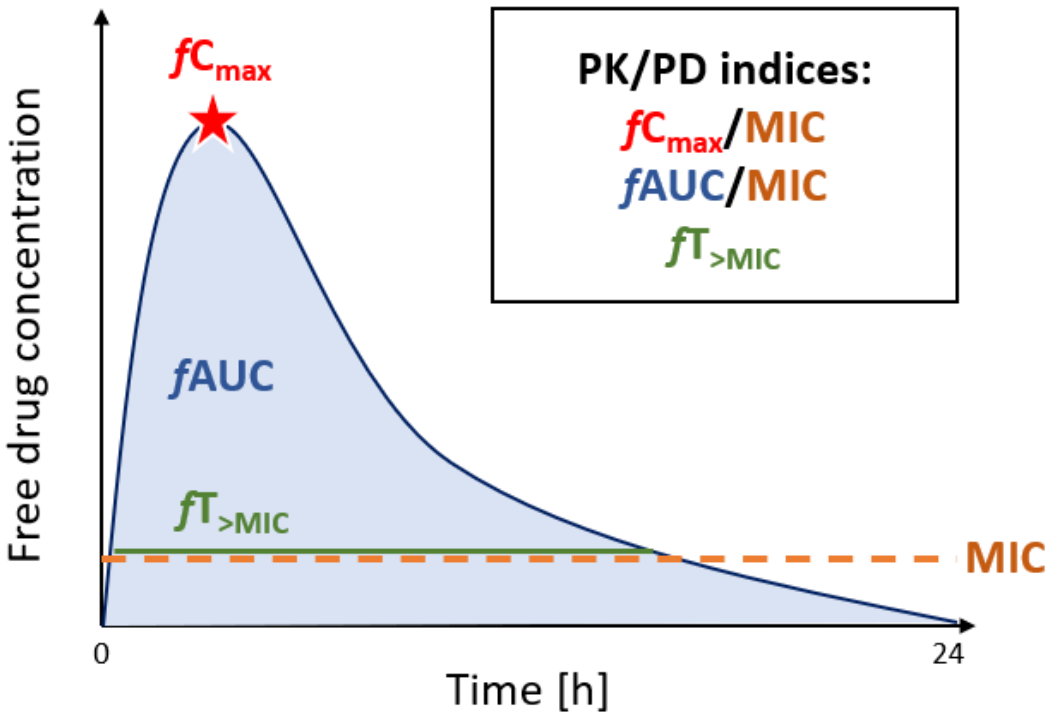

Figure 1.2: Illustration of different antibiotic pharmacokinetic (PK)/pharmacodynamic (PD) indices in a drug concentration-time profile.
Abbreviations: *MIC:* Minimum inhibitory concentration, *fC_{max}:* Maximum unbound i.e. "free" drug concentration, *fAUC:* Area under the unbound drug concentration-time curve, *$fT_{>MIC}$*: Time period of the free drug concentration exceeding the MIC

1.2.3 Investigated antibiotic drugs

In this chapter, the antibiotic drug meropenem and the drug combination piperacillin/tazobactam, investigated in the presented thesis will be introduced.

1.2.3.1 Piperacillin/Tazobactam

Indication and spectrum of activity

The fixed drug combination piperacillin and tazobactam is commonly administered as empirical therapy (the pathogen causing the infection is not yet identified) and as targeted therapy (the pathogen has been identified) to treat severe infections in the hospital [44–46]. Piperacillin is a broad spectrum ureidopenicillin antibiotic while tazobactam is a β-lactamase inhibitor preventing the enzymatic degradation of piperacillin by bacterial β-lactamases [47,48]. As a combination the two drugs exhibit a broad antimicrobial activity against many gram-negative and gram-positive aerobic and anaerobic pathogens [44,47]. The daily dose in adults with non-impaired kidney function ranges between 12-16 g piperacillin and 1.5-2 g tazobactam depending on type and severity of infection, the pathogen and patient condition and is administered with a fixed piperacillin/tazobactam ratio of 8/1. The doses are usually administered as short-term (1-30 min) infusions [49], but recent pharmacokinetic investigations led to a shift towards prolonged and continuous infusions [50–53]

Pharmacokinetics

Piperacillin and tazobactam can be classified as small molecule drugs due to their low molar mass (517.6 g/mol and 300.3 g/mol, respectively) and are orally not absorbed [44,48]. The distribution of the two drugs into different tissues is fast (<30 minutes after end of infusion) and exposures similar to plasma (>50% of plasma concentrations) are reached in multiple tissues including intestines, lung and skin [48]. Both drugs are primarily excreted via the kidney by passive glomerular filtration and active tubular secretion via the organic anion transporters 1 and 3 [44,47]. The saturation of the active tubular secretion is assumed to be the reason for the observed non-linear clearance and competitive inhibition between the two co-administered drugs [44,47,54,55]. To a small extent both drugs degrade into inactive metabolites by cleavage of the β-lactam ring: 70% - 80% of piperacillin can be recovered as parent compound while up to 26% of tazobactam is metabolised [44,47].

PK/PD target values

β-lactam antibiotics like piperacillin/tazobactam show time-dependent antimicrobial activity: their efficacy is linked to the time the unbound drug concentration is above the MIC value of the targeted pathogen ($fT_{>MIC}$) [44,47,56]. The determination of a defined PK/PD target for different β-lactam antibiotics, infections and patient populations was the aim of various *in vitro* and *in vivo*

investigations. For gram-negative pathogens the maximum activity is obtained with 60-70% $fT_{>MIC}$ while 40-50% $fT_{>MIC}$ is sufficient for gram-positive pathogens [44,47]. In a joint extensive review of β-lactams in critically ill patients, the French Society of Pharmacology and Therapeutics and the French Society of Anaesthesia and Intensive Care Medicine suggest a PK/PD target of 100% $fT_{4-8xMIC}$ in critically ill patients [57].

Safety

Overall piperacillin/tazobactam is well tolerated by patients [44,47,49]. The most common adverse events observed during piperacillin/tazobactam therapy are diarrhoea, infused vain complication, rash and nausea [44,47,49]. Furthermore, piperacillin minimum concentrations above 360 mg/L and 452.65 mg/L have been linked to an increased risk of neuro- and nephrotoxicity, respectively [57,58].

1.2.3.2 Meropenem

Indication and spectrum of activity

Meropenem is broad-spectrum carbapenem β-lactam antibiotic. The bactericidal activity of meropenem originates from the inactivation of penicillin binding proteins and the resulting inhibition of the bacterial cell wall synthesis [59]. It is frequently used for empirical therapy, i.e. before identification of the infection pathogen, in critically ill patients due to the activity against both gram-negative and gram-positive pathogens, including commonly less susceptible pathogens like *Pseudomonas aeruginosa* and *Acinetobacter spp.* [59,60]. Meropenem is administered to treat various infections including nosocomial pneumonia, febrile neutropenia, bacterial meningitis and complicated urinary tract infections [59]. The daily dose in adults ranges between 1.5-6.0 g depending on type and severity of infection, the pathogen and patient condition. Doses were usually administered as short-term (15-30 min) infusion [59], but based on various pharmacokinetic studies a shift towards prolonged and continuous infusions is observable [61–65]

Pharmacokinetics

Meropenem can be classified as a small molecule drug due to its low molar mass (383 g/mol), is orally not absorbed and rapidly penetrates most body fluids and tissues [66,67]. As a hydrophilic molecule ($\log D_{pH7.4}$=4.36 [68]), meropenem and its metabolite are primarily excreted via the kidney both by passive glomerular filtration and active tubular secretion via the organic anion transporters 1 and 3 [66,69]. The majority of the administered dose (∼70%) is excreted unchanged as parent compound, while roughly 28% is excreted as inactivated metabolite [3]. The metabolite is most likely formed via opening of the beta-lactam ring by the renal dehydropeptidase-1 [59].

PK/PD target values

Like piperacillin, meropenem shows time-dependent antimicrobial activity: the efficacy is linked to the time the unbound drug concentration is above the MIC value of the targeted pathogen ($fT_{>MIC}$) [56]. The determination of a defined PK/PD target for different β-lactam antibiotics, infections and patient populations was the aim of various *in vitro* and *in vivo* investigations. Based on their investigations of *Escherichia coli* and *P. aeruginosa* in a mouse thigh infection model, Drusano et al. linked the maximum bacterial kill activity to 40% $fT_{>MIC}$ [70,71]. A clinical study reported by Crandon et al. associated 19.2% and 47.9% of $fT_{>MIC}$ with clinical success and survival respectively in patients with ventilator-associated pneumonia and *Pseudomonas aeruginosa* infections [72]. Ariano et al. observed a clinical response rate of 80% for febrile neutropenic patients with bacteraemia and a $fT_{>MIC}$ greater than 76% [73]. Further investigations suggested an improved antibiotic efficacy for meropenem if minimum drug concentrations achieved 5 times [74] or 6.2 times the MIC [75]. In an joint extensive review of β-lactams in critically ill patients, the French Society of Pharmacology and Therapeutics and the French Society of Anaesthesia and Intensive Care

Medicine suggest a PK/PD target of 100% $fT_{4—8xMIC}$, based on multiple *in vitro* and *in vivo* studies reporting efficacy and adverse events [57].

Safety

The most common adverse events observed during meropenem therapy are diarrhoea, rash and nausea [76,77]. Furthermore, meropenem minimum concentrations above 64.2 mg/L and 44.5 mg/L have been linked to an increased risk of neuro- and nephrotoxicity, respectively [57,58]. Overall, meropenem is considered to be a relatively safe drug [77].

1.3 Critically ill patients

The selection of an appropriate dosing regimen depends on the individual patient. Physiological factors (e.g. weight), pathophysiological factors (e.g. renal impairment), genetic factors (e.g. CYP genotype), comedications (e.g. possible drug-drug interactions) or environmental factors can all have an impact on the PK of the administered drug and hence need to be considered for dosing decisions [78–84]. The research presented in this thesis focused on antibiotic drug therapy in critically ill patients and critically ill patients receiving CytoSorb® treatment. Therefore the special characteristics of these patient populations are further elucidated in the following.

Effective antibiotic treatment of critically ill patients is both particularly important and challenging. Adequate antibiotic treatment is important due to the high vulnerability of this patient population characterised by severe and life-threatening illnesses: critically ill patients require specialised care, aggressive medical intervention and intensive monitoring on their long way of recovery [10–12,85,86]. They often face severe infections (prevalence ~50% [85]) and, due to their vulnerable conditions, have particularly high mortality rates reaching up to 60% during sepsis or septic shock [10–12,85,86]. Effective antibiotic treatment is mandatory, yet challenging due to several heterogeneous changes in PK processes based on the pathophysiology of their severe illnesses (Figure 1.3) [79]. One frequently observed alteration concerns the haemodynamics of critically ill patients [87]. The systematic inflammatory response syndrome (SIRS) – caused by e.g. sepsis, burns or major surgeries – can lead to decreased vascular resistance and increased cardiac output [84,87,88]. Together with treatment interventions like vasopressors, a hyperdynamic state can be caused, leading to an increased blood flow through eliminating organs (i.e. kidney) and potentially to a higher drug clearance [79]. Furthermore, critically ill patients often display altered fluid balances. Increased vascular permeability and endothelial cell damage can lead to extravasation of fluid into tissues or interstitial space [79,83]. This so-called ‘third spacing’ can be further amplified by fluid resuscitation frequently administered to avoid hypotension in critically ill patients. In addition to the extravasation and also due to the increased permeability, albumin can leak into the interstitial space fluid and cause hypoalbuminemia [89,90]. Both phenomena can have an impact on the PK of an antibiotic drug: the altered fluid balance might affect the drug distribution (especially for hydrophilic, nonionised drugs) and the decrease in serum albumin might affect the unbound fraction of a drug [79,91,92]. As a consequence of an altered fraction unbound, both the drug clearance and its distribution might deviate [89,90]. Another major contribution to the uncertainty in the expected PK of a drug and common in critically ill patients are organ dysfunctions and the extracorporeal organ support the affected patients might receive [93]. The dysfunction of drug eliminating organs can lead to a gradual or rapid decrease in drug clearance [79], while extracorporeal organ support might increase drug clearance [94–96]. In both cases, the impact is highly variable, dependent on various

factors and hard to predict. Patient-specific characteristics (e.g. remaining organ function), extracorporeal organ support characteristics (in the case of renal replacement therapy e.g. mode, filter type, different flow rates) and drug-specific characteristics (e.g. lipophilicity, protein binding) all play an important and interconnected role [96,97].

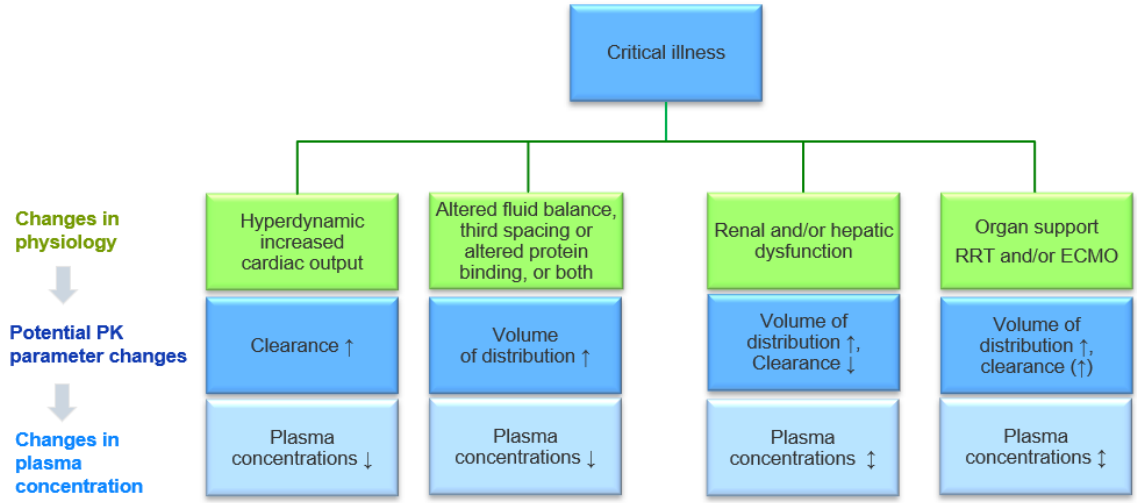

Figure 1.3: Possible impact of critical illness on physiology, pharmacokinetics and drug exposure. Modified from Roberts et al. [79].
Abbreviations: *RRT:* Renal replacement therapy, *ECMO:* Extracorporeal membrane oxygenation

A new therapeutic option to regain “immune homeostasis” in the dysregulated inflammatory state of septic shock with a potentially impact on drug pharmacokinetics - the haemadsorption of cytokines – has recently been promoted [98]. In this context, the CytoSorb® filter (CytoSorbents Corporation, NJ, USA) is licensed for extracorporeal cytokine elimination in hyperinflammatory conditions within the European Union [99]. CytoSorb® cartridges can be easily installed within ordinary haemodialysis-, haemofiltration-, extracorporeal membrane oxygenation- and heart-lung-machines. The mode of action is based on the adsorption of cytokines by highly porous high-tech polymer beads with a large surface area of about 45.000 m^2. Molecules up to a molar mass of 55 kDa are potentially adsorbed by the filter (molar mass range of cytokines 6-70 kDa) due to hydrophobic interactions and therefore eliminated from the patient [100]. In addition to its utility in sepsis therapy, the CytoSorb® filter is also employed to rapidly reduce drug concentrations in case of intoxications [101–103]. Up to now, the CytoSorb® filter has been installed 121.000 times worldwide [19].

The ability of the CytoSorb® filter to adsorb drugs implies that this might also happen unintentionally. Particularly feared in this context is the adsorption of antibiotics, which play the key role in the causal therapy of septic shock. Indeed, previously published *in vitro* and *in vivo* data indicated significant adsorption of antibiotics by the CytoSorb® filter [104–106].

1.4 Pharmacometrics

Pharmacometric research amalgamates and extends methods and knowledge from diverse disciplines such as medicine, clinical pharmacy, pharmacology, mathematics, statistics and computational science with the aim to quantitatively characterise the relationship between a system and an drug intervention [107–109]. Most commonly the investigated system is a patient and the observed intervention the administration of a drug. The focus of the analysis is to mathematically model the concentration-time profile of the drug in the patient after administration (PK), the drug effect-time profile (PD) in relationship to the PK (PK/PD) and/or the therapeutic outcome [108]. After development, a pharmacometric model can be used to explore and visualise the relationship between system and intervention, including the prediction of not observed events (e.g. different dosing regimen, data points outside the observation period) [107,110].

In pharmaceutical industry, pharmacometric modelling and simulation approaches are routinely employed to optimally utilise and combine data collected during different phases of drug development [111–113]. This so called 'model-informed drug discovery and development' strategy is encouraged by regulatory agencies such as the European Medicines Agency (EMA) or the Food and Drug Administration (FDA) in the United States of America [113,114] and supports decision making during drug discovery and development (e.g. biomarker or dose selection), extrapolation of knowledge to other diseases or populations and provides evidence needed for regulatory submissions [115–117]. Furthermore, pharmacometric analyses enable a separation and therapy optimisation for subpopulations of patients, thereby increasing the probability of therapeutic and regulatory success [118]. However, the detection and separation of special patient subgroups is often restricted by the design of clinical phase III studies: Strict inclusion/exclusion criteria usually exclude special patient populations (e.g. critically ill patients) with patient characteristics that might alter PK and/or PD of the investigated drug [119]. As a result, thorough PK/PD analyses of special patient populations often are only conducted after regulatory approval.

In addition to their frequent use in pharmaceutical industry, pharmacometic modelling and simulation approaches are slowly integrated into clinical practice [118,120–122]. Under the concept of 'model-informed precision dosing' (MIPD) drug therapy is individualised based on pharmacometric models and patient-specific characteristics [118,122–125]. Prior to the initiation of drug therapy patient characteristics can be used to predict the PK of that specific patient and the dosing regimen most likely to reach an adequate drug exposure can be selected. The uncertainty of this prediction can be further reduced by the integration of patient-specific drug measurement(s): Based on the patients characteristics and the measured drug concentration(s) the most likely model parameters are calculated and the prediction of the individual PK updated [126]. To enable their implementation into clinical practice the results of pharmacometric analyses can be integrated into user-friendly

model-informed dosing tools such as dosing algorithms or software [124,127–131]. Unfortunately, in many hospitals reliable and frequent concentration measurements of antibiotic drugs other than aminoglycosides, are not implemented and the use of model-informed dosing tools to inform dosing is rare [132,133]. The lack of specialised expertise, costs (e.g. software, drug measurement service), missing structured processes and indistinct global, national and local regulations (e.g. concerning liability) currently impede the widespread implementation of model-informed dosing tools [121,122]. To overcome these obstacles local initiatives are needed to build up the missing structures and to develop, implement and evaluate model-informed dosing tools according to local needs and possibilities.

While pharmacometrics has already demonstrated its potential in supporting drug development and dosing optimisation in the clinic in the last decades, the use and development of pharmacometric approaches is expected to further advance in the future [134].

1.5 Objectives

As introduced in the last chapters (see 1.1 - 1.3), realizing an appropriate antibiotic therapy for critically ill patients constitutes a major challenge, crucial not only for the individual patient but also for the fight against antimicrobial resistance. One key element of an appropriate antibiotic therapy - the selection of an adequate dosing regimen for each individual patient – could substantially benefit from the routine use of pharmacometric approaches under the concept of MIPD. Unfortunately, the implementation of MIPD into real world clinical application is still far from being complete. In many hospitals reliable and frequent concentration measurements of antibiotic drugs are not available. Even for some commonly administered and supposedly 'well-known' drugs, the PK is not fully characterised in special populations and the translation of accumulated knowledge into clinical application remains unsatisfactory: The growing repertoire of published PK models is seldom integrated into user-friendly tools or comprehensive dosing strategies and therefore remains inaccessible for most healthcare professionals. In addition to this, a majority of available tools has not been evaluated in a real-world scenario, which lowers trust in the reliability of their predictions and further hinders implementation.

Therefore, the overall objective of the presented thesis was to accelerate the implementation of MIPD into clinical practice following an *iterative*, *integrative* and *translational* approach (Figure 1.4). The initial and reoccurring central question in this *iterative* approach 'Is the current antibiotic dosing appropriate?', was addressed *integrating* expertise from a diverse interprofessional team of healthcare professionals and can be segmented into four intermediate steps, all vital to the main objective:

(i) **PK/PD data collection:** Establish reliable and frequent antibiotic drug concentration measurements and pathogen susceptibility determinations in clinical routine

(ii) **Pharmacometric data analysis**: Elucidate the PK/PD of antibiotic drugs in critically ill patients and assess local factors influencing antibiotic therapy (e.g. local pathogen susceptibility)

(iii) **Tailored improvement strategy**: Develop easy-to-use, model-informed dosing tools fit for clinical practice

(iv) **Clinical implementation + Evaluation:** Implement, evaluate and optimise existing model-informed dosing tools

The detailed objectives for each of the four projects presented in this thesis are introduced in the following. Furthermore, a short outline of the research strategy is provided.

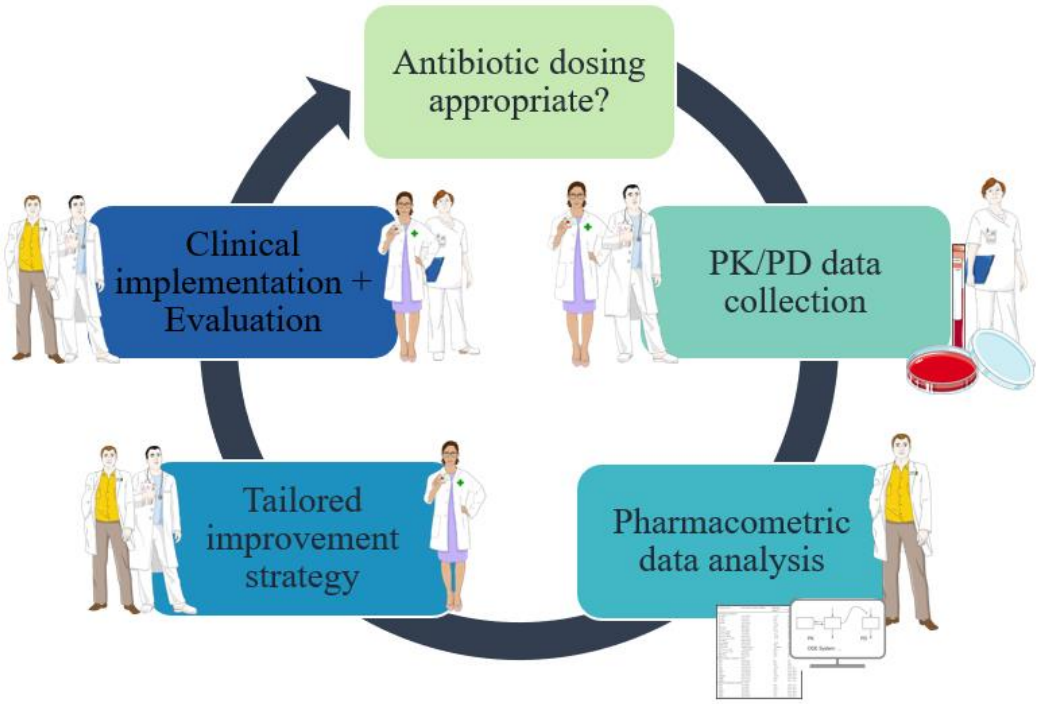

Figure 1.4 Graphical overview of the iterative, integrative and translational approach employed to accelerate the implementation of model-informed precision dosing in order to improve antibiotic therapy in critically ill patients.

Figures next to each step indicate the responsible healthcare professionals: *PK/PD data collection*: Physicians, pharmacists and clinical laboratory; *Pharmacometric data analysis*: Pharmacometrician; *Tailored improvement strategy*: Physicians, pharmacists and pharmacometrican; *Clinical implementation + Evaluation*: Physicians, pharmacists, pharmacometrican and clinical laboratory.

Figures representing healthcare professionals from smart.servier.com.

Project I: Characterising meropenem adsorption abilities at the cytokine adsorber CytoSorb®

Step: Pharmacometric data analysis

Objectives: The objective of this project was to (i) quantify a potential meropenem adsorption at the CytoSorb® filter and (ii) evaluate if meropenem dosing needs to be intensified during CytoSorb® therapy.

Research strategy: For this project a NLME modelling and simulation approach was chosen. A population pharmacokinetic model was developed leveraging therapeutic drug monitoring data in critically ill patients undergoing continuous veno-venous haemodialysis with and without CytoSorb® treatment and three distinct approaches to assess if clearance differed without or during CytoSorb® treatment were applied: (i) quantification of a possible proportional increase in clearance during CytoSorb® treatment (ii) investigation of (non)saturable adsorption at the CytoSorb® filter using different adsorption submodels and (iii) evaluating the predictive performance for concentrations during CytoSorb® treatment by a PK model developed excluding samples collected during CytoSorb® treatment.

Project II: Utilising pharmacokinetic models to improve meropenem and piperacillin/tazobactam dosing

Steps: PK/PD data collection, Pharmacometric data analysis, Tailored improvement strategy, Clinical implementation + Evaluation

Objectives: The objectives of this project were to (i) assess and evaluate the current piperacillin/tazobactam and meropenem dosing decisions at the Charité-Universitätzmedizin Berlin, to (ii) develop model-informed dosing tools optimised for integration into clinical practices at Charitè-Universitätsmedizin Berlin and to (iii) integrate and assess the developed dosing tools in clinical routine use.

Research strategy: In 2019 a clinical study for piperacillin/tazobactam and meropenem was initiated as a coordinated intervention of the antimicrobial stewardship (AMS) team at Charité-Universitätsmedizin Berlin. The study was separated into 3 stages. In stage I, current antibiotic dosing practices in two intensive care units were assessed. Furthermore, the data collected in stage I was used to select and evaluate published NLME models. A model-informed tabular dosing tool for initial antibiotic therapy and an interactive dosing software were developed based on the evaluated NLME models and assessed during clinical practice in stage II and stage III of the study, respectively.

Project III: Evaluation and extension of the MeroRisk Calculator

Classification: Implementation + Evaluation

Objectives: The objectives of this project were (i) to evaluate the performance of the MeroRisk Calculator, a previously developed user-friendly tool to predict the risk of meropenem target non-attainment in critically ill patients, using routine clinical data and (ii) to extend the risk predictions of the MeroRisk Calculator to include pathogen sensitivity information in case no individual MIC value is available.

Research strategy: A direct data-based evaluation of the MeroRisk Calculator was not feasible using the available clinical routine dataset without censoring most of the available data: While the MeroRisk Calculator uses the provided creatinine clearance to predict the meropenem concentration 8 h after standard dosing (1 g, 0.5 h infusion, q8h), i.e., at one specific time point, a large proportion of the concentration measurements of the retrospective dataset, were taken at different time points (not exactly 8 h after dose). Therefore, a two-step approach was chosen: In step 1, the potential of a population pharmacokinetic model to predict the clinical routine dataset was evaluated. In step 2, the PK model was used for a model-based evaluation of the MeroRisk Calculator. Furthermore, a method to calculate the risk of target non-attainment based on causative pathogens prior to MIC determination was developed employing susceptibility patterns reported by EUCAST.

2 Methods

To achieve the objectives of the projects introduced in section 1.5, different pharmacometric modelling and simulation techniques were employed. The first part of the methods section will focus on the general principles and methods of pharmacometric modelling shared by all presented projects. In the second part of the methods section, project-specific methodology and the clinical data underlying the respective analyses will be introduced.

2.1 Pharmacometric modelling and simulation approaches

Pharmacometric approaches are often categorised either as bottom-up or as top-down (Figure 2.1). Bottom-up approaches typically rely on and combine prior knowledge of the investigated system (e.g. human or animal physiology) and information about an agent interacting with the system (e.g. physicochemical properties of a drug) to predict reciprocal effects [135]. Top-down approaches on the other hand are based on (non-)clinical data.

In the context of the PK analyses described in this thesis, the clinical data are plasma drug concentrations determined over time, the corresponding dosing regimens and the characteristics of the associated patients.

Within the classification of top-down approaches, methodologies are further divided into (i) non-compartmental or compartmental and (ii) individual or population approaches.

The compartmental approach for analysing PK data is based on the assumption that a body consists of kinetically homogenous regions that can be represented by distinct ‘compartments’ in a mathematical model [107,136]. For example, a two-compartment model describes a body to consist of two kinetically distinct compartments. The central compartment of a two-compartment model typically includes blood and highly perfused regions of the body, while the peripheral compartment comprises less perfused regions.

Whereas individual approaches focus on the analysis of the available data on an individual patient level, population approaches include the information of all individuals in a joint analysis [137,138]. The naïve pooling approach pools the data of all patients in a population prior to the analysis. Consequently, the information which data originates from which patient is lost and interpatient variability cannot be quantified. One way of quantifying the observed interpatient variability in a population is using the two-stage approach [139]. In the first stage, the data of each patient is analysed

individually. In the second stage, descriptive summary statistics of the individual parameter estimates from stage I are computed to describe central tendencies and interpatient variability for the whole population. A serious limitation of the two-stage approach is the prerequisite of a rich and balanced dataset for each patient [139]. Furthermore, only accounting for one level of variability will lead to an overestimation of interpatient variability. The nonlinear mixed-effects (NLME) modelling approach does not have the these limitations [139]. It analyses the data of all individuals simultaneously and describes the central tendencies within a population while quantifying different levels of variability (e.g. residual unexplained variability, interpatient variability, intrapatient variability). Therefore, even unbalanced datasets including sparse data for some patients can be used for model development. Patient-specific characteristics that explain some of the observed variability can be integrated into NLME models as so-called 'covariates'. The integration of covariates enables the model to predict typical concentrations for subgroups of patients with specific patient characteristics and forms the foundation for subsequent simulation-based investigations e.g. dosing optimisations [140,141].

Because of the described advantages, the NLME approach was used primarily in the presented work and is further explained in detail in section 2.3.

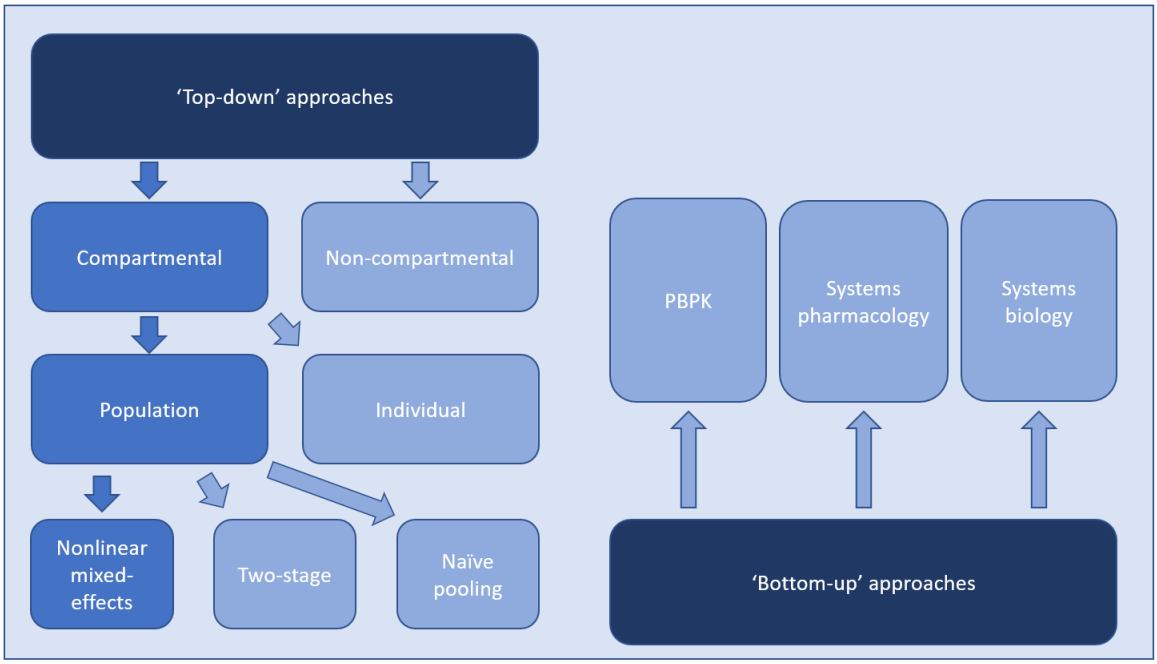

Figure 2.1: Overview of pharmacometric methods categorised into 'top-down' and 'bottom-up' approaches.
Abbreviations: *PBPK:* Physiologically based pharmacokinetics.

2.2 Data management and exploratory data analysis

The basis of every pharmacometric analysis is the underlying data set. It can originate from different sources (e.g clinical studies, clinical routine) and include different types of information (e.g. drug measurements in different matrices, patient-specific data). Data management and the exploratory data analysis are crucial steps in a successful pharmacometric analysis providing reliable results.

2.2.1 Dataset generation

For pharmacometric analyses, different software can be used, all of them requiring a specific structure of the investigated dataset. NONMEM was the main software used for modelling in the presented thesis and therefore the dataset requirements described in the following were applied to be compatible with using this software. The data of each individual patient included in the analysis needed to be combined in one dataset [142,143]. Within this dataset, data originating form one patient needed to be contiguous and arranged chronologically. Furthermore, NONMEM-specific data items had to be used (e.g. required data items: ID= individual identifier, DV=dependent variable) and non-numerical entries were not supported [142,143]. Datasets corresponding to the required dataset structure were generated from clinical study data received as Microsoft Excel files using the R/RStudio software environment. Missing data for planned covariate observations was imputed following different strategies depending on the availability of data before and after the missing information [144–146]:

1. Data values available both before and after the missing time point:
    a. Last observation carried forward: Imputation of the last available data point
    b. Next observation carried backwards: Imputation of the next available data point
    c. Linear interpolation: Imputation of the value derived from linear interpolation (Formula: see 5.3)
2. Data values only available before the missing time point:
    a. Last observation carried forward: Imputation of the last available data point
3. Data values only available after the missing time point:
    a. Next observation carried backwards: Imputation of the next available data point

Patient characteristics that might have an influence on the PK of a drug had been collected less frequently (e.g. once per day) than the dependent variable. Consequently, to include patient characteristics as time-dependent continuous covariates (e.g. creatinine clearance), additional time

points between the planned observations needed to be calculated. For this interpolation, the same methods were used than for missing planned observations.

2.2.2 Dataset checkout

Both during data collection and dataset generation errors may occur and negatively affect the quality of the data and every subsequent analysis. Therefore, a detailed examination of the dataset prior to model development is necessary. To evaluate the dataset for plausibility and completeness, different dataset quality check procedures were performed [143]. In ‘index plots’ each data item was plotted versus the ID, not only revealing missing and implausible data but also giving a first impression of the characteristics of the dataset. ‘Cross column checks’ were used to confirm plausible combinations of dataset items.

2.2.3 Exploratory data analysis

To get a first impression of the patient population in the dataset and to inform the model development strategy, an extensive exploratory data analysis was carried out prior to model development [143]. The numerical and graphical output (e.g. histograms) of statistical analyses were used to describe distributional characteristics of the data and to identify possible trends and relationships (Section 5.3). The focus of an additional graphical analysis was twofold. First, by visualising the concentration-time profiles in a semi-logarithmic plot, the number of disposition phases were identifiable and helped to select potential model structures. Second, possible trends between the dependent variable (e.g. drug concentration) and independent variables (e.g. patient characteristics) could be detected and marked for further analysis during the (covariate) model development.

2.3 Nonlinear mixed-effects modelling

As described in section 2.1, the NLME modelling approach allows a simultaneous analysis of data from all individuals in a population. 'Nonlinear' refers to the nonlinear functions characterising the relationships between the dependent variable (e.g. drug concentration) and the independent variables (e.g. time, dose) via the model structure and the estimated model parameters (e.g. volume of distribution). The term 'mixed-effects' is indicating the simultaneous estimation of two different types of parameters. Random-effect parameters quantify the variability observed in the data, while fixed-effect parameters are assumed to be constant in the population. In the following section, the components of NLME models, the parameter estimation process and evaluation of and discrimination between NLME models will be introduced.

2.3.1 Model components

A full NLME model consists of two components: the base model comprising (i) the structural submodel and (ii) the statistical submodel and the covariate submodel (Figure 2.2). In this section, a general overview of the submodels is provided.

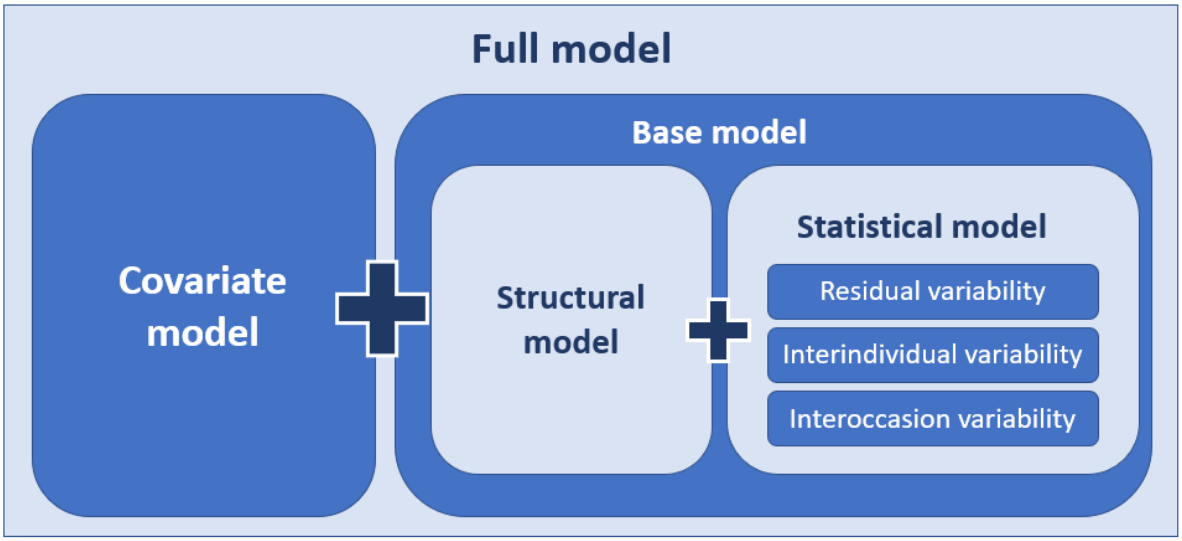

Figure 2.2: The two elements (base model and covariate model) of a full nonlinear mixed-effects model.

2.3.1.1 Structural submodel

The structural submodel described the general link and 'central tendency' between the dependent and independent variable of the model. In the case of PK data, the change in drug concentration (dependent variable) was characterised over time (independent variable) using a compartmental approach and a system of ordinary differential equations (ODEs). Exemplified for a one-compartment model (first-order elimination) and a i.v. dose the amount (A) of drug over time (t) can be described based on the two fixed-effects parameters clearance (CL) and volume of distribution (V) using the following ODE (Eq. 2.1).

$$\frac{dA(t)}{dt} = -\frac{CL}{V} \cdot A(t) \qquad \text{(Eq.2.1)}$$

The drug concentration (C) over time (t) is:

$$C(t) = \frac{A(t)}{V} \qquad \text{(Eq.2.2)}$$

For the simple case of a one-compartment model and a single i.v. bolus dose the ODE system can be solved and expressed as an exponential equation (Eq. 2.3):

$$C(t) = \frac{D}{V} \cdot e^{-\frac{\theta_{CL}}{\theta_V} \cdot t} \qquad \text{(Eq.2.3)}$$

In this case, the drug concentration (C) is a function of time (t), the two fixed effects PK parameters volume of distribution (θ_V) and clearance (θ_{CL}) and dose (D).

Assuming there is no discrepancy between model predictions and observations, the structural model can be mathematically represented in a more general way (Eq 2.4).

$$Y_{ij} = f\left(\emptyset_i, x_{ij}\right) \qquad \text{(Eq.2.4)}$$

The nonlinear function (f) represents the structural model describing the dependent variable (Y) of the i^{th} individual and j^{th} observation. It depends on the vector of structural model parameters of the i^{th} individual $\emptyset_i$ (e.g. volume of distribution, clearance) and the known study design variables x_{ij} (e.g. sampling time, dose, infusion duration).

2.3.1.2 Statistical submodel

Different levels of variability observed in the data were described and quantified by the statistical submodel. Depending on the available data, interindividual and interoccasion variability in model parameters and residual unexplained variability in the dependent variable were included. In combination with the structural model, the statistical model allowed the description of the individual behaviour of the dependent variable.

Interindividual variability

Unexplained deviations of the individual parameter value (Empirical Bayes estimate, EBE) from the population parameter value were quantified by the interindividual variability (IIV). To prevent negative and therefore physiologically implausible parameter values the IIV in PK models was implemented using an exponential relationship (Eq. 2.5.)

$$\emptyset_{ik} = \emptyset_k \cdot e^{\eta_{ik}} \qquad \eta_k \sim N\left(0, \omega_k^2\right) \tag{Eq.2.5}$$

The structural model parameter of the i^{th} individual and the k^{th} parameter ($\emptyset_{ik}$) was characterised by the population value for the k^{th} parameter and the influence of the individual patient ($e^{\eta_{ik}}$). The random effects parameters of all individuals (η_k) were assumed to follow a normal distribution with a mean of zero and the estimated random-effects parameter ω_k^2 as variance. Due to the assumed normal distribution of the random-effects parameters and their exponential implementation in the model, model parameters were log-normal distributed.

In addition to the variance of the random-effect parameters, the covariance between random-effect parameters on different structural parameters was estimated. In the omega matrix (Ω) (Eq. 2.6. example with three IIV parameters), the variances (ω_k^2) of the parameters $k = 1,2,3$ are displayed as diagonal elements while the off-diagonal elements represent the covariances between the corresponding variances.

$$\Omega = \begin{bmatrix} \omega_{1,1}^2 & & \\ \omega_{1,2} & \omega_{2,2}^2 & \\ \omega_{1,3} & \omega_{2,3} & \omega_{3,3}^2 \end{bmatrix} \tag{Eq.2.6}$$

For easier interpretation of random-effect parameters, the variance was converted to the coefficient of variation (CV). In the case of log-normally distributed parameters, the CV was computed according to Eq. 2.7.

$$CV, \% = \sqrt{e^{\omega_k^2} - 1} \cdot 100 \qquad \text{(Eq.2.7)}$$

The covariance was reported as correlation coefficient ρ:

$$\rho_{1,2}, \% = \frac{cov\left(\omega_{1,1}^2, \omega_{2,2}^2\right)}{\sqrt{\omega_{1,1}^2} \cdot \sqrt{\omega_{2,2}^2}} \cdot 100 = \frac{\omega_{1,2}}{\sqrt{\omega_{1,1}^2} \cdot \sqrt{\omega_{2,2}^2}} \cdot 100 \qquad \text{(Eq.2.8)}$$

Interoccasion variability

As an additional level of variability, interoccasion variability (IOV) was included in the model if observations of the dependent variable were available for multiple occasions (e.g. separate dosing events). By including IOV, unexplained deviations of individual parameter values from the typical individual model parameter values could be quantified at each occasion. To prevent negative parameter values, the IOV was implemented on the model parameters using an exponential model (Eq 2.9.):

$$\emptyset_{ikq} = \emptyset_k \cdot e^{\eta_{ik} + \kappa_{ikq}} \qquad \eta_k \sim N\left(0, \omega_k^2\right) \quad \kappa_k \sim N\left(0, \pi_k^2\right) \qquad \text{(Eq.2.9)}$$

The structural model parameter of the i^{th} individual, the q^{th} occasion and the k^{th} parameter ($\emptyset_{ikq}$) is characterised by the population value for the k^{th} parameter, the influence of the individual patient ($e^{\eta_{ik}}$) and the impact of the occasion ($e^{\kappa_{ikq}}$). The random effects parameters of all individuals (η_k) and the random effects parameters of all individuals at all occasions (κ_k) were assumed to follow a normal distribution with a mean of zero and the estimated random-effects parameters ω_k^2 and π_k^2 as respective variances. Like the IIV, the IOV is usually reported as CV. Eq. 2.7 can be used to convert π_k^2.

Residual unexplained variability

Imprecision in the bioanalytical method used to measure the dependent variable (e.g. drug concentration), erroneous documentation, model misspecification or other factors can be sources of variability on the level of the dependent variable. To quantify the discrepancy between the predicted to the observed dependent variable, a residual unexplained variability (RUV) model was used (Eq 2.10).

$$Y_{ij} = f\left(\emptyset_i, x_{ij}\right) + \varepsilon_{ij} \qquad \varepsilon \sim N(0, \sigma^2) \qquad \text{(Eq.2.10)}$$

The deviation between the j^{th} observation of the i^{th} individual (Y_{ij}) and the model prediction ($f(\emptyset_i, x_{ij})$) is described by ε_{ij}. The random effects parameters ε_{ij} of all individuals i and at all observations j (ε) were assumed to follow a normal distribution with a mean of zero and the estimated random-effects parameter σ^2 as variance.

In NLME models, RUV is typically implemented as one out of three distinct models:

1. The additive RUV model (Eq.2.10) assumes the variance to be constant and independent of model predictions.
2. The proportional RUV model (Eq.2.11) assumes a proportional increase of the variance with increasing model predictions.
3. The 'combined RUV model' combines the additive and the proportional RUV models (Eq. 2.12). At lower predictions, the additive component and at higher predictions the proportional component has a higher impact on the overall combined RUV model.

$$Y_{ij} = f(\emptyset_i, x_{ij}) \cdot (1 + \varepsilon_{ij}) \qquad \varepsilon \sim N(0, \sigma^2) \tag{Eq.2.11}$$

$$\begin{aligned} Y_{ij} &= f(\emptyset_i, x_{ij}) \cdot (1 + \varepsilon_{prop,ij}) + \varepsilon_{add,ij} \\ \varepsilon_{prop,ij} &\sim N(0, \sigma^2_{prop}) \\ \varepsilon_{add,ij} &\sim N(0, \sigma^2_{add}) \end{aligned} \tag{Eq.2.12}$$

2.3.1.3 Covariate submodel

One key objective of pharmacometric modelling is to elucidate the observed and quantified variability using patient- and/or occasion-specific covariates. The implementation of covariates into the PK model is important to inform clinical relevant decisions for individual patients and is described by the following equation (Eq.2.13):

$$\phi_i = g(\Theta, Z_i) \qquad \text{(Eq.2.13)}$$

For the i^{th} individual the vector of the fixed-effects model parameters (ϕ_i) is defined by the covariate function g describing the relationship between the vector of the fixed parameters of the population (Θ) and the observed covariate values of the i^{th} individual (Z_i). Potential covariates are pre-selected based on prior knowledge and graphical evaluation. For the graphical evaluation, potential covariates are typically plotted vs. the structural model parameters of each individual.

Covariates are either characterised as categorical (e.g. sex) or continuous (e.g. creatinine clearance) and can be based on a single or multiple time-varying measurements per patient. Depending on the type of covariate different ways of implementation into the PK model are possible. The different options used to implement the effect of one covariate on the structural parameter θ_k are described for both categorical and continuous covariates.

Categorical covariates can be implemented using a fractional change model or by estimating separate parameters for each category. In Eq 2.14 a fractional change model with two categories (COV = 1,2) is presented:

$$\begin{aligned} IF\ (COV = 1)\text{:}\ \theta_{k,COV=1} &= \theta_k \\ ELSE\text{:}\ \theta_{k,COV=2} &= \theta_k \cdot\ (1 + \theta_Z) \end{aligned} \qquad \text{(Eq.2.14)}$$

The structural parameter in case of the - typically more frequently occurring - first covariate category (COV=1) is defined as θ_k. The fractional change of θ_k observed for the second category is quantified by θ_Z.

The effect of **continuous covariates** on structural parameters can for example be implemented as a linear or power relationship. Typically the effect is centred to the median covariate value or normalised to a reference value to enhance interpretability. In the presented examples, the covariate effect is centred to the median covariate value of the population (Z_{median}).

In a linear covariate model (Eq.2.15), the structural model parameter is linearly modified with increasing or decreasing covariate values:

$$g(\theta_{ik}, Z) = \theta_k \cdot \left(1 + \theta_Z \cdot (Z - Z_{median})\right) \quad \text{(Eq.2.15)}$$

For the the specific covariate value Z the k^{th} fixed-effects parameter (θ_k) is defined by the k^{th} fixed-effects parameter for the median covariate value in the population (Z_{median}) and the covariate effect θ_Z quantifying the change of θ_k for the deviation between the specific (Z) and the median covariate value (Z_{median}).

In a power covariate model (Eq.2.16) θ_{ik} is defined by the ratio between the individual (Z_i) and the median covariate value (Z_{median}) and the estimated coefficient parameter θ_Z:

$$g(\theta_{ik}, Z_i) = \theta_k \cdot \left(\frac{Z_i}{Z_{median}}\right)^{\theta_Z} \quad \text{(Eq.2.16)}$$

If the principle of allometry is applied in a PK model, body weight is implemented as a power covariate model and θ_Z is set to 0.75 for clearance parameters and to 1 for volume of distribution parameters [147,148].

The general mathematical equation for NLME models combines the three submodels (Eq 2.17):

$$Y_{ij} = f\left(g(\Theta_i, Z_i), \eta_i, \kappa_i, x_{ij}, \varepsilon_{ij}\right) \quad \text{(Eq.2.17)}$$

2.3.2 Parameter estimation

To identify the NLME model parameter estimates best describing the observed data, a maximum likelihood estimation approach was chosen (Eq. 2.18):

$$\sum \mathcal{L}_i(\theta, \omega^2, \sigma^2|Y_i) = \sum p(Y_i|\theta, \omega^2, \sigma^2) = \prod_{j=1}^{n} \mathcal{L}\left(\theta, \omega^2, \sigma^2|Y_{ij}\right) \qquad \text{(Eq.2.18)}$$

Given the parameters $\theta, \omega^2, \sigma^2$, the individual contribution to the likelihood of observing the data Y_i for the i^{th} individual is $\mathcal{L}_i$. The corresponding probability density function is denoted by the variable p.

Due to the advantages of sums over products in maximisation or minimisation problems, the log of likelihoods $\mathcal{LL}$ was used to compute maximum likelihood estimates. In NONMEM –the software used for all parameter estimations presented in this thesis- the 'objective function value (OFV)' is defined as minus twice the natural logarithm of the likelihood (Eq. 2.19.). During parameter estimation, the OFV is minimised and therefore the model parameters with the lowest OFV are the maximum likelihood estimates.

$$OFV = -2\mathcal{LL} = -2 \cdot log\left(\mathcal{L}(\theta, \omega^2, \sigma^2|Y)\right) = \sum_{i=1}^{n} -2 \cdot log\left(\mathcal{L}_i(\theta, \omega^2, \sigma^2|Y_i)\right) \qquad \text{(Eq.2.19)}$$

For more complex NLME models, the likelihood cannot be computed analytically and consequently needs to be approximated numerically. In the projects presented in this thesis, the first-order conditional expectation method including interaction (FOCE+I) was used for the approximation in NONMEM.

In general, the maximum likelihood estimates are determined employing an iterative process. The selected algorithm starts by evaluating the OFV for the provided initial parameter estimates. Then, the model parameters are updated in the direction of decreasing OFV values until certain convergence criteria are met and the minimum OFV, i.e. the maximum likelihood, is found. The FOCE method is based on a gradient linearisation algorithm applying Laplace transformation and Taylor series expansion and the additional interaction method allows interaction between interindividual random-effects (η) and residual random-effects (ε) parameters.

In addition to the population parameters provided by the estimation method, individual parameter estimates (EBEs) are calculated in a second *post-hoc* estimation. If the FOCE method is used, EBEs

are estimated after each iteration based on the minimisation of the Bayes objective function (Eq. 2.20):

$$OFV_{Bayes} = \sum_{k=1}^{m} \frac{\left(\theta_{k,EBE} - \theta_{k,pop}\right)^2}{\omega_k^2} + \sum_{j=1}^{n} \frac{\left(Y_{ij} - \hat{Y}_{lj}\right)^2}{\sigma^2} \qquad \text{(Eq.2.20)}$$

The Bayes objective function (OFV_{Bayes}) is determined by the sum of the squared deviations of the k^{th} individual parameter ($\theta_{k,EBE}$) from the k^{th} population parameter ($\theta_{k,pop}$) weighted by the k^{th} interindividual random-effects parameter (ω_k^2) and the sum of the squared deviations of the observed data for the i^{th} individual on the j^{th} observation from the respective predicted data ($\hat{Y}_{lj}$) weighted by the residual random-effects parameter (σ^2).

2.3.3 Model evaluation and discrimination

The aim of PK model development is to ultimately obtain a model that adequately describes the observed data and can be used to gain information about the research question (e.g. investigate different dosing regimens and their probability of target attainment in a specific patient). To obtain the model best fitting, i.e. predicting, the data, a thorough model evaluation employing various evaluation techniques throughout the model development process is necessary. Based on their characteristics, model evaluation techniques can be classified into different categories:

- **Dataset:** '*External'* evaluation techniques are based on a dataset independent of the dataset used in model development while '*internal'* evaluation techniques rely on the dataset used during model development.
- **Representation:** '*Numerical'* evaluation techniques quantify the model fit (e.g. precision of parameter estimates) as numerical values while '*graphical'* evaluation techniques help to assess model (mis)specifications based on graphical outputs.

Evaluation techniques important in the context of this thesis are presented and discussed in more detailed in the following.

2.3.3.1 Goodness-of-fit plots

Goodness of fit (GOF) plots are graphical evaluation plots that were used to assess the appropriateness of a NLME model. Both on the population and the individual level the observed dependent variable (observations e.g. drug concentrations), the predicted dependent variable (prediction) and their deviation (residuals) were examined. Furthermore, the distributions of random effects parameters and EBEs were explored.

Observations vs. predictions

Both predictions based on the estimated population parameters (PRED) and on the estimated individual parameters (IPRED) were plotted against observations for the population, subgroups of the population and single individuals. Data points symmetrically scattered around the line of identity without systematic deviations indicated an appropriate structural submodel and the spread around the line of identity provided further information to assess the statistical submodel. For PRED vs. observation, a spread around the line of identity were expected while the data points in the IPRED vs. observation plot should be more narrowly distributed around the line of identity.

Residuals

For their graphical evaluation, residuals were weighted to enable interpretation independent of the absolute magnitude of the observations. All projects presented in this thesis employed the FOCE algorithm in NONMEM and therefore conditional weighted residuals (CWRES) were evaluated. The distribution of CWRES was assessed against both the independent variable (e.g. time) and the dependent variable (e.g. drug concentrations). Model misspecifications can be detected by an uneven distribution around zero and a high number of data points outside ± 2 standard deviations ($\sim 2.5^{th}$ - 97.5^{th} percentiles in a normal distribution).

Individually predicted concentration-time profiles

To identify inadequately described individuals and possible measurement errors on a sample level, the observations of each individual were plotted against the independent variable and overlayed with a continuous prediction, i.e. full concentration-time profile, based on both the population and the individual parameter estimates. The observations of the individual should be narrowly and evenly distributed around the individual prediction line while the population prediction will give an impression on how much the individual deviates from the central tendency of the model.

Distribution of random-effects

Histograms or density plots were used to investigate if the distribution of the individual-/occasion-specific random-effect parameters η and κ follow the assumed normal distribution. The mean of the distribution should not significantly differ from 0 and the width of the distribution indicated the

magnitude of the variability. Deviations from a normal distribution (like a binormal distribution) could indicate distinct subgroups in the population and need to be further investigated.

2.3.3.2 Parameter precision, accuracy and identifiability

Different methods were used to assess parameter precision, accuracy and identifiability. Imprecise, inaccurate and unidentifiable parameter estimates are a strong indication for model misspecification or overparametrisation (e.g. the observed data is not able to inform all model parameters).

Parameter precision based on the variance-covariance matrix

Parameter precision can be calculated and assessed based on the variance-covariance matrix of the parameter estimation. In this case the standard errors (SE) of the model parameters are derived by taking the square root of the diagonal elements of the variance-covariance matrix. SE were reported as relative standard errors (RSE, Eq. 2.21 and Eq.2.22) to facilitate comparability and an easier interpretation. Random effects parameters were not reported as the estimated variance but as %CV. As a consequence, the RSE were also transformed into the approximate standard deviation scale (Eq. 2.23).

$$RSE_{\theta},\% = \frac{SE}{\theta} \cdot 100 \quad \text{(Eq.2.21)}$$

$$RSE_{\omega^2_{variance\ scale}},\% = \frac{SE_{\omega^2}}{\omega^2} \cdot 100 \quad \text{(Eq.2.22)}$$

$$RSE_{\omega^2_{standard\ deviation\ scale}},\% = \frac{SE_{\omega^2}}{2 \cdot \omega^2} \cdot 100 \quad \text{(Eq.2.23)}$$

Complementary formulas were used for other levels of random-effects parameters and all RSE reported in this thesis are on standard deviation scale.

Based on the SE of the k^{th} fixed effects-parameter SE_{θ_k} and assuming a normal distribution, the 95% CI can be calculated:

$$Lower\ limit\ of\ 95\%\ CI = \theta_k - \left(SE_{\theta_k} \cdot 1.96\right) \quad \text{(Eq.2.24)}$$

$$Upper\ limit\ of\ 95\%\ CI = \theta_k + \left(SE_{\theta_k} \cdot 1.96\right) \quad \text{(Eq.2.25)}$$

Parameter precision and accuracy based on a bootstrap

A bootstrap is an advanced evaluation technique used to assess parameter precision and accuracy without assuming an underlying distribution. In a non-parametric bootstrap, replicate datasets with the same number of individuals as the original dataset were created by repeated random sampling with replacement on the individual level. The number of replicates used in a bootstrap analysis to derive the CI for the parameter estimates is recommended to be >1000 [149]. For each of the replicate datasets the model parameters were estimated. The median of the new parameter estimates of the k^{th} fixed effects-parameter ($P_{bs,k}$) were used to assess the accuracy (bias) of the original parameter estimate ($P_{orig,k}$) (Eq. 2.26) while the precision of the parameters was evaluated by computing their 95% CI, i.e. the range between the 2.5th and 97.5th percentile of the new parameter estimates.

$$Relative\ bias, \% = \frac{P_{orig,k} - P_{bs,k}}{P_{orig,k}} \cdot 100 \quad \text{(Eq.2.26)}$$

In addition to precision and accuracy a bootstrap also provides information about the robustness of a model: the convergence rate was calculated as the percentage of successful parameter estimations in the replicated datasets.

Parameter stability and model robustness based on case deletion diagnostics

Case deletion diagnostics (also jackknife, leave-one-out technique or leverage analysis) is an advanced evaluation technique to assess parameter stability and model robustness. In PK modelling case deletion diagnostics were performed on an individual level to detect individuals with a substantial influence on parameter estimates. One-by-one each individual was excluded from the dataset and model parameters were estimated. If the exclusion of an individual lead to parameter estimates outside the 95% CI of the original parameter estimates, that individual was considered influential and a further investigation of the individual and its characteristics was performed.

Assessment of parameters based on shrinkage

Individual parameters (i.e. EBEs) tend to shrink towards the typical fixed-effects parameter values, if insufficient individual information is available. This behaviour is called shrinkage and elevated shrinkage values (>20%-30%) can lead to a misinterpretation of diagnostic plots based on EBEs. Shrinkage is quantified based on the standard deviation of the individual values of EBEs of η (SD_{EBE_η}) and the estimated variance of η (ω^2):

$$\eta - shrinkage = 1 - \frac{SD_{EBE_\eta}}{\sqrt{\omega^2}} \cdot 100 \quad \text{(Eq.2.27)}$$

Similarly the distribution of individual weighted residuals (IWRES) can shrink in the case of a sparse data situation. This so called ε-shrinkage is quantified based on the standard deviation of the IWRES:

$$\varepsilon - shrinkage = 1 - SD_{IWRES} \quad \text{(Eq.2.28)}$$

2.3.3.3 Visual predictive checks

Visual predictive checks (VPCs) were used to assess the ability of the model to predict the central tendency and variability of the observed data. For a VPC, a large number of stochastic simulations (typically n=1000) were performed and the 5th, 50th and 95th percentiles were calculated for both the simulated and the observed values. Next, the median and 95% CI of the percentiles of the simulated values were evaluated based on the percentiles of the observed values. VPCs can be stratified by e.g. specific patient characteristics to assess the predictive performance of the model in a patient subgroup. Furthermore, VPCs can be presented using a covariate as independent value to investigate the predictive performance across its range.

2.3.3.4 Prediction errors

The predictive performance of a model can numerically be assessed based on prediction errors (PE). Prediction errors were calculated as the difference between observed (Y_{ij}) and predicted dependent variable ($\hat{Y}_{ij}$) of the i^{th} individual at time point j (Eq. 2.29) and were reported either as absolute or relative values. The accuracy (bias) of the predicted dependent variable was evaluated using the mean or median of the prediction errors while the mean or median of the absolute prediction errors (APE; Eq. 2.30) was used as a measure of the observed model precision.

$$PE_{ij} = \hat{Y}_{ij} - Y_{ij} \quad \text{(Eq.2.29)}$$

$$APE_{ij} = |PE_{ij}| \qquad \text{(Eq.2.30)}$$

PE and APE can be calculated for a specific subset of individuals to investigate the model performance in this group.

2.3.3.5 Objective function value and Akaike information criterion

During the model development process it is necessary to discriminate between different models and select the model best describing/predicting the observed data. The likelihood ratio test (LRT) was used to statistically compare two competing nested models. Two models were considered nested if one model (M_1) is a subset of the other model (M_2), i.e. if it is possible to reduce M_2 to M_1 by setting one or more parameters to the null hypotheses value(s). For the LRT the difference between the OFV values of two nested models was calculated, since the OFV is defined as minus twice the logarithm of the likelihood (see 2.3.2):

$$LR = OFV_{M2} - OFV_{M1} \qquad LR \sim X^2(df = \Delta n_p) \qquad \text{(Eq.2.31)}$$

The likelihood ratio (LR) was assumed to be chi-squared (x^2) distributed. The degrees of freedom (df) are equal to the difference in number of parameters between the two nested models (Δn_p). To conclude if one of the two models provided a significantly improved description of the data the LR was compared to the defined test statistic. The defined test statistic (Table 2.1) was dependent on the significance level α and the degrees of freedom df.

Table 2.1: Chi-squared (x^2) value for selected degrees of freedom (df) and significant levels (α).

df	**x^2 value (=test statistic)**		
	$\alpha = 0.1$	$\alpha = 0.05$	$\alpha = 0.01$
1	2.71	3.84	6.64
2	4.60	5.99	9.21
3	6.25	7.82	11.3

The Akaike information criterion (AIC) can also be used to compare non-nested models. The AIC is defined as minus twice the logarithm of the likelihood ($-2LL$) plus two times the total number of model parameters (n_p) (Eq. 2.32):

$$AIC = -2LL + 2 \cdot n_p \quad \text{(Eq.2.32)}$$

The addition of two times the total number of model parameters to the OFV can be considered as a penalising term for additional parameters. The model with a lower AIC value was deemed to better describe/predict the observed data.

2.3.4 Model application

2.3.4.1 Simulations

Simulations based on the developed NLME model are a major strength of this quantitative approach: simulations allowed to explore and visualise the relationship between patient, disease and drug and to address specific research questions [107]. Questions relevant for therapeutic decision making like '*Which dosing regimen results in adequate drug exposure for a patient with a creatinine clearance of 60 mL/min?*' were answered and potentially will help to improve drug therapy. Simulations are classified as deterministic (non-stochastic) or stochastic based on the inclusion of random-effects parameters in the simulation [143].

Deterministic simulations

In deterministic simulations, random-effects parameters were not considered and therefore only the typical behaviour of the dependent variable was predicted. Deterministic simulations of PK models predicted the typical concentration-time profile for a given dosing regimen and covariate combination. They were used for a first exploratory analysis on the effect of changing covariates or dosing regimen, since they are (i) easy to visualise and (ii) need less computational power and consequently are faster than stochastic simulations.

Stochastic simulations

For stochastic simulations (in the context of this thesis Monte Carlo (MC) simulations), all or some random-effects parameters of the model were considered and therefore the behaviour of the dependent variable for a population of individuals could be predicted. Which random-effects parameters (i.e. IIV, IOV and/or RUV) were included in the stochastic simulations varied depending

on the research question that was addressed. By sampling from the respective variability distributions, a large population of virtual patients (e.g. n = 1000) was generated and used for the simulation. If IOV was included on a parameter, the individual parameter of a virtual patient varied between each simulated occasion and the inclusion of RUV added variability on the sample level. Stochastic simulations were used to assess and visualize the variability in drug exposure following the same dosing regimen in a population.

2.3.4.2 Probability of target attainment and cumulative fraction of response analysis

A powerful tool to assess the adequacy of dosing regimens is the probability of target attainment (PTA) analysis. For a PTA analysis, stochastic simulations were used to generate individual concentration-time predictions for a virtual population of patients (typically n = 1000). The patient individual concentration-time predictions were then evaluated with regards to a predefined PK/PD target (e.g. in the case of time-dependent antibiotic drugs 100%$fT_{>MIC}$) and the PTA of the population was calculated based on the percentage of patients achieving the investigated target [150]. A PTA analysis cannot only help to identify patient subgroups at risk of suboptimal drug exposure after receiving the standard dosing regimen, but also facilitates the systematic investigation of alternative dosing regimens to ultimately identify the most suitable dosing regimen. For the selection of an appropriate antibiotic dosing regimen, a PTA of 90% was considered as adequate therapy by the EMA [151]. The PK/PD target for antibiotic drugs usually include the pathogen-specific MIC. Therefore the PTA of antibiotic drugs was assessed over a range of clinically relevant MIC values.

If the MIC of an individual pathogen was unknown, the cumulative fraction of response (CFR) could be calculated based on the PTA of a dosing regimen for different MIC values and the MIC distribution of the species (Eq.2.33)[43,152]:

$$CFR = \sum_{i=1}^{n} PTA_i \cdot f_i \qquad \text{(Eq.2.33)}$$

The index of MIC values of a population of pathogens is represented by i, the PTA for each MIC value by PTA_i and the fraction of the respective MIC value in the MIC distribution by f_i. For the CFR calculation, commonly MIC distributions collected in cross-national databases (e.g. EUCAST) were used but locally observed distributions can be used as well.

2.3.4.3 Bayesian forecasting: Maximum a-posteriori estimates and normal approximation

The Bayesian approach can be used to derive the individual parameter estimates (posterior) based on a population model (prior) and patient specific observations of the dependent variable [153,154]. In the case of PK modelling, the Bayesian approach enabled both the assessment of drug exposure (e.g. area under the concentration-time profile, time of the drug concentration above a threshold) for already administered and planned dosing regimens. It therefore is a powerful tool to improve drug therapy on an individual patient level. The maximum a-posteriori (MAP) estimates for each individual are the mode of the posterior parameter distributions and computed by minimising the Bayes objective function (OFV_{Bayes}, see 2.3.2, Eq. 2.20)[126].

As point estimates, the MAP parameter estimates do not contain any information about the uncertainty included in the estimation. To overcome this limitation, the posterior parameter distribution $\left(p(\cdot\,|y_{1:n})\right)$ can be approximated by a normal distribution centred at the MAP estimate [126]. The variance of the normal distribution is approximated by the curvature of the mode:

$$p(\cdot\,|y_{1:n}) \approx \mathcal{N}\left(\hat{\theta}_n^{\,MAP},\, I^{-1}\left(\hat{\theta}_n^{\,MAP}\right)\right) \qquad \text{(Eq.2.33)}$$

Here I denotes the observed Fisher Information Matrix.

2.4 Software

The software and key functionalities used in the presented thesis are summarised in Table 2.2 and Table 2.3, respectively.

Table 2.2 Software used in the presented projects.

Software	Version	Reference	Project
NONMEM®	7.4.1	Icon Development Solutions, Ellicott City, MD, USA. (www.iconplc.com/innovation/nonmem)	I, II, III
PsN	4.7.0	Uppsala University, Uppsala, Sweden. (uupharmacometrics.github.io/PsN)[155]	I, II, III
Pirana	2.9.6-2.9.9	Pirana Software & Consulting BV (www.pirana-software.com)[156]	I, II, III
R	3.6.3-3.5.0	The project for statistical computing. Vienna, Austria. (www.CRAN.R-project.org)	I, II, III
RStudio	1.1.447-1.3.959	Integrated development environment for R, Boston, MA. (www.rstudio.org)	I, II, III
Microsoft Office Excel®	2109	Microsoft Corporation, Redmond, Washington, USA.	III

Abbreviations: PsN: Pearl speaks NONMEM.

Table 2.3 Key functionalities and packages.

Software	Functionalities, packages	Project
PsN	vpc functionality	I, II, III
	Bootstrap functionality	I, II, III
	sse functionality	II
R	ggplot2 package	I, II, III
	Xpose4 package	I, II, III
	mrgsolve package	I, II, III
	shiny package	II
	TDMxR package [157]	II
	npde package [158]	III
Microsoft Office Excel®	Visual basics for application	III

Abbreviations: *vpc*: visual predictive check, *sse*: stochastic simulation and estimation

For computationally intensive activities the high performance computing cluster ‘Curta’ of the Freie Universität Berlin was employed (https://www.fu-berlin.de/sites/high-performance-computing/index.html) [159].

2.5 Project I: Characterising meropenem adsorption abilities at the cytokine adsorber CytoSorb®

2.5.1 Objectives and research strategy

The objective of this project was to (i) quantify a potential meropenem adsorption at the CytoSorb® filter and (ii) evaluate if meropenem dosing needs to be intensified during CytoSorb® therapy.

To achieve this objective a NLME modelling and simulation approach was chosen. A population pharmacokinetic model was developed leveraging therapeutic drug monitoring data in critically ill patients undergoing continuous veno-venous haemodialysis with and without CytoSorb® treatment and three distinct approaches to assess if clearance differed without or during CytoSorb® treatment were applied: (i) quantification of a possible proportional increase in clearance during CytoSorb® treatment (ii) investigation of (non)saturable adsorption at the CytoSorb® filter using different adsorption submodels and (iii) evaluating the predictive performance for concentrations during CytoSorb® treatment by a PK model developed excluding samples collected during CytoSorb® treatment.

2.5.2 Database

This analysis was based on a subset of critically ill patients from two prospective observational studies conducted at University Hospital, Ludwigs-Maximilian-University (LMU) Munich, Germany (ClinicalTrials.gov identifiers NCT01793012 and NCT03985605). Both study protocols were approved by the Institutional Review Board of the Medical Faculty of the LMU Munich (registration number NCT01793012: 428-12 and NCT03985605: 18-578). All patients on continuous veno-venous haemodialysis (CVVHD) or haemodiafiltration (CVVHDF) with at least two serum meropenem samples (n=25) in the same dosing interval were included. CytoSorb® and dialysis treatment was initiated and controlled by the responsible physician and the CytoSorb® cartridge was installed in predialyser position. In both studies meropenem was administered as infusion according to the assessment of the responsible physician. During NCT01793012, serum samples were collected in a dense-sampling scheme without predefined schedule, but only 1 of the 6 patients included in this analysis received CytoSorb® treatment. NCT03985605 included 19 patients receiving CytoSorb® treatments, but a sparse-sampling scheme was performed. Blood samples were immediately sent to the laboratory (< 30 min) and centrifuged at 2000 g for 10 min. During NCT01793012, serum samples were then stored at -80°C until total meropenem serum concentrations were quantified within 4 weeks. During NCT03985605, samples were frozen overnight at -20°C and analysed once a day. In both studies meropenem serum concentrations were quantified according to validated LC-MS/MS methods [160,161]. Demographic patient data (sex, age, weight) and laboratory data (serum albumin concentration, serum creatinine concentration) were collected daily.

2.5.3 Population pharmacokinetic modelling

To accurately quantify the potential effect of CytoSorb® treatment on meropenem concentrations, the model development strategy was divided into two stages: First, a basis PK model was developed, characterising the pharmacokinetic variability and investigating the effect of patient and dialysis characteristics — other than CytoSorb® treatment — on meropenem PK. Second, the effect of CytoSorb® treatment on meropenem exposure was investigated using three distinct approaches. Data from all patients of both studies were analysed collectively to ensure precise PK parameter estimates in the absence of CytoSorb® treatment (major contribution by NCT01793012) and an adequate number of meropenem concentrations during CytoSorb® treatment (major contribution by NCT03985605).

2.5.3.1 Basis PK model development

Based on the graphical analysis 1- and 2-compartmental PK disposition models with zero-order input and first-order elimination were investigated. Interindividual variability was implemented in a stepwise process using exponential models. Different residual variability models (additive, proportional and combined) were considered. Models were evaluated and discriminated based on the OFV, precision of the parameter estimates, GOF plots and VPCs (see 2.3.3). Due to the large variability in dosing regimens, prediction-corrected VPCs were used to account for the variability in observed concentrations [162]. Patient and dialysis characteristics — other than CytoSorb® treatment — potentially influencing meropenem PK were investigated as possible covariates on the volume of distribution and clearance parameters. Candidates for the covariate analysis were pre-selected based on graphical exploration and literature information. Covariate selection was based on statistical significance (alpha level ≤ 0.05, i.e. $\Delta OFV < -3.84$ for the integration of a single covariate), the reduction in unexplained and interindividual variability, higher precision of parameter estimates and biological plausibility (see 2.3.1.3).

2.5.3.2 Effect of CytoSorb® treatment on meropenem exposure

Three distinct approaches were chosen to investigate the effect of CytoSorb® treatment on meropenem exposure.

Approach 1: CytoSorb® treatment as categorical covariate on clearance

The potential effect of CytoSorb® treatment on clearance was investigated by means of a categorical covariate (i.e. meropenem concentrations while on or off CytoSorb® treatment) implemented as proportional clearance increase during CytoSorb® treatment (see 2.3.1.3). A statistically significant drop in objective function value (ΔOFV < -3.84, df=1) and a precise and plausible parameter estimate for the parameter characterising the covariate effect would indicate an change in clearance and thus adsorption of meropenem at the CytoSorb® filter. Furthermore, an increase of clearance >10% during CytoSorb® treatment was defined as clinically relevant adsorption.

Approach 2: Adsorption submodels

Three possible adsorption models of meropenem at the CytoSorb® filter were examined by implementing an additional elimination pathway associated with the CytoSorb® filter: A constant adsorption, a linear decrease in adsorption and a hyperbolic decrease in adsorption. In the constant adsorption model (Eq.2.46) the meropenem clearance via adsorption by the CytoSorb® filter ($CL_{Cytosorb}$) was dependent on the central volume of distribution (V_1) and the adsorption rate constant ($k_{Cytosorb}$). In the linear decrease (Eq.2.47) and the hyperbolic decrease models (Eq.2.48), the adsorption was linked to the maximum adsorption rate constant (k_{max}), the drug amount already adsorbed at the filter ($A_{Cytosorb}(t)$) and either the maximum drug amount that can be adsorbed (A_{max}) or the drug amount linked to the half of the maximum adsorption capacity (A_{50}) for an assumed maximum reduction in adsorption rate of 100%. In Figure 2.3 the impact of the three adsorption models on the total clearance of a patient is illustrated.

$$CL_{Cytosorb} = V_1 \cdot k_{Cytosorb} \quad \text{(Eq.2.46)}$$

$$CL_{Cytosorb}(t) = V_1 \cdot k_{max} \cdot \left(1 - \frac{A_{Cytosorb}(t)}{A_{max}}\right) \quad \text{(Eq.2.47)}$$

$$CL_{Cytosorb}(t) = V_1 \cdot k_{max} \cdot \left(1 - \frac{A_{Cytosorb}(t)}{A_{Cytosorb}(t) + A_{50}}\right) \quad \text{(Eq.2.48)}$$

A statistically significant drop in objective function value (i.e. ΔOFV ≤ -3.84 for the constant adsorption and ΔOFV ≤ -5.99 for the linear and hyperbolic decrease of adsorption) and precise and plausible parameter estimates would indicate an adsorption of meropenem at the CytoSorb® filter. Furthermore, a fraction of > 10% of the total meropenem clearance by the maximum $CL_{Cytosorb}$ was defined as clinically relevant adsorption.

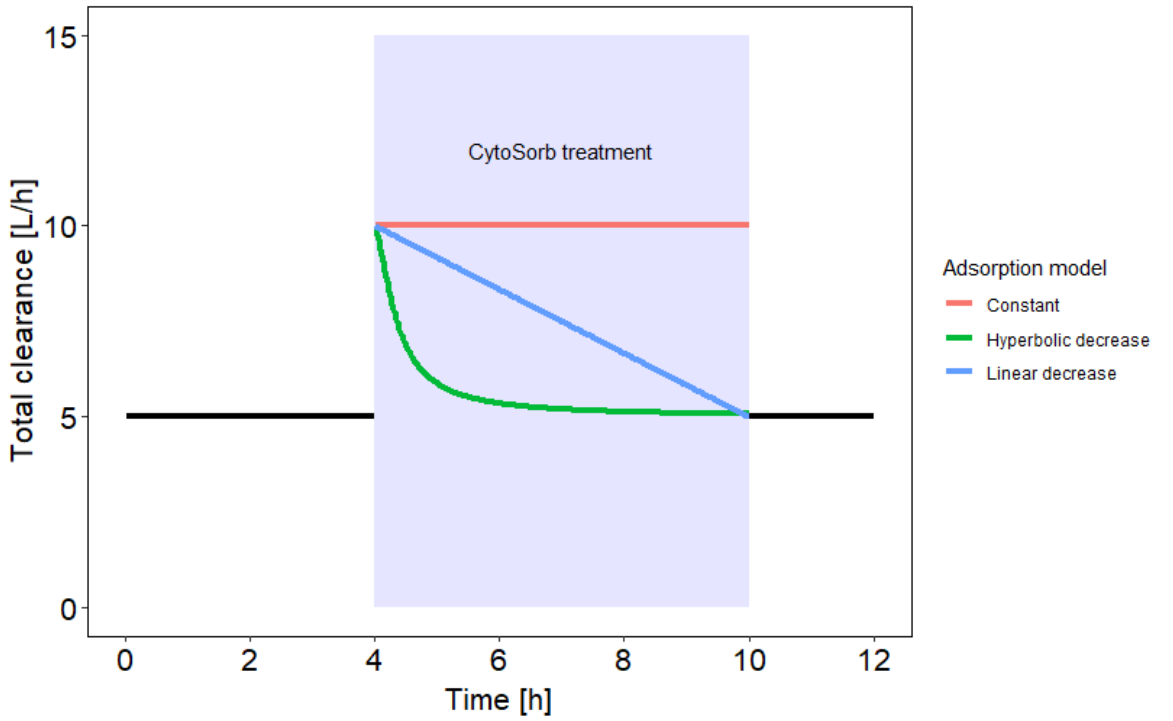

Figure 2.3: Graphical illustration of the different possible adsorption kinetics of meropenem at the CytoSorb® filter investigated using the three different adsorption models.
In the illustration a clearance of 5 L/h prior to CytoSorb® treatment is assumed. During implementation of the CytoSorb® filter the constant adsorption model describes a constant increase of the clearance to 10 L/h (red line) and both the linear (blue line) and hyperbolic (green line) adsorption models describe a temporary increase in clearance falling with increasing amounts of meropenem adsoprt at the filter.

Approach 3: Re-estimation of the model parameters excluding samples during CytoSorb® treatment

The parameters of the final basis PK model (not yet including any parameters describing the effect of CytoSorb® therapy) were re-estimated excluding drug measurements during CytoSorb® treatment. The resulting EBEs (individual parameter estimates, see 2.3.2) and their uncertainty for each patient were used to stochastically simulate (n=1000) the observed meropenem concentrations during CytoSorb® therapy. Per patient, the median predicted concentration-time profile and the 50% prediction intervals were plotted together with all individual observed concentrations to assess for systematic deviations between samples collected during and outside of CytoSorb® treatment. Furthermore, the median prediction error was calculated to assess the bias of the predictions. A substantial bias (> 5%) in predictions using the re-estimated model (i.e. that was based on non-CytoSorb® concentrations) to overpredict the concentrations during CytoSorb® therapy on the patient or population level was considered to indicate a clinically relevant adsorption of meropenem.

2.6 Project II: Utilising pharmacokinetic models to improve meropenem and piperacillin dosing

2.6.1 Objectives and research strategy

The objectives of this project were to (i) assess and evaluate the current meropenem and piperacillin/tazobactam dosing decisions at the Charité-Universitätzmedizin Berlin, to (ii) develop model-informed dosing tools optimised for integration into clinical practices at Charitè-Universitätsmedizin Berlin and to (iii) integrate and assess the developed dosing tools in clinical routine use.

To achieve this objective a clinical study for piperacillin/tazobactam and meropenem was initiated as a coordinated intervention of the antimicrobial stewardship (AMS) team at Charité-Universitätsmedizin Berlin. The study was separated into 3 stages. In stage I, current antibiotic dosing practices in two intensive care units were assessed. Furthermore, the data collected in stage I was used to select and evaluate published NLME models. A model-informed tabular dosing tool for initial antibiotic therapy and an interactive dosing software were developed based on the evaluated NLME models and assessed during clinical practice in stage II and stage III of the study, respectively.

2.6.2 Clinical study design

This study was developed as a monocentric, prospective, observational study planned and carried out in two intensive care units (Department of Infectious Diseases and Respiratory Medicine; Department of Surgery) at Charité-Universitätsmedizin Berlin. The study protocol was approved by the local institutional review board (Charité Ethics Committee, application number: EA4/053/19). Patients diagnosed with severe infections susceptible for antibiotic therapy either with meropenem or the drug combination piperacillin/tazobactam were included in the study. For both treatment options the study was separated into distinct stages assessing antibiotic treatment prior to and after the implementation of model-informed dosing tools (Figure 2.4). . For both drugs, 'stage I' focused on the assessment of 'standard practice', i.e. the current antibiotic treatment (see 2.6.5). In 'stage II' a model-informed tabular dosing tool providing individual dosing suggestions for initial meropenem therapy was to be developed and applied (see 2.6.6). For piperacillin/tazobactam treatment no changes compared to 'stage I' were made during 'stage II'. For 'stage III' of the study, an interactive web application was to be developed deriving the optimal individual initial dose for both drugs and integrating individual concentration measurements to update subsequent dosing suggestions (see 2.6.7). Overall, while one model informed-dosing tool was developed, implemented and its effect investigated for piperacillin/tazobactam treatment, two different model-informed dosing tools were developed, implemented and investigated for meropenem treatment

Throughout the study antibiotic drug concentrations were measured by Labor Berlin (Labor Berlin – Charité Vivantes GmbH, Berlin) using high-performance liquid chromatography coupled with tandem mass spectrometry. Within 1 hour after blood sample collection samples were sent to the laboratory, centrifuged and serum stored at −20 °C until drug concentrations were determined. The validation of the bioanalytical method revealed good analytical performance (Meropenem: inaccuracy $< \pm 5.9\%$ relative error, imprecision $\leq 6.3\%$ coefficient of variation, calibration range 2-30 µg/mL; Piperacillin: inaccuracy $< \pm 5.3\%$ relative error, imprecision $\leq 5.0\%$ coefficient of variation, calibration range 20-120 µg/mL). Serum concentrations outside the calibration range were diluted and re-evaluated. The results of the concentration measurement were available to the attending physician within 24 hours after sampling.

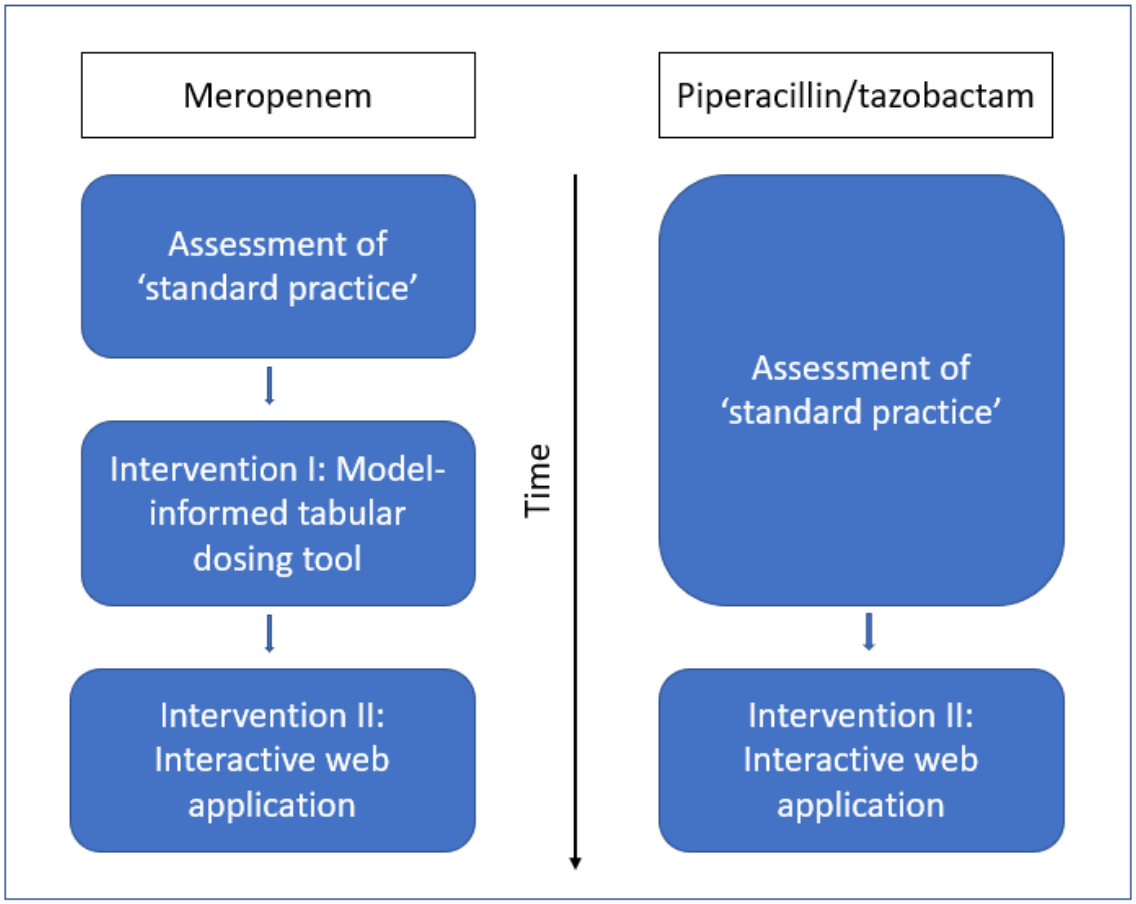

Figure 2.4: Stages of the clinical study at Charitè-Universitätsmedizin Berlin.
For meropenem two interventions (model-informed tabular dosing tool and interactive web application) were planned while only one intervention (interactive web application) was planned for piperacillin/tazobactam.

2.6.3 Pharmacokinetic/pharmacodynamic targets

Based on current literature evidence [57,73,74] and after discussion with the antimicrobial stewardship team, the PK/PD target for critically ill patients receiving short-time or prolonged infusions was defined as 100%$fT_{>MIC}$ whereas for patients receiving continuous infusions it was defined as 100%$fT_{>4*MIC}$ to prevent steady state antibiotic concentrations within the mutant selection window [163,164]. Given the non-achievability of 100%$T_{>MIC}$ on the first day of therapy, attainment of 98%$T_{>MIC}$/98%$T_{>4*MIC}$ was assessed in all simulation-based analysis. Due to the low (~2%) protein binding of meropenem total concentrations were evaluated for meropenem [66,165], while unbound piperacillin concentrations were calculated based on a literature reported fraction unbound (f_u) of 91% in critically ill patients [166]. To assess target attainment based on a single observed minimum drug concentration and to limit toxicities arising from high minimum drug concentrations an additional target was introduced for the evaluation of the collected data: If a MIC value can be determined the target range for minimum plasma concentrations was defined to be 1-5 x MIC for short-time or prolonged infusions (Figure 2.5) and 4-8 x MIC for continuous infusions. For meropenem, MIC values below 1 mg/L were treated as 1 mg/L while for piperacillin, MIC values below 4 mg/L were treated as 4 mg/L.

If no MIC value can be determined (i.e. empirical therapy), the target range for minimum plasma concentrations was defined to be the highest MIC value still susceptible to either of the two antimicrobial drugs to account for the less susceptible pathogens expected at ICUs [167,168]. Based on anti-pseudomonal activity (i.e. the least susceptible pathogen still treated using the two investigated antibiotics) the target range for meropenem was therefore 8-40 mg/L (EUCAST breakpoint 8 mg/L [38]) and 16-80 mg/L for piperacillin/tazobactam (EUCAST breakpoint 16 mg/L [38]) for critically ill patients without an identified pathogen and MIC.

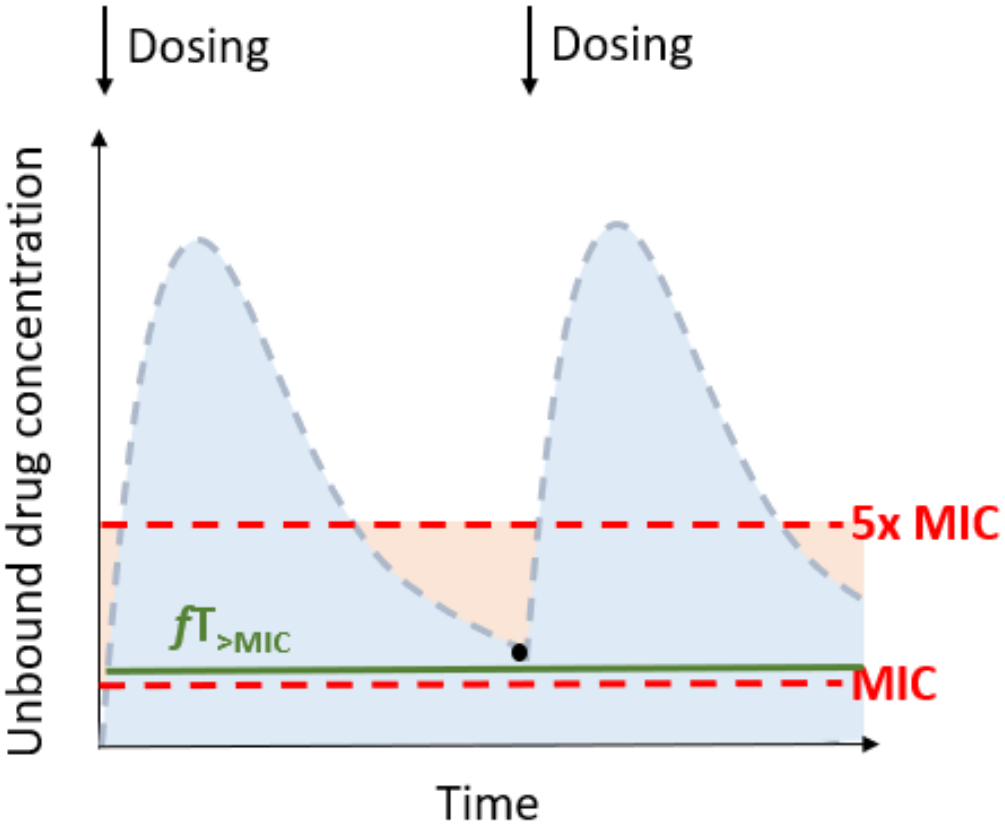

Figure 2.5 Illustration of the pharmacokinetic/pharmacodynamic (PK/PD) target range for minimum antibiotic drug concentrations after short-time or prolonged infusion of meropenem or piperacillin/tazobactam.

Black point: Observed minimum antibiotic concentration, *dotted blue line:* Expected concentration-time profile, *red dotted lines and red area:* PK/PD target range for minimum plasma concentrations; *green line:* Time period of the unbound drug concentration exceeding the MIC; *black arrows*: antibiotic dosing.

Abbreviations: *MIC:* Minimum inhibitory concentration, , $fT_{>MIC}$: Time period of the free drug concentration exceeding the MIC

2.6.4 Data management and exploratory data analysis

2.6.4.1 Dataset generation

The original datasets (overview of included data items: Table S1) received form the AMS and ICU teams at Charité-Universitätsmedizin Berlin were transferred into R readable datasets (see 2.2.1). As additional patient characteristic, creatinine clearance was estimated based on Cockcroft-Gault formula [169]. Missing covariate values were imputed using the last observation carried forward approach or next observation carried backwards approach if only data values after the missing time point were available (see 2.2.1).

2.6.4.2 Dataset checkout

A comprehensive dataset checkout (see 2.2.2) was performed for all datasets received from the AMS and ICU teams at Charité-Universitätsmedizin Berlin.

2.6.4.3 Statistical analysis

Statistical measures used to characterise the central tendency and dispersion of distributions (see 5.3.1) were calculated for continuous data. Furthermore, different statistical tests were used to address specific research questions.

2.6.5 Stage I: Evaluating the 'Status quo' of meropenem and piperacillin/tazobactam therapy

2.6.5.1 Antibiotic treatment in 'stage I'

Antibiotic dosing prior to and dosing adjustments after concentration measurements were determined by the attending physician based on the patient's clinical condition. No structured procedure for dose adjustments following concentration measurements outside the target range was pre-specified. For all prolonged or continuous infusions, a loading dose (0.5 h infusion) of 1 g meropenem or 4 g piperacillin/0.5 g tazobactam was recommended by the AMS team.

Pathogens with determined MIC values above the EUCAST breakpoint for anti-pseudomonal activity of the investigated drugs (meropenem: 8 mg/L, piperacillin/tazobactam: 16 mg/L) were defined as resistant and a change of antibiotic was recommended to the attending physician.

2.6.5.2 Data collection in 'stage I'

'Stage I' of the study was initiated in January 2019 and completed in August 2020. Blood samples for drug concentration determination were taken based on the decision of the treating intensive care physician. Diagnosis, antibiotic dosing history prior to sampling and clinical parameters including scores to assess the extent of organ function (e.g. SOFA score, creatinine clearance) were recorded. The available MIC values of relevant isolated pathogens were documented. To enable the selection of and an extensive PK model evaluation for the PK models underlying the model-informed dosing tools, the full dosing history was recorded for a subset of 66 meropenem and 101 piperacillin samples.

2.6.5.3 Target attainment assessment

Overall target attainment assessment

The proportion of measured concentrations in the target range was determined for both drugs depending on the availability of microbiological data (i.e. the target range either 1-5xMIC or in empirical therapy if no MIC was available 8-40 mg/L for meropenem and 16-80 mg/L for piperacillin/tazobactam (see 2.6.3)). Furthermore, the proportion of drug concentrations below the toxicity thresholds (64 mg/L meropenem, 157 mg/L piperacillin [57]) was calculated.

Target attainment assessment in different renal function groups

To assess if target attainment (TA) was independent of patients' renal function, target attainment was stratified by renal function (assessed by creatinine clearance estimated based on the Cockcroft-Gault formula [169]: severe renal impairment (RI) 0-30 mL/min, moderate RI >30-60 mL/min, mild RI >60-90 mL/min, normal renal function (RF) >90-130 mL/min, augmented RF: >130 mL/min) [170] and subjected to a chi-squared test of independence. A significant difference in target attainment between renal function groups (p-value < 0.01) would indicate lack of evidence for adequately adjusted dosing based on renal function.

Drug concentration assessment between different target range groups

If higher individual MIC values and therefore higher antibiotic concentrations to be targeted were adequately incorporated into dosing decisions, samples with higher targets should display higher drug concentrations. The Kruskal-Wallis test was used to assess if measured antibiotic drug concentrations were significantly higher for patients with higher targets. A non-significant difference between different targeted concentrations (p-value > 0.01) would indicate lack of evidence for adequately adjusted dosing based on the targeted concentration range of the individual patient.

2.6.5.4 Dosing adaptations

The frequency and nature of dosing adaptations after measured concentrations below, in and above the target range was assessed. To investigate if dosing adaptations after measured concentrations outside the target range were more frequent than dose adaptations after measured concentrations inside the target range, the Kruskal-Wallis test was used.

2.6.6 Stage II: Developing and implementing a model-informed tabular meropenem dosing decision tool

2.6.6.1 Pharmacokinetic model selection and evaluation

In 'stage I' of the clinical study exclusively minimum meropenem concentrations and only 66 samples including the full dosing history were collected. As a consequence, the PK data was unsuitable for model development. Instead, a published PK model needed to be selected, evaluated for its appropriateness to predict the observed concentrations and applied for the development of the dosing decision tool. The selection of the PK model was based on a high similarity of relevant patient characteristics between the local study population and the model-underlying population.

To ensure the adequacy of the selected PK model an extensive external model evaluation was conducted: Bias and precision were assessed based on median prediction errors (see 2.3.3.4) and normalized prediction distribution errors (NPDEs) [171,172]. For this purpose model-predicted concentrations were stochastically simulated (n=500) based on the design and patient characteristics in the subdataset with the full dosing history collected during 'stage I' of the study. To include parameter uncertainty, stochastic simulations were repeated for 1000 PK parameter sets obtained by bootstrapping of the dataset and re-estimation of the PK model (see 2.3.3.2). Possible deviations of the NPDEs from the standard normal distribution were assessed by the Wilcoxon signed-rank test (mean≠0), Fisher ratio test (variance≠1) and Shapiro-Wilks test (normality assumption) [158].

2.6.6.2 Development of the tabular dosing decision tool for meropenem

Selection and evaluation of dosing regimens

Based on their ease of integration into clinical routine, possible dosing regimens were preselected by the AMS and ICU teams. To reduce the number of eligible dosing regimen emerging from the possible combinations of the four variables (loading dose, infusion dose, infusion duration, dosing interval) prior to the comprehensive probability of target attainment analysis, deterministic simulations were performed. First, concentration-time profiles of four virtual patients with different creatinine clearance values (45, 90, 135, 180 mL/min) were simulated for potential loading doses (1000 mg and 2000 mg), infusion durations (0.5 h and 4 h), a fixed infusion dose (2000 mg) and a fixed dosing interval (8 h). The dosing regimens achieving higher predicted minimum meropenem concentrations and lower predicted maximum meropenem concentrations were included for the PTA analysis (see 2.3.4.2). PTA (selected targets see 2.6.3) was computed for treatment days 1 and 2 for creatinine clearance values estimated according to Cockcroft and Gault ($CLCR_{CG}$) ranging from 10-

300 mL/min (between 10-150 mL/min in steps of 10 mL/min, above in steps of 50 mL/min) and across MIC values ranging from 1 to 32 mg/L. PK model parameter uncertainty was incorporated by repeating each Monte Carlo simulation and the respective PTA analysis 1000 times using the PK parameter sets obtained from a non-parametric bootstrap. A dosing regimen leading to a PTA≥90% for the median of the 1000 computed PTA values was considered adequate [151]. All dosing regimens considered adequate based on the PTA analysis were further ranked according to higher probability of minimum concentrations being in the defined target range (1–5xMIC) and subsequently to lower total daily dose. Thus, for each MIC value and $CRCL_{CG}$ group one dosing recommendation was derived.

Integration of locally available pathogen information

As a high number of antibiotic therapies need to be initiated *prior* to pathogen detection, dosing recommendations accounting for this situation were developed. Based on the PTA results for MIC values ranging from 0.25 mg/L – 512 mg/L and the pathogen-independent MIC distribution observed at Charité-Universitätsmedizin Berlin during 'stage I' of the study (see 2.6.2 and 3.2.1.3), the local pathogen-independent mean fraction of response (LPIFR) was introduced as a metric for each dosing regimen: To determine the LPIFR for a dosing regimen ($LPIFR_{DR}$), first the PTA for each investigated MIC level ($PTA_{MIC,DR}$) was multiplied by the relative MIC frequency at this level in the distribution of MIC values. Next, the resulting MIC frequency-weighted PTA values were summarised per dosing regimen (Eq.2.49):

$$\mathrm{LPIFR_{DR}} = \sum_{\mathrm{MIC}} \left(\mathrm{PTA_{MIC,DR}} \times \frac{n_{\mathrm{MIC}}}{N_{MIC,total}} \right) \qquad \text{(Eq.2.49)}$$

In the equation, DR represents the investigated dosing, n_{MIC} the number of observed MIC values per MIC level and $N_{MIC,total}$ the total number of observed MIC values. Dosing regimen with a LPIFR ≥ 90% were considered adequate. For each $CRCL_{CG}$ group all dosing regimens considered adequate based on the LPIFR analysis were selected and subsequently ranked by lower total daily dose. Thus, for each $CRCL_{CG}$ group, one dosing recommendation was derived if the pathogen and its susceptibility was unknown.

2.6.6.3 Evaluation of the tabular dosing decision tool

To ensure patient safety and assess the potential benefit of the developed model-informed dosing decision tool, it was evaluated prior to implementation into clinical practice: The total daily doses of the dosing regimens recommended by the dosing decision tool were compared to the total daily doses of the actually administered dosing regimens in 'stage I' of the clinical study. For this purpose, the 'stage I' dataset was stratified based on target attainment (above, below and in defined target range of 1–5xMIC) and the administered and recommended daily doses were compared.

'Stage II' of the study was initiated in December 2020 with the aim of evaluating the tubular dosing decision tool in clinical practice at Charité-Universitätsmedizin Berlin. Healthcare personal in the participating ICU wards were trained in the use of the tool by members of the AMS team on multiple occasions. In addition to the training, a simple step-by-step flow-chart explaining the use of the dosing tool was provided to be displayed in the wards (Figure S5). Samples collected during a 4 weeks long transition period were flagged. Like in 'stage I' of the study, dosing information immediately prior to sampling and patient-specific data were collected (Table S1). Furthermore, to be able to retrace and to evaluate the correct use of the developed tool, the target selected by the intensive care physician was recorded on the sample collection sheet (Figure S6).

2.6.7 Stage III: Developing and implementing an interactive model-informed dosing software

2.6.7.1 Pharmacokinetic model selection and evaluation

For meropenem the evaluated PK model (see 3.2.2.1) underlying the tabular model-informed dosing decision tool developed in 'stage II' was selected. To identify a suitable PK model for piperacillin, possible candidates were identified from scientific literature and evaluated using the piperacillin subdataset with full dosing history collected in 'stage I' of the clinical study (see 2.6.2). First a PubMed search with the term 'piperacillin' in combination with one or multiple of the 25 selected terms (Table S11) indicating the development/use of a pharmacokinetic model was conducted. Subsequently, the pre-selected publications from the PubMed search were individually examined focusing on (i) patient population characteristics, (ii) modelling approach and (iii) the availability of all information needed to reconstruct the PK model. Only parametric PK models of critically ill patients or patients during sepsis were selected for model evaluation.

Next, to select the most appropriate of the preselected piperacillin PK models for the integration into the model-informed dosing software external model evaluations were conducted. Model-predicted concentrations were stochastically simulated (n=500) using the administered dosing regimens and patient characteristics observed in the subdataset with full dosing history (see 2.6.5.2). To assess bias and precision, median prediction errors and absolute median prediction errors were calculated (see 2.3.3.4). If the literature-identified PK models incorporated patient characteristics not available in the dataset, the respective characteristics were fixed to the median patient characteristic observed in the model development datasets. The PK model with the lowest bias and highest precision was selected as best performing model and subjected to further evaluation.

To evaluate the predictive performance of the best performing PK model in the context of intended use (i.e. updating the predictions for each induvial patient with every new antibiotic concentration becoming available), a step-wise maximum a-posteriori likelihood (MAP, see 2.3.4.3) estimation was conducted: for each patient the concentration at the sampling time point was predicted using stochastic simulations (500 virtual patients) based on the prior distribution of PK model parameter estimates and every subsequent concentration was predicted using stochastic simulations based on the posterior parameter distribution. The posterior parameter distribution was estimated using the MAP and normal approximation approach (see 2.3.4.3) and the preceding samples of an individual patient. As for the evaluation of the a-priori predictive performance (i.e. without MAP estimation), median prediction errors were calculated based on the simulations and used to assess bias and precision.

2.6.7.2 Simulation framework including maximum a-posteriori parameter estimation

The model-informed dosing software was developed as a web application utilising TDMxR and shiny in R/RStudio. To predict the concentration-time profile for an individual patient the two selected and evaluated PK models for meropenem and piperacillin (see 3.2.2.1 and 3.2.3.1) were incorporated in the software. To calculate the probability of a dosing regimen to attain the defined PK/PD target, stochastic simulations (n = 250) were implemented integrating the selected antibiotic drug, the provided patient characteristics and the chosen dosing regimen. To incorporate an individual patient's drug measurement(s) that become(s) available in the course of antibiotic treatment, maximum a-posteriori (MAP) parameter estimation and the estimation of the individual posterior parameter distribution based on the normal approximation approach was integrated using the estimate.map function in TDMxR.

2.6.7.3 Assessment of the potential of the dosing decision software using real patient data

The developed model-informed dosing software was evaluated prior to implementation into clinical practice. For patients with complete dosing history in 'stage I' of the study and determined MIC value (63 meropenem and 90 piperacillin samples), the DoseCalculator was used to select the most suitable dosing regimens integrating the available information throughout a typical clinical treatment period: Prior to the first concentration measurement the dosing regimen for each individual patient was selected based on stochastic simulations of the PK model integrating the patient's characteristics. After each subsequent antibiotic concentration measurement, MAP parameter estimation was conducted and the selected dosing regimen updated incorporating the individual PK of the patient. Next, the model-predicted target attainment (target: minimum antibiotic concentration 1-5xMIC) was calculated for the dosing regimens selected by the DoseCalculator and compared to the model-predicted target attainment for the dosing regimens administered to the ICU patients.

2.7 Project III: Evaluation and extension of the MeroRisk Calculator

2.7.1 Objectives and research strategy

The objectives of this project were (i) to evaluate the performance of the MeroRisk Calculator, a previously developed user-friendly tool to predict the risk of meropenem target non-attainment in critically ill patients, using routine clinical data and (ii) to extend the risk predictions of the MeroRisk Calculator to include pathogen sensitivity information in case no individual MIC value is available.

A direct data-based evaluation of the MeroRisk Calculator was not feasible using the available clinical routine dataset without censoring most of the available data: While the MeroRisk Calculator uses the provided creatinine clearance to predict the meropenem concentration 8 h after standard dosing (1 g, 0.5 h infusion, q8h), i.e., at one specific time point, a large proportion of the concentration measurements of the retrospective dataset, were taken at different time points (not exactly 8 h after dose). Therefore, a two-step approach was chosen: In step 1, the potential of a population pharmacokinetic model to predict the clinical routine dataset was evaluated. In step 2, the PK model was used for a model-based evaluation of the MeroRisk Calculator. Furthermore, a method to calculate the risk of target non-attainment based on causative pathogens prior to MIC determination was developed employing susceptibility patterns reported by EUCAST.

2.7.2 Database

This analysis was based on a monocentric, observational study at two anaesthesiological intensive care units (ICU) of the University Hospital, LMU Munich, Germany (ClinicalTrials.gov identifier: NCT03985605). The study protocol was approved by the local Institutional Review Board (registration number 18-578). Patients diagnosed with severe infections susceptible for antibiotic therapy with meropenem were included in the study and received meropenem treatment according to clinical need assessed by the responsible physician. Once-daily blood samples were collected to quantified meropenem according to a validated LC-MS/MS method [160]. Furthermore, the available demographic patient data (e.g. sex, age, weight) and laboratory data (e.g. serum albumin concentration, serum creatinine concentration) were collected from the hospital information system. Creatinine clearance was estimated as marker for renal function based on Cockcroft and Gault equation [169]. Patients undergoing renal replacement therapy and patients with creatinine clearances outside the current range of application of the MeroRisk Calculator (25 – 255 mL/min) [131] were excluded from the analysis. PK, laboratory and demographic data were analysed using the exploratory analysis methods introduced in section 2.2.3.

2.7.3 Evaluation of the MeroRisk Calculator

2.7.3.1 Evaluation strategy

The dataset used for the evaluation of the MeroRisk Calculator was collected during clinical routine and not in a controlled clinical trial with a fixed and accurate sampling schedule. As a consequence, it consisted of concentration measurements at various timepoints and after administration of different dosing regimens. The MeroRisk Calculator links the creatinine clearance estimated according to Cockcroft and Gault ($CLCR_{CG}$) to meropenem concentrations 8 hours after standard meropenem dosing (1 g, 0.5 h infusion, q8h) i.e. to one specific timepoint. Therefore, a direct evaluation based on the comparison of measured meropenem concentrations with concentrations predicted by the MeroRisk Calculator was not feasible. In contrast to the MeroRisk Calculator, compartmental PK models are able to predict the expected drug concentration-time profile, i.e. the meropenem concentration at any timepoint including the 8 hour timepoint, following every conceivable dosing regimen. To enable an evaluation based on the available clinical dataset, a two-step evaluation strategy was employed (Figure 2.6):

- Step 1: Data-based evaluation of a published NLME meropenem population PK model using the clinical dataset.
- Step 2: PK model-based evaluation of the MeroRisk Calculator by comparing the meropenem and risk of target nonattainment predictions of the evaluated PK model (Step 1) to the predictions of the MeroRisk Calculator.

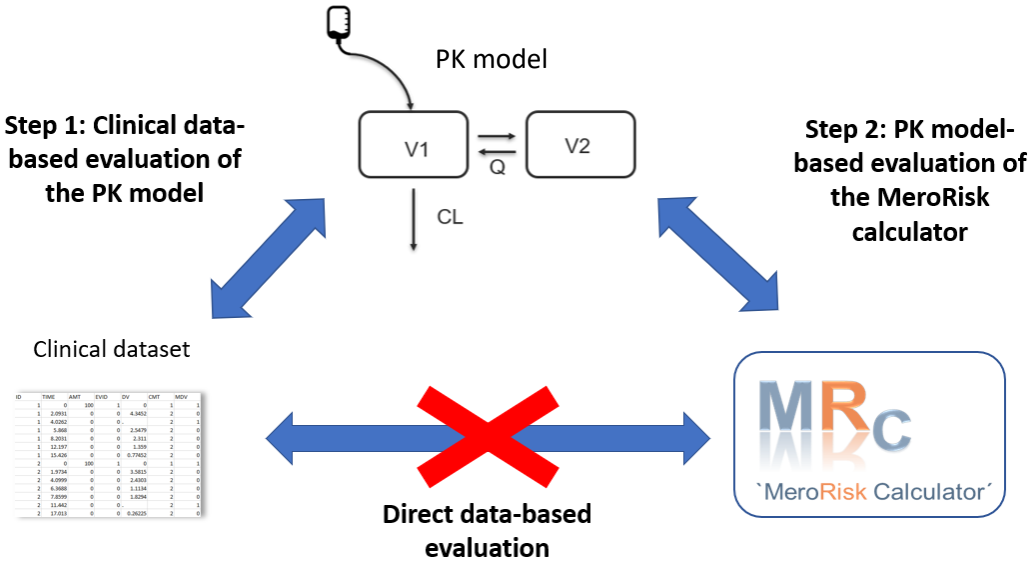

Figure 2.6: Work-flow for the stepwise evaluation strategy of the MeroRisk Calculator using a clinical routine dataset [173].

A direct, data-based evaluation of the MeroRisk Calculator (bottom right) employing the clinical dataset (bottom left) was not feasible due to the time variable sampling time points under routine conditions in the dataset. Therefore, a population pharmacokinetic (PK) model (top) was evaluated for its potential to predict the concentrations observed at variable time points (Step 1) and the predictions by the evaluated PK model were then used as a benchmark for the predictions of the MeroRisk Calculator (Step 2)

2.7.3.2 Evaluation step 1: Data-based evaluation of the two-compartment PK model

The two-compartment meropenem PK model selected for the evaluation included three covariates: CLCRCG as covariate on meropenem clearance, total body weight on the central volume of distribution and serum albumin concentration on the peripheral volume of distribution, implemented as piecewise linear, power and linear relationship, respectively [129].

For the external model evaluation of the PK model, patients with characteristics outside of the 90% range of patient characteristics observed in the model development dataset were excluded (n=28 (15.3%)). Stochastic simulations (n=2000) of the clinical dataset were performed and prediction errors were calculated and used to assess bias and precision of the PK model (see 2.3.3.4).

2.7.3.3 Evaluation step 2: PK model-based evaluation of the MeroRisk Calculator

For the evaluation of the MeroRisk Calculator, both predicted meropenem concentrations and predicted risks of target non-attainment by the MeroRisk Calculator were compared to predictions by the evaluated PK model of step 1.First, the conformity of predictions for the patients included in the clinical dataset was examined. Second, virtual patients were generated to investigated possible deviations between the predictions of the PK model and the MeroRisk Calculator for patient characteristics with a high impact on meropenem pharmacokinetics.

Conformity between the predictions for real patients

To assess the conformity of meropenem predictions between the MeroRisk Calculator and the PK model for a real patient population, concentrations 8 hours after standard dosing were simulated for the 155 patients included in the clinical dataset using stochastic simulations (n = 2000) for the PK model and classic theory of linear models and standardised residuals [131] for the model underlying the MeroRisk Calculator. Median predictions were calculated for each patient and method and compared visually.

To assess the conformity of risk predictions between the MeroRisk Calculator and the PK model a target of 100% $T_{>MIC}$, MIC values ranging from 0.125 – 16 mg/L and the characteristics of the 155 patients of the evaluation dataset were chosen. Due to the low protein binding of meropenem (~2%) [66] total meropenem concentrations were evaluated. The risk predictions of the PK model were calculated based on stochastically simulated (n=2000) meropenem concentrations 8 hours after standard dosing, while risk predictions of the MeroRisk Calculator were derived using classic theory of linear models and standardised residuals [131]. Lin's concordance correlation coefficient (CCC) [174] - a common way to assess the agreement of a new test or measurement (here: the MeroRisk

Calculator) to an established test or measurement (here evaluated PK model) -was chosen to quantitatively examine the conformity of both risk predictions. Based on the strength-of-agreement criteria for CCC defined by McBride (Table 2.4) [174] the evaluation of the MeroRisk Calculator was considered successful, if the lower one-sided 95% confidence limit of the calculated CCC value was ≥0.95 for the combined analysis of all investigated MIC values (0.125 – 16 mg/L).

Table 2.4: Strength of agreement criteria defined by McBride for Lin's concordance correlation coefficient [174].

Strength of agreement	Continuous variable
Almost perfect	>0.99
Substantial	0.95-0.99
Moderate	0.90-0.95
Poor	<0.90

Conformity between the predictions for virtual patients

To assess the impact of varying patient characteristics on the meropenem predictions and to identify possible characteristic-dependent deviations between the predictions of the MeroRisk Calculator and the PK model, three virtual patient populations of 50 individuals each were generated. In each of the virtual populations two of the three covariates implemented in the PK model were fixed to the median value of the model development dataset (weight: 70 kg, serum albumin concentrations: 2.8 g/dL, serum creatinine concentrations: 1.24 mg/dL) [129] while the third ranged in equally sized steps from the 5^{th} to 95^{th} percentile of the respective distributions. Based on the weight and serum creatinine concentration of each virtual patient, a fixed age of 53.9 years and male sex, creatinine clearance was estimated according to Cockcroft-Gault formula [169]. Meropenem concentrations 8 hours after standard dosing of meropenem were predicted for the three virtual populations using both the linear model underlying the MeroRisk Calculator and the evaluated PK model of step 1. For the PK model, stochastic simulations (n=2000) were performed, and the median prediction and 95% prediction interval calculated. The same metrics (median prediction and 95% prediction interval) were derived for the model underlying the MeroRisk Calculator using classic theory of linear models and standardised residuals [131]. The median predictions and 95% prediction intervals were graphically analysed over the range of investigated patient characteristics.

2.7.4 Integration of a new feature in the MeroRisk Calculator: Risk assessment based on pathogen specific MIC distribution

The previous version of the MeroRisk Calculator allowed a user-friendly way to predict the risk of meropenem target non-attainment in critically ill patients, if the pathogen causing the infection and its susceptible (i.e. MIC) are known. To extend the applicability of the tool to clinical situations in which the pathogen but not its susceptibility are known, the risk assessment for target non-attainment of an individual patient (characterised by the CLCRCG) and a specific pathogen (characterised by the MIC distribution) was implemented into the MeroRisk Calculator using Excel. The risk calculation was based on CFR analysis (see 2.3.4.2) for the 74 pathogens included in the current report of meropenem MIC value distributions by EUCAST [38]. To assess the appropriateness of standard dosing for a real patient population and all clinically relevant pathogens, the extended MeroRisk Calculator was used to determine the risk of target non-attainment for the 155 critically ill patients in the evaluation dataset and all 74 currently in the EUCAST database available pathogens.

3 Results

3.1 Project I: Characterising meropenem adsorption abilities at the cytokine adsorber CytoSorb®

3.1.1 Database

A total of 333 meropenem serum samples from 25 patients were included in the analysis (Table 3.1). One third of the samples (n = 114; 34.2%) were collected during CytoSorb®-treatment. The investigated patient population covered a broad range of age (19 - 97 years), was severely ill (median APACHE II score on study day 1: 34, range 11 - 43) and typically had a low residual diuresis (median 240 mL/day, range 0 – 3900 mL/day). Patients received meropenem either as a continuous (19%), prolonged (> 0.5 h - < 4 h) (14%) or short-term (≤ 0.5 h) (67%) infusion. The median daily dose was 5 g (range: 1 - 7 g) of meropenem. The CytoSorb® filter was installed after a median time of 3.26 hours (range: 0.08 – 8.5 hours) post dose for patients with short or prolonged infusion was. Since there was no fixed sampling schedule, there were no missing values for meropenem concentrations. All relevant patient characteristics were comparable between the two studies (Table 3.1), justifying to pool the data for the subsequent PK analysis. A first graphical evaluation of meropenem concentrations after short-term (0.5 h) infusion of 2000 mg meropenem did not indicate clear deviations between meropenem samples taken during renal replacement therapy, during renal replacement therapy including the CytoSorb® filter and outside of renal replacement therapy (Figure 3.1).

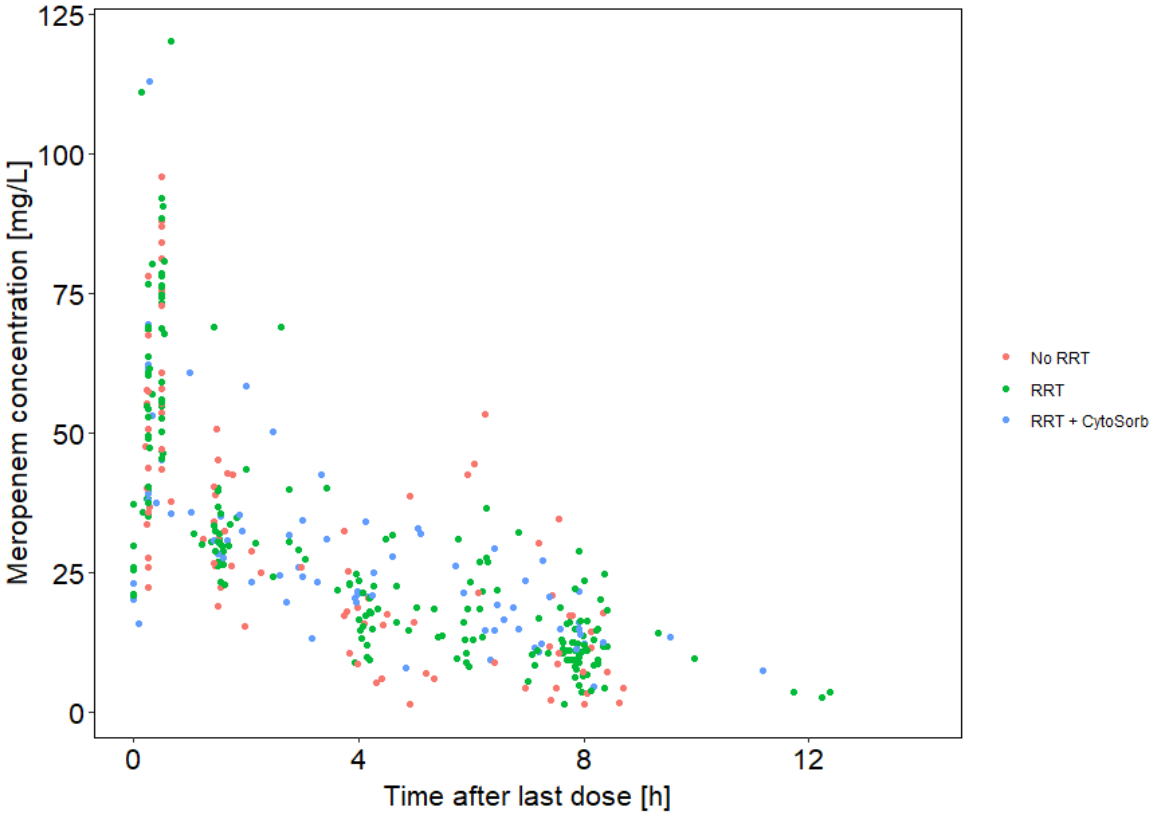

Figure 3.1: Observed meropenem concentrations (n=186) following a short-term infusions (0.5 h) of 2000 mg meropenem stratified by type of renal replacement therapy (RRT).
Meropenem samples taken during periods without RRT (red dots), during RRT (green dots) or during RRT including CytoSorb® filter (blue dots).

Table 3.1: Overview of patient characteristics also stratified by study.

Patient characteristic	**Total dataset**	**NCT01793012**	**NCT03985605**
Categorical variables		*n (%)*	
No. of patients	25 (100)	6 (100)	19 (100)
No. of male patients	20 (80)	2 (33)	18 (95)
No. of samples	333 (100)	117 (100)	216 (100)
Patients with CytoSorb®	20 (80)	1 (17)	19 (100)
Total no. of CytoSorb® treatments	44	2	42
No. of samples during CytoSorb®	114 (34.2)	17 (15)	97 (45)
No. of patients with CRRT	25 (100)	6 (100)	19 (100)
CVVHD/CVVHDF	19 (76)/12 (48)[a]	3 (50)/3 (50)	16 (84)/9 (47)[a]
Continuous variables [unit]		*Median (range)*	
CytoSorb® treatment duration [h]	9.3 (1.7 - 27.4)	22.8 (18.3 – 27.4)	9.23 (1.7 – 26.8)
Median daily dose [g]	5 (1 – 7)	3 (1 – 5)	6 (2 - 7)
Continuous variables on study day 1 [unit]		*Median (range)*	
Age [years]	54 (19 - 97)	53.5 (40 – 56)	56 (19 – 57)
Weight [kg]	80 (52 - 140)	75.5 (52 – 120)	87 (56 – 140)
Serum albumin concentration [g/dL]	2.6 (1.6 – 3.5)	2.8 (2.2 – 3.3)	2.5 (1.6 – 3.5)
APACHE II	34 (11 – 43)	34 (11 – 38)	35 (23 – 43)
Bilirubin [mg/dL]	2.6 (0.2 – 33.2)	8.2 (1.0 – 24.9)	1.5 (0.2 – 33.2)
IL-6 concentration [pg/mL]	1945 (0.2 – 370000)	1956 (82 – 197000)	1945 (2.6 – 370000)
CRP concentration [mg/dL]	15.4 (0.5 – 48.6)	2.5 (1.9 – 24.7)	16.9 (0.5 – 48.6)
Residual Diuresis [mL/day]	240 (0 – 3900)	650 (0 – 1700)	240 (0 – 3900)
Dialysate flow [L/h]	2.0 (1.0 – 4.8)	1.5 (1.0 – 3)	2.0 (1.2 - 4.8)
Replacement fluid [L/h][b]	2.0 (1.0 – 3.5)	1.0 (1.0 – 1.5)	2.2 (1.2 – 3.5)
Blood flow [L/h]	6.0 (4.8 – 24)	6.0 (4.8 – 12)	6.0 (6.0 -24)

Abbreviations: *APACHE II*: Acute Physiology And Chronic Health Evaluation II, *CRP:* C-reactive protein, *CRRT*: Continuous renal replacement therapy, *CVVHD*: Continuous veno-venous haemodialysis, *CVVHDF:* Continuous veno-venous haemodiafiltration, *IL-6*: Interleukin 6.

[a] in 6 patients the dialysis-type was switched

[b] when CVVHDF on.

3.1.2 Population pharmacokinetic modelling

3.1.2.1 Basis model development

A two-compartment PK disposition model with zero-order input and first-order elimination best described the data. IIV was included on clearance (CL) and both volumes of distribution (V1, V2) and residual variability was described using a proportional model (Table 3.2). None of the examined covariates fulfilled the criteria for inclusion in the model. Both goodness-of-fit plots and a visual predictive check demonstrated an adequate representation of the observed data by the developed PK model (Figure 3.2). The slight overprediction of the observed variability (identifiable in the VPC) can be attributed to a few outliers in the dataset.

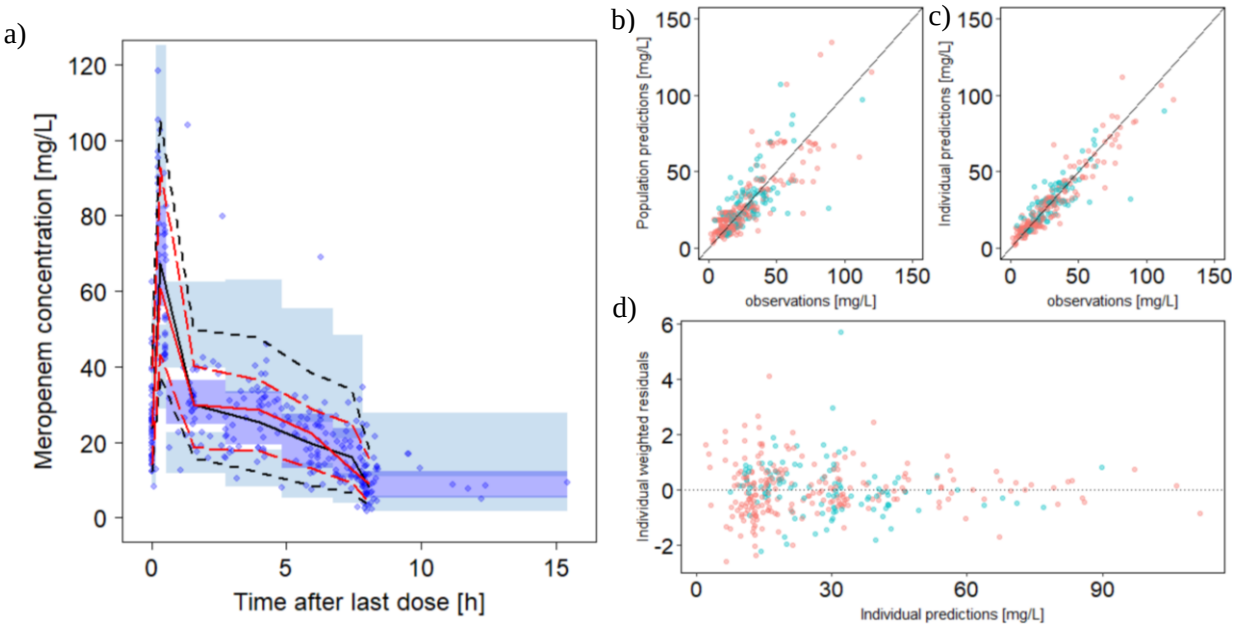

Figure 3.2. Prediction-corrected visual predictive check (n=1000 simulations, left) and goodness-of-fit plots (right) for the population pharmacokinetic model of meropenem in critically ill patients undergoing renal replacement therapy.
a): *Points*: Observations, *Lines*: 10th, 90th percentile (dashed), 50th percentile (solid) of the observed (red) and simulated (black) data. *Shaded areas:* 95% confidence interval around 10th, 50th and 90th percentile of simulated data. b-d): *Points*: Observations with (blue) and without (red) CytoSorb® b, c): *Lines*: Line of unity. d): *Horizontal line*: Reference line at y=0.

3.1.2.2 Effect of CytoSorb®-treatment on meropenem concentrations

Approach 1: CytoSorb®-treatment as categorical covariate on clearance

Implementing CytoSorb® as a categorical covariate on clearance did neither result in a statistically significant drop in objective function value (ΔOFV: -0.018) nor in a reduction of unexplained variability (30.0 %CV vs. 30.8 %CV, Table 3.2). Furthermore, the estimated increase in clearance during CytoSorb® treatment was not clinically relevant (0.73%) and the parameter was estimate imprecisely, i.e., the relative standard error (RSE) for the parameter estimate was 627% and therefore the 95% confidence interval of the parameter estimate included 0 (i.e. no-effect).

Approach 2: Adsorption submodels

None of the three investigated adsorption submodels for meropenem during CytoSorb® therapy led to a significant drop in OFV (ΔOFV: -0.024, -0.78, -0.78 for constant adsorption model, linear decrease adsorption model and hyperbolic decrease adsorption model, respectively). The precision of the parameter estimates was low for all three models (ranging from 110% RSE to 1557% RSE) and the maximum CytoSorb® clearance was not clinically relevant (Table 3.2). Directly after implementation of the CytoSorb® filter when no meropenem is yet adsorpt at the filter and therefore the adsorption in all three adsorption models is at the maximum, the adsorption clearance was equivalent to 0.75%, 3.7% and 3.84% of total clearance for the constant adsorption model, the linear decrease adsorption model and the hyperbolic decrease in adsorption model, respectively.

Approach 3: Re-estimation of the model parameters excluding samples during CytoSorb® treatment

Re-estimation of the parameters of the final basis model without samples of meropenem concentrations collected during CytoSorb® treatment, did not substantially change parameter estimates (Table 3.2): CL even increased slightly while still remaining within the 95% CI of the original parameter estimates. In Figure 3.3 the individual median meropenem concentration predicted by the re-estimated model and the 50% prediction interval are plotted against the observed concentrations during CytoSorb® therapy (n=114). The re-estimated model showed a tendency to predict concentrations lower than those measured during CytoSorb® therapy: The median bias of the predictions was -0.42 mg/L (2.6%) and for the majority (81.7%) of samples the 50% prediction interval included the line of identity. For 61 (53.5%) of the samples the median predicted concentration was below the observed concentration. In Figure 3.4 the predicted concentration-time profile and all observed concentrations from one individual patient from study NCT01793012 are displayed as an example, while the individual concentration-time profiles of all other patients are presented in the supplementary data (Figure S1): Both the meropenem concentrations with and without CytoSorb® therapy were randomly scattered around the individual median predicted

concentration. Hence, a difference between samples taken with and without CytoSorb® therapy could not be detected across all patients with very different dosing regimens and numbers of meropenem samples taken.

Table 3.2: Parameter estimates (RSE %) [shrinkage %] for the pharmacokinetic models investigating the effect of CytoSorb® treatment on meropenem concentrations.

Parameter [unit]	Basis model	Model with CytoSorb® as categorical covariate	Adsorption submodels			CytoSorb® excluded ($n_{remaining}$=219)
			Constant	Linear decrease	Hyperbolic decrease	
Fixed-effects parameter						
CL [L/h]	6.39 (6)	6.38 (6)	6.37 (7)	6.31 (5)	6.31 (24)	6.63 (5)
V1 [L]	11.6 (21)	12.0 (17)	12.0 (23)	11.6 (77)	11.6 (259)	10.8 (36)
V2 [L]	29.8 (25)	29.8 (20)	29.8 (26)	30.1 (45)	31.1 (20)	28.6 (23)
Q [L/h]	11.4 (39)	11.0 (36)	11.0 (38)	11.0 (59)	11.0 (274)	21.2 (40)
COV CL		0.007 (627)				
k_{max} [1/h]			0.004 (248)	0.02 (110)	0.02 (686)	
A_{max}[mg]				$3*10^7$ (1557)		
A_{50} [mg]					$4*10^8$ (711)	
Interindividual variability						
ω CL, CV %	20.2 (19) [9]	20.6 (19) [9]	20.5 (19) [9]	20.5 (20.0) [9]	20.5 (64) [9]	20 (18) [14]
ω V1, CV %	69.5 (33) [28]	72.4 (33) [28]	64.9 (32) [28]	73.9 (56) [28]	73.9 (166) [28]	57.2 (31) [41]
ω V2, CV %	69.9 (27) [27]	79.6 (27) [27]	70.1 (25) [27]	80.5 (32) [27]	80.4 (118) [27]	51.7 (122) [40]
Residual variability						
σ Prop. CV %	30.0 (11)	30.8 (11)	30.8 (11)	30.7 (10)	30.7 (84)	30.2 (11)

Abbreviations: *CL*: Clearance, *V1*: Volume of central compartment, *V2*: Volume of the peripheral compartment, *Q*: Clearance between V1and V2, *COV CL*: proportional increase of clearance during CytoSorb® therapy, k_{max}: maximum adsorption rate, *Amax*: maximum drug amount adsorbed at the CytoSorb® filter, A_{50}: absorbed drug amount connected to a the half maximum adsorption rate, *CV*: Coefficient of variation, *Prop*.: Proportional, *RSE*: relative standard error, ω: Random-effects parameters for interindividual variability, σ: Random-effects parameters for residual variability

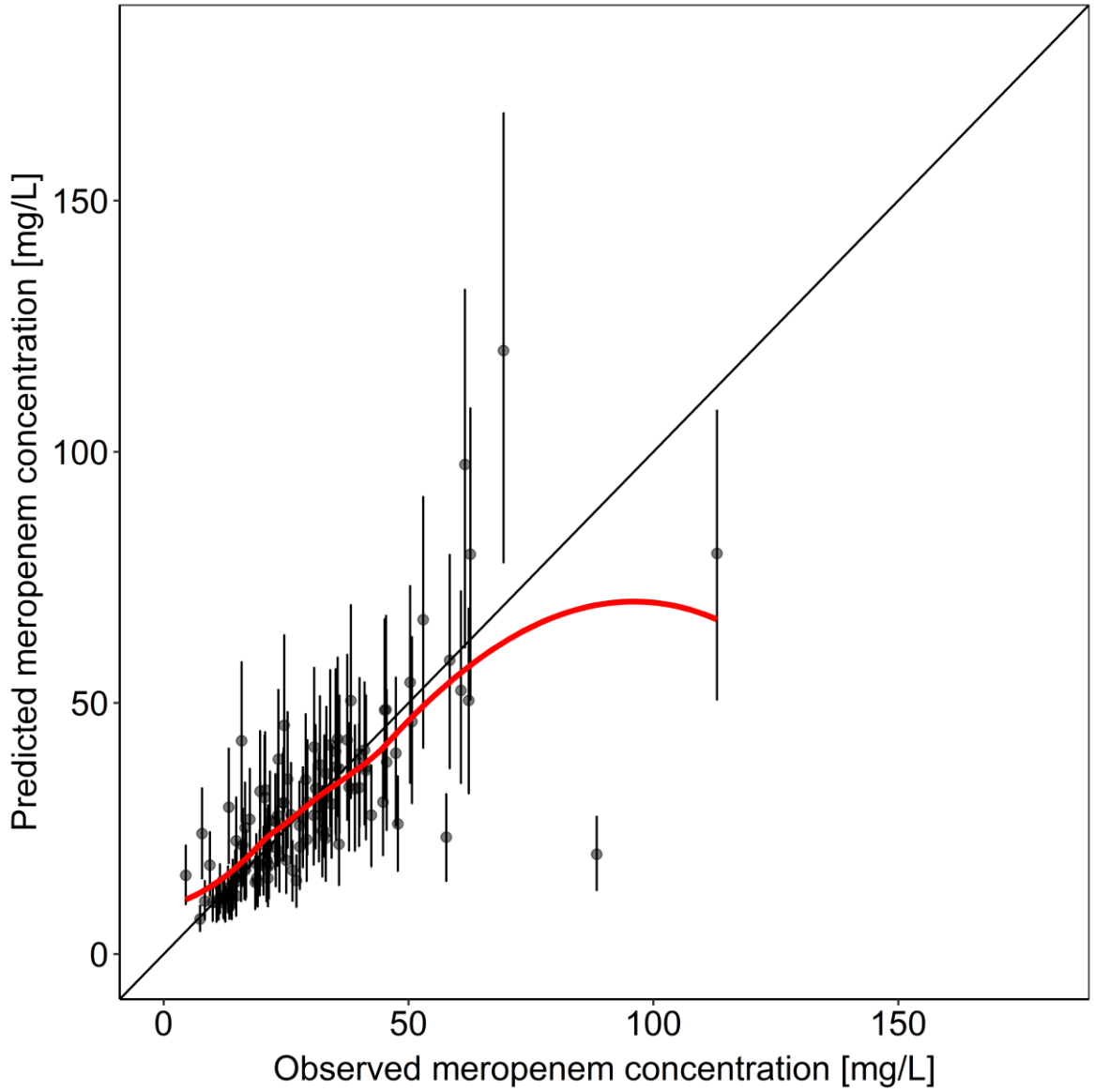

Figure 3.3: Predicted meropenem concentrations based on pharmacokinetic model excluding CytoSorb® samples vs. meropenem concentrations observed during CytoSorb® therapy (n=114). Dots: Median predictions, Error bars: 50% prediction interval, Black line: Line of identity. Red line: Loess smoother

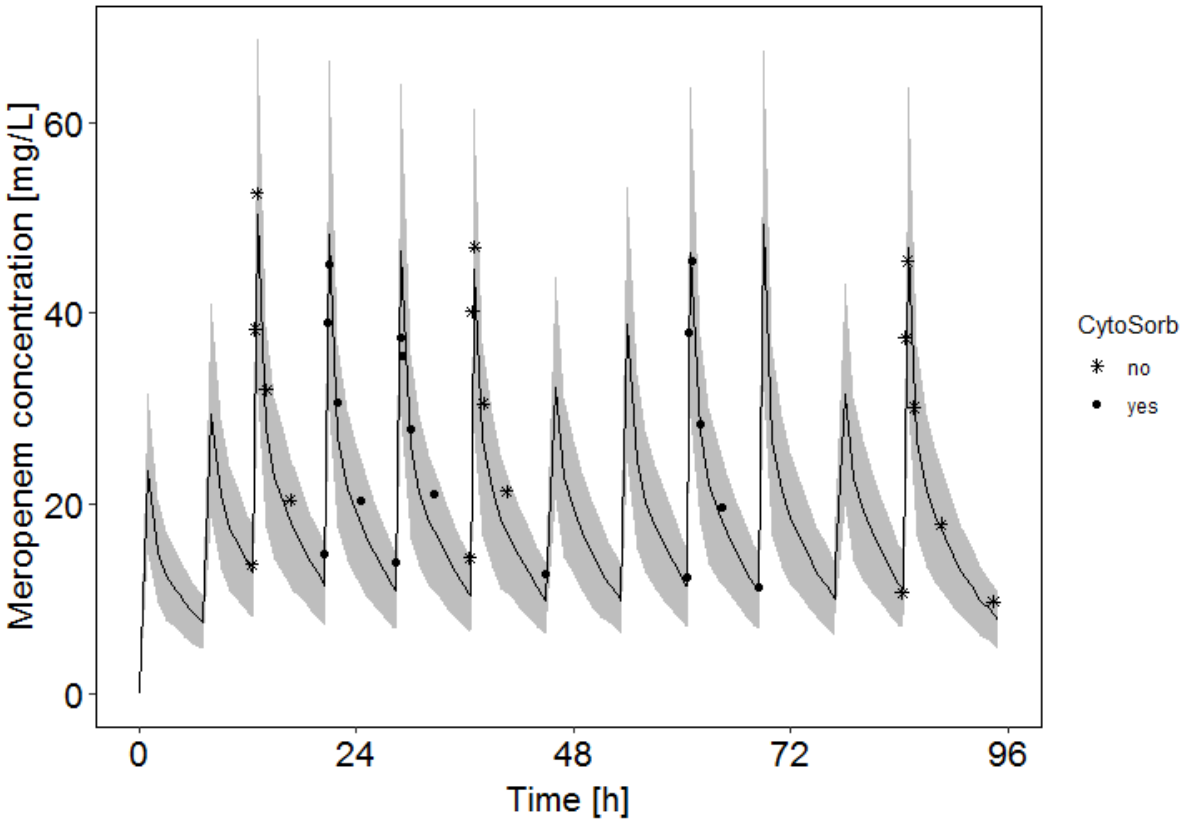

Figure 3.4: Observed meropenem concentrations and predicted meropenem concentration-time profile based on a pharmacokinetic model excluding CytoSorb® samples for one individual patient of the dataset.

Black line: Median prediction, Grey shade: 50% prediction interval, Symbols: Meropenem samples with (points) and without (stars) CytoSorb®-treatment.

3.2 Project II: Utilising pharmacokinetic models to improve piperacillin/tazobactam and meropenem dosing

3.2.1 Stage I: Evaluating the 'status quo' of meropenem and piperacillin/tazobactam therapy

3.2.1.1 Database

In 'stage I' of the clinical study 375 meropenem samples and 230 piperacillin blood samples were collected from 108 and 96 ICU patients, respectively. For 19 (5%) blood samples taken for meropenem measurements and 14 (6%) blood samples taken for piperacillin measurements, the drug concentrations could not be determined by the laboratory due to delays in sample transportation resulting in the disbarment of the affected samples. For both drugs the patients included in the study were predominantly male (meropenem: 64.8%, piperacillin/tazobactam: 63.5%), aged over 60 years (median: meropenem 62.0 years, piperacillin/tazobactam 65.0 years) and had a median weight of 76.0 kg. Creatinine clearance estimated based on the Cockcroft-Gault equation [169], serum albumin concentrations and location of infection were similar for patients receiving meropenem and piperacillin/tazobactam (Table 3.3). Patients receiving meropenem were found to be more severely ill, with increased SOFA and APACHE scores (median score for meropenem vs. piperacillin/tazobactam: SOFA: 8 vs. 6, APACHE: 23 vs. 20) and a higher proportion of extracorporeal organ support (percentage of samples during organ support for meropenem vs. piperacillin/tazobactam: renal replacement therapy (RRT): 38.1% vs. 23.0%, extracorporeal membrane oxygenation (ECMO): 8.80% vs 5.22%). All other patient characteristics where found to be highly similar between the two groups (Table 3.3 and Figure S2).

Table 3.3: Overview of patient and blood sampling characteristics

Characteristic	Meropenem	Piperacillin/tazobactam
	Patient level	
Categorical	***n (%)***	***n (%)***
Patients	108	96
Male	70 (64.8)	61 (63.5)
Continuous [unit]	***Median (5^{th}-95^{th} percentile)***	***Median (5^{th}-95^{th} percentile)***
Age [years]	62.0 (36.0-80.0)	65.0 (36.0-81.0)
Weight [kg]	76.0 (49.0-126)	76.0 (49.6-128)
	Sample level	
Categorical	*n (%)*	*n (%)*
Blood samples	375	230
• Samples during RRT	143 (38.1)	53 (23.0)
• Samples during ECMO	33 (8.80)	12 (5.22)
Location of infection		
• Intraabdominal	166 (44.6)	101 (43.9)
• Pneumonia	131 (35.2)	102 (44.3)
• Blood stream	60 (16.1)	18 (7.83)
• Skin-/soft tissue	15 (4.00)	4 (1.74)
• Other	0 (0)	5 (2.17)
• Unknown	3 (0.80)	0 (0)
Continuous [unit]	***Median (5^{th}-95^{th} percentile)***	***Median (5^{th}-95^{th} percentile)***
Blood samples per patient	2 (1-10)	2 (1-5)
Creatinine clearance[#] [mL/min]	76.6 (24.8-241)	71.1 (17.8-171)
Serum albumin concentration [g/dL]	2.68 (1.99-3.58)	2.70 (2.00-3.50)
SOFA score	8.00 (1.90-17.0)	6.00 (1.00-14.0)
APACHE score	23.0 (12.0 – 37.0)	20.0 (11.0-34.0)

[#]estiamted according to Cockcroft-Gault formula [169].

Abbreviations: n: number, RRT: renal replacement therapy, ECMO: extracorporeal membrane oxygenation, SOFA: Sepsis-related Organ Failure Assessment, APACHE: Acute Physiology and Chronic Health Evaluation

3.2.1.2 Antibiotic treatment

The monitored meropenem dosing regimens prior to the concentration measurements were diverse: In most cases (63.5%), 2 g meropenem were administered as loading dose, while in the remaining cases, it was 1 g meropenem. Administered meropenem maintenance doses included 0.5, 1, 2, 3, 6 and 8 g, with 1 g (50.2%) and 2 g (40.7%) being the two most frequently administered doses. The majority of doses (92.7%) was administered as prolonged infusions over 3 hours (31.2%) or 4 hours (61.5%) and a further 7.26% as continuous infusion. The most common dosing interval for meropenem was 8 hours (77.0%), followed by 6 hours (11.0%), 24 hours (8.52%) and 12 hours (3.15%).

Piperacillin/tazobactam dosing regimens monitored during the study did not substantially vary between patients regarding to the administered dose, infusion duration and dosing interval. For piperacillin, almost all administered doses (98.6% of loading and 99.5% of maintenance doses) consisted of 4 g in combination with 0.5 g tazobactam (others: 1 g piperacillin/0.125 g tazobactam and 2 g piperacillin/0.25 g tazobactam). The majority (98.0%) of doses was administered as prolonged infusion over 3 hours (34.3%) or 4 hours (63.7%); the others were prolonged infusions over 2 h (1.50%) or short infusions over 0.5 h (0.50%). The most common dosing interval was 8 hours (72.4%), followed by 6 hours (18.6%), 12 hours (8.54%) and 24 hours (0.50%).

3.2.1.3 Pathogen susceptibility

For 49.1% of patients receiving meropenem and 34.4% of patients receiving piperacillin/tazobactam, the MIC value of the pathogen causing the infection could be determined and was available for the attending physician approximately two days after therapy start (median time (range) after therapy start: meropenem 2.1 days (0-120 days), piperacillin 2.3 days (0-103 days)). The majority of observed pathogens was susceptible to the administered antibiotics (meropenem: 93.3%, piperacillin: 97.0%) and most observed MIC values (meropenem: 90.0%, piperacillin: 93.9%) were found to be lower than 8 mg/L for meropenem and 16 mg/L for piperacillin, which represented the lower threshold of the target range set by the AMS team for empirical antibiotic therapy (see 2.6.3). For meropenem, 75% of the pathogens with a determined MIC value had a MIC value 32 times smaller than the lower threshold of the defined empirical target range. For piperacillin, more than one fifth (21.2%) of the determined MIC values were within a 2-fold deviation and 93.9% within a 4-fold deviation from the selected empirical target. An overview of the observed MIC values independent of their pathogen is presented in Table 3.4 and a detailed overview of the detected pathogens and MIC values can be found in the supplementary (Table S2 and Table S3).

Table 3.4: Observed minimum inhibitory concentration (MIC) values independent of pathogen.

	Meropenem	**Piperacillin/Tazobactam**
	n (%)	n (%)
Patients with determined MIC	53 (49.1)	33 (34.4)
Unique[#] MIC determinations	60	33
MIC [mg/L]:		
≤0.25	45 (75.0*)	2 (6.06 *)
0.5	2 (3.33*)	-
1	2 (3.33 *)	-
2	2 (3.33*)	-
4	3 (5.00*)	24 (72.7*)
8	2 (3.33*)	5 (15.2*)
16	4 (6.67*)	1 (3.03*)
32	-	1 (3.03 *)

[#]if a second MIC determination in the same patient was equal to the first determination it was not considered in this table. *in relation to the number of unique MIC determinations (n=60 for meropenem, n=33 for piperacillin) ***Abbreviations:*** *MIC:* minimum inhibitory concentration, *n:* number of samples.

3.2.1.4 Target attainment assessment

Of the 356 meropenem samples with a reported antibiotic drug concentration, 127 (35.7%) were within the targeted concentration range, while 49 (13.8%) were below and 180 (50.6%) above. One in forty (2.5%) meropenem concentration measurements exceeded concentrations linked to an increased risk for neurotoxicity. For piperacillin, 109 of 216 (50.5%) measured drug concentrations were in the targeted concentration range, 32 (14.8%) below and 75 (34.7%) above. One in ten (10.2%) piperacillin concentrations exceeded the toxicity threshold.

For both drugs, concentration measurements from patients without a determined MIC value for the causative pathogen (i.e. empirical therapy) had a higher but yet unsatisfying proportion of target attainment (meropenem 56.8%, piperacillin 57.0%) than measurements with a determined MIC value (meropenem 20.6%, piperacillin 33.9%; Figure 3.5).

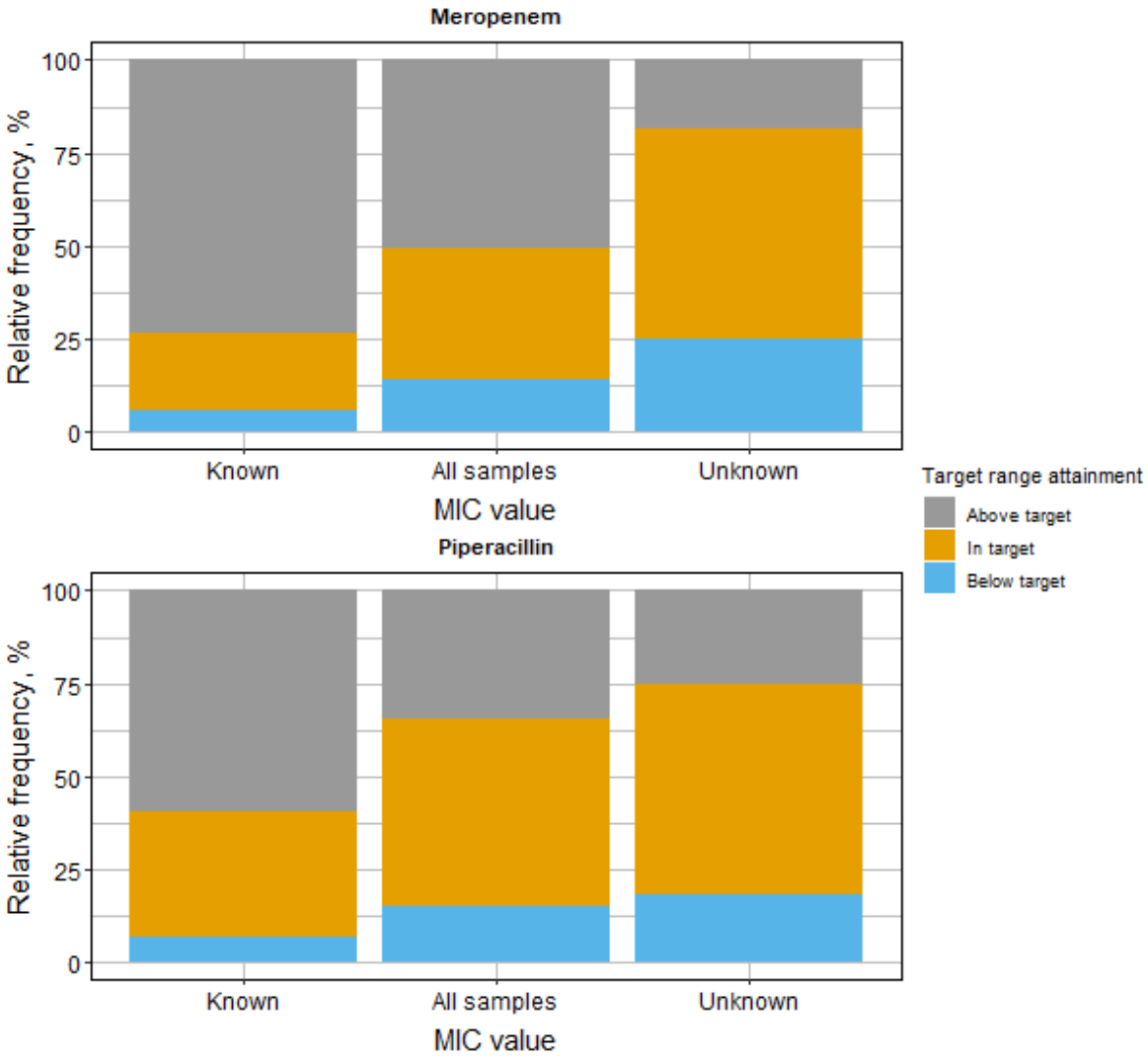

Figure 3.5: Target range attainment of minimum meropenem or piperacillin concentrations stratified by the availability of susceptibility data (MIC value) for the pathogen causing the infection.

Target range for the minimum drug concentration defined as 1-5xMIC. If no MIC values was determined an empirical target of 8-40 mg/L and 16-80 mg/L was used for meropenem and piperacillin, respectively.

Abbreviations: MIC: minimum inhibitory concentration

3.2.1.5 Target attainment assessment in different renal function groups

Target attainment (considering both samples with and without determined MIC value) significantly differed between patients with different renal functions (p-value < 0.01 for both drugs). Patients with severe renal impairment had a higher proportion of samples above the target (target attainment meropenem: 2.78% below, 13.9% in target, 83.3% above; target attainment piperacillin: 4.17% below, 29.2% in target, 66.7% above) compared to patients with augmented renal clearance (target attainment meropenem: 36.9% below, 44.0% in target, 19.0% above; target attainment piperacillin: 25.0% below, 47.2% in target, 27.8% above). The highest frequency of target attainment for both drugs was found in patients with 'normal' RF (49.2% for meropenem, 58.8% for piperacillin; Figure 3.6).

3.2.1.6 Drug concentrations in different target range groups

Neither for meropenem (p-value = 0.4) nor for piperacillin (p-value = 0.5) the measured drug concentrations stratified by their targeted concentration range differed significantly. A boxplot of the observed drug concentrations per targeted concentration range and drug can be found in the supplementary (Figure S3 and Figure S4).

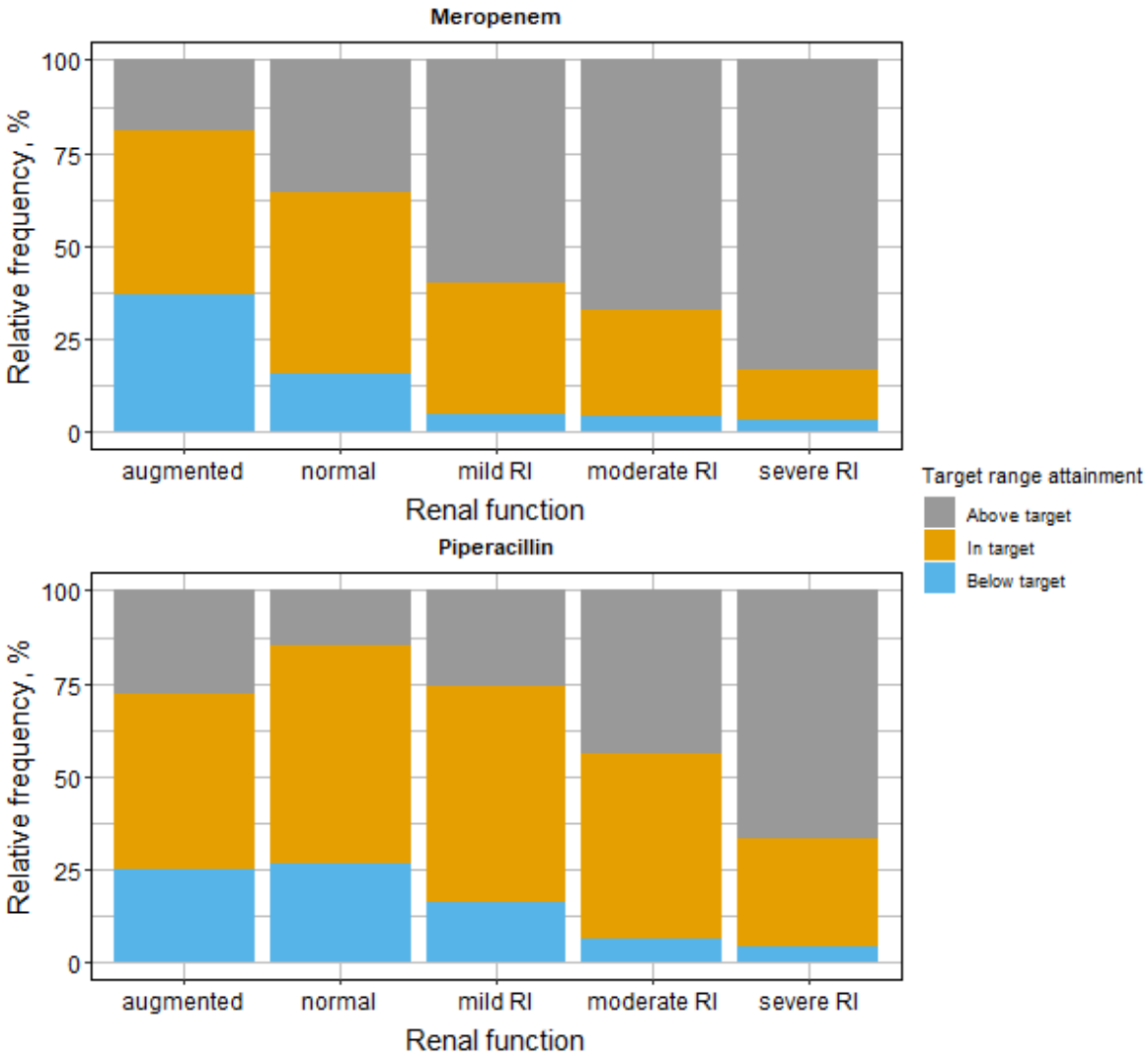

Figure 3.6: Target range attainment of minimum meropenem or piperacillin concentrations stratified by renal function.

Target range for the minimum drug concentration defined as 1-5xMIC. If no MIC values was determined an empirical target of 8-40 mg/L and 16-80 mg/L was used for meropenem and piperacillin/tazobactam, respectively.

Abbreviations: MIC: Minimum inhibitory concentration

3.2.1.7 Dosing adaptations

Dosing was adjusted in 6.18% and 4.63% of monitored drug concentrations for meropenem and piperacillin, respectively. While the majority of meropenem dosing adaptations were realised via a change in the administered dose (68.2%), piperacillin dosing was predominantly adjusted by modifying the dosing interval (90.0%) (Table 3.5). Dosing was not adapted for piperacillin after samples in the target range. The overall proportion of dosing adaptations following samples outside versus in the target range did not significantly differ for meropenem (p-value = 0.8) but differed for piperacillin (p-value = 0.005).

Table 3.5: Overview of dosing adaptations for meropenem and piperacillin.

Samples	**Dosing adaptations, n (%)**			
	All	Below target range	In target range	Above target range
Meropenem				
Total	22 (6.18*)	3 (6.12*)	7 (5.51*)	12 (6.67*)
Dose reduction	7 (31.8#)	0 (0#)	0 (0#)	7 (58.0#)
Dose increase	8 (36.4#)	3 (100#)	3 (43.0#)	2 (17.0#)
Dosing interval reduction	2 (9.09#)	0 (0#)	1 (14.0#)	1 (8.3#)
Dosing interval increase	2 (9.09#)	0 (0#)	1 (14.0#)	1 (8.3#)
Infusion duration reduction	2 (9.09#)	0 (0#)	1 (14.0#)	1 (8.3#)
Infusion duration increase	1 (4.54#)	0 (0#)	1 (14.0#)	0 (0#)
Piperacillin				
Total	10 (4.63*)	4 (12.5*)	0 (0*)	6 (8.00*)
Dose reduction	0 (0#)	0 (0#)	0 (0#)	0 (0#)
Dose increase	0 (0#)	0 (0#)	0 (0#)	0 (0#)
Interval reduction	4 (40.0#)	3 (75.0#)	0 (0#)	1 (17.0#)
Interval increase	5 (50.0#)	0 (0#)	0 (0#)	5 (83.0#)
Infusion duration reduction	1 (10.0#)	1 (25.0#)	0 (0#)	0 (0#)
Infusion duration increase	0 (0#)	0 (0#)	0 (0#)	0 (0#)

*in relation to the number of determined drug concentrations per column and antibiotic (see 3.2.1.4),
#in relation to the total number of dose adaptations.
Abbreviations: n: Number of samples.

3.2.2 Stage II: Developing and implementing a model-informed tabular meropenem dosing decision tool

3.2.2.1 Pharmacokinetic model selection and evaluation

Based on the high similarity of patient characteristics between the local study population (data collection up to September 2019) and the patient population underlying the PK model development (Table 3.6 and Figure 3.7) the PK model by Ehmann et al. was selected for further evaluation [129]. This two-compartment model with first-order elimination, a combined residual variability model, interindividual variability on clearance (CL) and both volumes of distribution and interoccasion variability on CL included a piecewise linear relation between $CLCR_{CG}$ and clearance (CL), a power relation between body weight and the central volume of distribution (V_1), and a linear relation between serum albumin concentration and the peripheral volume of distribution (V_2). Of these three covariates, Ehmann et al. demonstrated that only $CLCR_{CG}$ had a clinically relevant impact on PTA [129]. Therefore, for the development of the dosing tool the effect of $CLCR_{CG}$ on clearance was kept as the only covariate in the model and PK parameters were re-estimated for the new reduced PK model using the underlying dataset of the original full model [129].

Table 3.6: Comparison of relevant patient characteristics between the local study population and the population investigated by Ehmann et al. [129].

Patient characteristic	**Charité-Universitätsmedizin Berlin**	**Ehmann et al.**
Categorical	*n (%)*	*n (%)*
No. of patients	81	42
No. of meropenem samples	306	1376
Male	55 (67.9)	27 (56.3)
No. of patients with extracorporeal membrane oxygenation	8 (9.88)	6 (12.5)
Continuous [unit]	*Median (5^{th}-95^{th} percentile)*	*Median (5^{th}-95^{th} percentile)*
Age [years]	64.0 (40.0-81.0)	55.5 (32.0-69.9)
Weight [kg]	75.0 (48.0-116)	70.5 (47.4-121)
Creatinine clearance[#,*] [mL/min]	74.4 (24.7.-253)	80.8 (24.8-191)
Serum albumin concentration* [g/dL]	2.68 (2.00-3.60)	2.80 (2.20-3.56)

[#]Calculated using Cockcroft-Gault formula [169]. [*]Creatinine clearance and serum albumin concentration determined on sample level, all other characteristics on patient level.

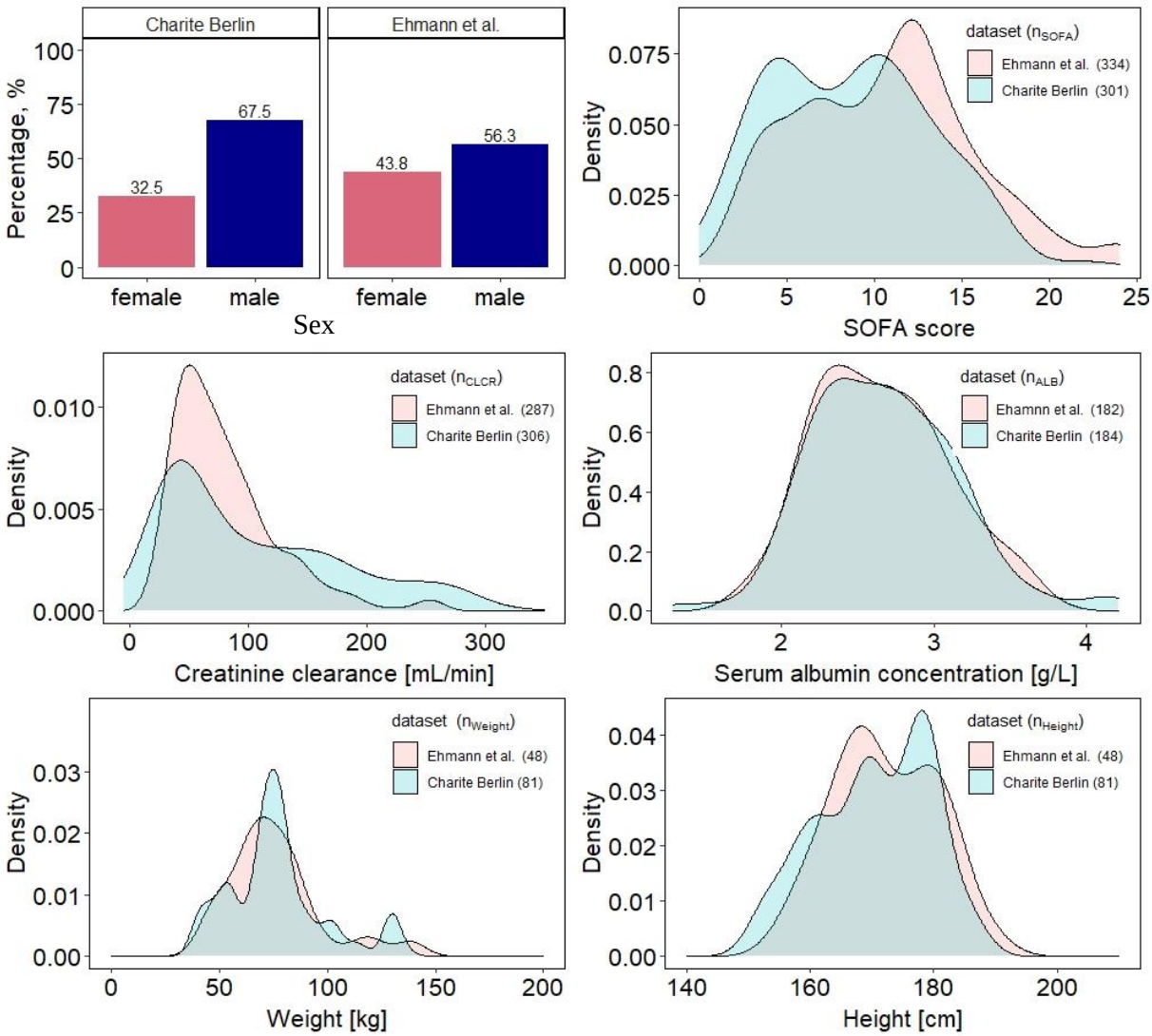

Figure 3.7: Comparison of relevant patient characteristics between the local study population labelled "Charite Berlin" and the population investigated by Ehmann et al [129].
Numbers in brackets represent the available number of data points.

The new reduced PK model was a two-compartment model with first-order elimination, interindividual variability on CL, V1 and V2, inter-occasion variability on CL and a combined proportional and additive residual variability model. CL was shown to linearly increase with increasing $CLCR_{CG}$ up to an inflection point of 154 mL/min where the maximum clearance was reached (Table 3.7). After parameter re-estimation an extensive internal model evaluation was conducted: Standard goodness-of-fit plots (see 2.3.3.1) indicated adequate model predictions and the VPC (see 2.3.3.3) revealed good predictive performance both for the typical trend and variability of the meropenem concentration-time profiles (Figure 3.8). Furthermore, the nonparametric bootstrap confirmed model robustness (convergence rate=90.4%) and narrow 95% confidence intervals for the parameter estimates (Table 3.7).

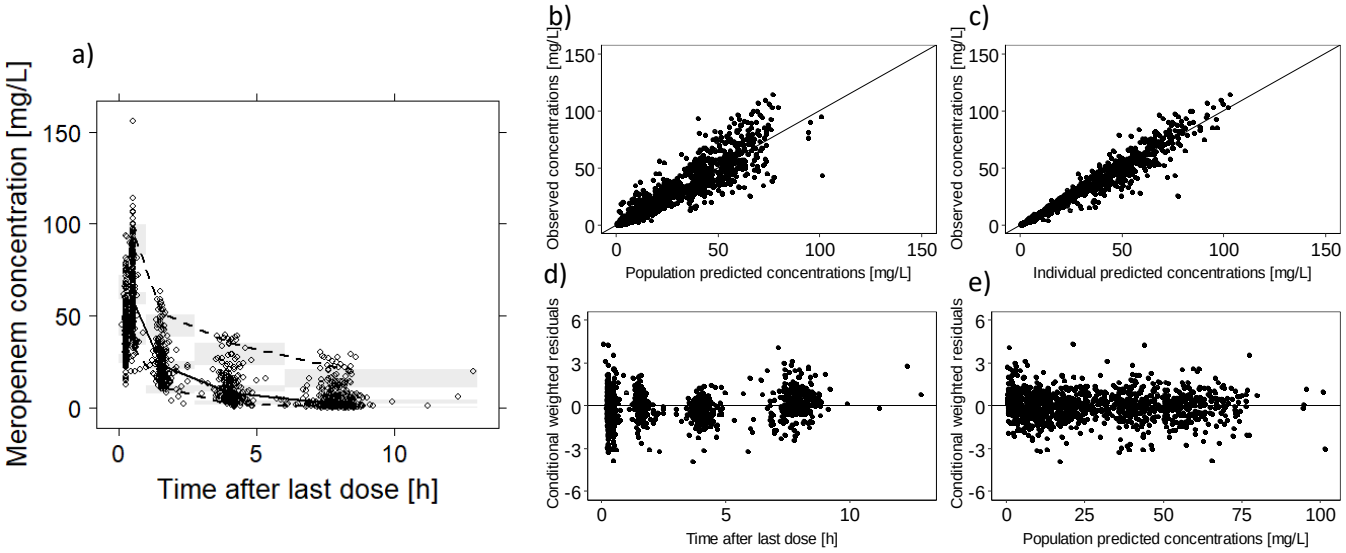

Figure 3.8: Visual predictive check (a) (n=1000 simulations) and goodness-of-fit plots (b)-e)) for the final reduced population pharmacokinetic model of meropenem.
a): *Circles*: Observations, *Lines*: 5th, 95th percentile (dashed), 50th percentile (solid) of the observed data. *Shaded areas:* 95% confidence interval around 5th, 50th and 95th percentile of simulated data. b, c: *Lines*: Line of unity. d, e: *Horizontal lines*: Reference lines at y=0.

Table 3.7: Parameter estimates for the reduced pharmacokinetic model of meropenem.

Parameter [unit]	Final model		Bootstrap[2]	
	Estimate (RSE, %)	95% CI[1]	Median	95% CI
Fixed-effects				
CL[3] [L/h]	9.25 (4.5)	8.43-10.1	9.29	8.39-10.2
V1 [L]	8.22 (11.8)	6.32–10.1	8.14	6.27-11.8
V2 [L]	28.3 (15.8)	19.5–37.1	28.7	11.4-37.6
Q [L/h]	16.3 (7.40)	13.9-18.6	16.2	12.3-18.7
$CLCR_{CG}$_CL[4]	0.00984 (9.10)	0.00808-0.0116	0.00993	0.00725-0.0113
$CLCR_{CG}$_INF [mL/min]	154 (7.20)	132-176	154	113-173
Interindividual variability				
ω CL, CV %	27.1 (19.5)	16.7-37.5	26.6	17.3-38.0
ω V1, CV %	41.5 (12.1)	31.7-51.3	40.7	27.1-53.0
ω V2, CV %	20.2 (15.0)	14.3 -26.1	20.1	12.1-28.9
Interoccasion variability[5]				
Κ CL, CV %	12.7 (12.4)	9.61-15.8	12.4	9.27-15.4
Residual variability				
σ Prop. (CV %)	16.5 (6.30)	14.5-18.5	16.4	14.2-18.6
Additive, SD [mg/L]	0.251 (26.1)	0.122-0.379	0.243	0.110-0.343

[1]Limits of 95% confidence intervals computed as: parameter estimate ± 1.96·SE; [2]Non-parametric bootstrap (n=1000) with a convergence rate of 90.4%; [3]CL for a patient with $CLCR_{CG}$ of 80,8 mL/min; [4]Change in CL in linear $CLCR_{CG}$-CL relationship for every mL/min change in $CLCR_{CG}$, centred to median in overall population (80.8 mL/min); [5]Occasion was defined as intensively monitored dosing interval.

Abbreviations: *CL*: Clearance; *V1*: Volume of central compartment; *V2*: Volume of the first peripheral compartment; *Q*: Intercompartmental clearance between V1and V2; $CLCR_{CG}$: Creatinine clearance estimated according to Cockcroft-Gault; $CCLCR_{CG}$_*CL*: $CLCR_{CG}$ effect on CL; $CLCR_{CG}$_*INF*: $CLCR_{CG}$ value serving as inflection point from which clearance is not longer increasing with increasing $CLCR_{CG}$ values; *CV*: Coefficient of variation; *Add*.: Additive; *Prop*.: Proportional; *SD*: standard deviation; *RSE*: relative standard error; ω: Random-effects parameters for interindivual variability; *K*: Random-effects parameter for interocassion variability, σ: Random-effects parameters for residual variability.

In Figure 3.9, prediction errors for 66 samples with drug concentrations were plotted against observed meropenem concentrations in the 34 ICU patients with full dosing history. The median prediction error across all observations was -1.2 mg/L, indicating a slight bias towards underprediction. The 50% prediction error interval ranging from -3.5 to +2.5 mg/L indicated acceptable precision for the ICU patient population the model was applied to with a single sample deviating by more then 50 mg/L (Figure 3.9). Other samples of the same patient showed acceptable prediction errors and therefore this suspected outlier sample was excluded from the subsequent NPDE analysis. While the overall NPDE distribution did not significantly differ from the standard normal distribution (global adjusted p-value: 0.0976, Fisher ratio test: 0.283 and Shapiro-Wilks test: 0.784, Table S4), the Wilcoxon signed-rank test revealed a significant (p-value 0.0325) deviation from a mean of 0 and therefore confirmed a small bias (NPDE mean: 0.296; Table S5) The graphical results of the NPDE analysis in the supplementary showed a random distribution of NPDEs versus time after therapy start and over the range of predicted concentrations (Figure S7).

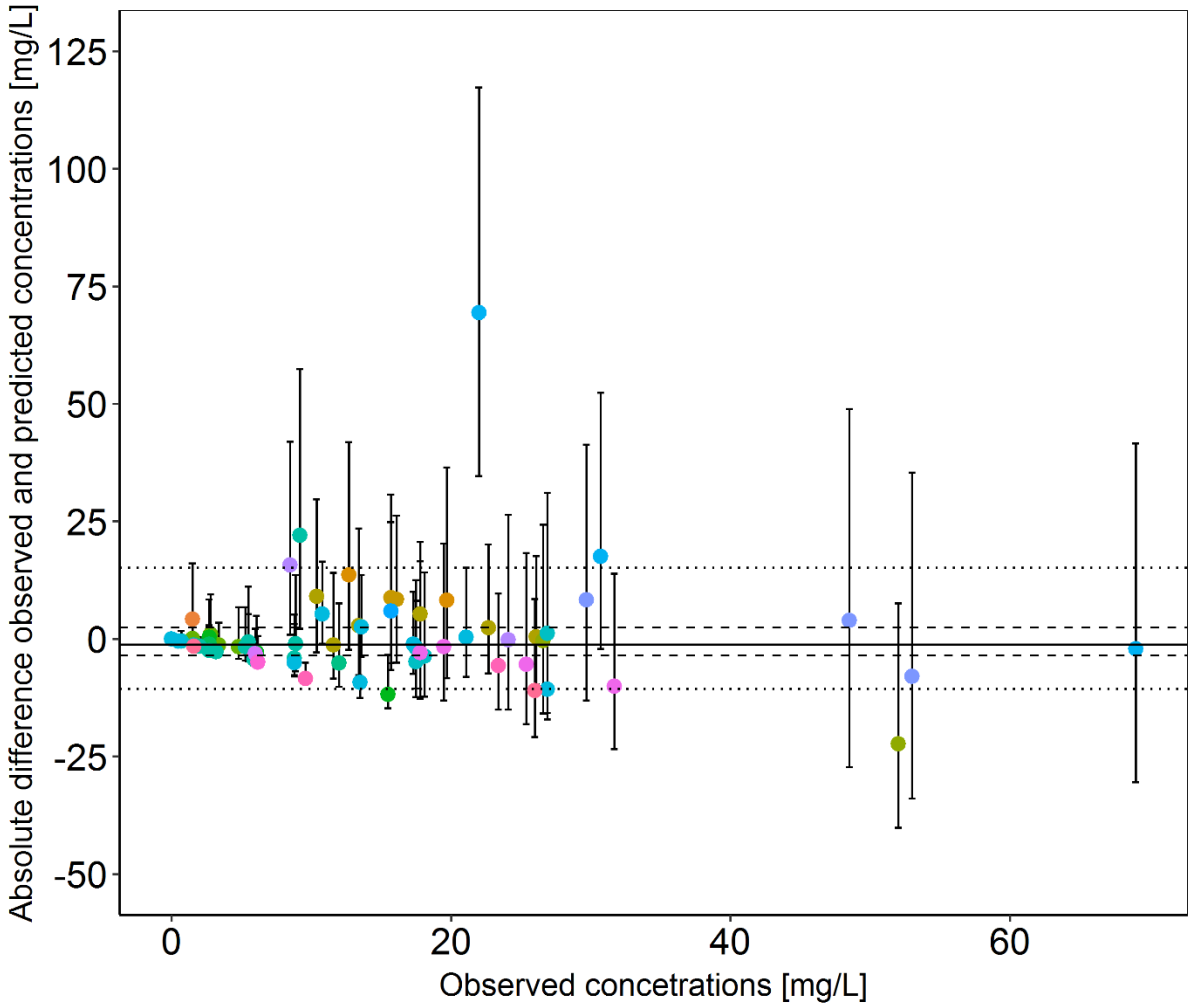

Figure 3.9: Absolute prediction error (mg/L) plotted against observed meropenem concentrations (n=66) when predicting concentration based on the reduced pharmacokinetic model for the patients from 'stage I' of the study with complete dosing history.
Points: median prediction error per sample. *Colors:* individual patients (i=34). *Error bar:* 90% prediction interval of prediction error per sample. *Solid horizontal line:* Median prediction error. *Dashed line:* 50% prediction interval of median prediction error. *Dotted line:* 90% prediction interval of median prediction error.

3.2.2.2 Development of the tabular dosing decision tool for meropenem

Selection and evaluation of dosing regimens

Based on their ease of integration into clinical routine, dosing regimens with infusion durations of 0.5, 4 and 24 hours, dosing intervals of 6, 8, 12 and 24 hours and meropenem doses as a multiple of 1000 mg were preselected. Deterministic simulations demonstrated that 2000 mg loading doses provided little further benefit over 1000 mg loading doses, the latter being sufficient to reach minimum meropenem concentrations above minimum meropenem concentrations at steady state (Figure 3.10A). Furthermore, short-term (0.5 h) infusions were inferior to prolonged infusions (4 h) with short-term infusions generally having unfavourable higher maximum and lower minimum concentrations for the same daily dose (Figure 3.10B). Consequently, dosing regimens with a 2000 mg loading dose and short-term infusions were not further considered for PTA analysis (Table 3.8). PTA analysis of the 15 remaining dosing regimens (Table 3.8) showed that for the same daily dose, prolonged (4 h) infusions reached higher PTA than continuous infusions due to higher targets for continuous infusions (Table S6). As illustrated, a patient with a CLCRCG=120 mL/min, a pathogen with MIC=8 mg/L and a daily dose of 8 g meropenem had a PTA of 75.0% receiving prolonged infusions and a PTA of 1.80% receiving continuous infusions. Furthermore, four-times-daily dosing was superior to three-times-daily-dosing (Table S6). As illustrated, a patient with a CLCRCG=120 mL/min, a pathogen with MIC=8 mg/L and a daily dose of 12 g meropenem achieved a PTA of 91.7% receiving four-times-daily dosing or versus a PTA of 58.0% receiving three-times-daily-dosing. For pathogens with MIC≥8 mg/L in patients with augmented renal clearance (≥150 mL/min) none of the investigated dosing regimens reached a PTA≥90%.

After the analysis, dosing recommendations stratified by patient's $CLCR_{CG}$ and determined MIC were summarized in a simple tabular model-informed dosing tool (Figure 3.11). Detailed results (PTA, probability of minimum meropenem concentration in target range, distribution of minimum concentrations) for each investigated dosing regimen and one exemplary MIC value (8 mg/L) can be found in the supplementary Table S6.

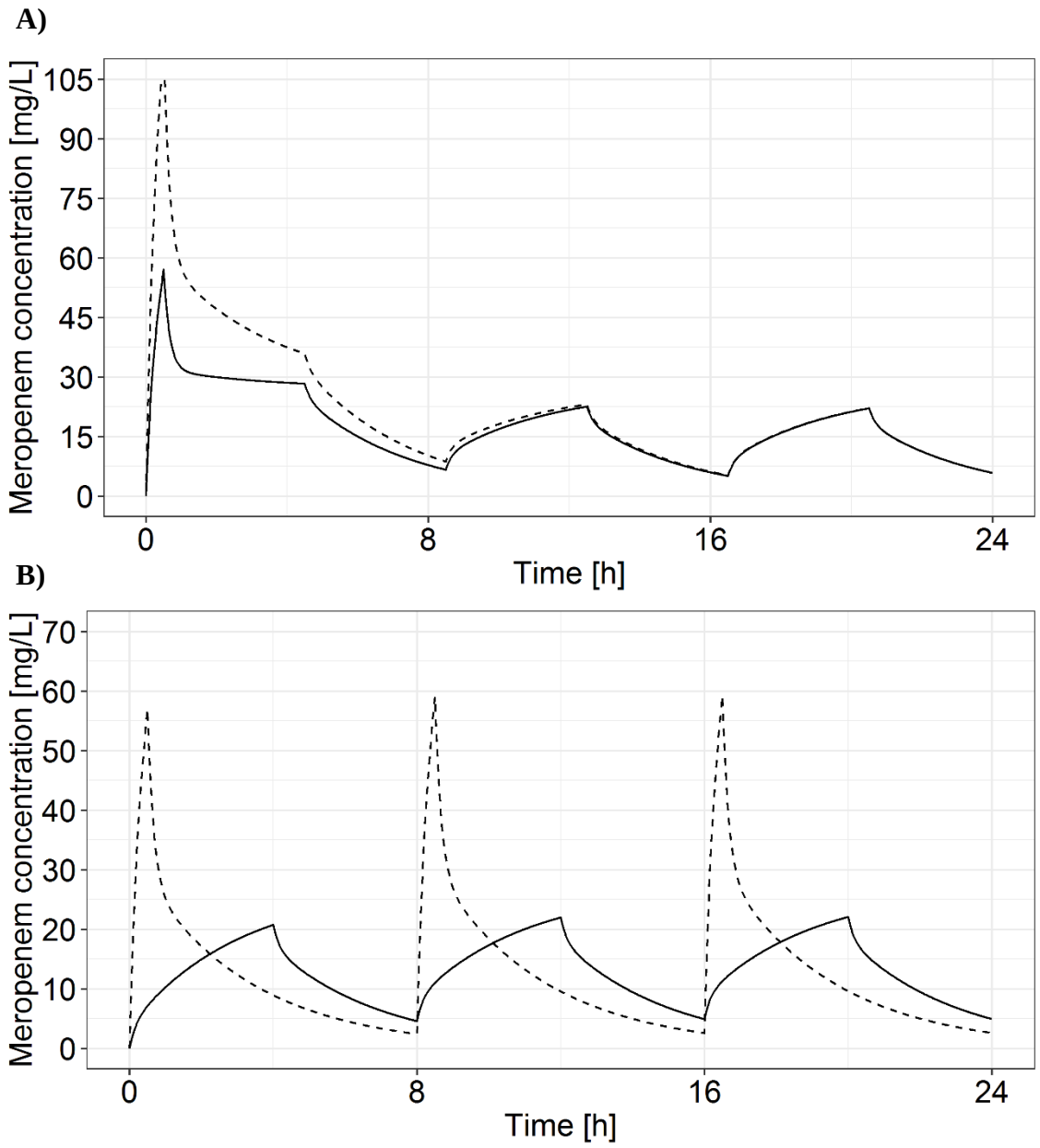

Figure 3.10: Predicted meropenem concentration-time profiles based on deterministic simulations using the reduced population pharmacokinetic model for a patient with a creatinine clearance of 80.8 mL/min. A) After either a 1000 (solid line) or a 2000 mg (dashed line) loading dose followed by prolonged (4 h) 1000 mg meropenem infusions with a dosing interval of 8 h. B) After either a short-term (0.5 h; dashed line) or a prolonged (4 h; solid line) 1000 mg meropenem infusions administered every 8 h.

Table 3.8. Meropenem dosing regimens investigated in probability of target attainment analysis for potential inclusion in the tabular dosing decision tool.

Dosing regimen	Dose per infusion [mg]	Infusion duration [h]	Dosing Interval [h]	Total daily dose [mg]
1	1000	4	6	4000
2	1000	4	8	3000
3	1000	4	12	2000
4	2000	4	6	8000
5	2000	4	8	6000
6	2000	4	12	4000
7	3000	4	6	12000
8	3000	4	8	9000
9	3000	4	12	6000
10	4000	4	6	16000
11	4000	4	8	12000
12	4000	4	12	8000
13	4000	24	24	4000
14	6000	24	24	6000
15	8000	24	24	8000

Grey shading: Dosing regimen ultimately implemented in the developed tabular dosing tool.

Integration of locally available pathogen information

If the pathogen and its MIC value are not known at the time of dosing selection, two options are implemented in the dosing tool: An empirical dosing regimen based on non-species related EUCAST breakpoints for meropenem or a dosing regimen based on the LPIFR metric and pathogen-independent MIC distribution data from ‘stage I’ of the study. A short summary of both options was added on the backside of the dosing decision table (Figure 3.12). Compared to targeting the pathogen independent ‘susceptible/susceptible at increased exposure’ (2 mg/L) or the ‘susceptible at increased exposure/resistant’ (8 mg/L) EUCAST breakpoints, the LPIFR substantially reduced the drug exposure in patients, while still assuring a desired percentage of 90% of patients being above the PK/PD target of 98%$T_{> MIC}$. Based on the LPIFR the daily dose for a patient with unknown pathogen and MIC and a creatinine clearance of 120 mL/min was 4000 mg whereas there was a three-fold higher dose of 12000 mg when the current recommendation at Charité-Universitätsmedizin Berlin (see 2.6.3) was followed and a meropenem concentration above the EUCAST susceptible at increased exposure/resistant breakpoint (8 mg/L) was targeted.

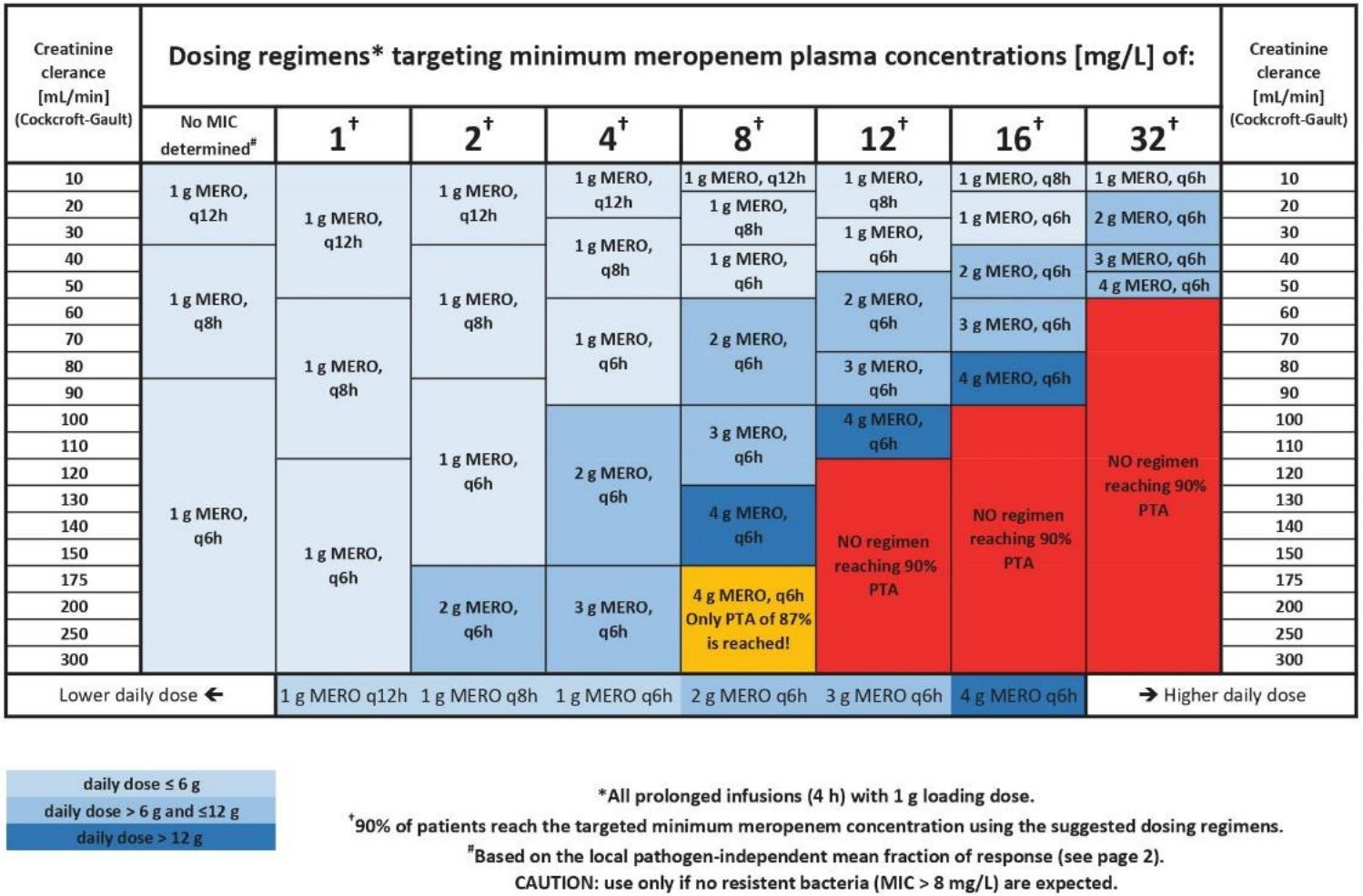

Figure 3.11: Front page of the developed tabular dosing decision tool for initial meropenem dosing in intensive care patients.
Dosing recommendations are stratified for creatinine clearance according to Cockcroft and Gault and target (Local pathogen-independent mean fraction of response (LPIFR, see 2.6.6.2) in column "No MIC determined" or minimal meropenem concentration in columns "1" to "32")
Abbreviations: *MERO:* Meropenem; *q6h:* Every 6 h dosing ; *q8h;* Every 8 h dosing; *q12h*: Every 12 h dosing; *PTA:* Probability of target attainment; *MIC:* Minimum inhibitory concentration.

Options if MIC is unknown:

1. Targeting the EUCAST breakpoints
(2 mg/L susceptible/intermediate and
8 mg/L intermediate/resistent)

NOTE: Targeting 8 mg/L leads to high concentrations in all patients. Figure 1 shows the predicted distribution of minimum meropenem plasma concentrations in patients with a creatinine clearances of 70 mL/min (median of the observed clearances at Charité-Universitätsmedizin Berlin in 2019) receiving 2 g meropenem every 6 h. More than 90% of the patients reach the target of 8 mg/L (blue line). At the same time the minimum meropenem concentration of more than 81% of the patients are above 16 mg/L.

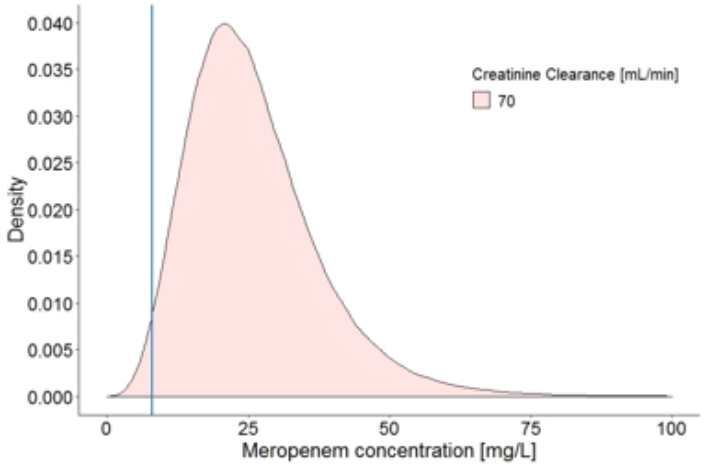

Figure 1: Distribution of simulated meropenem minimum concentrations at steady state. 500 000 virtual patients with a creatine clearance of 70 mL/min receiving 2 g meropenem every 6 hours as a prolonged (4 h) infusion, blue line represents the target of 8 mg/L.

2. Targeting the distribution of MIC values present at at Charité-Universitätsmedizin Berlin in 2019

In figure 2 the MIC distribution of patients receving Meropenem at Charité-Universitätsmedizin Berlin in 2019 is shown. The suggested dosing regimens for patients without determind MIC have a probabillity of ≥90 % to be over a randomly choosen MIC from this distribution.

CAUTION: ONLY USE IF NO RESISTANT BACTERIA ARE EXPECTED!

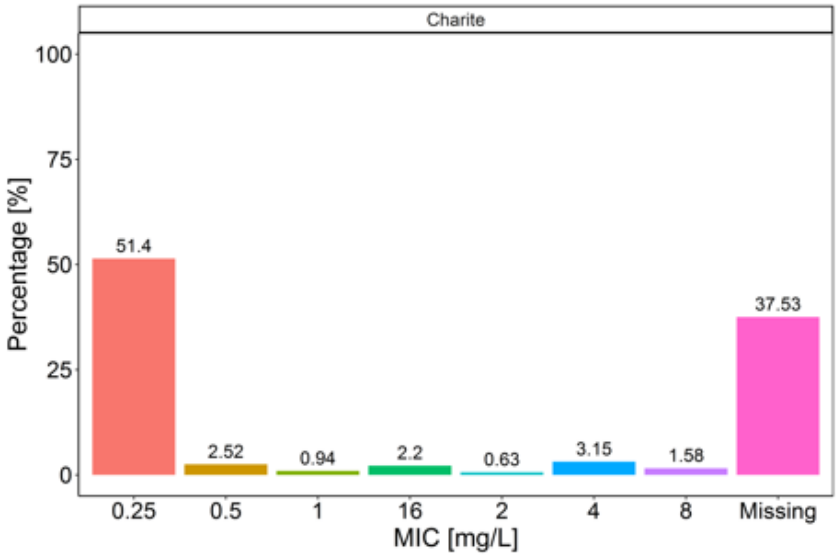

Figure 2: Distribution of observed minimal inhibitory concentrations of different bacteria in patients treated with meropenem at the Charite in 2019.

Figure 3.12: Back page of the developed dosing decision tool for initial meropenem dosing in intensive care patients.
Abbreviations: *MIC:* Minimum inhibitory concentration.

3.2.2.3 Retrospective evaluation of the dosing decision tool

Out of 306 meropenem samples collected during ‘stage I’ of the study, 46 (15.0%) were found to be below and 160 (52.3%) to be above the defined target range. The retrospective application of the developed tool recommended a change in dosing for the majority (77%) of patients with concentrations observed outside the target range (Figure 3.13). For 72% of the patients with minimum meropenem concentration below the target range the developed dosing tool recommended an increased daily dose, while for 78% of the patients with samples above the target range a lower daily dose was recommended.

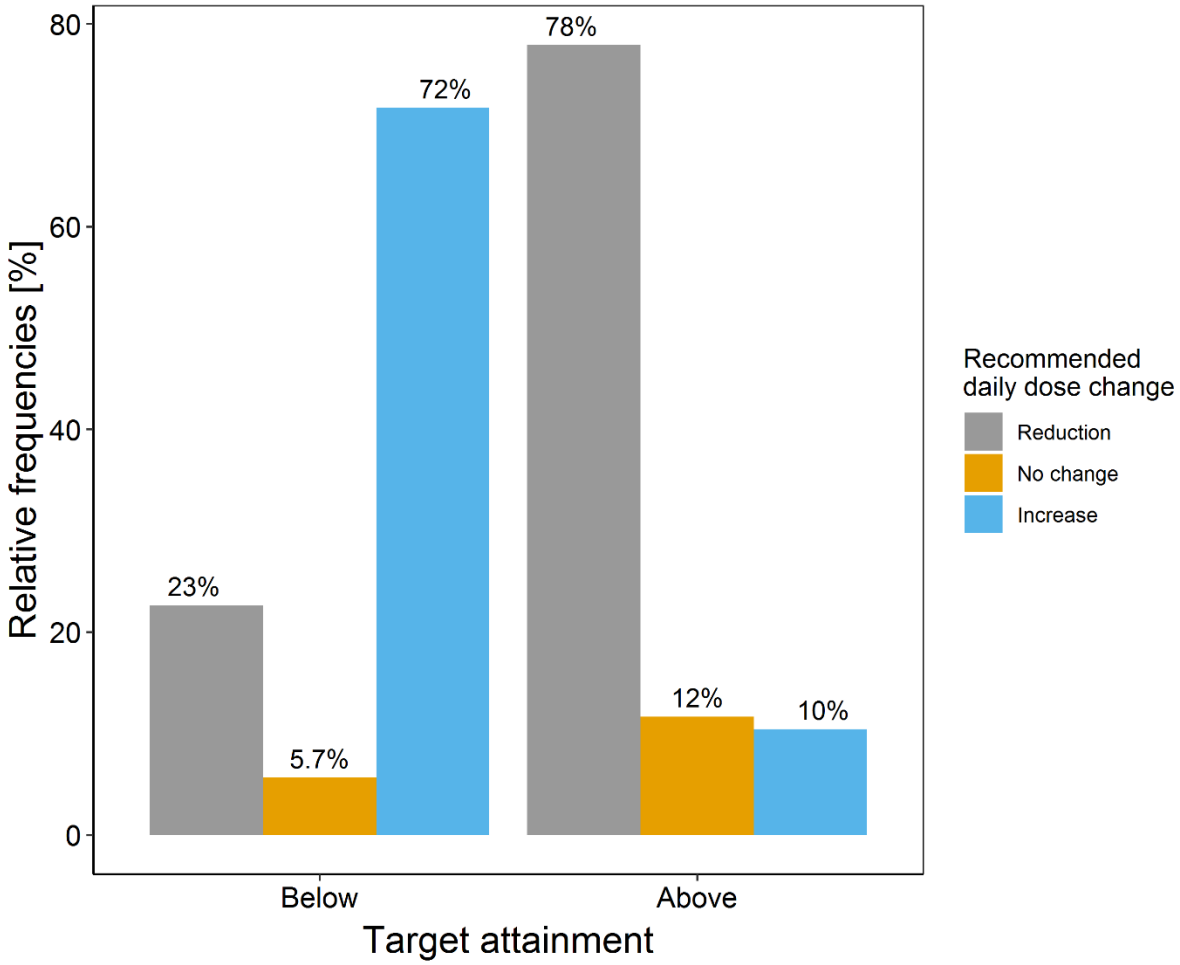

Figure 3.13: Frequency of daily meropenem dose adjustments by comparing the recommended daily dose to the actual administered daily dose at Charité-Universitätsmedizin Berlin, stratified by non-attainment of the target range of the administered dosing regimen.
Out of 306 samples 46 were below and 160 above the target range.

3.2.3 Stage III: Developing and implementing an interactive model-informed dosing software

3.2.3.1 Pharmacokinetic model selection and evaluation

For meropenem the evaluated PK model (see 3.2.2.1) underlying the tabular model-informed dosing decision tool developed in 'stage II' was selected for integration into the interactive model-informed dosing software.

For piperacillin five PK models were identified by the literature research for further evaluation (Table 3.9) [50,175–178]. Mean arterial blood pressure (MABP) implemented as a linear covariate on clearance in the PK model by Sukarnjanaset et al. was not available in the dataset and as a consequence MABP was fixed to the median value reported by Sukarnjanaset et al. The first evaluation step revealed a widely varying predictive performance between the five PK models: the observed bias, i.e. the median prediction errors, ranged between -32.0 mg/L and +15.3 mg/L (median relative prediction error -87.5% and +51.4%, respectively) and the imprecision, i.e. absolute median prediction errors, between 18.0 mg/L and 48.9 mg/L (absolute median relative prediction error 65.0% and 97.6%, respectively) (Table 3.10). The two-compartment PK model integrating creatinine clearance and mean arterial blood pressure as influential covariates on clearance and adjusted body weight on the central volume of distribution by Sukarnjanaset et al. [50] showed the best predictive performance (bias: -2.73 mg/L (-10.9%), imprecision: 20.2 mg/L (60.3%)) but a bias to underpredict high (>100 mg/L, 16.7% of documented concentrations) piperacillin concentrations (Figure 3.14, all other PK models Figure S8-Figure S11). The individual piperacillin concentration-time profile predicted by the PK model by Sukarnjanaset et al. [50] overlaid by the observed piperacillin concentrations for every patient (supplementary Figure S12) revealed well predicted individual concentrations with 82.2% of concentration measurements within the 90% prediction intervals. As best performing of the five models it was selected for the second evaluation step.

Table 3.9: Overview of identified published piperacillin pharmacokinetic models included in the model evaluation and compared to the local patient population at Charité-Universitätsmedizin Berlin.[50,175–178].

	Sukarnjanaset et al.	**Andersen et al.**	**Öbrink-Hansen et al.**	**Roberts et al.**	**Li et al.**	**Charité Berlin**
Clinical study characteristics						
No. of patients	48	22	15	16	56	46
Type of infusion	Intermittent	Intermittent	Intermittent	Intermittent/ continuous	Intermittent/ continuous	Intermittent
No. of PK samples/day	5	2-3	8	10-17	5	1
Patient characteristics						
Disease	Critically ill with septic shock	Sepsis	Critically ill with septic shock	Critically ill with sepsis	Complicated intra-abdominal infection	Intensive care unit patients
CREA [mg/dL]	1.1 (0.7-1.5)[1]	1.09 (0.74-1.49)[1]	1.92 (1.34-3.19)[1]	-	II: 0.9 (0.5-2)[2] CI: 1 (0.5-1.8)[2]	0.98 (0.71-1.50)
CLCR [mL/min]	54.9 (41.6-86.5)[1]	83.9 (46-152) [1]	-	II: 88.3 (53.3-101)[1] CI: 96.7 (31.7-148.3)[1]	II: 84 (36-136)[2] CI: 93 (22-150)[2]	71.1 (46.2-109.5)
TBW [kg]	56.6 (49.6-69.5)[1]	76 (64-82)[1]	80 (70.2-95)[1]	II: 80 (74-86)[1] CI: 73 (64-83)[1]	II: 82.6 (55-136)[2] CI: 80 (55.5-115)[2]	76.0 (49.6-128.3)
ABW [kg]	56.0 (48.1-65.0)[1]	-	-	-	-	-
MABP [mmHg]	68 (61-75)[1]	-	-	-	-	-
Pharmacokinetic model characteristics/parameters						
No. of compartments	2	2	2	2	1	
CL [L/h]	5.37*	8.58*	3.6*	17.1[#]	14.8*	
V1 [L]	9.35*	12.4	7.3*	7.2	22.3*	
V2 [L]	7.77	3.48	3.9	17.8	-	
Q [L/h]	21.3	3.54	6.58	52	-	
Covariate relations	CLCR and MABP as linear function on CL, ABW as linear function on V1	CLCR as linear function on CL	CREA as linear function on CL	TBW as linear function on CL	CLCR as linear function on CL, TBW as linear function on V1	
Interindividual variability model	CL, V1	CL	CL, V1	CL, V1, Q, V2	CL, V1	
Residual variability model	Proportional	Proportional	Proportional	Additive + proportional	Additive + proportional	

Abbreviations: CL: Clearance; Q: Intercompartmental clearance; V1: Central volume of distribution; V2: Peripheral volume of distribution, CREA: Serum creatinine concentration, CLCR: Creatinine clearance, TBW: Total body weight, MABP: Mean arterial blood pressure, ABW: Adjusted body weight, II: Intermittent infusion, CI: Continuous infusion
[1]Patient characteristics reported as median (IQR), [2]Patient characteristics reported as median (range)
*Population parameter reported for the median patient characteristics of the model development dataset, [#]Population parameter reported for a weight of 70 kg

Table 3.10: Predictive performance of the literature-identified piperacillin pharmacokinetic models applied to the local patient population [50,175–178].

	Sukarnjanaset et al.	**Andersen et al.**	**Öbring-Hansen et al.**	**Roberts et al.**	**Li et al.**
Bias* [mg/L] (%)	-2.73 (-10.9)	-12.9 (-52.1)	+15.3 (51.4)	-26.0 (-82.6)	-32.0 (-87.5)
Precision# [mg/L] (%)	20.2 (60.3)	18.0 (65.0)	48.9 (97.6)	27.7 (86.0)	34.0 (91.5)

*Bias calculated as median prediction error (see 2.3.3.4).
#Precision calculated as median absolute prediction error (see 2.3.3.4).

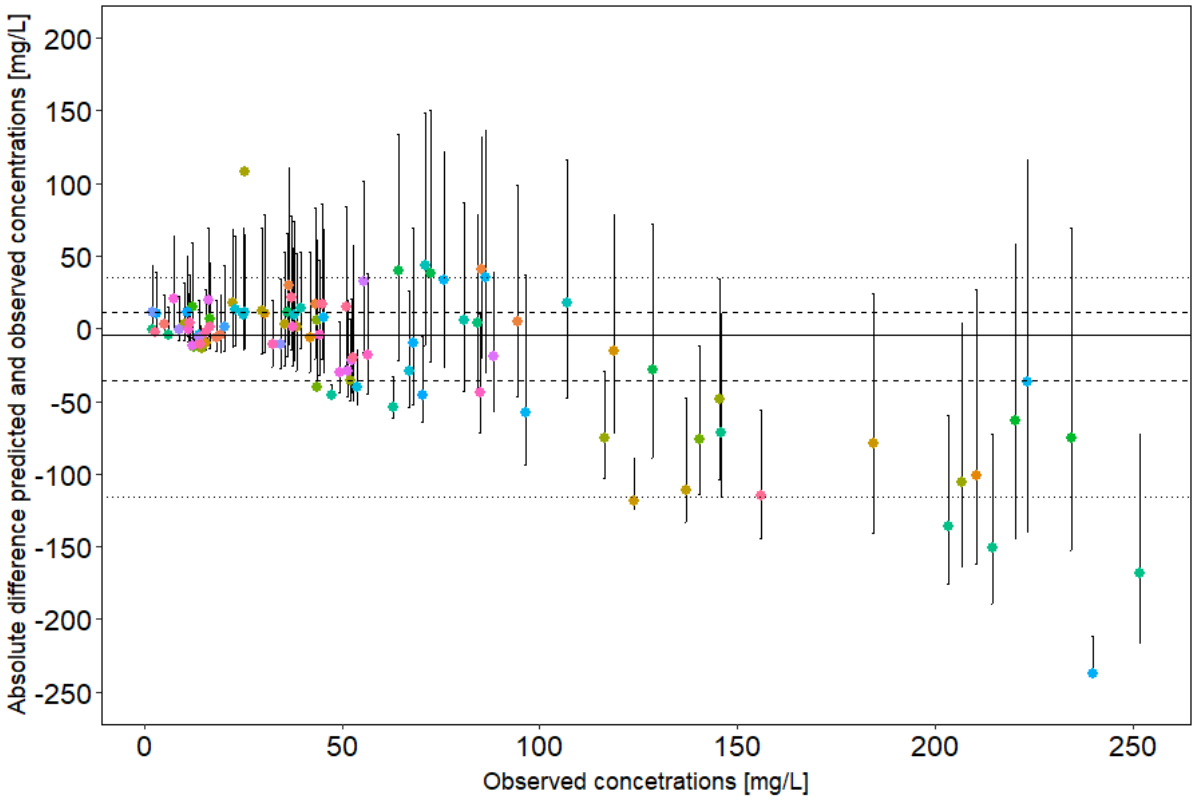

Figure 3.14: Absolute difference between predicted and observed concentrations (prediction error) (mg/L) plotted against observed piperacillin concentrations (n=90) when predicting concentration employing the pharmacokinetic model by Sukarnjanaset et al. [50]
Points: median prediction error per observed concentration. *Colours:* individual patients (i=46). *Error bar:* 90% prediction interval of prediction error per sample. *Solid horizontal line:* median prediction error. *Dashed line:* 50% prediction interval of median prediction error. *Dotted line:* 90% prediction interval of median prediction error.

The step-wise MAP estimation improved the predictive performance of the selected model: The observed bias was reduced by 78.8% from -2.73 mg/L to -0.58 mg/L while the precision was reduced by 21.8% from 20.2 mg/L to 16.0 mg/L. In Figure 3.15 the deviation of the median prediction based on the prior (star) and on the posterior (point) and their respective 90% prediction interval (error bars) from the observed concentrations are displayed. After MAP estimation the model was still biased to underpredict high observed concentrations (>100 mg/L) and the spread around no prediction error was not noticeably reduced compared to Figure 3.14 highlighting the small increase in precision.

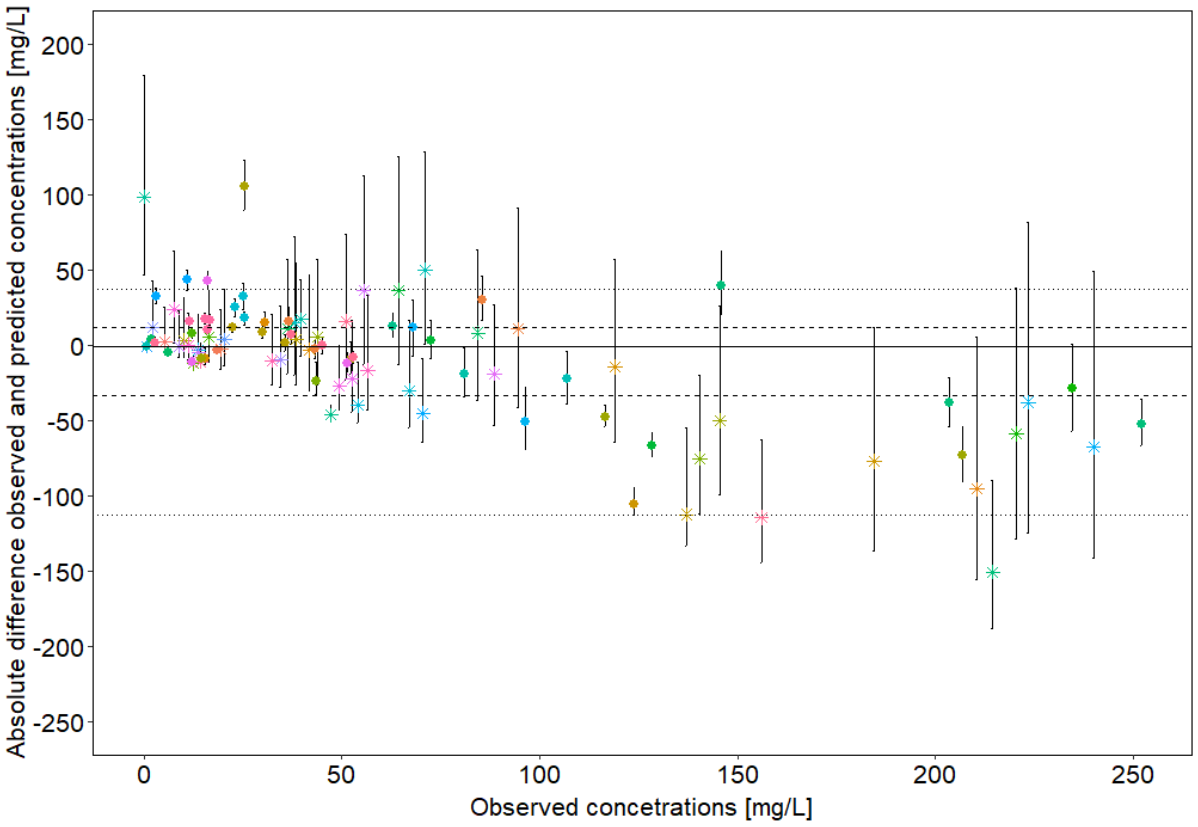

Figure 3.15: Absolute difference between predicted and observed concentrations (prediction error) (mg/L) plotted against observed piperacillin concentrations (n=90) when predicting concentrations employing the pharmacokinetic model by Sukarnjanaset et al. [50] and maximum a-posteriori estimation of preceding samples for the data in the subdataset.
Stars: median prediction error per observed concentration based on prior distribution, *Points:* median prediction error per observed concentration based on posterior distribution. *Colors:* individual patients (i=46). *Error bar:* 90% prediction interval of prediction error per sample. *Solid horizontal line:* median prediction error. *Dashed line:* 50% prediction interval of median prediction error. *Dotted line:* 90% prediction interval of median prediction error.

3.2.3.2 The DoseCalculator

Within the interprofessional collaboration two major features were identified for a successful MIPD software software in clinical routine: First, a clear, intuitive user interface including a comprehensible and informative ranking output of the investigated dosing regimens. Second, the ability to select the appropriate dosing regimen for each patient based on (i) a patient's characteristics and if available prior antibiotic concentration measurements and (ii) the current level of knowledge about the infecting pathogen.

(i) Developed user interface and visualisation of analysis results

In Figure 3.16 a screenshot of the developed dosing software, the DoseCalculator, is displayed. The user interface of the DoseCalculator is separated into 2 main sections:

1) Input module: On the left side of the interface is an input module for entering information about the selected antibiotic agent, the infecting pathogen, the PK/PD target and the patient by the user (highlighted here by the green box in Figure 3.16). The input module also includes buttons to start and reset the analysis and to download (as .csv file) and re-upload the entered data for further analyses to enable a quick and easy follow-up for each individual patient over multiple dosing cycles. After entering/uploading the required information and clicking the "Start analysis"-button, a pop-up window with commonly used dosing regimens appears (Table S12). The user can select dosing regimens from the pop-up window and/or add additional dosing regimens to be included in the analysis.

2) The results of the PK/PD target attainment analysis are displayed in three output sections in the main window:

1. Dosing recommendation: In a brightly coloured box on the top of the interface (highlighted here by the orange box in Figure 3.16), the highest ranked dosing regimen for a specific patient and PK/PD target is prominently presented.

2. Detailed analysis results: Below graphical illustrations of the results are displayed (highlighted here by the blue box in Figure 3.16 for a patient with known pathogen but unknown MIC value, and without antibiotic drug measurements). By default, the predicted concentration-time profile (median and 90%, 95% and 99% prediction intervals, left plot in the highlighted blue box) and the distribution of predicted minimum drug concentration (including the median prediction, right plot in the highlighted blue box) are shown for the recommended dosing regimen and the individual patient. Furthermore, both plots displayed in the default setting (i.e. the predicted concentration-time profile and the predicted distribution of minimum concentrations), the EUCAST distribution of MIC values for the selected pathogen and the results of the MAP analysis can be selected and displayed separately by selecting the

tabs highlighted by the black box in Figure 3.16. If the analysis is conducted based on the results of the MAP estimation both the stochastic simulations based on the prior and the posterior are displayed in all graphical illustrations.

3. A ranking table of all dosing regimens included in the analysis and their numeric results (i.e. probability to reach the PK/PD target, daily dose and, if selected, probability to exceed the toxicity threshold) can be found below the graphical results. Dosing regimens attaining the PK/PD target in ≥90% of simulations are considered adequate and are further ranked according to lower probability of minimum concentrations exceeding a user-defined toxicity threshold (if selected by the user) and subsequently by lower total daily dose. By selecting an alternative dosing regimen in the ranking table the box on the top displaying the selected dosing regimen and the graphical output are updated to show the results of the dosing regimen now selected by the user.

(ii) Integration of patient characteristics and concentration measurements

All analyses and subsequent dosing recommendations are adapted to patient-specific factors: Patient characteristics with a high impact on the pharmacokinetics of the selected antibiotic drug (e.g. $CLCR_{CG}$), and if available, observed drug concentrations and the preceding dosing history, are included in the analysis. If antibiotic concentration measurements are supplied, the subsequent analysis is conducted based on MAP estimation and stochastic simulation of the posterior PK parameter distribution. To ensure that very high or very low concentration measurements potentially associated with non-patient related inaccuracies do not result in inadequate and potentially dangerous dosing recommendations, a warning was integrated and is displayed if the observed concentration is outside the 95% prediction interval of the observed dosing.

(iii) Integration of currently available knowledge about the infecting pathogen

For each of the three knowledge levels about the pathogen identified (pathogen un-/known, MIC determined/not determined), an appropriate method to calculate the probability of a dosing regimen to reach the user-defined PK/PD target was implemented.

Knowledge level 1 - pathogen unknown and thus MIC unknown: a local pathogen-independent mean fraction of response (LPIFR, see 3.2.2.2) analysis was included based on the local MIC distribution, i.e. at the Charité-Universitätsmedizin Berlin (see 3.2.2.2).

Knowledge level 2 - pathogen known but MIC unknown: the EUCAST-reported MIC value distribution of the selected pathogen was used for a cumulative fraction of response (CFR) analysis (see 2.3.4.2). To reduce the risk of erroneously treating a pathogen unsuitable for meropenem or

piperacillin/tazobactam therapy instead of changing the antibiotic drug, only pathogens with a clear recommendation of meropenem or piperacillin/tazobactam treatment by the local AMS team were included in the DoseCalculator.

Knowledge level 3- pathogen and MIC known: If the MIC value had been determined, it was considered to be the most informative indicator of the susceptibility of a pathogen and becomes the preselected target antibiotic concentration for a probability of target attainment (PTA) analysis (see 2.3.4.2). Additionally, the target antibiotic concentration can be increased or decreased by the user to account for particular circumstances of a patient (e.g. site of infection, severity of illness). For all three scenarios, the preselected PK/PD target value of 99%fT>MIC can be adjusted without restriction between 0% and 99%.

Figure 3.16: Display of graphical user interface of the DoseCalculator after performing cumulative fraction of response analysis for a specific patient. *Green box:* Input module for Patient and treatment information, *Orange box:* Recommended dosing regimen , *Blue box:* Detailed illustration of results: predicted concentration-time profile (left figure) and distribution of predicted minimum concentrations at steady state (right figure) for the recommended dosing regimen in the specific patient; *Black box:* Tabs to individually display the result of the MAP estimation, the MIC distribution of a pathogen, the concentration-time profile or the distribution of minimum concentrations.Example for illustration: *Antibiotic:* Meropenem, *Patient and microbiological data*: Creatinine clearance = 70 mL/min, infected with *Pseudomonas aeruginosa* and MIC value not determined, *PK/PD target:*99% $fT_{>MIC}$

3.2.3.3 Assessment of the potential of the DoseCalculator using real patient data

For knowledge level 3, i.e. pathogen and MIC known, the dosing regimens recommended by the DoseCalculator for meropenem therapy, led to a >3 times increase (28.6% vs. 92.0%) in predicted target attainment compared to the documented dosing at Charité-Universitätsmedizin Berlin (Table 3.11) while reducing the daily dose by a median of 77.8%. For piperacillin, a smaller increase in predicted target attainment (16.7% vs. 23.3%) was observed if the DoseCalculator was restricted to select only from the dosing regimens currently available at Charité-Universitätsmedizin Berlin implemented in the software (supplementary Table S12). However, including further dosing regimens (supplementary Table S13) into the DoseCalculator increased the predicted target attainment >5 times (16.7% vs. 84.4%) compared to the documented dosing (Table 3.11) and reduced the daily dose by a median of 83.4%. The target-normalised (i.e. MIC-normalised) predicted antibiotic concentrations including the 90% prediction interval for the observed and recommended dosing regimens (Figure 3.17-Figure 3.19) demonstrated that samples outside the target range were closer to the target range for the dosing regimen recommended by the DoseCalculator compared to the documented dosing.

Table 3.11: Predicted median antibiotic concentrations in relation to target range either by the dosing regimen selected/recommended by the DoseCalculator or documented meropenem and piperacillin dosing regimens.

Based on:	**Predicted median antibiotic concentrations in relation to target range**					
	Below	In	Above	Below	In	Above
	Meropenem, % (n)			Piperacillin, % (n)		
Documented dosing regimens	27.0 (17)	28.6 (18)	44.4 (28)	8.89 (8)	16.7 (15)	74.4 (67)
DoseCalculator selected dosing regimens*	0 (0)	92.0. (58)	7.90 (5)	0 (0)	23.3 (21)	76.7 (69)
DoseCalculator selected dosing regimens including additional dosing regimens currently not available at Charité-Universitätsmedizin Berlin#	-	-	-	0 (0)	84.4 (76)	15.6 (14)

*Included dosing regimens in Table S12.
#Included dosing regimens in Table S13.

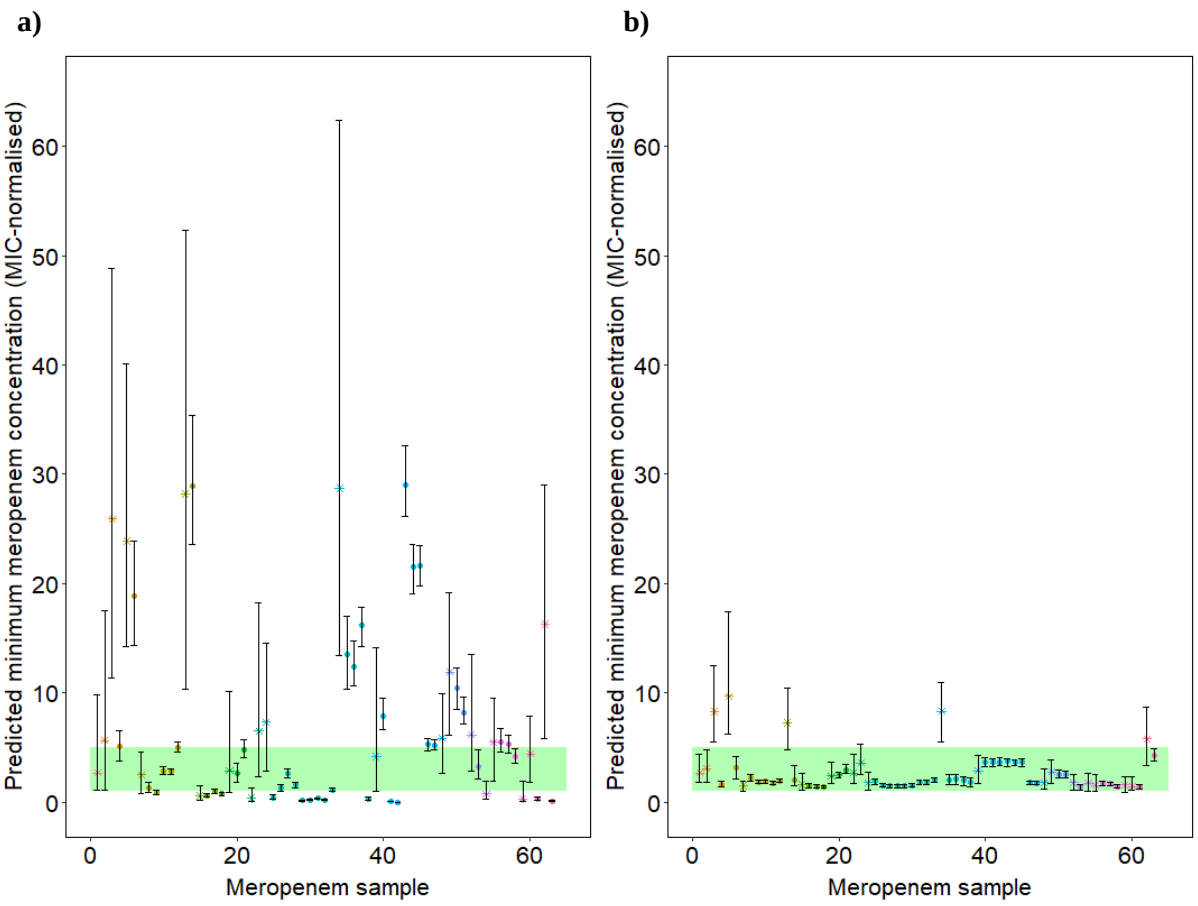

Figure 3.17: MIC-normalised predicted meropenem concentrations for the dosing regimens documented at Charité-Universitätsmedizin Berlin (a) and recommended by the DoseCalculator (b). *Stars:* median prediction based on prior distribution, *Points:* median prediction based on posterior distribution.. *Colors:* individual patients (i=34). *Error bar:* 90% prediction interval. *Green shaded box:* target range, i.e. 1-5x minimum inhibitory concentration of the pathogen..

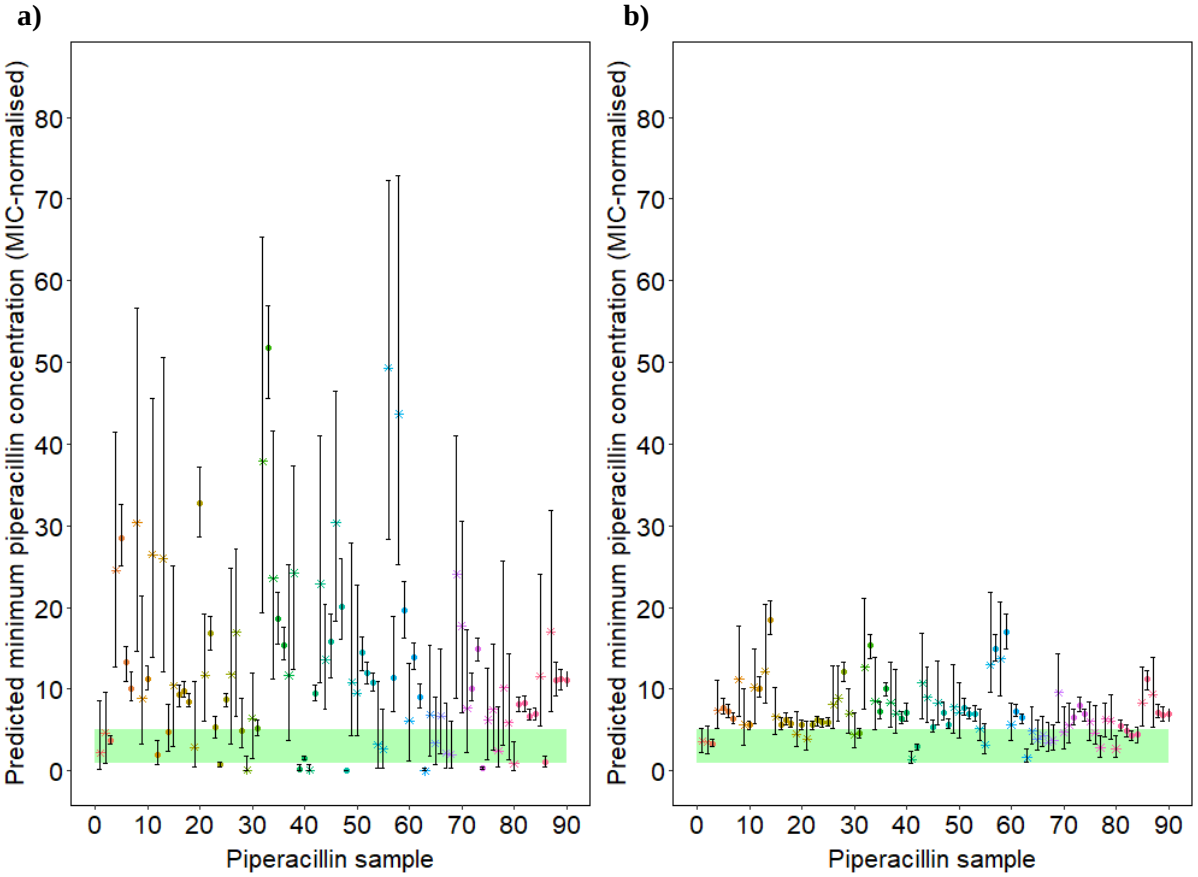

Figure 3.18: MIC-normalised predicted piperacillin concentrations for the dosing regimens documented at Charité-Universitätsmedizin Berlin (a) and recommended by the DoseCalculator for currently available dosing regimens at Charité-Universitätsmedizin Berlin (b).
Stars: median prediction based on prior distribution, *Points:* median prediction based on posterior distribution. *Colors:* individual patients (i=46). *Error bar:* 90% prediction interval. *Green shaded box:* target range, i.e. 1-5x minimum inhibitory concentration of the pathogen.

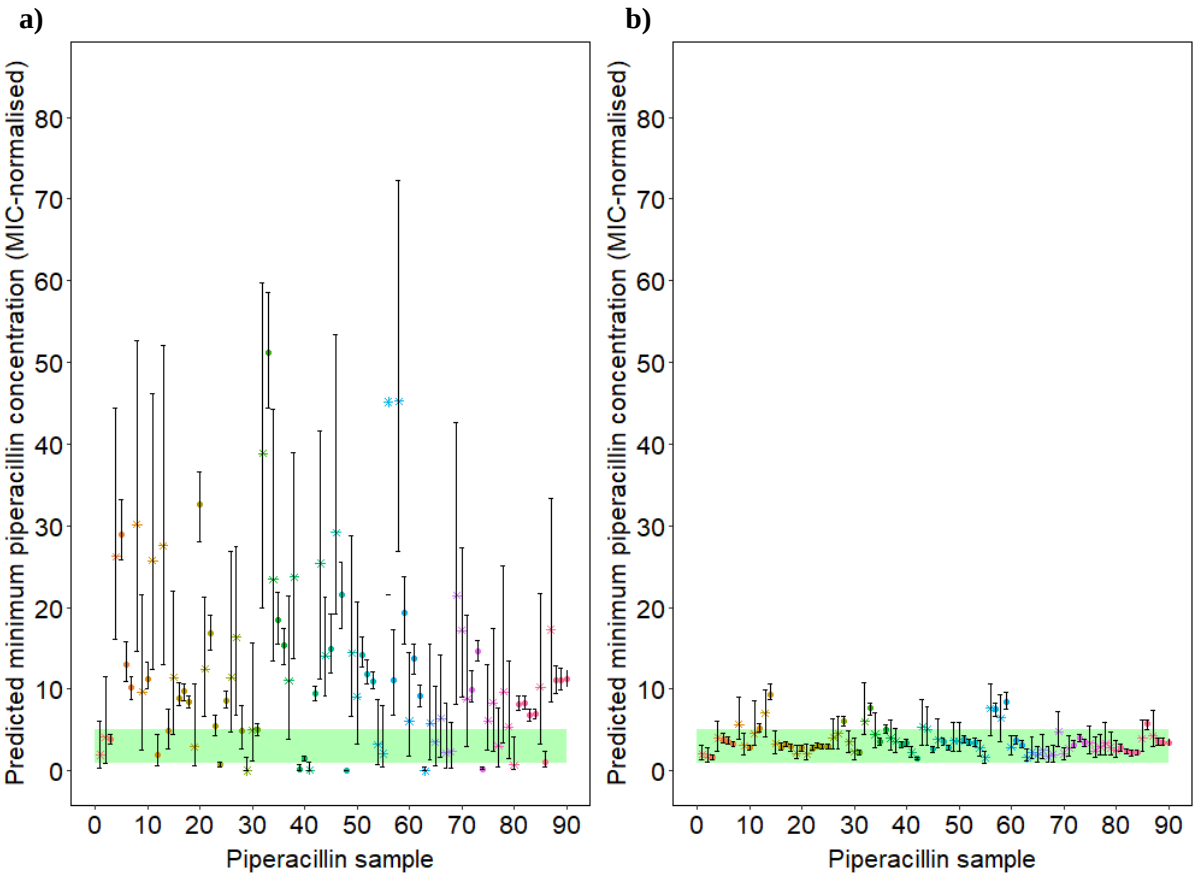

Figure 3.19: MIC-normalised predicted piperacillin concentrations for the dosing regimens documented at Charité-Universitätsmedizin Berlin (a) and recommended by the DoseCalculator after implementing currently not available formulations (2 g piperacillin/0.25 g tazobactam) (b). *Stars:* median prediction based on prior distribution, *Points:* median prediction based on posterior distribution. *Colors:* individual patients (i=46). *Error bar:* 90% prediction interval. *Green shaded box:* target range, i.e. 1-5x minimum inhibitory concentration of the pathogen.

3.3 Project III: Evaluation and extension of the MeroRisk Calculator

3.3.1 Database

891 meropenem TDM samples from 155 patients were included in the evaluation. Meropenem was administered as short-term infusion (0.5 h) at doses of 1000 mg, 1500 mg or 2000 mg (67.9%, 1.8% and 30.3% of administered doses, respectively) .In Table 3.12, a summary of patient and sample characteristics is displayed. The patients included in the study were predominantly male (65.2%) and had a median creatinine clearance estimated based on Cockcroft-Gault formula of 86.4 mL/min, i.e. mild renal impairment [170]. However, the renal function observed in the study ranged from moderate renal impairment (>30-60 mL/min [170]) to augmented renal function (>130 mL/min [170]). Furthermore, most patients in the dataset experienced hypoalbuminemia (serum albumin $\leq$3.5 g/dL). The dataset had sparse and variable sampling data: For each monitored dosing regimen only one PK sample was collected and sampling timepoints deviated from the planned sampling timepoint 8 hours after dose (median time after last dose: 6.2 h, 5^{th}-95^{th} percentile: 3.72-8.13 h). In Figure 3.20 the measured meropenem concentrations are plotted against the time after last dose for the three different administered doses of meropenem (1000 mg, 1500 mg and 2000 mg) observed in the dataset.

Table 3.12: Comparison of relevant patient characteristics between the clinical dataset used for the evaluation and dataset used for model development by Ehmann et al.

Patient characteristic	**Clinical dataset**	**Ehmann et al.** [129]
Categorical	*n (%)*	
No. of patients	155	42
No. of male patients	101 (65.2)	27 (56.3)
No. of meropenem samples	891	1376
No. of meropenem samples collected during extracorporeal membrane oxygenation	64 (7.18)	-
Continuous [unit]	*Median (5^{th}-95^{th} percentile)*	
Meropenem concentration [mg/L]	9.05 (1.09-36.5)	-
Age [years]	57.0 (33.7-79.0)	55.5 (32.0-69.9)
Weight [kg]	73.0 (50.0-97.3)	70.5 (47.4-121)
Creatinine clearance[#] [mL/min]	86.4 (35.4-161)	80.8 (24.8-191)
Serum albumin concentration [g/dL]	2.5 (2.3-3.2)	2.80 (2.20-3.56)

[#]Calculated using Cockcroft-Gault formula [169]. Meropenem concentration, creatinine clearance and serum albumin concentration determined on sample level, all other continuous characteristics on patient level.

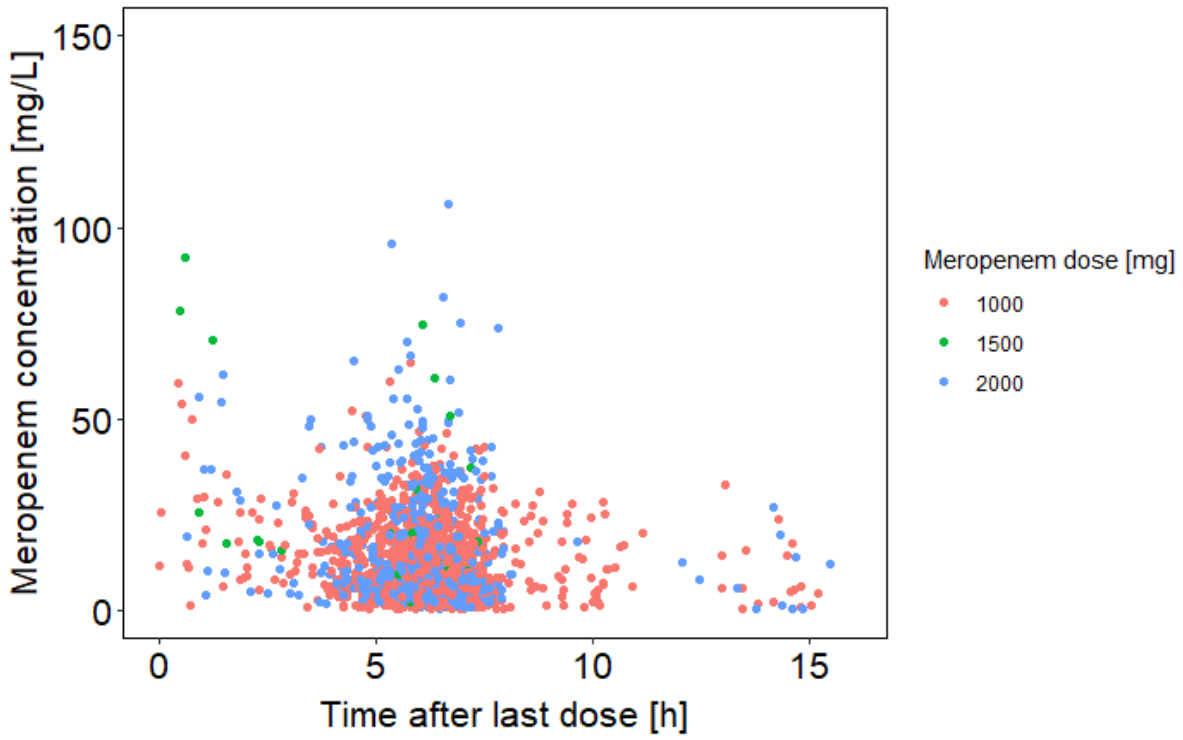

Figure 3.20: Observed meropenem concentrations vs. time after last dose (n=891) following a short-term infusions (0.5 h) of 1000 mg (red dots), 1500 mg (green dots) or 2000 mg (blue dots) of meropenem.

3.3.2 Evaluation of the MeroRisk Calculator

3.3.2.1 Step 1: Data-based evaluation of the two-compartment PK model

The comparison of the measured meropenem concentrations (clinical dataset) with the concentrations predicted by the PK model revealed a median prediction error and therefore bias of -0.84 mg/L (-16%), i.e. the PK model slightly underpredicted the observed concentrations. In Figure 3.21 a Bland-Altman plot is used to visualise the deviations between observations and predictions, i.e. the prediction errors. The prediction errors seem to be randomly distributed around 0 which is equivalent to no deviation between observations and predictions. However, the median prediction error included in the figure shows the prediction errors are in fact distributed around -0.84 mg/L. Furthermore, the 50% and 90% prediction error interval are not equally spaced around the median prediction error revealing that the prediction errors are not normally distributed. Nevertheless, the 50% prediction error interval ranged from -5.0 mg/L (-59%) to +1.2 mg/L (+32%) proving acceptable precision for a critically ill patient population and routine clinical data. The PK model evaluation was therefore considered successful and the model was subsequently used to predict the meropenem concentrations 8 hours after standard dose for every patient, enabling the evaluation of the MeroRisk Calculator in step 2 of the evaluation process.

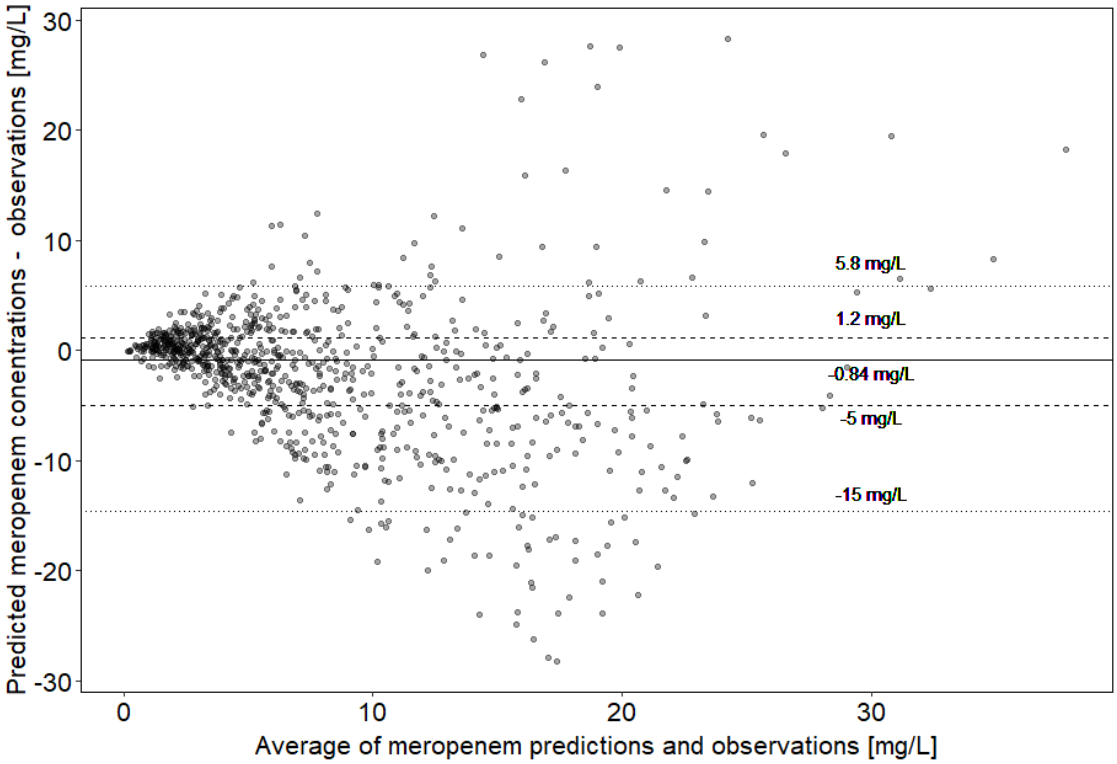

Figure 3.21: Bland-Altman plot for observed and predicted meropenem concentrations**.** Predictions are based on deterministic simulations of the investigated pharmacokinetic model. *Solid Line:* Median of deviations between observed and median predicted concentrations. *Dashed Lines:* 50% prediction error interval, *Dotted Line:* 90%prediction error interval.

3.3.2.2 Step 2: PK-model-based evaluation of the MeroRisk calculator

Conformity between the predictions for real patients

The comparison of median predicted concentrations 8 hours after dosing for a real patient population (Figure 3.22) confirmed a high level of agreement for patients with a $CLCR_{CG}$ above 50 mL/min (green squares) while the patients below 50 mL/min (red triangles) displayed increasing deviations with the MeroRisk Calculator predicting higher concentrations compared to the PK model.

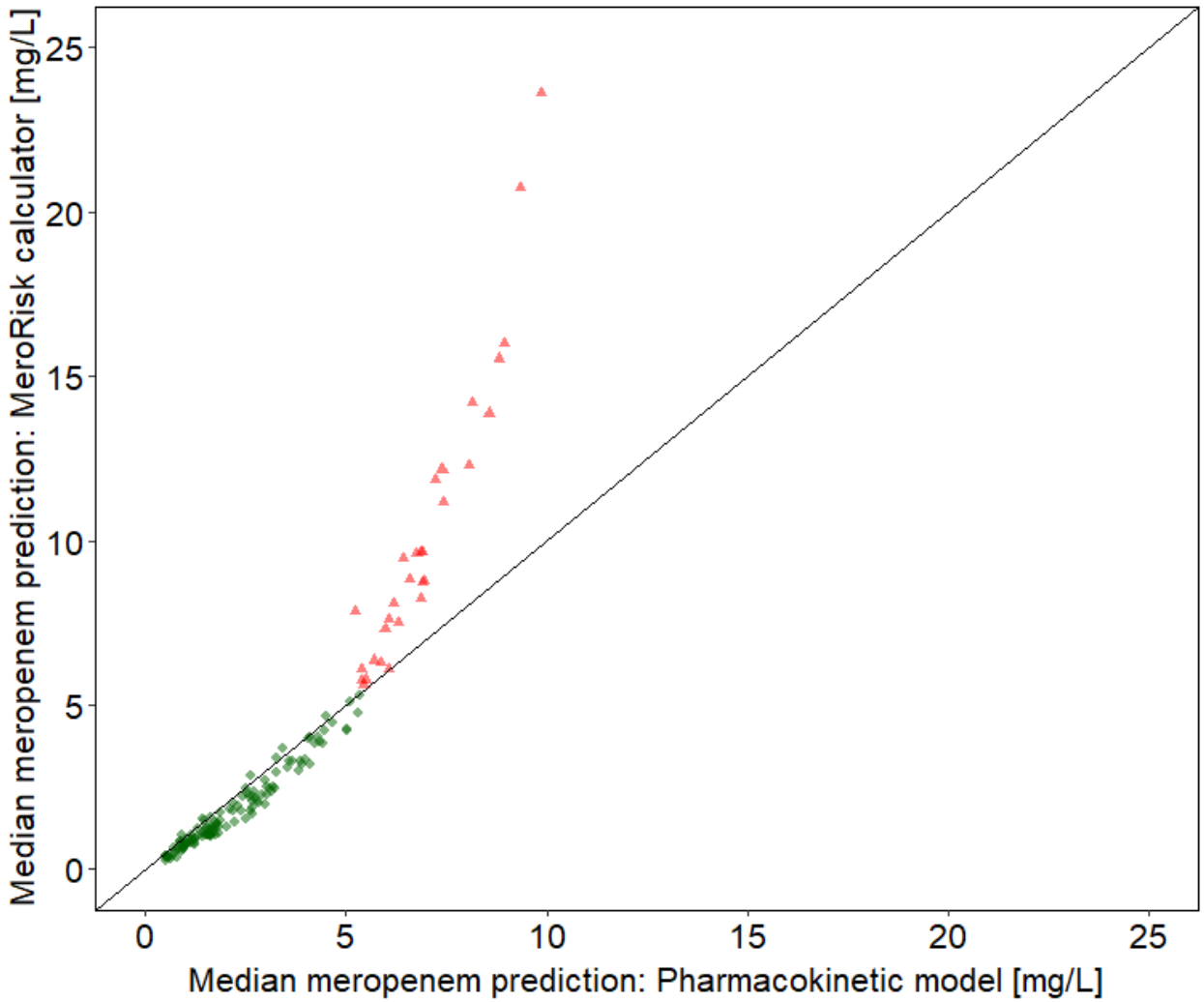

Figure 3.22 :Median meropenem concentrations 8 h after dose predicted by pharmacokinetic model and MeroRisk Calculator [173].
Median predictions (PK model: stochastic simulations (n = 2000), MeroRisk Calculator: classic theory of linear models [11]) for patients (n = 124) with creatinine clearance calculated using Cockcroft–Gault Equation ($CLCR_{CG}$) > 50 mL/min (green triangles) and patients (n = 31) with $CLCR_{CG} \leq 50$ mL/min (red points) 8 h after standard dose (1 g meropenem, 0.5 h infusion). Line: Line of identity

The risk of target non-attainment (i.e. the risk of meropenem concentrations 8 hours after standard dose being below the MIC) for 8 MIC levels ranging from 0.125 mg/L to 16 mg/L and the 155 critically ill patients predicted by the MeroRisk Calculator and the PK model evaluated in step 1 is displayed in Figure 3.23. The graphical comparison showed an overall good agreement between the two investigated methods. The risk predictions by the MeroRisk Calculator for MIC values of 8 mg/L and 16 mg/L are biased towards lower risks compared to the PK model. However, for these two high MIC values the risk of target non-attainment for most patients was predicted to be very high (patients with PK model predicted risk above 95%: 65.8% (MIC=8 mg/L), 100% (MIC=16 mg/L)). As a consequence most data points in the figure are clustered in the upper right corner near the line of identity for both predictions and only a small fraction of patients with an estimated creatinine clearance below 50 mL/min (n=31, red triangles in Figure 3.23) led to the strong deviation observed in the graphical analysis.

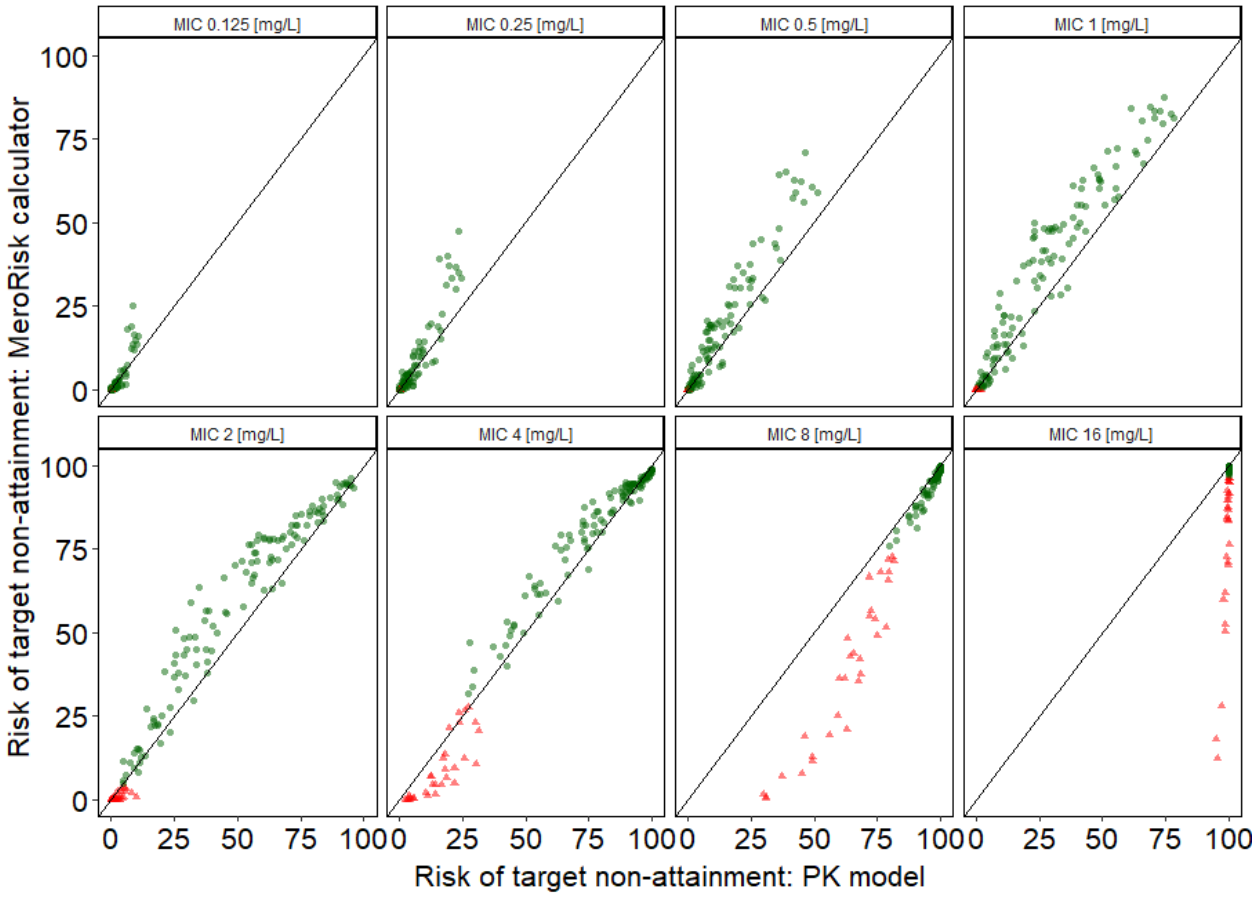

Figure 3.23: Risk of target non-attainment predicted by the MeroRisk Calculator and by the pharmacokinetic (PK) model for different minimum inhibitory concentrations (MIC).
The risk of target non-attainment (i.e. drug concentration below the MIC) 8 h after standard dose (1 g meropenem, 0.5 h infusion)) was assessed for 155 critically ill patients. Solid line: Line of identity, Green points: Risk predictions for patients with creatinine clearance calculated using Cockcroft-Gault equation ($CLCR_{CG}$) $\geq$ 50 mL/min, Red triangles: Risk predictions for patients with $CLCR_{CG}$ < 50 mL/min.

The numerical analysis using Lin's concordance correlation coefficient (CCC) confirmed the conclusion based on the graphical analysis. The lower one-sided 95% confidence limit of the calculated CCC value for all investigated MIC values and all patients was 0.98 and therefore, according to the interpretation by McBride, the agreement between the predictions was substantial (Table 2.4). Overall agreement between the risk predictions of the PK model and the MeroRisk Calculator improved considerably (shown by an increasing CCC value), if patients with a $CLCR_{CG}$ below 50 mL/min were excluded from the analysis. A full overview of the CCC values for the investigated MIC values is displayed in Table 3.13.

Table 3.13: Lin's concordance correlation coefficient for risk predictions by the pharmacokinetic model and the MeroRisk Calculator.

MIC [mg/L]	Lin's concordance correlation coefficient[#] (95% CI)	
	All Patients	**$CLCR_{CG}$ > 50 mL/min**
0.125 – 16	**0.983 (0.981-0.984)*** **	**0.990 (0.988-0.991)*** **
0.125	0.791 (0.746-0.830)*	0.999 (0.998-0.999)****
0.25	0.845 (0.811-0.872)*	0.997 (0.996-0.998)****
0.5	0.894 (0.869-0.914)*	0.992 (0.991-0.994)****
1	0.921 (0.899-0.938)*	0.930 (0.910-0.946)**
2	0.957 (0.942-0.967)**	0.919 (0.893-0.938)*
4	0.979 (0.972-0.984)***	0.954 (0.938-0.967)**
8	0.857 (0.834-0.877)*	0.978 (0.970-0.984)***
16	0.087 (0.077-0.097)*	0.945 (0.925-0.960)**

Abbreviations: *MIC*: Minimum inhibitory concentration; *$CLCR_{CG}$*: Creatinine clearance estimated using Cockcroft-Gault equation;
[#]Strength of agreement criteria defined by McBride [174]: poor:*, moderate**, substantial***, almost perfect****

Conformity between the predictions for virtual patients

The predicted minimum meropenem concentrations for the three virtual patient populations with one varying patient characteristic (out of three implemented as covariates in the PK model) showed an overall good agreement between the MeroRisk Calculator and the PK model (Figure 3.24 and Figure 3.25). Nevertheless, two differences can be observed in Figure 3.25: First, the 95% prediction interval of the MeroRisk calculator was considerably broader than the 95% prediction interval of the PK model. This was most evident for patients with fixed weight and serum creatinine concentrations (70 kg and 1.24 mg/dL, respectively) and varying serum albumin concentrations (Figure 3.25d). Second, for an estimated creatinine clearance below 50 mL/min the MeroRisk Calculator predicted median minimum meropenem concentrations up to 3 times above the PK model: The median predicted minimum meropenem concentration for a patient with a $CLCR_{CG}$ of 25 mL/min was 10.4 mg/L for the PK model and 27.0 mg/L for the MeroRisk Calculator (Figure 3.25a). This deviation in meropenem predictions is linked to the deviations in risk predictions for patients with low $CLCR_{CG}$. Compared to the evaluated PK model, the MeroRisk Calculator overpredicts meropenem concentrations and as direct consequence underestimates the risk of target non-attainment.

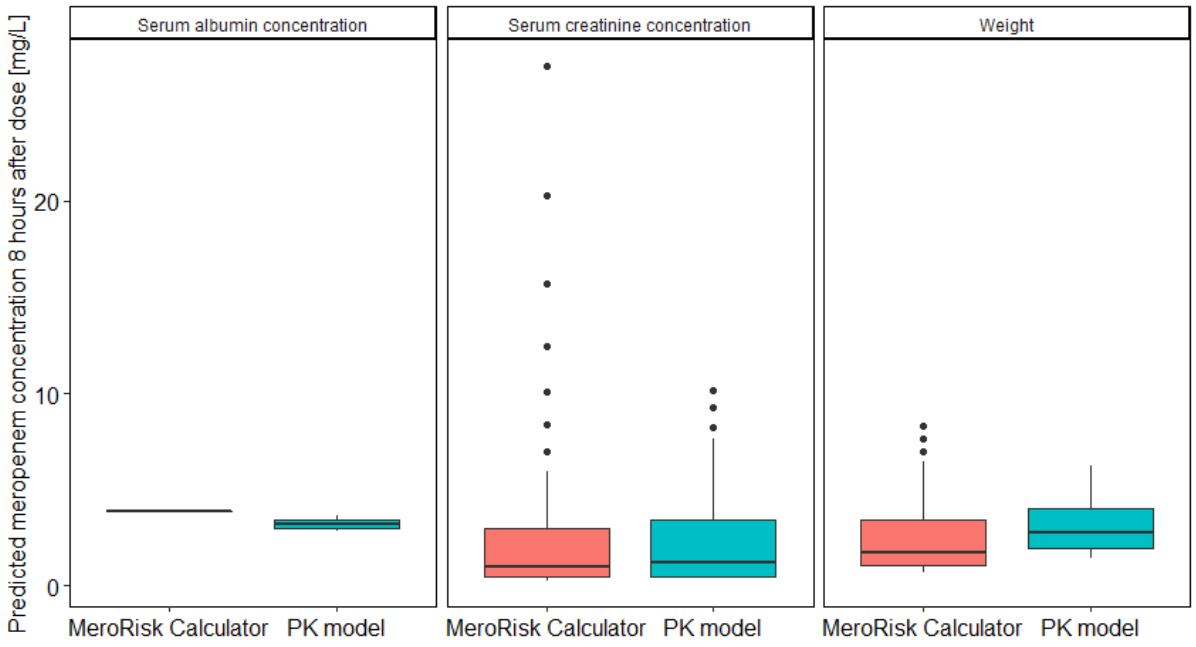

Figure 3.24: Boxplot of the median predicted meropenem concentrations 8 hours after standard dose (1 g meropenem, 0.5-hour infusion) by the pharmacokinetic (PK) model and the model underlying the MeroRisk Calculator for varying patient characteristics.
Serum albumin concentrations ranging from 2.20 to 3.56 g/dL , serum creatinine concentrations ranging from 0.44 to 3.35 mg/dL and weight ranging from 40 to 120 kg. Median derived based on 50 virtual patients using stochastic simulations (n = 2000) for the PK model (green) and classic theory of linear models and standardised residual [131] for the model underlying the MeroRisk Calculator (red).

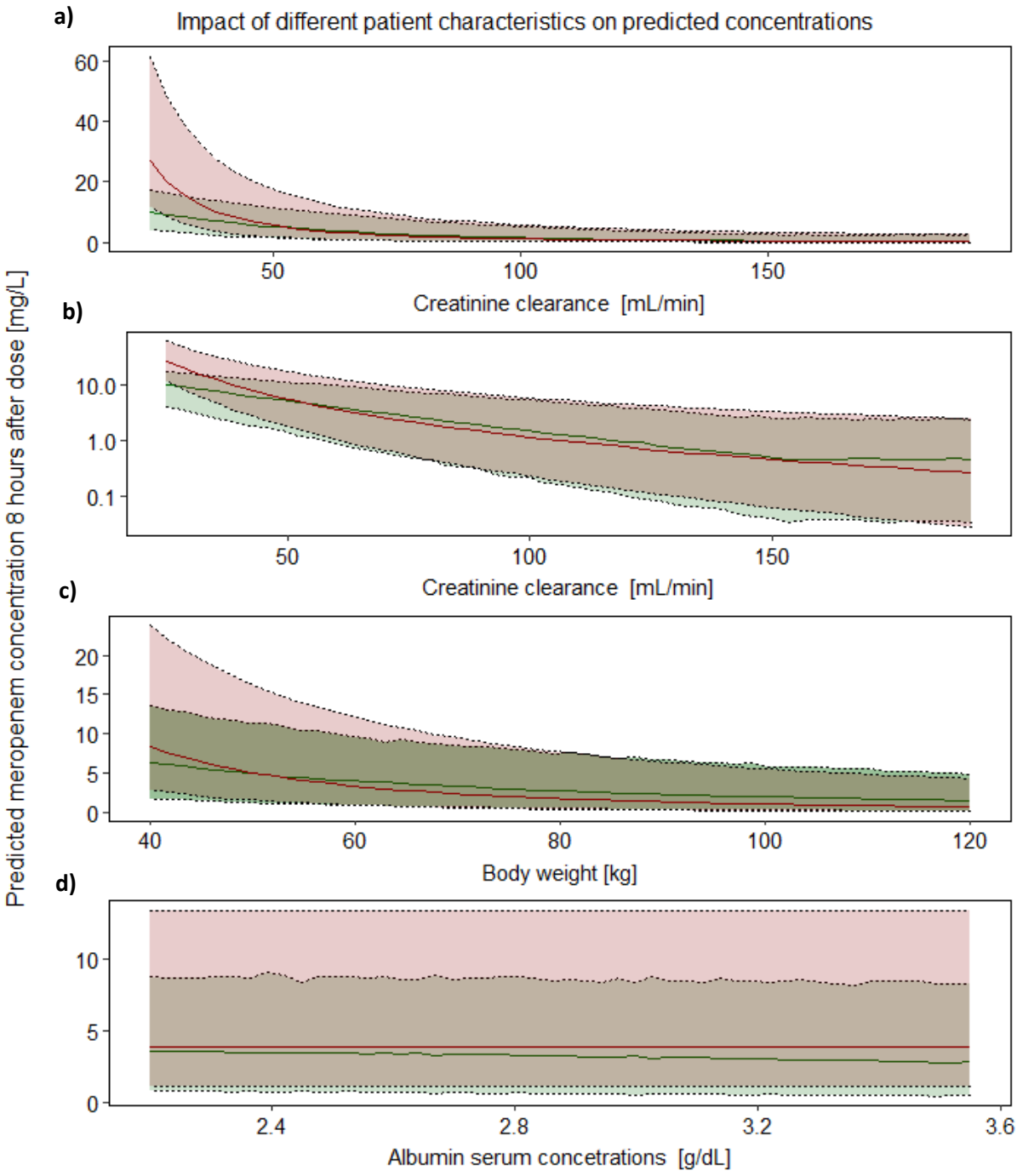

Figure 3.25: Comparison of the influence of patient characteristics (creatinine clearance, body weight and albumin serum concentrations) on meropenem concentrations 8 hours after standard dose (1 g meropenem, 0.5-hour infusion) predicted by the pharmacokinetic (PK) model and the model underlying the MeroRisk Calculator**.**

Solid and dashed lines: Median and 95% prediction interval of predicted meropenem concentrations derived based on 50 virtual patients using stochastic simulations (n = 2000) for the PK model (green) and classic theory of linear models and standardised residual [131] for the model underlying the MeroRisk Calculator (red).

3.3.3 Integration of a new feature in the MeroRisk Calculator: risk assessment based on pathogen

In the new extended version of the MeroRisk Calculator the intuitive user interface remained largely unchanged by the addition of the new feature but now all information about the pathogen becoming available over the course of antibiotic treatment can be used to calculate the risk of target non-attainment (Figure 3.26). If at the beginning of the antibiotic therapy no information about the pathogen and its MIC value is available, and the pathogen entry remains "unknown" and the MIC entry blank. Risk calculations are then based on pathogen unspecific EUCAST breakpoints chosen by the user. If the pathogen is known to the user, but the MIC value of the pathogen is unknown the MIC entry remains empty and the pathogen is selected from the dropdown list of implemented pathogens. The risk of target non-attainment for the patient is then calculated based on CFR analysis and the EUCAST MIC distribution of the selected pathogen. If both the pathogen and its MIC value are known, the information is entered into the MeroRisk Calculator and risk calculation is based on the pathogen's MIC value. For all risk assessments, either the $CLCR_{CG}$ of a patient or its determinants (sex, age, total body weight, serum creatinine concentration) need to be provided by the user. As in the first version of the MeroRisk Calculator, the result of the risk assessment for target non-attainment are displayed in the original colour coded box (green $\leq$10%, orange >10% to <50%, red $\geq$50%). Furthermore, a graphical illustration of the relationship between $CLCR_{CG}$ and minimum meropenem concentration 8 hours after standard dosing including the 95% prediction interval is provided for the user.

The extended version of the MeroRisk Calculator containing the new feature to assess the risk of target non-attainment based on a selected pathogen is publicly available as additional file in the article by Liebchen et al. [173]. Additionally, and due to changing MIC distributions an up-to-date version of the MeroRisk Calculator based on the latest reported MIC distributions can be found online (https://www.bcp.fu-berlin.de/en/pharmazie/faecher/klinische_pharmazie/arbeitsgruppe_kloft/forschung/MRc/index.html). The tool is compatible with all Windows operating systems and different Excel versions (2010 and onwards).

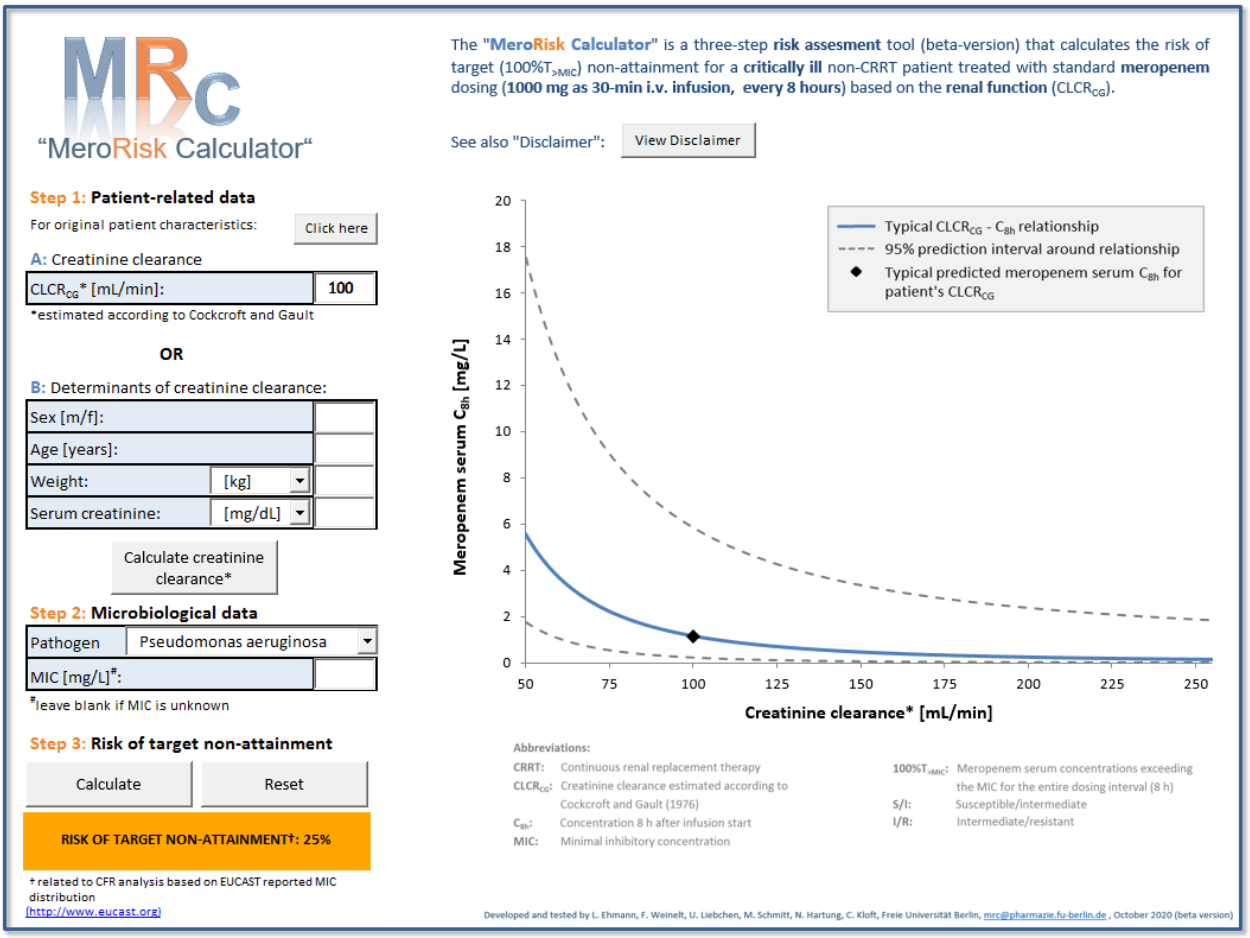

Figure 3.26: Graphical user interface of the extended MeroRisk Calculator after risk calculation. Example for illustration: *Patient-related and microbiological data (left):* Female, aged 60 years, body weight 65 kg, serum creatinine concentration 0.6 mg/dL (Step 1), infected with *Pseudomonas aeruginosa* and no MIC value available (Step 2). The predicted risk of target non-attainment of 25% is displayed in the colour coded box (Step 3) and the typical meropenem prediction 8 hours after dose including the 95% prediction interval is visualised on the right.
Abbreviations: $CLCR_{CG}$ Creatinine clearance estimated according to Cockcroft and Gault equation [24], CRRT Continuous renal replacement therapy, C8h Meropenem serum concentration 8 h after infusion start, MIC Minimum inhibitory concentration.

To illustrate the impact of the pathogen on the risk of target non-attainment, the risk predictions by the MeroRisk Calculator for six selected clinically relevant pathogens and the investigated 155 critically ill patients are displayed in Figure 3.27. For all pathogens patients with higher creatinine clearance experienced a higher risk of target non-attainment after standard dosing of meropenem. For susceptible pathogens like *Escherichia coli* or *Streptococcus pneumoniae*, the risk of target non-attainment after standard dose was found to be low in all investigated patients. More resistant pathogens like *Pseudomonas aeruginosa* or *Acinetobacter baumannii* displayed increased risks of target non-attainment after standard meropenem dosing for the majority of the investigated patients. The results for all 74 pathogens in the EUCAST database can be found in the supplementary (Figure S13). Overall the risk of target non-attainment predicted by the MeroRisk Calculator was found to be low for the majority of pathogens and the investigated 155 critically ill patients: 73.0 % of pathogens revealed median risks below 10%, 18.9 % between 10% and 50% and 8.1 % above 50%.

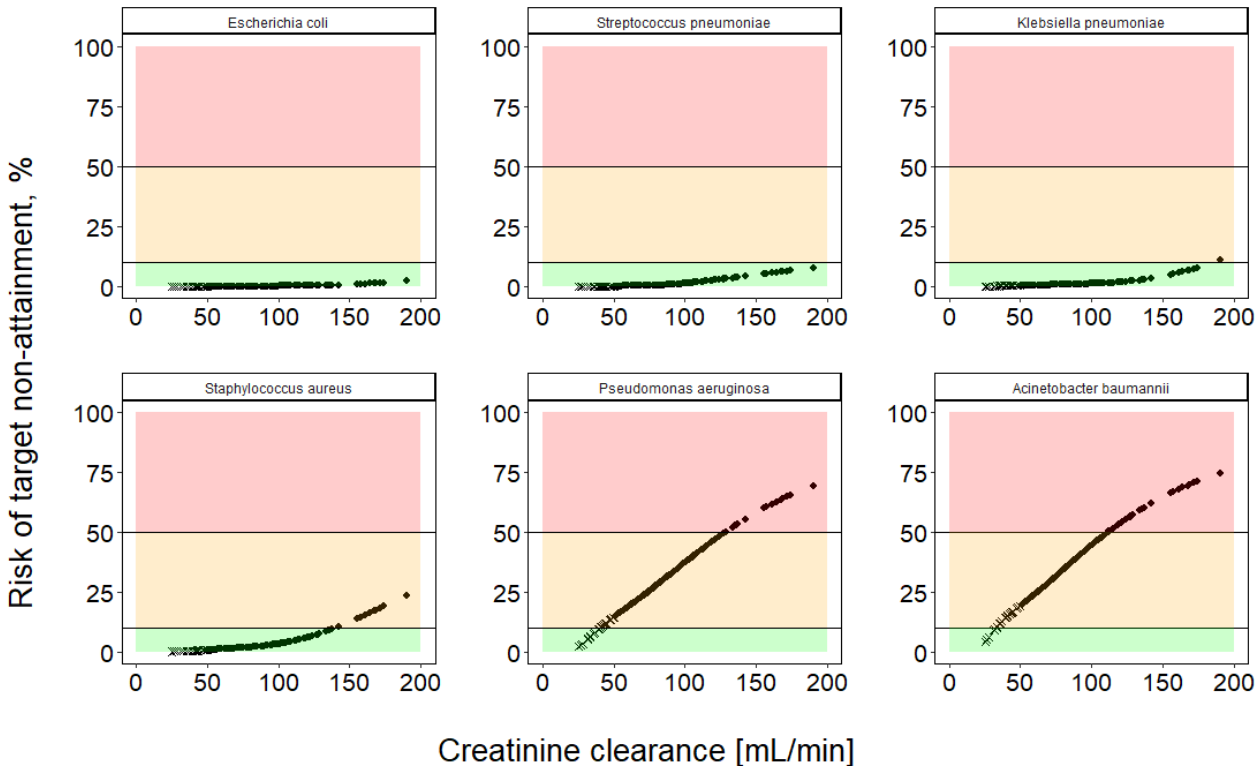

Figure 3.27: MeroRisk Calculator predicted risk of target non-attainment for critically ill patients (n = 155) and six clinically relevant pathogens (modified from [173]).
The risk of target non-attainment (unbound drug concentration being above the minimum inhibitory concentration (MIC) for 100% of the time) was assessed using EUCAST MIC distributions of the investigated pathogens and cumulative fraction of response analysis. Risk predictions for patients with creatinine clearance calculated using Cockcroft-Gault equation ($CLCR_{CG}$) $\geq$ 50 mL/min (points) and for patients with $CLCR_{CG}$ < 50 mL/min (x). Risk predictions $\leq$10% (green), >10% to $\leq$ 50% (orange) and >50% (red).

4 Discussion

In the presented thesis, quantitative analyses were employed to assess and improve antibiotic dosing in critically ill patients following an iterative, integrative and translational approach (Figure 4.1). Using nonlinear mixed-effects modelling and simulation, a possible adsorption of meropenem at the cytokine adsorber CytoSorb® was investigated. By analysing current antibiotic dosing strategies, pathogen susceptibility and target attainment in intensive care wards patients at risk of subtherapeutic or toxic concentrations were identified. In close collaboration with the AMS and ICU teams, easy-to-use model-informed dosing tools were developed to specifically address the needs of local ICUs and improve antibiotic dosing for patients at risk. Furthermore, the MeroRisk Calculator, an previously at our department developed tool, was extended to include risk assessment based on a pathogens genus and evaluated using new data to improve trust in its predictions.

In the following section, the key results of each of the presented projects will be summarised and discussed in light of currently available scientific literature. In the subsequent and final chapter of this thesis, an overall conclusion and outlook will be provided.

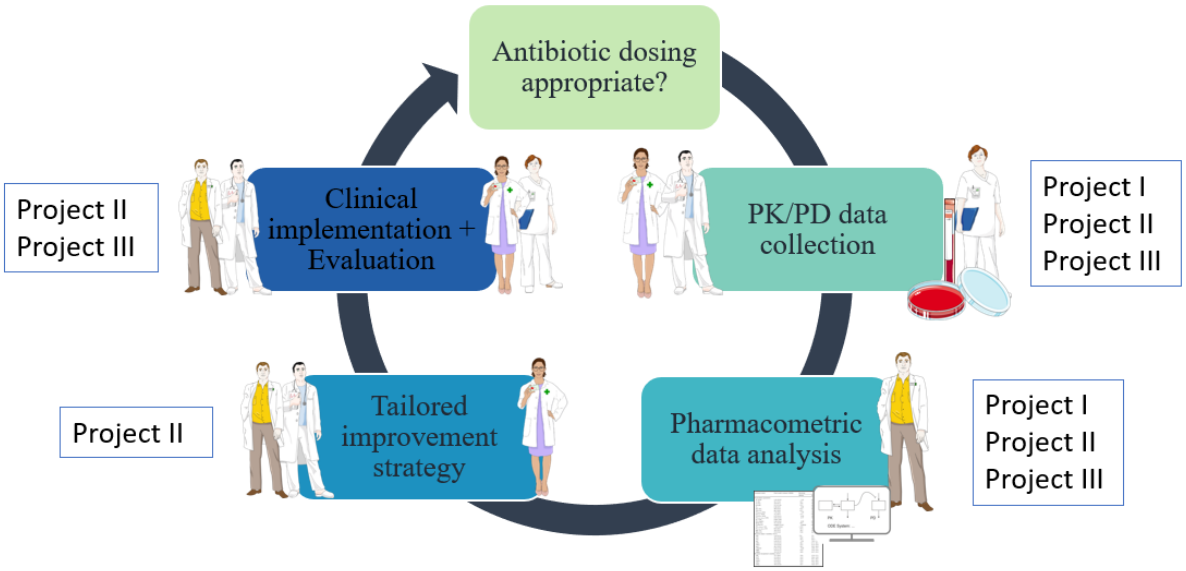

Figure 4.1: Graphical representation of the iterative, integrative and translational approach employed to accelerate the implementation of model-informed precision dosing highlighting steps which were addressed in each of the presented projects.
Figures next to each step indicate the responsible healthcare professionals: *PK/PD data collection*: Physicians, pharmacists and clinical laboratory; *Pharmacometric data analysis*: Pharmacometrician; *Tailored improvement strategy*: Physicians, pharmacists and pharmacometrican; *Clinical implementation + Evaluation*: Physicians, pharmacists, pharmacometrican and clinical laboratory.
Figures representing healthcare professionals from smart.servier.com.

4.1 Project I: Investigation of possible meropenem adsorption at the cytokine adsorber CytoSorb®

Project I focused on the quantification of a possible meropenem adsorption at the cytokine filter CytoSorb® and its effect on meropenem exposure in critically ill patients. No clinically relevant adsorption of meropenem by the cytokine adsorber CytoSorb® was observed in the investigated critically ill patient population. Therefore the hypothesis (based on *in vitro* experiments) that each CytoSorb® filter adsorbs approximately 400 mg of meropenem [105] was rejected.

The presented analysis included 333 meropenem concentrations from 25 critically ill patients collected during two prospective observational studies at the same study centre. All patients suffered from sepsis or septic shock and were undergoing continuous veno-venous haemodialysis or haemodiafiltration. Overall, the dataset represented a large population (20 patients with concomitant CytoSorb®-treatment) for the research question. So far, previous clinical/*in vivo* investigations addressing the potential adsorption of antibiotics by the CytoSorb® filter were either case reports or case series ($n \leq 3$) [179,180]. Therefore, to the best of our knowledge, this analysis represents the most comprehensive analysis of meropenem adsorption at the CytoSorb® filter to date. The dosing regimens covering typical dosing regimens for this patient population and the sampling timepoints of the dataset (collected during clinical routine) were overall heterogeneous and therefore the sole comparison of measured concentrations would not have allowed a valid conclusion. As clearly illustrated in this project, NLME modelling approaches can successfully be employed to quantitatively investigate such a heterogeneous dataset.

In a first step, a two-compartment structural model with first-order elimination was developed and adequately described the measured meropenem concentrations. Neither the type nor the intensity of dialysis proved to be an influencing covariate in the graphical or statistical analysis. Even if this result is counterintuitively at first, it is in agreement with previous studies that also did not demonstrate any effect of dialysis characteristics on drug concentrations [181,182]. Ulldemolins et al. hypothesised that already at the lowest dialysis intensity the meropenem clearance by the dialysis filter is at its maximum, explaining the repeated finding that dialysis intensity is not a determinant of meropenem clearance [181].

In a second step, the influence of CytoSorb®-treatment on meropenem concentrations was examined using three distinct approaches and all three approaches supported the same conclusion: No clinically relevant amount of meropenem is adsorbed by the cytokine adsorber CytoSorb®. Both the proportional increase of clearance during CytoSorb® treatment in the covariate model and the maximum adsorption in the adsorption submodels were negligibly small ($\leq 3.84\%$ of the total clearance) and therefore clinically irrelevant. Moreover, neither the integration of CytoSorb® treatment as a proportional categorial covariate on clearance nor the inclusion of different adsorption submodels at the CytoSorb®

filter showed a significant improvement in the model fit (i.e. a non-significant reduction in OFV). Furthermore, all parameters characterising the adsorption at the CytoSorb® filter and thus an additional elimination pathway in the different models (covariate effect, adsorption and maximum adsorption capacities) could not be estimated precisely and for each of the adsorption parameters the 90% confidence interval included zero. A low adsorption clearance and the resulting negligible meropenem amount adsorpt are supported by recent *in vivo* data from pigs reported by Schneider et al. [106] reporting an increase in clearance during CytoSorb® use of 6.3%. The parameters representing the maximum adsorption capacity in the adsorption submodels were found to be implausibly high (A_{max} = 33 kg, A_{50} = 400 kg, administered daily doses ranging from 1 g – 7 g), reducing both the linear decrease and the hyperbolic decrease models to the constant adsorption model and suggesting an nonsaturable adsorption process. However, a nonsaturable adsorption process is both physically improbable and contradicting the available *in vivo* pig data for meropenem and other antibiotics: for all investigated drugs Schneider et al. observed a decrease in adsorption clearance over time [106]. However, this contradiction can be explained by the available dataset: Most likely the collection timepoints during CytoSorb® therapy in the investigated study were not dense enough to adequately quantify the low saturable adsorption process. To adequately characterise the saturation of the adsorption process, a denser sampling scheme after installation of the CytoSorb® filter, in the best case with pre- and post-CytoSorb® filter samples, would be required and should be implemented in future trials investigating drug adsorption at the CytoSorb® filter. Furthermore, to measure the exact drug amount adsorbed, future trials could also include an examination of the CytoSorb® cartridge after use.

The findings of this project contradict the conclusions previously drawn based on *in vitro* data. König et al. investigated the adsorption capacity in an *in vitro* experiment perfusing the CytoSorb® cartridge with NaCl (0.9%), human albumin (5%) solution or reconstituted blood and suspected a saturable adsorption of 400 mg meropenem occurring mainly in the first 200 minutes after installation of the CytoSorb® filter [105]. The presented analyses did not confirm such a substantial adsorption. One possible explanation could be that even reconstituted blood obtained from healthy blood donors does not represent the composition of blood from critically ill patients. The latter contains multiple drugs as well as numerous endogenous compounds in higher concentrations than in healthy donors (e.g. bilirubin, cytokines, platelets) that could potentially interact with the adsorption capacity of meropenem by the CytoSorb® filter. In addition, the results of the *in vitro* study by König et al. have been questioned due to possible stability issues during the experiment [183] and are in conflict with the *in vivo* experiments in pigs conducted by Schneider et al. investigating the adsorption and elimination of 17 different drugs by the CytoSorb® filter in pigs [106]. While Schneider et al. found an insignificant adsorption and insignificant increase in clearance (+6.3%) for meropenem (logP=-0.6), more lipophilic drugs (e.g. fluconazole (logP=0.4), linezolid (logP=0.23)) revealed a major increase (>100%) in total drug clearance. Even if the results of an animal study cannot be easily transferred to critically ill human

patients, the results reported by Schneider et al. support the conclusion drawn from our clinical investigation. Furthermore, the larger number of patients included in our analyses provided a robust clinical result compared to previously published data and excluded clinically relevant adsorption of meropenem. Consequently, no additional meropenem dosing is required during or after CytoSorb®-treatment.

It needs to be emphasised that the findings of this project most likely do not translate to other drugs and antibiotics and therefore highlighted that every drug needs to be investigated separately. Especially for more lipophilic and larger drugs than meropenem (logP=-0.6, 383,464 g/mol), clinical studies investigating adsorption at the CytoSorb® filter should be conducted, to rule out or quantify possible adsorption. The knowledge gained by these studies can then serve as basis for dosing decisions of antibiotics after CytoSorb® treatment in critically ill patients. The proposed adsorption models and the work-flow presented in this project presents a framework for future trials and analyses.

Conclusion

Using NLME modelling, a clinically significant adsorption of meropenem at the CytoSorb® filter and thus additional elimination in critically ill patients with sepsis or septic shock was ruled out. Consequently, neither additional dosing nor a more frequent drug measurement routine is necessary during simultaneous application of meropenem and CytoSorb®-treatment.

4.2 Project II: Utilising pharmacokinetic models to improve meropenem and piperacillin/tazobactam dosing

Project II focused on improving meropenem and piperacillin/tazobactam treatment for critically ill patients at the Charité-Universitätsmedizin Berlin. For this purpose, a 3-staged clinical study was initiated as a coordinated intervention (Figure 4.2). In 'stage I', frequent and reliable concentrations measurements were implemented and the current antibiotic therapy was assessed. In 'stage II', a tabular model-informed dosing tool was developed and implemented for meropenem therapy and for 'stage III' an interactive model-informed dosing software termed 'DoseCalculator' was developed for both drugs.

First, the key results of the 3 individual stages of the study will be summarised and discussed separately followed by a general conclusion and outlook for the project.

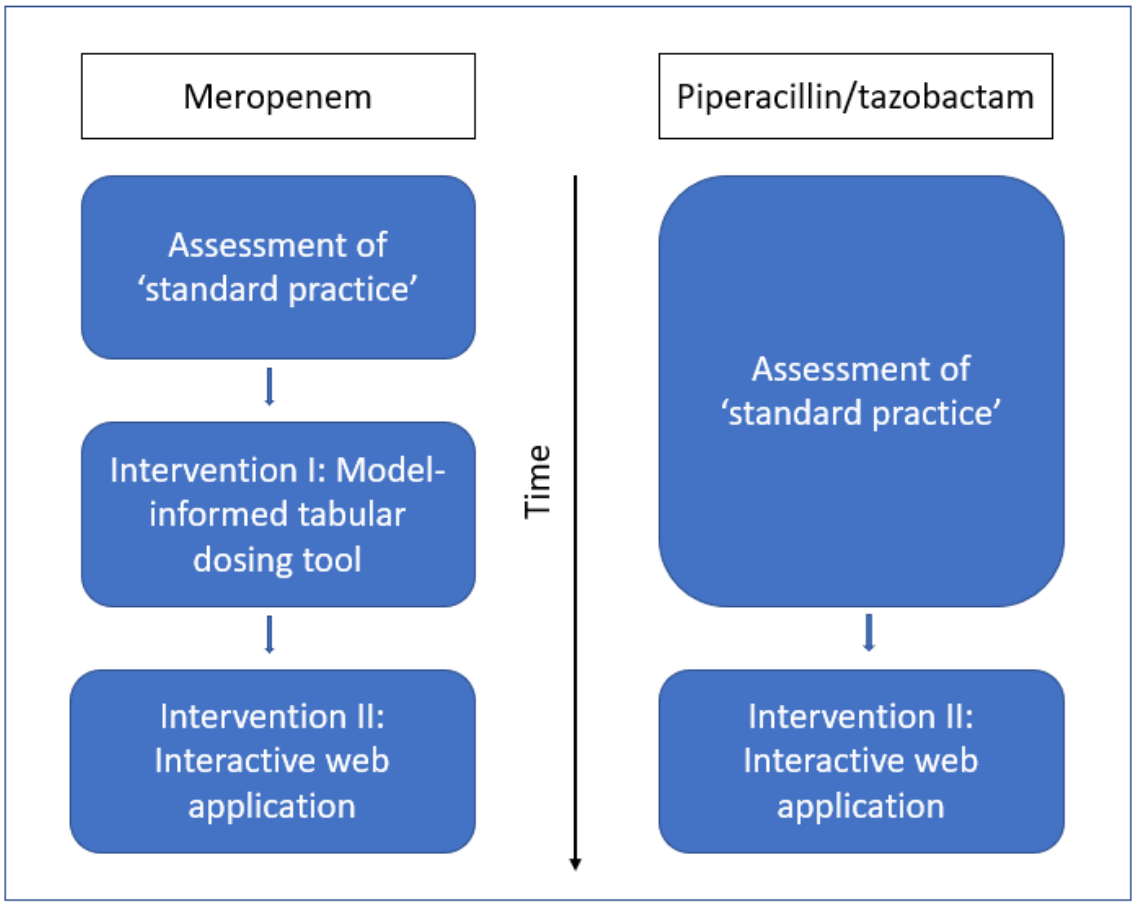

Figure 4.2: Stages of the clinical study at Charitè-Universitätsmedizin Berlin.
For meropenem two interventions (model-informed tabular dosing tool and interactive web application) were planned while only one intervention (interactive web application) was planned for piperacillin/tazobactam.

4.2.1 Stage I: Evaluating the 'status quo' of meropenem and piperacillin/tazobactam therapy

The antibiotic monitoring program conducted during stage I of the study provided two key insights into current dosing practice for the two frequently used antibiotics meropenem and piperacillin: Currently, neither the local pathogen susceptibility data was comprehensively exploited for PK/PD target selection nor was the relationship between renal function and antibiotic clearance for dosing decisions. This lead to poor target attainment (only 4 out of 10 meropenem samples and 5 out of 10 piperacillin samples were found to be in the target range, see 3.2.1.4). Hence, the regular assessment of PK targets and easy-to-use dosing decision tools are warranted.

Observed antibiotic dosing

Both meropenem and piperacillin/tazobactam were found to be most commonly administered as prolonged infusion (92.7% and 98%, respectively) at Charité-Universitätsmedizin Berlin. The prolonged infusion of both drugs was corresponding to the latest dosing recommendations, but not yet standard in every major German hospital. For example, at the university hospital Munich, short-term (0.5 h) infusions were found to be the most frequent way of administration for both meropenem (see 3.3.1) and piperacillin/tazobactam. The variations in infusion time (3 h and 4 h) for the prolonged infusions observed were attributable to the two different intensive care wards included in the study and point to non-standardised dosing regimens among different ICUs across the hospital prior to the study.

Even though most patients received either 1 g or 2 g of meropenem (50.2% and 40.7%, respectively), a wide range of doses from 0.5 g to 8 g was observed. Compared to meropenem, piperacillin/tazobactam dosing regimens observed during the study did not substantially vary between patients in regards to the administered dose, infusion duration and dosing interval. The overwhelming majority of administered doses (99.5% of maintenance doses) were 4 g piperacillin and 0.5 g tazobactam administered as a prolonged infusion. The only way piperacillin/tazobactam dosing was adjusted to the individual patient was via the length of the dosing interval. Nevertheless, the majority of patients (72.4%) received piperacillin/tazobactam every 8 hours. Most probable this was due to the non-availability of other doses than the standard preparation of 4 g piperacillin and 0.5 g tazobactam. Introducing a new combination in the hospital would simplify adjusting piperacillin/tazobactam dosing.

Pathogen susceptibility

At the two ICUs at Charité-Universitätsmedizin Berlin, the MIC of a causative pathogen was determined for only 49.1% of patients receiving meropenem and 34.4% of patients receiving piperacillin/tazobactam. The value was available to the attending intensive care physician approximately two days after the initiation of antimicrobial therapy. This finding corresponded well

with those reported by Esteve-Pitarch et al. [184] and once again highlights the need for safe and effective dosing strategies prior to pathogen and MIC detection. To determine if an antibiotic drug is the right choice for a safe and effective therapy, it is important to closely monitor the local susceptibility to the antibiotic. Fortunately, in our analysis the high number of pathogens susceptible to the investigated drugs confirmed that both drugs were suitable for empirical antimicrobial therapy. However, the question arises if the selected targets for empirical therapy were appropriate. For both drugs, more than 90% of the determined MIC values were found to be lower than the lower threshold of the selected empirical target range. Nevertheless, the conclusion based on the assessment of the selected empirical targets differed between meropenem and piperacillin/tazobactam due to two considerations: (i) the percentage of samples without determined MIC values and (ii) the fold difference between the observed MIC values and the selected empirical targets. First, for patients treated with meropenem the corresponding MIC value of the pathogen was available more often compared to piperacillin (49.1% vs. 34.4%). As a consequence, the reliability that the collected susceptibility data represented the underlying MIC value distribution at the two intensive care wards was higher for meropenem. Second, for meropenem the lower threshold of the empirical target range was 32-times higher then 75% of MIC values observed, while for piperacillin more than a fifth (21.3%) of the determined MIC values were within a 2-fold deviation and 93.9% within a 4-fold deviation from the selected empirical target. Given the high uncertainty in MIC value determination [185], this deviation of the observed susceptibility to piperacillin from the selected empirical target was judged to be too low to justify a target reduction for piperacillin. Detecting more causative pathogens, including a concomitant MIC determination, would help to further elucidate the local piperacillin susceptibility and will hopefully increase the reliability of the selected empirical target in future. For meropenem adjusting (i.e. reducing) the empirical target from 8-40 mg/L to 4-20 mg/L was recommended by the AMS team based on the analysis. Furthermore, the local pathogen-independent mean fraction of response (LPIFR) was introduced and integrated in the dosing decision tools developed for stage II and III of the clinical study to provide dosing recommendations based on the observed pathogen susceptibility pattern at the two ICU wards (see 2.6.6.2).

Target attainment and dose adjustments

Corresponding to multiple other studies [131,186,187], the observed TA was found to be low. However, in our analysis the majority of samples (meropenem: 87.2%, piperacillin: 85.2%) was above the lower limit of the defined target range. At the same time the observed TA strongly varied between patients with different renal functions for both drugs: The highest proportion of TA was observed for patients with a normal renal function, while TA decreased both for worsening and elevated renal functions. This clearly indicated that the well-known impact of a patient's individual renal function on the clearance of both antibiotics [50,131,188–191] had not been adequately taken into account for dosing decisions. Furthermore, the susceptibility of the causative pathogen or the empirical target (if the MIC was not

determined) did not impact measured concentrations. Neither for meropenem nor for piperacillin, the observed drug concentrations differed significantly between patients with different targeted concentrations, indicating that the individual target range was not adequately considered during dosing decisions. In addition, the proportion of dosing adaptations after drug concentration measurement was found to be low (<10%) and the frequency of dosing adaptations after samples below the target range was not notably higher than after samples above the target range. For meropenem the proportion of dosing adjustments was found to be completely independent from TA, suggesting that the observed dosing adaptations might not be due to the measured concentrations.

Conclusion

Overall, the real-word assessment revealed the need for actions on multiple levels to enable an optimal meropenem and piperacillin/tazobactam therapy: First, the empirical targets should regularly be assessed based on the local susceptibility pattern to ensure drug concentration targets sufficiently high to effectively treat local pathogens while at the same time avoiding unnecessary high drug burdens, [192]. Second, the renal function of the patient should be adequately taken into account [79,129,131]. And third, once additional information - i.e. MIC values or antibiotic concentration measurements - becomes available these should be thoroughly analysed and if required lead to dosing adjustments [79]. As exemplified by the analysis of two intensive care units at Charité-Universitätsmedizin Berlin, current dosing was not adjusted based on the well-known link between the clearance of both drugs and the renal function of the individual patient. The observed data furthermore highlighted the difficulty of integrating target information (e.g. infecting pathogen, MIC value) into individual initial dosing decisions. Adjusting dosing based on updated target information or individual drug measurements appeared to be an additional challenge. Evidently the availability of information alone was not sufficient to encourage dose individualisation at the bedside. As seen in other antibiotics [193,194] and indications [195,196], meropenem and piperacillin dosing decisions need to be supported by clear and comprehensive dosing strategies developed and evaluated by e.g. the local AMS team. Dosing algorithms for initial antibiotic therapy integrating patient characteristics and target information will help to increase target attainment while standardising dosing. Clear guidelines on when and how to adjust dosing if new information becomes available, might increase the impact and benefit of a concentration monitoring program: De Waele et al. reported a substantial increase of target attainment when implementing a simple algorithm to adjust dosing after concentration measurements outside the target range [197]. A more structured and standardised approach to individualise antibiotic dosing at the bedside is needed to fully utilise all available information.

4.2.2 Stage II: Developing and implementing a model-informed tabular dosing decision tool for meropenem

After identifying an elevated risk of inadequate antibiotic drug exposure in the local ICU patient population (see 3.2.1.4) a strategy was developed in collaboration with the AMS and ICU teams to improve antibiotic dosing. As a first step model-informed tabular dosing tables for initial meropenem dosing were developed and integrated into clinical routine.

Pharmacokinetic model selection, reduction and evaluation

The PK model developed by Ehmann et al. was selected for further model evaluation based on the high similarity of patient characteristics between the local patient population at Charité-Universitätsmedizin Berlin and the patient population used for model development (see 3.2.2.1). In the two-compartment model three covariates were included ($CLCR_{CG}$ on clearance, body weight on the central volume of distribution, and serum albumin concentration on the peripheral volume of distribution as piecewise linear, power and linear relationship, respectively), but only $CLCR_{CG}$ proved to have a clinical relevant impact on PTA [129]. To enable dosing recommendations depending only on the single patient characteristic with clinically relevant impact on PTA ($CLCR_{CG}$), the two clinically less relevant patient characteristics (serum albumin concentration and weight) were removed from the model and all PK parameters were re-estimated using the original dataset.

The subsequent external PK model evaluation using data collected during 'stage I' of the study (Section 3.2.2.1) confirmed a good predictive performance of the selected model for the local patient population. A slight bias to underpredict the observed meropenem concentrations (-1.2 mg/L) was identified and accepted as an additional safety margin since it led to slightly lower PTA values for each investigated dosing regimen. The 50% prediction error interval (-3.5 mg/L to 2.5 mg/L) observed was considered to be satisfactory for the data situation and the patient population: The inaccuracies (e.g. sampling and dosing time) often observed in data from clinical routine can inflate the observed imprecision [198] and the high PK variability observed in critically ill patients [79,199–202] can also contribute to higher imprecisions during external model evaluation. The 90% prediction interval of most samples included the observed concentration (Figure 3.9), confirming that the observed imprecision was in line with the unexplained variability characterised in the PK model. To conclude, the selected PK model adequately represented the observed data and it could therefore be used to derive optimal initial antibiotic dosing for the critically ill patients at Charité-Universitätsmedizin Berlin.

Development of the tabular dosing tool for meropenem

The dosing regimen included in the investigation were preselected by the AMS and ICU teams to guarantee a good integrability into local clinical routine. To ensure sufficiently high meropenem concentrations at the start of antibiotic therapy [57,73,74], while at the same time avoiding unnecessary high drug exposures [57], the effect of different loading doses on target attainment was analysed. Regardless of the loading dose used (1000 mg vs 2000 mg) the minimum meropenem concentration after the first maintenance dose was higher than or equal to minimum concentrations in steady state (see 3.2.2.2). Therefore, a 2000 mg loading dose had no additional benefit compared to a 1000 mg loading dose and consequently all dosing regimens recommended by the dosing tool included a 1000 mg loading dose.

For continuous infusions a higher PK/PD target ($T_{>4MIC}$) was chosen to exclude the possibility of antibiotic concentrations being inside a pathogens mutant selection window over an extended period of time. Drug concentrations inside the mutant selection window supress the growth of susceptible strains of a pathogen, thereby giving a growth advantage to already available resistant strains in the pathogen population [163,164]. Over a longer period of time, drug concentrations within the mutant selection window increase the proportion of resistant pathogens and the risk for resistant mutations to prevail [163,164]. Due to the higher target, the PTA for continuous infusions was found to be lower compared to the PTA of prolonged infusions with the same daily dose. As a consequence, continuous infusions were not included in the dosing recommendations of the dosing tool.

To inform dosing selection prior to pathogen identification, local, hospital specific and pathogen-independent MIC values were integrated into the dosing decision tool (see 2.6.6.2). While this approach is a good opportunity to reduce unnecessary high meropenem dosing, it also carries some risks and should be applied with care. First, dosing suggestions based on LPIFR need to be updated regularly since local MIC distributions vary over time [203]. Second, in the rare event of a pathogen with low susceptibility (MIC values >8-32 mg/L), the risk of target non-attainment will be underestimated until the susceptibility of the pathogen is determined. Therefore, it is vital to communicate those limitations to the decision-making team and encourage a dose increase or change of antibiotic if higher MIC values are expected. In general, the dosing regimen recommended based on the LPIFR metric should only be administered as long as there is no further information about the pathogen (e.g. MIC) available.

For each individual creatinine clearance and target, only the best performing dosing regimen was included as a dosing recommendation into the dosing decision tool. As a result, the dosing decision tool has a simple, explicit and clear structure. This structure allows to provide the initial dose individualisation needed to optimise dosing in critically ill patients while maintaining a level of standardisation that will help to avoid complication of ICU ward process.

Patients receiving renal replacement therapy (RRT) were not included in the development of the dosing tool. Consequently, the derived dosing recommendations do not apply to the roughly 20% of patients receiving RRT.

Retrospective evaluation of the dosing tool

Prior to implementation the dosing decision tool was evaluated using data collected during stage I of the clinical trial. For 72% of the samples found to be below the target range, the dosing decision tool suggested an increase in daily dose, while suggesting a decrease in the daily dose for 78% of the samples above the target range. The suggested reduction of daily dose for 23% of samples below the target can be explained by the transition towards four-times-daily dosing: The more frequent administration of meropenem provided higher PTAs, while reducing daily dose compared to three-times-daily dosing. At the same time the suggested increase in daily dose for 10% of the samples above the target range is mostly likely due to sampling prior to the minimum drug concentration: While the median meropenem sample was collected 20 minutes before the planed end of the dosing interval, the median sample that was both above the target range and had a recommendation to increase the daily dose was collected 60 minutes before the planned end of the dosing interval. The positive results obtained by this evaluation strengthened the case to integrate the tool into the clinical practice without delay.

Conclusion

After observing the low target attainment rooted in the difficulty of integrating target and relevant patient information into individual dosing decisions, a concise dosing tool for initial meropenem dosing was developed. Based on the observed local susceptibility pattern (MIC distribution) or if available the susceptibility (MIC value) of the pathogen causing the infection and the renal function (assessed by creatinine clearance estimated using Cockcroft-Gault formula) of an individual patient, a single dosing regimen for initial meropenem therapy is recommended by the dosing tool. The retrospective evaluation using data collected during stage I of the clinical trial, suggested a high potential for the tool to increase target attainment.

4.2.3 Stage III: Developing and implementing an interactive model-informed dosing software

To allow for more flexibility, such as the integration of patient-individual antibiotic drug concentration measurements, various levels of prior knowledge on the pathogen and individually-to-chose PK/PD targets a model-informed, interactive dosing tool was developed in stage III of project II.

Selection and evaluation of the pharmacokinetic models

The software was designed to easily integrate additional antibiotics and patient populations. The current version supports dosing decisions in critically ill patients receiving either meropenem or piperacillin/tazobactam therapy. For meropenem the previously evaluated (see 3.2.2.1) PK model underlying the model-informed dosing tables developed for stage II was implemented in the dosing software. For piperacillin/tazobactam the five potentially suitable PK models [50,175–178] identified in a literature research showed a widely varying predictive performance for the data collected in stage I of the clinical study. While observed bias, i.e. the median prediction errors, ranged between – 32.0 mg/L and 15.3 mg/L and the imprecision, i.e. absolute median prediction errors, between 18.0 mg/L and 48.9 mg/L, the graphical evaluation of the absolute prediction errors clearly demonstrated some of the models to be inadequate to describe the pharmacokinetics of piperacillin in our local patient population: The PK models by Andersen et al. [178] (Figure S8), Roberts et al. [175] (Figure S10) and by Li et al. [177] (Figure S11) all demonstrated a strong bias to underpredict high meropenem concentrations and the PK model by Öbrink-Hansen et al. [176] displayed an extremely high variability in predicted concentrations (Figure S9). Only the two-compartment model by Sukarnjanaset et al. [50] showed an acceptable predictive performance (Bias: -2.73 mg/L (-10.9%), imprecision: 20.2 mg/L (60.3%)) even if a bias to underpredict high (> 100 mg/L) piperacillin concentrations (Figure 3.14) was detected. The wide prediction interval determined during model evaluation can be attributed to the typical high unexplained variability in a ICU patient population and is therefore expected [79,204,205]. While the slight bias of the PK model to underpredict observed piperacillin concentrations can be considered as an additional safety margin lowering the probability of each dosing regimen to achieve the PK/PD target and leading to slightly higher dose recommendations, the observed underprediction for piperacillin concentrations above 100 mg/L might indicate an inadequate predictive performance of the PK model for a subset of patients. However, inspecting the individual concentration-time course predictions and the documented piperacillin concentrations and observing the high deviations for some patients and concentration measurements (e.g. ID7, 2nd concentration measurement, Figure S12), the question arose if these high deviations between predicted and observed concentrations were not in fact due to inaccuracies during documentation of sampling or dosing time. For example, an additional dose not documented in the patient record or a concentration measurement taken during instead of prior to the drug infusion would lead to large discrepancies between predicted and observed concentrations.

Although such inaccuracies have been observed in clinical practice and are known to impact model-informed precision dosing [206,207], this hypothesis could neither be confirmed nor rejected with reasonable confidence for the concentration measurements in question. However, the origin of the observed deviation has no relevance for the warning system implemented in the software. To identify both erroneous measurements/sample data and individual patients not well predicted by the PK model, the user will be warned if documented antibiotic concentration(s) are found to be outside the 95% prediction interval for the administered dosing regimen and the characteristics of the patient. As a consequence, patients and samples not well predicted by the PK model are identified and can be further scrutinised after the first drug measurement. Due to possible inaccuracies in documentation and the high PK variability in ICU patients the implementation of similar warning systems in future MIPD software was recommend. Additionally, prior to the first measurement, the direction of the bias of the piperacillin model implemented in the DoseCalculator ensures concentrations exceeding the selected PK/PD targets. Therefore, the predictive performance of the PK model was judged to be acceptable. The insufficient predictive performance of the other four PK models once more highlights the necessity and importance of a thorough model evaluation prior to implementation and application of a PK model.

To assess the predictive performance of the PK model by Sukarnjanaset et al. if prior piperacillin concentration measurements are available, a step-wise MAP estimation and prediction of the next observed concentration was conducted. This second evaluation step provided two important insights: Frist, as expected, the additional patient-specific PK information overall improved the predictive performance which was illustrated by a 78.8% reduction in bias (-2.73 mg/L to -0.58 mg/L). Second, the graphical analysis of the MAP and population predicted concentration-time profiles and the observed concentrations for each patient repeatedly revealed single measurements outside the 90% prediction interval, while other observed concentration of the same patient were found to be well predicted. That individual measurements of otherwise well predicted patients were found to be far outside the prediction interval, supported the hypothesis of inaccuracies in data documentation. This uncertainty in the reported data needs to be taken into account when working with clinical routine data.

Development of the dosing tool

The DoseCalculator was designed to select the best dosing regimen for the three identified (different) levels of pathogen knowledge faced during the course of an antimicrobial therapy: In ICU patients, antibiotic therapy needs to be initiated at the first signs of infection [204] and as a consequence, typically neither the pathogen nor its MIC value are known at the start of antibiotic treatment. In this case, the user of the DoseCalculator can choose from three different targets: either the pathogen-unspecific breakpoints reported by EUCAST, the LPIFR based on the local pathogen-unspecific MIC distribution (in our case at the Charité-Universitätsmedizin Berlin) or a user-specified drug concentration. In stage I of the study, the defined empirical targets (based on EUCAST breakpoints for the least susceptible

pathogens) were found to be considerably higher than the observed susceptibility (see 3.2.1.3) [208]. For this situation, the LPIFR is therefore a valuable opportunity to reduce unnecessary high antibiotic dosing. However, since local MIC distributions might vary over time they need to be monitored and the MIC distribution implemented in the DoseCalculator updated regularly. Furthermore, in the rare event of a pathogen with high MIC values, the risk of target non-attainment could be underestimated until the MIC is determined. Therefore, it is vital to communicate those limitations to the decision-making team and encourage a dosing increase or change of antibiotic if higher MIC values are expected. In general, the dosing regimen recommendations based on the LPIFR metric should only be used as long as there is no further knowledge about the pathogen (e.g. MIC) available [209]. If the genus of the pathogen becomes available and is entered in the DoseCalculator, the EUCAST reported MIC value distribution for the selected pathogen will be used for a CFR analysis as default. To prevent the treatment of pathogens without a clear indication for meropenem or piperacillin/tazobactam, only pathogens with an explicit treatment recommendation by the AMS team were included in the MIPD software. During the initial introduction and training with the DoseCalculator, it needs to be emphasised that the non-availability of a pathogen in the DoseCalculator is equivalent to a recommendation by the AMS team to change the antibiotic drug. In this case, the responsible AMS team should be consulted to jointly decide on an appropriate antimicrobial therapy. Once the MIC value of the infection pathogen becomes available (approximately two days after treatment see 3.2.1.3 [208]) and is entered in the software, a PTA analysis will be conducted. By default, the MIC value will be chosen as target, but to allow for a more flexible target selection in case of severe infections, the user can adjust the targeted antibiotic concentration without restrictions. For all three possible levels of pathogen knowledge, a toxicity threshold for the minimum drug concentration can be entered to further discriminate between the dosing regimens included in the analysis based on their probability to reach toxic concentrations. Although the safety profile of both meropenem and piperacillin/tazobactam was overall considered to be favourable [47,77], adverse events (e.g. neurotoxicity, nephrotoxicity) have been linked to high minimum concentrations [57,58]. Since no additional benefit was expected once the drug exposure exceeds conservative PK/PD targets such as $100\%T_{>MIC}$ [57], even a low unnecessary risk of adverse events should be avoided. Both the optional toxicity threshold and the ranking based on lower daily dose for dosing regimen reaching the PK/PD target, will help to ensure effective and safe dosing recommendations.

The routine drug concentration measurement in ICU patients is an important tool to ensure adequate antibiotic drug exposure and can further improve the dosing recommendations by the DoseCalculator. If both a drug concentration measurement and the preceding dosing history is available for a patient it can be entered into the DoseCalculator. Based on the provided patient characteristics, the dosing history and the drug concentration(s), a MAP estimation will be conducted and the subsequent analyses will be based on the patient's individual posterior parameter distribution. Especially in the ICU population with

its high intra- and intererindividual variability [79,204,205,210,211], including individual PK information will help to provide more precise predictions and consequently better dosing recommendations for each patient.

Retrospective evaluation of the dosing tool

The first evaluation of the DoseCalculator using the data from stage I (i.e. patients with full dosing history and determined MIC value) suggested a substantial potential to improve target attainment while at the same time reducing the total daily dose. For meropenem, the median prediction of the dosing regimens suggested by the tool was inside the target range (1-5xMIC) in the majority of cases (92.0%). This constituted a >3 times increase (28.6% to 92.0%) in median meropenem samples predicted to be in the target range compared to the actually administered dosing regimen, while at the same time reducing the median daily dose by 77.8%.

For piperacillin, the dosing regimens suggested by the software led to a convergence of the median predicted piperacillin concentration towards the target range, but the percentage of samples within the target range was only increased by 139% (from a low 16.7% for the observed dosing regimens to 23.3%). Even if the median MIC-normalised piperacillin concentration decreased by 36.3% (6.5 vs. 10.2 mg/L), most of the samples were still predicted to be above the target range. By integrating an additional piperacillin formulation of 2 g into the DoseCalculator the predicted target attainment was increased by 405% to 84.4%, clearly highlighting the need of this additional formulation at Charité-Universitätsmedizin Berlin.

Conclusion

Compared to the tabular dosing tool developed for stage II, the newly developed dosing software allows for more flexibility and the integration of additional data like drug concentration(s) into the analyses forming the foundation for the dosing recommendations. Furthermore, the developed platform can be easily expanded to include other antibiotic drugs or patient populations like intensive care patients receiving renal replacement therapy. The retrospective application of the DoseCalculator for the patients included in stage I of the study, did not only suggest a high potential to increase target attainment and reduce daily doses, but also highlighted the need for additional piperacillin/tazobactam formulations.

4.2.4 Conclusion and outlook project II

Project II is not only a powerful illustration of the possibilities of model-informed precision dosing but first and foremost an example on the importance of interprofessional collaboration to achieve optimal patient care. As introduced in chapter 1.1, a rational antibiotic drug therapy entails the four vital components appropriate indication, appropriate choice of antibiotic, appropriate timing and appropriate dosing. To derive the optimal antibiotic dosing for an individual patient based on those four components is already a challenging endeavour in a hypothetical research setting focused only on antibiotic therapy. However, in clinical practice the focus is rarely on antibiotic therapy alone. Intensive care patients commonly receive treatment for multiple diseases in parallel and the infection is demoted to be just another complication the attending healthcare professional has to take care of. As a consequence, the antibiotic therapy of each individual patient is in constant competition for resources and attention, not only with other patients but other therapies for the same patient as well. Even if there are enough monetary resources and heath care personal available, other treatments, diagnostic measures and transfers between wards will always limit the possible options for the antibiotic therapy. To sustainably improve antibiotic therapy in intensive care patients, the reality in clinical routine needs to be taken into account and every intervention needs to be designed to account for local conditions. Similar to antibiotic therapy itself, a "one intervention fits all" approach covering multiple institutions with different prerequisites is unlikely to produce the best results. With this knowledge in mind, project II was planned and conducted as a close interprofessional collaboration between the local AMS team, infectious disease specialists, critical care specialists, hospital pharmacists, the clinical laboratory and pharmacometricians. From the design of the study and the target definition, to the development of the model-informed dosing tools and their implementation into clinical practices, bi-weekly meetings of the whole study team enabled continuous discussions and feedback and guaranteed the inclusion of all stakeholders. Although such an approach improves the chance of a successful intervention, unforeseen developments can still hinder their timely implementation. In the spring of 2020, the COVID-19 pandemic reached Germany. A surge of COVID-19 cases and the associated increase in intensive care patients suspended the study for multiple months and complicated the implementation of the developed dosing tools throughout 2021 and 2022.

The study was designed to not only integrate locally available expertise but also to incorporate local information collected during the study itself. While the main objective of stage I was to assess current clinical practices and target attainment, both the pharmacokinetic data and the observed local pathogen susceptibility pattern were utilised to inform dosing recommendations in stage II and III. Based on the observed antibiotic concentrations, dosing histories and patient characteristics, piperacillin and meropenem PK models were evaluated and the best performing models selected. The wide variation in predictive performance observed during the study (see 3.2.3.1), illustrated the importance of an

extensive model evaluation in the targeted population prior to implementation into a model-informed dosing tool. Based on the observed local pathogen susceptibility pattern the local pathogen-independent mean fraction of response was introduced, allowing a more targeted therapy prior to pathogen detection at the start of antibiotic therapy.

Both the retrospective evaluation of the tabular dosing decision tool for initial meropenem dosing and the DoseCalculator software initial and follow-up dosing revealed a high potential to increase target attainment, while at the same time reducing the daily dose for the individual patient. While these results give hope for the future of antibiotic therapy, the predicted target attainment for the suggested dosing regimens needs to be realistically interpreted as close to the best possible outcome. During the simulation study for the retrospective evaluation both the application rate of the tools and the adherence to their dose suggestions was assumed to be 100%. Even if it is impossible to estimate the real application rate and/or adherence, it is rather unlikely that even one of them will be close to 100%. As a consequence, the target attainment for the whole population will probably not rise as steep as predicted in the simulated best case scenario. Furthermore, even for the patients whose antibiotic dosing was informed by the developed dosing tools, the target attainment will probably not be as good as predicted: In addition to possible non adherence to the dosing suggestion, applying the tools only to inform dosing decisions for the most vulnerable and pharmacokinetically complicated patients might decrease the predictive performance of the PK models and therefore the quality of the dosing suggestions. Still, even if an >3-times increase in target attainment might not be achieved, a considerable increase in target attainment is still expected. How big this increase will be in a real world clinical setting can only be determined by prospective evaluations for both the tabular dosing decision tool and the DoseCalculator software.

4.3 Project III: Evaluation and extension of the MeroRisk Calculator

In Project III the MeroRisk Calculator, a dosing assessment tool for meropenem therapy in critically ill patients prior to the initiation of treatment, was evaluated and extended to integrate risk assessment for target non-attainment based on general pathogen sensitivity data.

Evaluation of the MeroRisk Calculator

Due to the high variability in sampling times observed in the real-world clinical dataset and the few samples included 8 hours after standard dose a direct evaluation of the MeroRisk Calculator was not feasible. Instead, the MeroRisk Calculator was evaluated using a two-step data- and model-based evaluation strategy allowing the inclusion of a large number of patients (n=155) and samples (n=891).

The evaluation of the selected PK model [129] revealed a small bias (-0.84 mg/L) to underpredict observed meropenem concentrations and a 50% prediction error interval ranging from -5.0 mg/L (-59%) to 1.2 mg/L (32%). Due to the small size of bias compared to the observed concentrations (mean meropenem concentration 13.0 mg/L) the bias was considered to be acceptable. Furthermore, the tendency to underpredict observed concentrations leads to more conservative risk predictions and thus adds a safety margin to the risk assessment. The precision, assessed based on the 50% prediction error interval, was judged to be acceptable for a critically ill patient population and the nature of the retrospective data collected during clinical routine. The imprecision observed during model evaluation using a dataset from clinical routine might be inflated by the higher degree of uncertainty (in e.g. sampling or dosing times) compared to a prospective dataset collected in a controlled clinical trial [198]. In a previously published evaluation of eight meropenem NLME PK models for critically ill patients, the observed bias ranged from -8.76 to +7.06 mg/L (mean meropenem concentration in the dataset: 16.3 mg/L) with +2.07 mg/L as the lowest observed bias [212]. The imprecision assessed based on root mean squared prediction errors was higher for all models investigated in the mentioned publication than for the model used to evaluate the MeroRisk Calculator (9.9 – 42.1 mg/L vs. 6.2 mg/L) [212]. To conclude, the selected PK model adequately represented the observed data and its predictions could therefore be used as a benchmark for the evaluation of the MeroRisk Calculator.

For patients with a creatinine clearance equal to or greater than 50 mL/min, the PK model and the MeroRisk Calculator predicted highly similar meropenem concentrations. For patients with a creatinine clearance below 50 mL/min however, the MeroRisk Calculator predicted higher concentrations than the PK model. This discrepancy can be explained by the different mathematical approaches underlying the NLME PK model and the model integrated in the MeroRisk Calculator. The MeroRisk Calculator has been based on a linear regression model on double natural logarithmic scale linking meropenem

concentrations 8 hours after standard dose to a patient's creatinine clearance. Therefore, the linear model of the MeroRisk Calculator cannot separate between renal and non-renal elimination (the latter accounting for up to 27% of meropenem clearance [213]) and with decreasing creatinine clearances, the renal and non-renal clearance is reduced at the same rate. As a consequence, the concentration 8 hours after standard dose of a patient with a creatinine clearance approaching zero would be wrongly predicted by the MeroRisk Calculator infinite. For the same patient, the NLME PK model would predict a clearance of roughly 20% of the median clearance, which corresponds well to the expected extent of non-renal clearance.

Differences in risk predictions between the NLME PK model and the MeroRisk Calculator were small for all patients and MIC values below 8 mg/L. The difference in concentration predictions had only a minor impact due to very low risk predictions for patients with creatinine clearance below 50 mL/min. However, for MIC values greater or equal to 8 mg/L, the risk of target non-attainment for patients with a creatinine clearance below 50 mL/min was substantially underestimated by the MeroRisk Calculator compared to the PK model. MIC values of 8 mg/L or higher are rare and would lead to a change in antibiotic in most cases. Nevertheless, the MeroRisk Calculator should not be used for patients with impaired renal function and high MIC values ($\geq$8 mg/L). The disclaimer of the MeroRisk Calculator was updated to integrate the knowledge gained from the evaluation and to exclude patients with a creatinine clearance below 50 mL/min.

For all other patients, the very good agreement between the risk predictions of the MeroRisk Calculator and the NLME PK model (see section 3.3.2.2) supports interchangeability. Therefore, the intuitive and easy-to-use MeroRisk Calculator can be utilised to assess the risk of target non-attainment of a patient prior to therapy start with the same confidence as the successfully evaluated NLME PK model.

Extension of the MeroRisk Calculator

The newly added possibility to assess the risk of target non-attainment based on the infecting pathogen if the MIC value is unknown considerably extends the applicability of the tool. This is especially helpful for all the hospitals not determining MIC values on a regular basis (in a recent survey of ICU physicians in Germany over half of the respondents reported not to receive any MIC values [36]) and early during antibiotic therapy when the MIC values is not yet available (in Project II the median time until the MIC value was reported to the attending physician was 2.1 days). To accommodate changing MIC distributions, an up-to-date version of the MeroRisk Calculator integrating the latest EUCAST MIC distributions is provided online (https://www.bcp.fu-berlin.de/en/pharmazie/faecher/klinische_pharmazie/arbeitsgruppe_kloft/forschung/MRc).

The elevated (>10%) median risk of target non-attainment for 27% out of the 74 pathogens included in the EUCAST database and the investigated critically ill patient population, highlights the need for an individual risk assessment prior to therapy start. In the evaluation of all pathogens, especially pathogens

of the genus *Acinetobacter*, *Pseudomonas* and *Staphylococcus* were identified as high-risk pathogens for standard dosing (Figure S13). For infections caused by pathogens of these genera alternative antibiotic drugs or intensified dosing is especially crucial even for patients with low renal function.

Conclusion and outlook

The MeroRisk-Calculator was successfully evaluated using a clinical routine dataset and a two-step data- and model-based evaluation approach. For patients with creatinine clearances equal to or greater than 50 mL/min, the user-friendly MeroRisk Calculator allows an equally good and reliable risk assessment as the successfully evaluated NLME PK model. For patients with creatinine clearance below 50 mL/min, the MeroRisk Calculator should not be used due to the observed tendency to underpredict the risk of target non-attainment. By including risk assessment based on general pathogen sensitivity data, the range of possible application of the MeroRisk Calculator was substantially extended to include situations where MIC values are not (yet) available. While the developed two-step evaluation approach allowed to exploit an already available large dataset from clinical routine and thereby increased the robustness of the results without the need for an expensive prospective study, a prospective clinical study remains the "gold standard" of evaluation and should follow next. A prospective study of the MeroRisk Calculator could also investigate the effect of the tool on treatment outcomet. Even if a prospective study is not possible, to ensure transferability to other intensive care wards, the results of this evaluation need to be verified using clinical data from the respective ICUs prior to the implementation of the MeroRisk Calculator.

Overall conclusion and perspective

The objective of this thesis was the development, implementation and evaluation of MIPD tools to ultimately improve antibiotic dosing in critically ill patients. To achieve this objective, the presented projects employed pharmacometric modelling and simulation techniques to (i) characterise antibiotic drug pharmacokinetics in critically ill patients, (ii) assess current antibiotic dosing in the intensive care wards, (iii) develop MIPD tools and (iv) implement and evaluate developed MIPD tools.

The presented research was focused on antibiotic therapy in critically ill patients for several reasons. Due to the frequent and sometimes inadequate antibiotic therapy in ICUs, the emergence and spread of antimicrobial resistance is especially prominent and dangerous in highly vulnerable ICU patients [214,215]. Reducing or even inverting the spread of antimicrobial resistances in ICUs, might therefore contribute disproportionately to the global fight against antimicrobial resistance. Meropenem and the drug combination piperacillin/tazobactam were chosen as investigated antibiotic drugs, due to their widespread use and their broad antimicrobial activity. While the widespread use of the two drugs improves the transferability and therefore expands the benefit of our research, improvements in the rational therapy of the two drugs will hopefully protect their broad antimicrobial activity and hold emerging antimicrobial resistances at bay. Besides the higher rates of resistance in ICUs, the presented research focused on ICU patients for two equally important additional reasons. First, ICU patients are especially vulnerable to bacterial infections: Due to their critical illness they often face mortality rates up to 60% during sepsis or septic shock [10–12,85,86]. Second, an effective antibiotic treatment of ICU patients is challenging due to several heterogeneous changes in PK processes, based on the pathophysiology of their severe illnesses [79]. As observed in stage I of the clinical trial presented in Project II, those changes in PK processes complicate the selection of a suitable dosing regimen and often lead to suboptimal target attainment.

Pharmacometric modelling and simulation approaches in general and MIPD in particular, can improve antibiotic treatment considerably by characterising the PK/PD of antibiotic drugs and supporting dosing decisions in the clinic [199,209,216–218]. However, while there are promising examples of model-informed tools improving drug therapy [219,220], implementation into real world clinical settings is still lagging behind for various reasons [221].

Even for some commonly administered and supposedly ‘well-known’ drugs, the PK is not fully characterised in special populations like ICU patients or patients receiving extracorporeal organ support (e.g. renal replacement therapy, extracorporeal membrane oxygenation, cytokine adsorber therapy). PK studies and subsequent NLME analyses are still needed to assess the effect of extracorporeal organ support on drug exposure and to determine if dose adaptations are needed. One crucial challenge often faced during model development in special populations is the data situation. To develop sophisticated

pharmacometric models, high quality data is needed. Depending on the research question the requirements can vary, but for population pharmacokinetic modelling the datasets ideally contain multiple patients, different dosing regimens, multiple concentration measurements per patient and dosing regimen, and a wide range of patient characteristics. If an investigation is focused on the elimination processes of a drug -like Project I-, additional drug measurements in urine and faeces are especially valuable. Unfortunately, the availability of accurate high quality data is rather limited. This is partly due to the smaller number of patients in special populations, and mainly due to the high effort and costs involved in conducting largescale clinical trials. In order to establish MIPD for a broad range of diseases and drugs in the future, it is therefore necessary to first enable the funding and conduct of clinical trials. In addition to this, the accessibility and use of available data in hospitals needs to be improved. Routine drug measurements and pathogen susceptibility data cannot only be used to monitor current antibiotic treatment, but can and should further be utilised –as illustrated in Project II- to evaluate the predictive performance of a PK model for the local population or to inform future dosing decisions based on local pathogen susceptibility. Unfortunately, so far extracting routine data from the electronic healthcare records is often tedious work, due to inconsistent data structures and incompatible software. At the same time, clinical routine data is often associated with a higher degree of uncertainty compared to prospective clinical trials, mostly due to less precise documentation [198]. To realise the full potential of the available clinical routine data in the future, a standardised data structure and good data management procedures should be implemented and the extractability of data from electronic healthcare records should be improved.

Closing the remaining knowledge gaps is a particularly important, but at the same time only the first step in enhancing the rational use of antibiotics. To improve antibiotic therapy, the knowledge gained during scientific research needs to find its way into individual dosing decisions at the bedside. Currently, the translation of accumulated knowledge into clinical application remains unsatisfactory: The growing repertoire of published PK models is seldom integrated into user-friendly tools and therefore remains inaccessible for most healthcare professionals [79,121]. Furthermore, the available tools often do not match local conditions, objectives or, in the case of commercial Bayesian dosing software, the available budget. This problem was also faced before Project II presented in this thesis. The dosing regimens frequently used at Charité-Universitätzmedizin Berlin were either not included in the available tools or part of a multitude of dosing regimen recommendations complicating the daily use of the tool [129,131,173,222]. All freely available Bayesian dosing software [223] did either not include the investigated drugs and patient population, or did not provide the envisaged user-friendliness and compatibility with the local clinical routine. Furthermore, the risk of reaching toxic minimum concentrations was not considered in the examined other tools and an evaluation of the underlying PK models would have been necessary. Most likely, this situation is similar for a wide range of drugs, model-based tools and hospitals. Even when model-based tools or PK models are available for a specific

drug in a specific patient population, the selected target or the clinical setting might hinder implementation and use. In those situations, local initiatives are needed to develop dosing decision tools fit for the situation on-site. The approach described in this thesis may serve as a blueprint to a wide range of hospitals, patient populations and drugs to develop sophisticated dosing decision tools providing optimised dosing adapted for local conditions and objectives.

In many hospitals reliable and frequent drug measurements are not yet available [132]. Since drug measurements are a prerequisite for MIPD software, such software cannot be implemented without a routine drug measurement program. As an alternative, tabular dosing decision tools integrating an evaluated PK model can be used for initial dose adaptation -as illustrated in *stage II* of Project II- based on individual patient characteristics. Furthermore, these tabular dosing decision tools can provide dosing recommendations prior to the first drug measurement, improving dosing in this especially crucial time window of antibiotic drug therapy [224].

If drug measurements are available, MIPD software has clear advantages over tabular model-based dosing algorithms. Both during the development of model-based dosing algorithms and during the application of MIPD software, stochastic simulations of PK models are employed to determine the probability of a selected dosing regimen to attain a defined target given specific patient characteristics (i.e. probability of target attainment (PTA)). By analysing each patient individually during the application of the MIPD software, it is more flexible in adapting to the individual situation of each patient compared to static dosing algorithms relying on analyses finalised during development and therefore prior to use: Multiple continuous patient characteristics (e.g., creatinine clearance) can be integrated into MIPD software simultaneously without categorisation, which is often applied to keep dosing algorithms concise and easy to use. As a consequence, dosing recommendations from MIPD software can be calculated based on the concrete individual patient characteristics. Furthermore, the PK/PD target can be flexibly adjusted in MIPD software to account for particular circumstances of individual patients: A higher PK/PD target in plasma might for example be warranted to treat an infection suspected to be located at a poorly perfused site of the body. In addition to this higher flexibility, the regular concentration measurements that are often performed in combination with MIPD software do not only detect inadequate drug exposures, but also provide valuable information about the PK of the individual patient. Especially in patient populations with high inter- and intraindividual variability, such as ICU patients, the additional PK information can be useful to subsequently adapt dosing for an individual patient. The complex task of deriving the subsequent most adequate dosing regimen based on drug concentration measurements of the individual patient, can then be supported by the MIPD software and is carried out based on clear quantitative metrics, e.g. the PTA [198]. In contrast to MIPD software, the integration of newly gained PK information in static dosing algorithms is not possible.

The constraint in the choice of MIPD tool (tabular vs. interactive MIPD software) due to the availability of a concentration measurement program, highlights the key factor in developing and implementing MIPD dosing tools: the local conditions. It is often not feasible to rearrange the complex processes during clinical routine to provide the necessary conditions needed for an already developed tool. Instead, new tools should be designed or already developed tools adapted specifically for local objectives, the local clinical routine and local conditions. To ensure the best possible adaptation to clinical processes and to integrate the broad expertise of different healthcare professions, the projects presented in this thesis were all conducted within a close interprofessional collaboration between local AMS teams, infectious disease specialists, critical care specialists, pharmacists, the clinical laboratory and pharmacometricans. In project I, the collaboration ensured the physiologically sound model development strategy and interpretation of the results. In project II and III, continuous discussions ranging from the choice of the optimal PK/PD targets to the user-friendliness of the developed tools guaranteed an optimal adaptation to local objectives and clinical routine. In all three projects, the straightforward and direct communication with the scientists responsible for data collection and bioanalysis was crucial to spot and interpret irregularities in the datasets.

In addition to the already mentioned challenges, a majority of available PK models and tools have not been evaluated, undermining trust in the reliability of their predictions and further hindering implementation. To illustrate the accuracy and potential of MIPD tools, a clinical routine dataset was used in Project III to evaluate an already developed tool and simulation studies were used in Project II to demonstrate the possible improvements in antibiotic dosing when using the developed tools. The prospective evaluation of the tools during clinical routine planned as next step, should asses the promising results of the simulation studies and further enhance trust in the tools and their potential.

MIPD is a powerful approach with the potential to improve drug therapy for a range of diseases and patient populations. It is one important tool to improve antibiotic drug therapy in ICU patients and will hopefully contribute to lower mortality rates and a reduction in antibiotic resistance in the near future. To accomplish these goals, first MIPD needs to be widely implemented into clinical routine. In this thesis potential challenges and opportunities for the implementation were presented and discussed in detail. The scientific findings and the dosing tools developed in this thesis will not only improve dosing at Charité Universitätsmedizin Berlin, but also serve as a blueprint for other institutions and drugs.

Bibliography

[1] G. Pappas, I.J. Kiriaze, M.E. Falagas. Insights into infectious disease in the era of Hippocrates. Int. J. Infect. Dis. 12: 347–350 (2008).

[2] The anthropology of infectious disease: International health perspectives. Routledge, London, 1st ed. (2013).

[3] L. Shaw-Taylor. An introduction to the history of infectious diseases, epidemics and the early phases of the long-run decline in mortality. Econ. Hist. Rev. 73: E1–E19 (2020).

[4] A.P. Dobson, E. Robin Carper. Infectious diseases and human population history. Bioscience 46: 115–126 (1996).

[5] Kathrin I. Mohr. History of antibiotics research. Curr. Top. Microbiol. Immunol. 37: 435 (2012).

[6] R.I. Aminov. A brief history of the antibiotic era: Lessons learned and challenges for the future. Front. Microbiol. 1: 1–7 (2010).

[7] K.C. Nicolaou, S. Rigol. A brief history of antibiotics and select advances in their synthesis. J. Antibiot. (Tokyo). 71: 153–184 (2018).

[8] L. Zaffiri, J. Gardner, L.H. Toledo-Pereyra. History of antibiotics: From salvarsan to cephalosporins. J. Investig. Surg. 25: 67–77 (2012).

[9] W. Adedeji. The treasure called antibiotics. Ann. Ibadan Postgrad. Med. 14: 56–57 (2016).

[10] Y. Sakr, U. Jaschinski, X. Wittebole, T. Szakmany, J. Lipman, S.A. Ñamendys-Silva, I. Martin-Loeches, M. Leone, M.N. Lupu, J.L. Vincent. Sepsis in intensive care unit patients: Worldwide data from the intensive care over nations audit. Open Forum Infect. Dis. 5: 1–9 (2018).

[11] J.A. Kempker, G.S. Martin. The changing epidemiology and definitions of sepsis. Clin. Chest Med. 37: 165–179 (2016).

[12] C. Engel, F.M. Brunkhorst, H.-G. Bone, R. Brunkhorst, H. Gerlach, S. Grond, M. Gruendling, G. Huhle, U. Jaschinski, S. John, K. Mayer, M. Oppert, D. Olthoff, M. Quintel, M. Ragaller, R. Rossaint, F. Stuber, N. Weiler, T. Welte, H. Bogatsch, C. Hartog, M. Loeffler, K. Reinhart. Epidemiology of sepsis in Germany: Results from a national prospective multicenter study. Intensive Care Med. 33: 606–618 (2007).

[13] K. Gould. Antibiotics: From prehistory to the present day. J. Antimicrob. Chemother. 71: 572–575 (2016).

[14] L. Morrison, T.R. Zembower. Antimicrobial resistance. Gastrointest. Endosc. Clin. N. Am. 30: 619–635 (2020).

[15] B.R. da Cunha, L.P. Fonseca, C.R.C. Calado. Antibiotic discovery: Where have we come from, where do we go? Antibiotics 8: 45 (2019).

[16] M. Nadimpalli, E. Delarocque-Astagneau, D.C. Love, L.B. Price, B.T. Huynh, J.M. Collard, K.S. Lay, L. Borand, A. Ndir, T.R. Walsh, D. Guillemot, A. De Lauzanne, A. Kerleguer, A. Tarantola, P. Piola, T. Chon, S. Lach, V. Ngo, S. Touch, Z.Z. Andrianirina, M. Vray, V. Richard, A. Seck, R. Bercion, A.G. Sow, J.B. Diouf, P.S. Dieye, B. Sy, B. Ndao, M. Seguy, L. Watier, A.Y. Abdou. Combating global antibiotic resistance: Emerging one health concerns in lower-and middle-income countries. Clin. Infect. Dis. 66: 963–969 (2018).

[17] S. Bin Zaman, M.A. Hussain, R. Nye, V. Mehta, K.T. Mamun, N. Hossain. A review on antibiotic resistance: Alarm bells are ringing. Cureus 9: 6 (2017).

[18] T.F. Schäberle, I.M. Hack. Overcoming the current deadlock in antibiotic research. Trends Microbiol. 22: 165–167 (2014).

[19] The Boston Consulting Group. Breaking through the wall: A call for concerted action on antibiotics research and development. (2001).

[20] L. Matthiessen, R. Bergström, S. Dustdar, P. Meulien, R. Draghia-Akli. Increased momentum in antimicrobial resistance research. Lancet 388: 865 (2016).

[21] J.A. Roberts, P. Kruger, D.L. Paterson, J. Lipman. Antibiotic resistance-What's dosing got to do with it? Crit. Care Med. 36: 2433–2440 (2008).

[22] G. Levy Hara, S.S. Kanj, L. Pagani, L. Abbo, A. Endimiani, H.F.L. Wertheim, C. Amábile-Cuevas, P. Tattevin, S. Mehtar, F. Lopes Cardoso, S. Unal, I. Gould. Ten key points for the appropriate use of antibiotics in hospitalised patients: a consensus from the Antimicrobial Stewardship and Resistance Working Groups of the International Society of Chemotherapy. Int. J. Antimicrob. Agents 48: 239–246 (2016).

[23] K. Lambrini. The rational use of antibiotics medicine. J. Healthc. Commun. 02: 1–4 (2017).

[24] T.G. Slama, A. Amin, S.A. Brunton, T.M. File, G. Milkovich, K.A. Rodvold, D.F. Sahm, J. Varon, D. Weiland. A clinician's guide to the appropriate and accurate use of antibiotics: The Council for Appropriate and Rational Antibiotic Therapy (CARAT) criteria. Am. J. Med. 118: 1–6 (2005).

[25] A. Kumar. Early antimicrobial therapy in severe sepsis and septic shock. Curr. Infect. Dis. Rep. 12: 336–344 (2010).

[26] S. Harbarth, J. Garbino, J. Pugin, J.A. Romand, D. Lew, D. Pittet. Inappropriate initial antimicrobial therapy and its effect on survival in a clinical trial of immunomodulating therapy for severe sepsis. Am. J. Med. 115: 529–535 (2003).

[27] R.D. MacArthur, M. Miller, T. Albertson, E. Panacek, D. Johnson, L. Teoh, W. Barchuk. Adequacy of early empiric antibiotic treatment and survival in severe sepsis: Experience from the MONARCS trial. Clin. Infect. Dis. 38: 284–288 (2004).

[28] M. Dryden, A.P. Johnson, D. Ashiru-oredope, M. Sharland. Using antibiotics responsibly: Right drug, right time, right dose, right duration. J. Antimicrob. Chemother. 66: 2441–2443 (2011).

[29] J.H. Jorgensen, M.J. Ferraro. Antimicrobial susceptibility testing: A review of general principles and contemporary practices. Clin. Infect. Dis. 49: 1749–1755 (2009).

[30] K. Syal, M. Mo, H. Yu, R. Iriya, W. Jing, S. Guodong, S. Wang, T.E. Grys, S.E. Haydel, N. Tao. Current and emerging techniques for antibiotic susceptibility tests. Theranostics 7: 1795–1805 (2017).

[31] M. Balouiri, M. Sadiki, S.K. Ibnsouda. Methods for in vitro evaluating antimicrobial activity: A review. J. Pharm. Anal. 6: 71–79 (2016).

[32] Methods for dilution antimicrobial susceptibility tests for bacteria that grow aerobically. Clinical and Laboratory Standards Institute, Wayne, Ninth ed. (2012).

[33] D.C. Broussou, P.L. Toutain, F. Woehrlé, F. El Garch, A. Bousquet-Melou, A.A. Ferran. Comparison of in vitro static and dynamic assays to evaluate the efficacy of an antimicrobial drug combination against Staphylococcus aureus. PLoS One 14: 1–13 (2019).

[34] J.B. Bulitta, W.W. Hope, A.E. Eakin, T. Guina, V.H. Tam, A. Louie, G.L. Drusano, J.L. Hoover. Generating robust and informative nonclinical in vitro and in vivo bacterial infection model efficacy data to support translation to humans. Antimicrob. Agents Chemother. 63: 1–25 (2019).

[35] B. Kowalska-Krochmal, R. Dudek-Wicher. The minimum inhibitory concentration of antibiotics: Methods, interpretation, clinical relevance. Pathogens 10: 1–21 (2021).

[36] U. Liebchen, M. Paal, C. Scharf, I. Schroeder, B. Grabein, J. Zander, C. Siebers, M. Zoller. The ONTAI study – a survey on antimicrobial dosing and the practice of therapeutic drug monitoring in German intensive care units. J. Crit. Care 60: 260–266 (2020).

[37] M. Benkova, O. Soukup, J. Marek. Antimicrobial susceptibility testing: currently used methods and devices and the near future in clinical practice. J. Appl. Microbiol. 129: 806–822 (2020).

[38] European Committee on Antimicrobial Susceptibility Testing. Breakpoint tables for interpretation of MICs and zone diameters. Version 8.1 (2018).

[39] J. Turnidge, D.L. Paterson. Setting and revising antibacterial susceptibility breakpoints. Clin. Microbiol. Rev. 20: 391–408 (2007).

[40] P.G. Ambrose, S.M. Bhavnani, C.M. Rubino, A. Louie, T. Gumbo, A. Forrest, G.L. Drusano. Pharmacokinetics-pharmacodynamics of antimicrobial therapy: It's not just for mice anymore. Clin. Infect. Dis. 44: 79–86 (2007).

[41] E.I. Nielsen, O. Cars, L.E. Friberg. Pharmacokinetic/Pharmacodynamic (PK/PD) indices of antibiotics predicted by a semimechanistic PKPD model: A step toward model-based dose optimization. Antimicrob. Agents Chemother. 55: 4619–4630 (2011).

[42] T. Velkov, P. Bergen, J. Lora-Tamayo, C. Landersdorfer, J. Li. PK/PD models in antibacterial development. Curr Opin Microbiol. 23: 1–7 (2013).

[43] J.W. Mouton, M.N. Dudley, O. Cars, H. Derendorf, G.L. Drusano. Standardization of pharmacokinetic/pharmacodynamic (PK/PD) terminology for anti-infective drugs: An update. J. Antimicrob. Chemother. 55: 601–607 (2005).

[44] Y. Hayashi, J.A. Roberts, D.L. Paterson, J. Lipman. Pharmacokinetic evaluation of piperacillin-tazobactam. Expert Opin. Drug Metab. Toxicol. 6: 1017–1031 (2010).

[45] A.E. Muller, B. Huttner, A. Huttner. Therapeutic drug monitoring of beta-lactams and other antibiotics in the intensive care unit: Which agents, which patients and which infections? Drugs 78: 439–451 (2018).

[46] G. Wong, A. Brinkman, R.J. Benefield, M. Carlier, J.J. De Waele, N. El Helali, O. Frey, S. Harbarth, A. Huttner, B. McWhinney, B. Misset, F. Pea, J. Preisenberger, M.S. Roberts, T.A. Robertson, A. Roehr, F.B. Sime, F.S. Taccone, J.P.J. Ungerer, J. Lipman, J.A. Roberts. An international, multicentre survey of β-lactam antibiotic therapeutic drug monitoring practice in intensive care units. J. Antimicrob. Chemother. 69: 1416–1423 (2014).

[47] A. Gin, L. Dilay, J.A. Karlowsky, A. Walkty, E. Rubinstein, G.G. Zhanel. Piperacillin-tazobactam: A β-lactam/β-lactamase inhibitor combination. Expert Rev. Anti. Infect. Ther. 5: 365–383 (2007).

[48] F. Sörgel, M. Kinzig. The chemistry, pharmacokinetics and tissue distribution of piperacillin/tazobactam. J. Antimicrob. Chemother. 31: 39–60 (1993).

[49] Pfizer Inc. Tazocin® (piperacillin and tazobactam powder for injection) - Summary of product characteristics. (2016).

[50] W. Sukarnjanaset, S. Jaruratanasirikul, T. Wattanavijitkul. Population pharmacokinetics and pharmacodynamics of piperacillin in critically ill patients during the early phase of sepsis. J. Pharmacokinet. Pharmacodyn. 46: 251–261 (2019).

[51] J.A. Jamal, D.M. Roberts, A.A. Udy, M.B. Mat-Nor, F.S. Mohamad-Nor, S.C. Wallis, J. Lipman, J.A. Roberts. Pharmacokinetics of piperacillin in critically ill patients receiving continuous venovenous haemofiltration: A randomised controlled trial of continuous infusion versus intermittent bolus administration. Int. J. Antimicrob. Agents 46: 39–44 (2015).

[52] K. Nichols, K. Chung, C.A. Knoderer, L.E. Buenger, D.P. Healy, J. Dees, A.S. Crumby, B. Kays. Population pharmacokinetics and pharmacodynamics of extended-infusion piperacillin and tazobactam in critically ill children. Antimicrob Agents Chemother 60: 522–531 (2016).

[53] J. Zander, G. Döbbeler, D. Nagel, B. Maier, C. Scharf, M. Huseyn-Zada, J. Jung, L. Frey, M. Vogeser, M. Zoller. Piperacillin concentration in relation to therapeutic range in critically ill patients - A prospective observational study. Crit. Care 20: 1–11 (2016).

[54] S. Wen, C. Wang, Y. Duan, X. Huo, Q. Meng, Z. Liu, S. Yang, Y. Zhu, H. Sun, X. Ma, S. Yang, K. Liu. OAT1 and OAT3 also mediate the drug-drug interaction between piperacillin and tazobactam. Int. J. Pharm. 437: 172–182 (2017).

[55] J.B. Bulitta, M. Kinzig, V. Jakob, U. Holzgrabe, F. Sörgel, N.H.G. Holford. Nonlinear pharmacokinetics of piperacillin in healthy volunteers - implications for optimal dosage regimens. Br. J. Clin. Pharmacol. 70: 682–693 (2010).

[56] F. de Velde, J.W. Mouton, B.C.M. de Winter, T. van Gelder, B.C.P. Koch. Clinical applications of population pharmacokinetic models of antibiotics: Challenges and perspectives. Pharmacol. Res. 134: 280–288 (2018).

[57] R. Guilhaumou, S. Benaboud, Y. Bennis, C. Dahyot-Fizelier, E. Dailly, P. Gandia, S. Goutelle, S. Lefeuvre, N. Mongardon, C. Roger, J. Scala-Bertola, F. Lemaitre, M. Garnier. Optimization of the treatment with beta-lactam antibiotics in critically ill patients - Guidelines from the French Society of Pharmacology and Therapeutics (Société Française de Pharmacologie et Thérapeutique - SFPT) and the French Society of Anaesthesia . Crit. Care 23: 1–20 (2019).

[58] S. Imani, H. Buscher, D. Marriott, S. Gentili, I. Sandaradura. Too much of a good thing: A retrospective study of β-lactam concentration-toxicity relationships. J. Antimicrob. Chemother. 72: 2891–2897 (2017).

[59] C.M. Baldwin, K.A. Lyseng-Williamson, S.J. Keam. Meropenem: A review of its use in the treatment of serious bacterial infections. Drugs 68: 803–838 (2008).

[60] M. Hurst, H.M. Lamb. Meropenem: A review of its use in patients in intensive care. Drugs 59: 653–680 (2000).

[61] L. Manning, C. Wright, P.R. Ingram, T.J. Whitmore, C.H. Heath, I. Manson, M. Page-Sharp, S. Salman, J. Dyer, T.M.E. Davis. Continuous infusions of meropenem in ambulatory care: Clinical efficacy, safety and stability. PLoS One 9: 7–9 (2014).

[62] Y.R. Lee, P.D. Miller, S.K. Alzghari, D.D. Blanco, J.D. Hager, K.S. Kuntz. Continuous infusion versus intermittent bolus of beta-lactams in critically ill patients with respiratory infections: A systematic review and meta-analysis. Eur. J. Drug Metab. Pharmacokinet. 43: 155–170 (2018).

[63] B. van Herendael, A. Jeurissen, P.M. Tulkens, E. Vlieghe, W. Verbrugghe, P.G. Jorens, M. Ieven. Continuous infusion of antibiotics in the critically ill: The new holy grail for beta-lactams and vancomycin? Ann. Intensive Care 2: 1 (2012).

[64] M.H. Abdul-Aziz, J. Lipman, M. Akova, M. Bassetti, J.J. De Waele, G. Dimopoulos, J. Dulhunty, K.M. Kaukonen, D. Koulenti, C. Martin, P. Montravers, J. Rello, A. Rhodes, T. Starr, S.C. Wallis, J.A. Roberts, S. Paul, A.M. Ribas, L.D. De Crop, H. Spapen, J. Wauters, T. Dugernier, P. Jorens, I. Dapper, D.D. De Backer, F.S. Taccone, L. Ruano, E. Afonso, F. Alvarez-Lerma, M.P. Gracia-Arnillas, F. Fernández, N. Feijoo, N. Bardolet, A. Rovira, P. Garro, D. Colon, C. Castillo, J. Fernado, M.J. Lopez, J.L. Fernandez, A.M. Arribas, J.L. Teja, E. Ots, J.C. Montejo, M. Catalan, I. Prieto, G. Gonzalo, B. Galvan, M.A. Blasco, E. Meyer, F. Del Nogal, L. Vidaur, R. Sebastian, P.M. Garde, M. del M.M. Velasco, R.Z. Crespo, M. Esperatti, A. Torres, O. Baldesi, H. Dupont, Y. Mahjoub, S. Lasocki, J.M. Constantin, J.F. Payen, J. Albanese, Y. Malledant, J. Pottecher, J.Y. Lefrant, S. Jaber, O. Joannes-Boyau, C. Orban, M. Ostermann, C. McKenzie, W. Berry, J. Smith, K. Lei, F. Rubulotta, A. Gordon, S. Brett, M. Stotz, M. Templeton, C. Ebm, C. Moran, V. Pettilä, A. Xristodoulou, V. Theodorou, G. Kouliatsis, E. Sertaridou, G. Anthopoulos, G. Choutas, T. Rantis, S. Karatzas, M. Balla, M. Papanikolaou, P. Myrianthefs, A. Gavala, G. Fildisis, A. Koutsoukou, M. Kyriakopoulou et al. Is prolonged infusion of piperacillin/tazobactam and meropenem in critically ill patients associated with improved pharmacokinetic/ pharmacodynamic and patient outcomes? J. Antimicrob. Chemother. 71: 196–207 (2016).

[65] A. Lal, P. Jaoude, A.A. El-Solh. Prolonged versus intermittent infusion of β-lactams for the treatment of nosocomial pneumonia: A meta-analysis. Infect. Chemother. 48: 81–90 (2016).

[66] W.A. Craig. The Pharmacology of meropenem, a new carbapenem antibiotic. Clin. Infect. Dis. 24: S266–S275 (1997).

[67] D.P. Nicolau. Pharmacokinetic and pharmacodynamic properties of meropenem. Clin. Infect. Dis. 47: 32–40 (2008).

[68] AstraZeneca. MERREM® I.V. (meropenem for injection). (2006).

[69] T. Shibayama, D. Sugiyama, E. Kamiyama, T. Tokui, T. Hirota, T. Ikeda. Characterization of CS-023 (RO4908463), a novel parenteral carbapenem antibiotic, and meropenem as substrates of human renal transporters. Drug Metab. Pharmacokinet. 22: 41–47 (2007).

[70] G.L. Drusano. Prevention of resistance: A goal for dose selection for antimicrobial agents. Clin. Infect. Dis. 36: 42–50 (2003).

[71] C.T. Ong, P.R. Tessier, C. Li, C.H. Nightingale, D.P. Nicolau. Comparative in vivo efficacy of meropenem, imipenem, and cefepime against Pseudomonas aeruginosa expressing MexA-MexB-OprM efflux pumps. Diagn. Microbiol. Infect. Dis. 57: 153–161 (2007).

[72] J.L. Crandon, C.E. Luyt, A. Aubry, J. Chastre, D.P. Nicolau. Pharmacodynamics of carbapenems for the treatment of Pseudomonas aeruginosa ventilator-associated pneumonia: Associations with clinical outcome and recurrence. J. Antimicrob. Chemother. 71: 2534–2537 (2016).

[73] R.E. Ariano, S.A. Zelenitsky, A. Nyhlén, D.S. Sitar. An evaluation of an optimal sampling strategy for meropenem in febrile neutropenics. J. Clin. Pharmacol. 45: 832–835 (2005).

[74] C. Li, X. Du, J.L. Kuti, D.P. Nicolau. Clinical pharmacodynamics of meropenem in patients with lower respiratory tract infections. Antimicrob. Agents Chemother. 51: 1725–1730 (2007).

[75] V.H. Tam, A.N. Schilling, S. Neshat, K. Poole, D.A. Melnick, E.A. Coyle. Optimization of meropenem minimum concentration/MIC ratio to suppress in vitro resistance of Pseudomonas aeruginosa. Antimicrob. Agents Chemother. 49: 4920–4927 (2005).

[76] Pfizer Inc. Meronem IV 500mg & 1g (Summary of Product Characteristics). Pfizer (2018).

[77] P. Linden. Safety profile of meropenem: An updated review of over 6000 patients treated with meropenem. Drug Saf. 30: 657–668 (2007).

[78] M. Hites, A.M. Dell'Anna, S. Scolletta, F.S. Taccone. The challenges of multiple organ dysfunction syndrome and extra-corporeal circuits for drug delivery in critically ill patients. Adv. Drug Deliv. Rev. 77: 12–21 (2014).

[79] J.A. Roberts, M.H. Abdul-Aziz, J. Lipman, J.W. Mouton, A.A. Vinks, T.W. Felton, W.W. Hope, A. Farkas, M.N. Neely, J.J. Schentag, G. Drusano, O.R. Frey, U. Theuretzbacher, J.L. Kuti. Individualised antibiotic dosing for patients who are critically ill: Challenges and potential solutions. Lancet Infect. Dis. 14: 498–509 (2014).

[80] J. Gonçalves-Pereira, P. Póvoa. Antibiotics in critically ill patients: A systematic review of the pharmacokinetics of β-lactams. Crit. Care 15: R206 (2011).

[81] T.W. Felton, W.W. Hope, J.A. Roberts. How severe is antibiotic pharmacokinetic variability in critically ill patients and what can be done about it? Diagn. Microbiol. Infect. Dis. 79: 441–447 (2014).

[82] J.F. Bugge. Influence of renal replacement therapy on pharmacokinetics in critically ill patients. Best Pract. Res. Clin. Anaesthesiol. 18: 175–187 (2004).

[83] B.L. Erstad. Albumin disposition in critically Ill patients. J. Clin. Pharm. Ther. 43: 746–751 (2018).

[84] S.H. Mahmoud, C. Shen. Augmented renal clearance in critical illness: An important consideration in drug dosing. Pharmaceutics 9: 3 (2017).

[85] J. Vincent, J. Marshall, A. Anzueto, C.D. Martin, C. Gomersall. International study of the prevalence and outcomes of infection in intensive care units. Jama 302: 2323–2329 (2009).

[86] R. Ferrer, I. Martin-Loeches, G. Phillips, T.M. Osborn, S. Townsend, R.P. Dellinger, A. Artigas, C. Schorr, M.M. Levy. Empiric antibiotic treatment reduces mortality in severe sepsis and septic shock from the first hour: Results from a guideline-based performance improvement program. Crit. Care Med. 42: 1749–1755 (2014).

[87] A. Vieillard-Baron, S. Prin, K. Chergui, O. Dubourg, F. Jardin. Hemodynamic instability in sepsis: Bedside assessment by doppler echocardiography. Am. J. Respir. Crit. Care Med. 168: 1270–1276 (2003).

[88] A.A. Udy, J.P. Baptista, N.L. Lim, G.M. Joynt, P. Jarrett, L. Wockner, R.J. Boots, J. Lipman. Augmented renal clearance in the ICU: Results of a multicenter observational study of renal function in critically ill patients with normal plasma creatinine concentrations. Crit. Care Med. 42: 520–527 (2014).

[89] M. Ulldemolins, J.A. Roberts, J. Rello, D.L. Paterson, J. Lipman. The effects of hypoalbuminaemia on optimizing antibacterial dosing in critically ill patients. Clin. Pharmacokinet. 50: 99–110 (2011).

[90] J.P. Nicholson, M.R. Wolmarans, G.R. Park. The role of albumin in critical illness. Br. J. Anaesth. 85: 599–610 (2000).

[91] J. Lipman, A.A. Udy, J.A. Roberts. Do we understand the impact of altered physiology, consequent interventions and resultant clinical scenarios in the intensive care unit? The antibiotic story. Anaesth. Intensive Care 39: 999–1000 (2011).

[92] C.Y. Yang, P. Xu, Y.J. Yang, B.Y. Li, S.Z. Sun, Q.Z. Yang, L.X. Wang. Systemic capillary leak syndrome due to systemic inflammatory response syndrome in infants: A report on 31 patients. Cent. Eur. J. Med. 9: 477–480 (2014).

[93] F. Husain-Syed, Z. Ricci, D. Brodie, J.L. Vincent, V.M. Ranieri, A.S. Slutsky, F.S. Taccone, L.

Gattinoni, C. Ronco. Extracorporeal organ support (ECOS) in critical illness and acute kidney injury: From native to artificial organ crosstalk. Intensive Care Med. 44: 1447–1459 (2018).

[94] K. Shekar, J.A. Roberts, S. Ghassabian, D. V. Mullany, S.C. Wallis, M.T. Smith, J.F. Fraser. Altered antibiotic pharmacokinetics during extracorporeal membrane oxygenation: Cause for concern? J. Antimicrob. Chemother. 68: 726–727 (2013).

[95] J.F. Bugge. Pharmacokinetics and drug dosing adjustments during continuous venovenous hemofiltration or hemodiafiltration in critically ill patients. Acta Anaesthesiol. Scand. 45: 929–934 (2001).

[96] D.M. Roberts, X. Liu, J.A. Roberts, P. Nair, L. Cole, M.S. Roberts, J. Lipman, R. Bellomo. A multicenter study on the effect of continuous hemodiafiltration intensity on antibiotic pharmacokinetics. Crit. Care 19: 1–9 (2015).

[97] J.A. Jamal, A.A. Udy, J. Lipman, J.A. Roberts. The impact of variation in renal replacement therapy settings on piperacillin, meropenem, and vancomycin drug clearance in the critically Ill: An analysis of published literature and dosing regimens. Crit. Care Med. 42: 1640–1650 (2014).

[98] P.M. Honore, E. Hoste, Z. Molnár, R. Jacobs, O. Joannes-Boyau, M.L.N.G. Malbrain, L.G. Forni. Cytokine removal in human septic shock: Where are we and where are we going? Ann. Intensive Care 9: 1 (2019).

[99] E.C. Poli, T. Rimmelé, A.G. Schneider. Hemoadsorption with CytoSorb ®. Intensive Care Med. 45: 236–239 (2019).

[100] J.A. Stenken, A.J. Poschenrieder. Bioanalytical chemistry of cytokines - A review. Anal. Chim. Acta 853: 95–115 (2015).

[101] V. Mendes, S. Colombier, F. Verdy, X. Bechtold, P. Schlaepfer, E. Scala, A. Schneider, M. Kirsch. Cytosorb® hemoadsorption of apixaban during emergent cardio-pulmonary bypass: a case report. Perfusion 1: 1–3 (2020).

[102] C.N. Lang, M.J. Sommer, M.A. Neukamm, D.L. Staudacher, A. Supady, C. Bode, D. Duerschmied, A. Lother. Use of the CytoSorb adsorption device in MDMA intoxication: a first-in-man application and in vitro study. Intensive Care Med. Exp. 8: 1 (2020).

[103] I. Schroeder, M. Zoller, M. Angstwurm, F. Kur, L. Frey. Venlafaxine intoxication with development of takotsubo cardiomyopathy: Successful use of extracorporeal life support, intravenous lipid emulsion and CytoSorb®. Int. J. Artif. Organs 40: 358–360 (2017).

[104] K. Reiter, V. Bordoni, G. Dall'Olio, M.G. Ricatti, M. Soli, S. Ruperti, G. Soffiati, E. Galloni, V. D'Intini, R. Bellomo, C. Ronco. In vitro removal of therapeutic drugs with a novel adsorbent system. Blood Purif. 20: 380–388 (2002).

[105] C. König, A.C. Röhr, O.R. Frey, A. Brinkmann, J.A. Roberts, D. Wichmann, S. Braune, S. Kluge, A. Nierhaus. In vitro removal of anti-infective agents by a novel cytokine adsorbent system. Int. J. Artif. Organs 42: 57–64 (2019).

[106] A.G. Schneider, P. André, J. Scheier, M. Schmidt, H. Ziervogel, T. Buclin, D. Kindgen-Milles. Pharmacokinetics of anti-infective agents during CytoSorb hemoadsorption. Sci. Rep. 11: 1–9 (2021).

[107] D.R. Mould, R.N. Upton. Basic concepts in population modeling, simulation, and model-based drug development. CPT Pharmacometrics Syst. Pharmacol. 1: 1–14 (2012).

[108] R.N. Upton, D.R. Mould. Basic concepts in population modeling, simulation, and model-based

drug development: Part 3-introduction to pharmacodynamic modeling methods. CPT Pharmacometrics Syst. Pharmacol. 3: 1–16 (2014).

[109] J.S. Barrett, M.J. Fossler, K.D. Cadieu, M.R. Gastonguay. Pharmacometrics: A multidisciplinary field to facilitate critical thinking in drug development and translational research settings. J. Clin. Pharmacol. 48: 632–649 (2008).

[110] H.M. Jones, K. Rowland-Yeo. Basic concepts in physiologically based pharmacokinetic modeling in drug discovery and development. CPT Pharmacometrics Syst. Pharmacol. 2: 1–12 (2013).

[111] J.A. Stone, C. Banfield, M. Pfister, S. Tannenbaum, S. Allerheiligen, J.D. Wetherington, R. Krishna, D.M. Grasela. Model-based drug development survey finds pharmacometrics impacting decision making in the pharmaceutical industry. J. Clin. Pharmacol. 50: (2010).

[112] S.F. Marshall, R. Burghaus, V. Cosson, S. Cheung, M. Chenel, O. DellaPasqua, N. Frey, B. Hamrén, L. Harnisch, F. Ivanow, T. Kerbusch, J. Lippert, P.A. Milligan, S. Rohou, A. Staab, J.L. Steimer, C. Tornøe, S.A.G. Visser. Good practices in model-informed drug discovery and development: Practice, application, and documentation. CPT Pharmacometrics Syst. Pharmacol. 5: 93–122 (2016).

[113] J.Y. Lee, C.E. Garnett, J.V.S. Gobburu, V.A. Bhattaram, S. Brar, J.C. Earp, P.R. Jadhav, K. Krudys, L.J. Lesko, F. Li, J. Liu, R. Madabushi, A. Marathe, N. Mehrotra, C. Tornoe, Y. Wang, H. Zhu. Impact of pharmacometric analyses on new drug approval and labelling decisions: A review of 198 submissions between 2000 and 2008. Clin. Pharmacokinet. 50: 627–635 (2011).

[114] European Medicines Agency. Activity report of the modelling and simulation working group. (2015).

[115] S. Marshall, R. Madabushi, E. Manolis, K. Krudys, A. Staab, K. Dykstra, S.A.G. Visser. Model-informed drug discovery and development: Current industry good practice and regulatory expectations and future perspectives. CPT Pharmacometrics Syst. Pharmacol. 8: 87–96 (2019).

[116] E. Manolis, R. Herold. Pharmacometrics for regulatory decision making: Status and perspective. Clin. Pharmacokinet. 50: 625–626 (2011).

[117] J.R. Powell, J.V.S. Gobburu. Pharmacometrics at FDA: Evolution and impact on decisions. Clin. Pharmacol. Ther. 82: 97–102 (2007).

[118] D. Gonzalez, G.G. Rao, S.C. Bailey, K.L.R. Brouwer, Y. Cao, D.J. Crona, A.D.M. Kashuba, C.R. Lee, K. Morbitzer, J.H. Patterson, T. Wiltshire, J. Easter, S.W. Savage, J.R. Powell. Precision dosing: Public health need, proposed framework, and anticipated impact. Clin. Transl. Sci. 10: 443–454 (2017).

[119] R.J. Temple, D.C. Crews, K. Vasisht, K. Goodrich, M.A. Bernard, R. Nelson, A.K. Parekh, R. Madabushi, R. Sridhara. Evaluating inclusion and exclusion criteria in clinical trials. Natl. Press Club (2018).

[120] T.M. Polasek, A. Rostami-Hodjegan, D.S. Yim, M. Jamei, H. Lee, H. Kimko, J.K. Kim, P.T.T. Nguyen, A.S. Darwich, J.G. Shin. What does it take to make model-informed precision dosing common practice? Report from the 1st asian symposium on precision dosing. AAPS J. 21: 1–9 (2019).

[121] A.S. Darwich, K. Ogungbenro, A.A. Vinks, J.R. Powell, J.L. Reny, N. Marsousi, Y. Daali, D. Fairman, J. Cook, L.J. Lesko, J.S. McCune, C.A.J. Knibbe, S.N. de Wildt, J.S. Leeder, M. Neely, A.F. Zuppa, P. Vicini, L. Aarons, T.N. Johnson, J. Boiani, A. Rostami-Hodjegan. Why has model-

informed precision dosing not yet become common clinical reality? Lessons from the past and a roadmap for the future. Clin. Pharmacol. Ther. 101: 646–656 (2017).

[122] F. Kluwe, R. Michelet, A. Mueller-Schoell, C. Maier, L. Klopp-Schulze, M. van Dyk, G. Mikus, W. Huisinga, C. Kloft. Perspectives on model-informed precision dosing in the digital health era: Challenges, opportunities, and recommendations. Clin. Pharmacol. Ther. 109: 29–36 (2021).

[123] D. Chan, V. Ivaturi, J. Long-Boyle. The time is now: Model-based dosing to optimize drug therapy. Int. J. Pharmacokinet. 2: 213–215 (2017).

[124] S.G. Wicha, M.G. Kees, A. Solms, I.K. Minichmayr, A. Kratzer, C. Kloft. TDMx: A novel web-based open-access support tool for optimising antimicrobial dosing regimens in clinical routine. Int. J. Antimicrob. Agents 45: 442–444 (2015).

[125] R.J. Keizer, R. ter Heine, A. Frymoyer, L.J. Lesko, R. Mangat, S. Goswami. Model-informed precision dosing at the bedside: Scientific challenges and opportunities. CPT Pharmacometrics Syst. Pharmacol. 7: 785–787 (2018).

[126] C. Maier, N. Hartung, J. de Wiljes, C. Kloft, W. Huisinga. Bayesian data assimilation to support informed decision making in individualized chemotherapy. CPT Pharmacometrics Syst. Pharmacol. 9: 153–164 (2020).

[127] A.A. Kumar, M. Burgard, S. Stacey, I. Sandaradura, T. Lai, C. Coorey, M. Cincunegui, C.E. Staatz, S. Hennig. An evaluation of the user-friendliness of Bayesian forecasting programs in a clinical setting. Br. J. Clin. Pharmacol. 85: 2436–2441 (2019).

[128] S.G. Wicha, A.C. Röhr, O.R. Frey, A. Brinkmann, C. Kloft. Pharmacometrics-based therapeutic drug monitoring of antibiotics. Krankenhauspharmazie 37: 212–221 (2016).

[129] L. Ehmann, M. Zoller, I.K. Minichmayr, C. Scharf, W. Huisinga, J. Zander, C. Kloft. Development of a dosing algorithm for meropenem in critically ill patients based on a population pharmacokinetic/pharmacodynamic analysis. Int. J. Antimicrob. Agents 54: 309–317 (2019).

[130] I.K. Minichmayr, J.A. Roberts, O.R. Frey, A.C. Roehr, C. Kloft, A. Brinkmann. Development of a dosing nomogram for continuous-infusion meropenem in critically ill patients based on a validated population pharmacokinetic model. J. Antimicrob. Chemother. 73: 1330–1339 (2018).

[131] L. Ehmann, M. Zoller, I.K. Minichmayr, C. Scharf, B. Maier, M. V. Schmitt, N. Hartung, W. Huisinga, M. Vogeser, L. Frey, J. Zander, C. Kloft. Role of renal function in risk assessment of target non-attainment after standard dosing of meropenem in critically ill patients: A prospective observational study. Crit. Care 21: 1–14 (2017).

[132] A. Tabah, J. de Waele, J. Lipman, J.R. Zahar, M.O. Cotta, G. Barton, J.F. Timsit, J.A. Roberts. The ADMIN-ICU survey: A survey on antimicrobial dosing and monitoring in ICUs. J. Antimicrob. Chemother. 70: 2671–2677 (2015).

[133] S. Paviour, S. Hennig, C.E. Staatz. Usage and monitoring of intravenous tobramycin in cystic fibrosis in Australia and the UK. J. Pharm. Pract. Res. 46: 15–21 (2016).

[134] F. Mentré, L.E. Friberg, S. Duffull, J. French, D.A. Lauffenburger, L. Li, D.E. Mager, V. Sinha, E. Sobie, P. Zhao. Pharmacometrics and systems pharmacology 2030. Clin. Pharmacol. Ther. 107: 76–78 (2020).

[135] L. Kuepfer, C. Niederalt, T. Wendl, J.F. Schlender, S. Willmann, J. Lippert, M. Block, T. Eissing, D. Teutonico. Applied concepts in PBPK modeling: How to build a PBPK/PD model. CPT Pharmacometrics Syst. Pharmacol. 5: 516–531 (2016).

[136] H. Zhou. PK/PD Approach. In: Pharmacokinetics in Drug Discovery and Development. CRC Press, 33–56 (2002).

[137] E.I. Ette, P.J. Williams. Population pharmacokinetics I: Background, concepts, and models. Ann. Pharmacother. 38: 1702–1706 (2004).

[138] L. Aarons. Population pharmacokinetics: theory and practice. Br. J. Clin. Pharmacol. 32: 669–670 (1991).

[139] L.B. Sheiner. The population approach to pharmacokinetic data analysis: Rationale and standard data analysis methods. Drug Metab. Rev. 15: 153–171 (1984).

[140] S.B. Duffull, D.F.B. Wright, H.R. Winter. Interpreting population pharmacokinetic-pharmacodynamic analyses - a clinical viewpoint. Br. J. Clin. Pharmacol. 71: 807–814 (2011).

[141] C.M.. Sherwin, T.K.L. Kiang, M.G. Spigarelli, M.H.H. Ensom. Fundamentals of population pharmacokinetic modelling. Clin. Pharmacokinet. 51: 573–590 (2012).

[142] S. Beal, L. Sheiner, A. Boeckmann, R. Bauer. NONMEM Users Guide. ICON Dev. Solut. (2013).

[143] Introduction to population pharmacokinetic/pharmacodynamic analysis with nonlinear mixed effects models. Wiley & Sons, Hoboken, New Jersey, (2014).

[144] Å.M. Johansson, M.O. Karlsson. Multiple imputation of missing covariates in NONMEM and evaluation of the method's sensitivity to η-shrinkage. AAPS J. 15: 1035–1042 (2013).

[145] M. Bergstrand, M.O. Karlsson. Handling data below the limit of quantification in mixed effect models. AAPS J. 11: 371–380 (2009).

[146] U. Wählby, A.H. Thomson, P.A. Milligan, M.O. Karlsson. Models for time-varying covariates in population pharmacokinetic- pharmacodynamic analysis. Br. J. Clin. Pharmacol. 58: 367–377 (2004).

[147] B.J. Anderson, N.H.G. Holford. Mechanism-based concepts of size and maturity in pharmacokinetics. Annu. Rev. Pharmacol. Toxicol. 48: 303–332 (2008).

[148] N.H.G. Holford, B.J. Anderson. Allometric size: The scientific theory and extension to normal fat mass. Eur. J. Pharm. Sci. 109: S59–S64 (2017).

[149] A. Yafune, M. Ishiguro. Bootstrap approach for constructing confidence intervals for population pharmacokinetic parameters. II: A bootstrap modification of standard two-stage (STS) method for phase I trial. Stat. Med. 18: 601–612 (1999).

[150] J.W. Mouton, D.F.J. Brown, P. Apfalter, R. Cantón, C.G. Giske, M. Ivanova, A.P. MacGowan, A. Rodloff, C.J. Soussy, M. Steinbakk, G. Kahlmeter. The role of pharmacokinetics/pharmacodynamics in setting clinical MIC breakpoints: The EUCAST approach. Clin. Microbiol. Infect. 18: (2012).

[151] Committee for Human Medicinal Products (CHMP). Guideline on the use of pharmacokinetics and pharmacodynamics in the development of antibacterial medicinal products. (2016).

[152] E. Asín-Prieto, A. Rodríguez-Gascón, A. Isla. Applications of the pharmacokinetic/pharmacodynamic (PK/PD) analysis of antimicrobial agents. J. Infect. Chemother. 21: 319–329 (2015).

[153] J.L. Puga, M. Krzywinski, N. Altman. Points of Significance: Bayes' theorem. Nat. Methods 12: 277–278 (2015).

[154] D.J. Lunn, N. Best, A. Thomas, J. Wakefield, D. Spiegelhalter. Bayesian analysis of population

PK/PD models: General concepts and software. J. Pharmacokinet. Pharmacodyn. 29: 271–307 (2002).

[155] L. Lindbom, P. Pihlgren, N. Jonsson. PsN-Toolkit - A collection of computer intensive statistical methods for non-linear mixed effect modeling using NONMEM. Comput. Methods Programs Biomed. 79: 241–257 (2005).

[156] R.J. Keizer, M. van Benten, J.H. Beijnen, J.H.M. Schellens, A.D.R. Huitema. Piraña and PCluster: A modeling environment and cluster infrastructure for NONMEM. Comput. Methods Programs Biomed. 101: 72–79 (2011).

[157] S.G. Wicha. TDMxR: an open-source package for model-based therapeutic drug monitoring in R. PAGE 28 - Abstr. 8973 (2019).

[158] E. Comets, K. Brendel, F. Mentré. Computing normalised prediction distribution errors to evaluate nonlinear mixed-effect models : The npde add-on package for R. Comput. Methods Programs Biomed. 90: 154–166 (2007).

[159] Refubium - Curta: A General-purpose High-Performance Computer at ZEDAT, Freie Universität Berlin.

[160] J. Zander, B. Maier, A. Suhr, M. Zoller, L. Frey, D. Teupser, M. Vogeser. Quantification of piperacillin, tazobactam, cefepime, meropenem, ciprofloxacin and linezolid in serum using an isotope dilution UHPLC-MS/MS method with semi-automated sample preparation. Clin. Chem. Lab. Med. 53: 781–791 (2015).

[161] M. Paal, M. Zoller, C. Schuster, M. Vogeser, G. Schütze. Simultaneous quantification of cefepime, meropenem, ciprofloxacin, moxifloxacin, linezolid and piperacillin in human serum using an isotope-dilution HPLC–MS/MS method. J. Pharm. Biomed. Anal. 152: 102–110 (2018).

[162] M. Bergstrand, A.C. Hooker, J.E. Wallin, M.O. Karlsson. Prediction-corrected visual predictive checks for diagnosing nonlinear mixed-effects models. AAPS J. 13: 143–151 (2011).

[163] K. Drlica, X. Zhao. Mutant selection window hypothesis updated. Clin. Infect. Dis. 44: 681–688 (2007).

[164] K. Drlica. The mutant selection window and antimicrobial resistance. J. Antimicrob. Chemother. 52: 11–17 (2003).

[165] M.H. Al-Shaer, W.A. Alghamdi, E. Graham, C.A. Peloquin. Meropenem, cefepime, and piperacillin protein binding in patient samples. Ther. Drug Monit. 42: 129–132 (2020).

[166] S. Colman, V. Stove, J.J. De Waele, A.G. Verstraete. Measuring unbound versus total piperacillin concentrations in plasma of critically ill patients: Methodological issues and relevance. Ther. Drug Monit. 41: 325–330 (2019).

[167] M. Bassetti, J.J. De Waele, P. Eggimann, J. Garnacho-Montero, G. Kahlmeter, F. Menichetti, D.P. Nicolau, J.A. Paiva, M. Tumbarello, T. Welte, M. Wilcox, J.R. Zahar, G. Poulakou. Preventive and therapeutic strategies in critically ill patients with highly resistant bacteria. Intensive Care Med. 41: 776–795 (2015).

[168] K.J. Eagye, M.A. Banevicius, D.P. Nicolau. Pseudomonas aeruginosa is not just in the intensive care unit any more: Implications for empirical therapy. Crit. Care Med. 40: 1329–1332 (2012).

[169] D.W. Cockcroft, M.H. Gault. Prediction of Creatinine Clearance from Serum Creatinine. Nephron 16: 31–41 (1976).

[170] Food and Drug Administration. Briefing document pharmaceutical science and clinical pharmacology advisory committee meeting. (2019).

[171] K. Brendel, E. Comets, C. Laffont, C. Laveille, F. Mentré. Metrics for external model evaluation with an application to the population pharmacokinetics of gliclazide. Pharm. Res. 23: 2036–2049 (2006).

[172] F. Mentré, S. Escolano. Prediction discrepancies for the evaluation of nonlinear mixed-effects models. J. Pharmacokinet. Pharmacodyn. 33: 345–367 (2006).

[173] U. Liebchen, M. Klose, M. Paal, M. Vogeser, M. Zoller, I. Schroeder, L. Schmitt, W. Huisinga, R. Michelet, J. Zander, C. Scharf, F.A. Weinelt, C. Kloft. Evaluation of the merorisk calculator, a user-friendly tool to predict the risk of meropenem target non-attainment in critically ill patients. Antibiotics 10: 468 (2021).

[174] L.I. Lin, G. McBride, J.M. Bland, D.G. Altman. A proposal for strength-of-agreement criteria for Lin's concordance correlation coefficient. (2005).

[175] J.A. Roberts, C.M.J. Kirkpatrick, M.S. Roberts, A.J. Dalley, J. Lipman. First-dose and steady-state population pharmacokinetics and pharmacodynamics of piperacillin by continuous or intermittent dosing in critically ill patients with sepsis. Int. J. Antimicrob. Agents 35: 156–163 (2010).

[176] K. Öbrink-Hansen, R.V. Juul, M. Storgaard, M.K. Thomsen, T.F. Hardlei, B. Brock, M. Kreilgaard, J. Gjedsted. Population pharmacokinetics of piperacillin in the early phase of septic shock: Does standard dosing result in therapeutic plasma concentrations? Antimicrob. Agents Chemother. 59: 7018–7026 (2015).

[177] C. Li, J.L. Kuti, C.H. Nightingale, D.L. Mansfield, A. Dana, D.P. Nicolau. Population pharmacokinetics and pharmacodynamics of piperacillin/ tazobactam in patients with complicated intra-abdominal infection. J. Antimicrob. Chemother. 56: 388–395 (2005).

[178] M.G. Andersen, A. Thorsted, M. Storgaard, A.N. Kristoffersson, L.E. Friberg, K. Öbrink-Hansen. Population pharmacokinetics of piperacillin in sepsis patients: Should alternative dosing strategies be considered? Antimicrob. Agents Chemother. 62: 1–11 (2018).

[179] M. Zoller, G. Döbbeler, B. Maier, M. Vogeser, L. Frey, J. Zander. Can cytokine adsorber treatment affect antibiotic concentrations? A case report. J. Antimicrob. Chemother. 70: 2169–2171 (2015).

[180] T. Dimski, T. Brandenburger, C. MacKenzie, D. Kindgen-Milles. Elimination of glycopeptide antibiotics by cytokine hemoadsorption in patients with septic shock: A study of three cases. Int. J. Artif. Organs 43: 753–757 (2020).

[181] M. Ulldemolins, D. Soy, M. Llaurado-Serra, S. Vaquer, P. Castro, A.H. Rodríguez, C. Pontes, G. Calvo, A. Torres, I. Martín-Loeches. Meropenem population pharmacokinetics in critically Ill patients with septic shock and continuous renal replacement therapy: Influence of residual diuresis on dose requirements. Antimicrob. Agents Chemother. 59: 5520–5528 (2015).

[182] D. Onichimowski, A. Będźkowska, H. Ziółkowski, J. Jaroszewski, M. Borys, M. Czuczwar, P. Wiczling. Population pharmacokinetics of standard-dose meropenem in critically ill patients on continuous renal replacement therapy: a prospective observational trial. Pharmacol. Reports 72: 719–729 (2020).

[183] F.J. Baud, P. Houzé. RE to manuscript 'In vitro removal of anti-infective agents by a novel cytokine adsorbent system.' Int. J. Artif. Organs 42: 528–529 (2019).

[184] E. Esteve-Pitarch, V.D. Gumucio-Sanguino, S. Cobo-Sacristán, E. Shaw, K. Maisterra-Santos, J. Sabater-Riera, X.L. Pérez-Fernandez, R. Rigo-Bonnin, F. Tubau-Quintano, J. Carratalà, H. Colom-Codina, A. Padullés-Zamora. Continuous infusion of piperacillin/tazobactam and meropenem in ICU patients without renal dysfunction: Are patients at risk of underexposure? Eur. J. Drug Metab. Pharmacokinet. 46: 527–538 (2021).

[185] J.W. Mouton, A.E. Muller, R. Canton, C.G. Giske, G. Kahlmeter, J. Turnidge. MIC-based dose adjustment: Facts and fables. J. Antimicrob. Chemother. 73: 564–568 (2018).

[186] J. Zander, G. Döbbeler, D. Nagel, C. Scharf, M. Huseyn-Zada, J. Jung, L. Frey, M. Vogeser, M. Zoller. Variability of piperacillin concentrations in relation to tazobactam concentrations in critically ill patients. Int. J. Antimicrob. Agents 48: 435–439 (2016).

[187] C. Scharf, M. Paal, I. Schroeder, M. Vogeser, R. Draenert, M. Irlbeck, M. Zoller, U. Liebchen. Therapeutic drug monitoring of meropenem and piperacillin in critical illness—experience and recommendations from one year in routine clinical practice. Antibiotics 9: 3 (2020).

[188] M. Carlier, S. Carrette, J.A. Roberts, V. Stove, A. Verstraete, E. Hoste, P. Depuydt, J. Decruyenaere, J. Lipman, S.C. Wallis, J.J. De Waele. Meropenem and piperacillin/tazobactam prescribing in critically ill patients: Does augmented renal clearance affect pharmacokinetic/pharmacodynamic target attainment when extended infusions are used? Crit. Care 17: R84 (2013).

[189] M. Chimata, M. Nagase, Y. Suzuki, M. Shimomura, S. Kakuta. Pharmacokinetics of meropenem in patients with various degrees of renal function, including patients with end-stage renal disease. Antimicrob. Agents Chemother. 37: 229–233 (1993).

[190] T. Tamatsukuri, M. Ohbayashi, N. Kohyama, Y. Kobayashi, T. Yamamoto, K. Fukuda, S. Nakamura, Y. Miyake, K. Dohi, M. Kogo. The exploration of population pharmacokinetic model for meropenem in augmented renal clearance and investigation of optimum setting of dose. J. Infect. Chemother. 24: 834–840 (2018).

[191] A.A. Udy, J. Lipman, P. Jarrett, K. Klein, S.C. Wallis, K. Patel, C.M.J. Kirkpatrick, P.S. Kruger, D.L. Paterson, M.S. Roberts, J.A. Roberts. Are standard doses of piperacillin sufficient for critically ill patients with augmented creatinine clearance? Crit. Care 19: 1 (2015).

[192] R. Masterton, G. Drusano, D.L. Paterson, G. Park. Appropriate antimicrobial treatment in nosocomial infections - The clinical challenges. J. Hosp. Infect. 55: 1–12 (2003).

[193] W. Zhao, E. Lopez, V. Biran, X. Durrmeyer, M. Fakhoury, E. Jacqz-Aigrain. Vancomycin continuous infusion in neonates: Dosing optimisation and therapeutic drug monitoring. Arch. Dis. Child. 98: 449–453 (2013).

[194] S. Leroux, E. Jacqz-Aigrain, V. Biran, E. Lopez, D. Madeleneau, C. Wallon, E. Zana-Taïeb, A.L. Virlouvet, S. Rioualen, W. Zhao. Clinical utility and safety of a model-based patient-tailored dose of vancomycin in neonates. Antimicrob. Agents Chemother. 60: 2039–2042 (2016).

[195] J.S. McCune, A. Batchelder, K.A. Guthrie, R. Witherspoon, F.R. Appelbaum, B. Phillips, P. Vicini, D.H. Salinger, G.B. McDonald. Personalized dosing of cyclophosphamide in the total body irradiation-cyclophosphamide conditioning regimen: A phase II trial in patients with hematologic malignancy. Clin. Pharmacol. Ther. 85: 615–622 (2009).

[196] N. Marsousi, C.F. Samer, P. Fontana, J.L. Reny, S. Rudaz, J.A. Desmeules, Y. Daali. Coadministration of ticagrelor and ritonavir: Toward prospective dose adjustment to maintain an optimal platelet inhibition using the PBPK approach. Clin. Pharmacol. Ther. 100: 295–304 (2016).

[197] J.J. De Waele, S. Carrette, M. Carlier, V. Stove, J. Boelens, G. Claeys, I. Leroux-Roels, E. Hoste, P. Depuydt, J. Decruyenaere, A.G. Verstraete. Therapeutic drug monitoring-based dose optimisation of piperacillin and meropenem: A randomised controlled trial. Intensive Care Med. 40: 380–387 (2014).

[198] R. ter Heine, R.J. Keizer, K. van Steeg, E.J. Smolders, M. van Luin, H.J. Derijks, C.P.C. de Jager, T. Frenzel, R. Brüggemann. Prospective validation of a model-informed precision dosing tool for vancomycin in intensive care patients. Br. J. Clin. Pharmacol. 86: 2497–2506 (2020).

[199] T.W. Felton, W.W. Hope, J.A. Roberts. How severe is antibiotic pharmacokinetic variability in critically ill patients and what can be done about it? Diagn. Microbiol. Infect. Dis. 79: 441–447 (2014).

[200] J.A. Roberts, S.K. Paul, M. Akova, M. Bassetti, J.J. De Waele, G. Dimopoulos, K.M. Kaukonen, D. Koulenti, C. Martin, P. Montravers, J. Rello, A. Rhodes, T. Starr, S.C. Wallis, J. Lipman, A. Margarit Ribas, L. De Crop, H. Spapen, J. Wauters, T. Dugernier, P. Jorens, I. Dapper, D. De Backer, F.S. Taccone, L. Ruano, E. Afonso, F. Alvarez-Lerma, M.P. Gracia-Arnillas, F. Fernández, N. Feijoo, N. Bardolet, A. Rovira, P. Garro, D. Colon, C. Castillo, J. Fernado, M.J. Lopez, J.L. Fernandez, A.M. Arribas, J.L. Teja, E. Ots, J. Carlos Montejo, M. Catalan, I. Prieto, G. Gonzalo, B. Galvan, M.A. Blasco, E. Meyer, F. Del Nogal, L. Vidaur, R. Sebastian, P.M. Garde, M.D.M. Martin Velasco, R. Zaragoza Crespo, M. Esperatti, A. Torres, O. Baldesi, H. Dupont, Y. Mahjoub, S. Lasocki, J.M. Constantin, J.F. Payen, J. Albanese, Y. Malledant, J. Pottecher, J.Y. Lefrant, S. Jaber, O. Joannes-Boyau, C. Orban, M. Ostermann, C. McKenzie, W. Berry, J. Smith, K. Lei, F. Rubulotta, A. Gordon, S. Brett, M. Stotz, M. Templeton, C. Ebm, C. Moran, V. Pettilä, A. Xristodoulou, V. Theodorou, G. Kouliatsis, E. Sertaridou, G. Anthopoulos, G. Choutas, T. Rantis, S. Karatzas, M. Balla, M. Papanikolaou, P. Myrianthefs, A. Gavala, G. Fildisis, A. Koutsoukou, M. Kyriakopoulou, K. Petrochilou, M. Kompoti et al. DALI: Defining antibiotic levels in intensive care unit patients: Are current ß-lactam antibiotic doses sufficient for critically ill patients? Clin. Infect. Dis. 58: 1072–1083 (2014).

[201] M.G. Sinnollareddy, M.S. Roberts, J. Lipman, S.L. Peake, J.A. Roberts. Pharmacokinetics of piperacillin in critically ill patients with acute kidney injury receiving sustained low-efficiency diafiltration. J. Antimicrob. Chemother. 73: 1647–1650 (2018).

[202] A.S. Alobaid, M. Hites, J. Lipman, F.S. Taccone, J.A. Roberts. Effect of obesity on the pharmacokinetics of antimicrobials in critically ill patients: A structured review. Int. J. Antimicrob. Agents 47: 259–268 (2016).

[203] C. Alpuche, J. Garau, V. Lim. Global and local variations in antimicrobial susceptibilities and resistance development in the major respiratory pathogens. Int. J. Antimicrob. Agents 30: 135–138 (2007).

[204] C. McKenzie. Antibiotic dosing in critical illness. J. Antimicrob. Chemother. 66: 25–31 (2011).

[205] M.G. Vossen, L. Ehmann, S. Pferschy, A. Maier-Salamon, M. Haidinger, C. Weiser, J.M. Wenisch, K. Saria, C. Kajahn, S. Jilch, R. Lemmerer, M. Bécède, M. Zeitlinger, C. Kloft, W. Jäger, F. Thalhammera. Elimination of doripenem during dialysis and pharmacokinetic evaluation of posthemodialysis dosing for patients undergoing intermittent renal replacement therapy. Antimicrob. Agents Chemother. 62: 1–23 (2018).

[206] D. Alihodzic, A. Broeker, M. Baehr, S. Kluge, C. Langebrake, S.G. Wicha. Impact of inaccurate documentation of sampling and infusion time in model-informed precision dosing. Front. Pharmacol. 11: 1–12 (2020).

[207] A.F. Van Der Meer, D.J. Touw, M.A.E. Marcus, C. Neef, J.H. Proost. Influence of erroneous patient records on population pharmacokinetic modeling and individual bayesian estimation.

Ther. Drug Monit. 34: 526–534 (2012).

[208] F.A. Weinelt, M.S. Stegemann, A. Theloe, F. Pfäfflin, S. Achterberg, F. Weber, L. Dübel, A. Mikolajewska, A. Uhrig, P. Kiessling, W. Huisinga, R. Michelet, S. Hennig, C. Kloft. Evaluation of a Meropenem and Piperacillin Monitoring Program in Intensive Care Unit Patients Calls for the Regular Assessment of Empirical Targets and Easy-to-Use Dosing Decision Tools. Antibiotics 11: 6 (2022).

[209] F.A. Weinelt, M.S. Stegemann, A. Theloe, F. Pfäfflin, S. Achterberg, L. Schmitt, W. Huisinga, R. Michelet, S. Hennig, C. Kloft. Development of a model-informed dosing tool to optimise initial antibiotic dosing—A translational example for intensive care units. Pharmaceutics 13: 12 (2021).

[210] M.G. Kees, I.K. Minichmayr, S. Moritz, S. Beck, S.G. Wicha, F. Kees, C. Kloft, T. Steinke. Population pharmacokinetics of meropenem during continuous infusion in surgical ICU patients. J. Clin. Pharmacol. 56: 307–315 (2016).

[211] I.K. Minichmayr, A. Schaeftlein, J.L. Kuti, M. Zeitlinger, C. Kloft. Clinical determinants of target non-attainment of linezolid in plasma and interstitial space fluid: A pooled population parmacokinetic analysis with focus on critically ill patients. Clin. Pharmacokinet. 56: 617–633 (2017).

[212] S.A.M. Dhaese, A. Farkas, P. Colin, J. Lipman, V. Stove, A.G. Verstraete, J.A. Roberts, J.J. De Waele. Population pharmacokinetics and evaluation of the predictive performance of pharmacokinetic models in critically ill patients receiving continuous infusion meropenem: A comparison of eight pharmacokinetic models. J. Antimicrob. Chemother. 74: 432–441 (2019).

[213] Y.S.K. Moon, K.C. Chung, M.A. Gill. Pharmacokinetics of meropenem in animals, healthy volunteers, and patients. Clin. Infect. Dis. 24: 249–255 (1997).

[214] N. Brusselaers, D. Vogelaers, S. Blot. The rising problem of antimicrobial resistance in the intensive care unit. Ann. Intensive Care 1: 47 (2011).

[215] C. Llor, L. Bjerrum. Antimicrobial resistance: Risk associated with antibiotic overuse and initiatives to reduce the problem. Ther. Adv. Drug Saf. 5: 229–241 (2014).

[216] S.G. Wicha, A.G. Märtson, E.I. Nielsen, B.C.P. Koch, L.E. Friberg, J.W. Alffenaar, I.K. Minichmayr. From therapeutic drug monitoring to model-informed precision dosing for antibiotics. Clin. Pharmacol. Ther. 109: 928–941 (2021).

[217] J.A. Cusumano, K.P. Klinker, A. Huttner, M.K. Luther, J.A. Roberts, K.L. LaPlante. Towards precision medicine: Therapeutic drug monitoring-guided dosing of vancomycin and β-lactam antibiotics to maximize effectiveness and minimize toxicity. Am. J. Heal. Pharm. 77: 1104–1112 (2020).

[218] U. Liebchen, F. Weinelt, C. Scharf, I. Schroeder, M. Paal, M. Zoller, C. Kloft, J. Jung, R. Michelet. Combination of pharmacokinetic and pathogen susceptibility information to optimize meropenem treatment of gram- negative infections in critically ill patients. Antimicrob. Agents Chemother. 66: 2 (2022).

[219] M. Neely, M. Philippe, T. Rushing, X. Fu, M. Van Guilder, D. Bayard, A. Schumitzky, N. Bleyzac, S. Goutelle. Accurately achieving target busulfan exposure in children and adolescents with very limited sampling and the bestdose software. Ther. Drug Monit. 38: 332–342 (2016).

[220] E.L. Heil, D.P. Nicolau, A. Farkas, J.A. Roberts, K.A. Thom. Pharmacodynamic target attainment for cefepime, meropenem, and piperacillin-tazobactam using a pharmacokinetic/pharmacodynamic-based dosing calculator in critically Ill patients.

Antimicrob. Agents Chemother. 62: 9 (2018).

[221] D.R. Mould, G. D'Haens, R.N. Upton. Clinical Decision Support Tools: The Evolution of a Revolution. Clin. Pharmacol. Ther. 99: 405–418 (2016).

[222] I.K. Minichmayr, J.A. Roberts, O.R. Frey, A.C. Roehr, C. Kloft, A. Brinkmann. Development of a dosing nomogram for continuous-infusion meropenem in critically ill patients based on a validated population pharmacokinetic model. J. Antimicrob. Chemother. 73: 1330–1339 (2018).

[223] W. Kantasiripitak, R. Van Daele, M. Gijsen, M. Ferrante, I. Spriet, E. Dreesen. Software tools for model-informed precision dosing: How well do they satisfy the needs? Front. Pharmacol. 11: 5 (2020).

[224] P. Nauclér, A. Huttner, C.H. van Werkhoven, M. Singer, P. Tattevin, S. Einav, T. Tängdén. Impact of time to antibiotic therapy on clinical outcome in patients with bacterial infections in the emergency department: implications for antimicrobial stewardship. Clin. Microbiol. Infect. 27: 175–181 (2021).

5 Appendix

5.1 Supplementary tables

Table S1: Overview of patient-specific characteristics collected during stage I of the clinical study at Charité-Universitätsmedizin Berlin.

Determined once		**Determined once per study day**
Categorical	**Continuous**	**Continuous**
• Sex • Location of Infection • General Diagnosis • RRT • ECMO • Pathogen • Immunosuppression status • Treatment outcome*	• Age • Height • Weight • MIC	• SOFA score • APACHE-II score • Serum creatinine concentration • Dosing change

*Possible treatment outcomes: free of pathogen, change of medication, death due to infection, death or transfer to different ward.

Abbreviations: *RRT:* Renal replacement therapy, *ECMO:* Extracorporeal membrane oxygenation, *MIC:* Minimum inhibitory concentration, *SOFA:* Sepsis-related Organ Failure Assessment, *APACHE-II:* Acute Physiology And Chronic Health Evaluation.

Table S2: Overview of determined Pathogens and minimum inhibitory concentrations for patients treated with meropenem.

Pathogen	**Pathogens determined, n (%)**	**MIC, n (%)**	**Minimum inhibitory concentration [mg/L], n (%)**						
			0.25	**0.5**	**1**	**2**	**4**	**8**	**16**
All Pathogens	244 (100)	217 (88.9)	176 (81.1)	8 (3.69)	3 (1.38)	4 (1.84)	11 (5.07)	7 (3.23)	8 (3.69)
Enterobacter cloacae	50 (20.5)	48 (96.0)	43 (89.6)	0 (0)	0 (0)	0 (0)	0 (0)	5 (10.4)	0 (0)
Pseudomonas aeruginosa	41 (16.8)	39 (95.1)	16 (41)	7 (17.9)	3 (7.69)	2 (5.13)	3 (7.69)	0 (0)	8 (20.5)
Escherichia coli	36 (14.8)	32 (88.9)	30 (93.8)	0 (0)	0 (0)	2 (6.25)	0 (0)	0 (0)	0 (0)
Klebsiella pneumonia	36 (14.8)	30 (83.3)	28 (93.3)	0 (0)	0 (0)	0 (0)	0 (0)	2 (6.67)	0 (0)
Serratia marcescens	25 (10.2)	24 (96.0)	24 (100)	0 (0)	0 (0)	0 (0)	0 (0)	0 (0)	0 (0)
Citrobacter freundii	14 (5.74)	14 (100)	6 (42.9)	0 (0)	0 (0)	0 (0)	8 (57.1)	0 (0)	0 (0)
Hafnia alvei	12 (4.91)	10 (83.3)	10 (100)	0 (0)	0 (0)	0 (0)	0 (0)	0 (0)	0 (0)
Klebsiella oxytoca	8 (3.28)	8 (100)	8 (100)	0 (0)	0 (0)	0 (0)	0 (0)	0 (0)	0 (0)
Pseudomonas stutzeri	5 (2.05)	5 (100)	5 (100)	0 (0)	0 (0)	0 (0)	0 (0)	0 (0)	0 (0)
Staphylococcus aureus	7 (2.87)	3 (42.9)	3 (100)	0 (0)	0 (0)	0 (0)	0 (0)	0 (0)	0 (0)
Proteus mirabilis	3 (1.23)	3 (100)	3 (100)	0 (0)	0 (0)	0 (0)	0 (0)	0 (0)	0 (0)
Providencia stuartii	1 (0.41)	1 (100)	0 (0)	1 (100)	0 (0)	0 (0)	0 (0)	0 (0)	0 (0)
Enterococcus faecalis	1 (0.41)	0 (0)	0 (0)	0 (0)	0 (0)	0 (0)	0 (0)	0 (0)	0 (0)
Streptococcus salivarius	1 (0.41)	0 (0)	0 (0)	0 (0)	0 (0)	0 (0)	0 (0)	0 (0)	0 (0)
Achromobacter xylosoxidans	1 (0.41)	0 (0)	0 (0)	0 (0)	0 (0)	0 (0)	0 (0)	0 (0)	0 (0)
Streptococcus agalactiae	1 (0.41)	0 (0)	0 (0)	0 (0)	0 (0)	0 (0)	0 (0)	0 (0)	0 (0)

Abbreviations: *MIC:* minimum inhibitory concentration, *n:* number of samples.

Table S3: Overview of determined Pathogens and minimum inhibitory concentrations for patients treated with piperacillin/tazobactam.

Pathogen	**Pathogens determined, n (%)**	**MIC, n (%)**	**Minimum inhibitory concentration [mg/L], n (%)**							
			0.25	**0.5**	**1**	**2**	**4**	**8**	**16**	**32**
All Pathogens	78 (100)	60 (76.9)	3 (5)	0 (0)	0 (0)	0 (0)	41 (68.3)	10 (16.7)	2 (3.33)	4 (6.67)
Pseudomonas aeruginosa	15 (19.2)	14 (93.3)	0 (0)	0 (0)	0 (0)	0 (0)	1 (7.14)	7 (50)	2 (14.3)	4 (28.6)
Escherichia coli	13 (16.7)	13 (100)	1 (7.69)	0 (0)	0 (0)	0 (0)	12 (92.3)	0 (0)	0 (0)	0 (0)
Enterococcus faecalis	13 (16.7)	0 (0)	0 (0)	0 (0)	0 (0)	0 (0)	0 (0)	0 (0)	0 (0)	0 (0)
Serratia marcescens	9 (11.5)	9 (100)	0 (0)	0 (0)	0 (0)	0 (0)	9 (100)	0 (0)	0 (0)	0 (0)
Achromobacter sp.	6 (7.70)	6 (100)	0 (0)	0 (0)	0 (0)	0 (0)	6 (100)	0 (0)	0 (0)	0 (0)
Klebsiella pneumoniae	5 (6.41)	4 (80.0)	0 (0)	0 (0)	0 (0)	0 (0)	2 (50)	2 (50)	0 (0)	0 (0)
Citrobacter freundii	4 (5.12)	4 (100)	0 (0)	0 (0)	0 (0)	0 (0)	4 (100)	0 (0)	0 (0)	0 (0)
Enterobacter cloacae	2 (2.56)	2 (100)	0 (0)	0 (0)	0 (0)	0 (0)	1 (50)	1 (50)	0 (0)	0 (0)
Staphylococcus aureus	2 (2.56)	2 (100)	0 (0)	0 (0)	0 (0)	0 (0)	2 (100)	0 (0)	0 (0)	0 (0)
Streptococcus agalactiae	2 (2.56)	0 (0)	0 (0)	0 (0)	0 (0)	0 (0)	0 (0)	0 (0)	0 (0)	0 (0)
Proteus mirabilis	2 (2.56)	2 (100)	0 (0)	0 (0)	0 (0)	0 (0)	2 (100)	0 (0)	0 (0)	0 (0)
Acinetobacter baumannii	2 (2.56)	2 (100)	2 (100)	0 (0)	0 (0)	0 (0)	0 (0)	0 (0)	0 (0)	0 (0)
Achromobacter xylosoxidans	2 (2.56)	2 (100)	0 (0)	0 (0)	0 (0)	0 (0)	2 (100)	0 (0)	0 (0)	0 (0)

Abbreviations: *MIC:* minimum inhibitory concentration, *n:* number of samples.

Table S4: Statistical tests to assess the normality assumption in the NPDE analysis.

Statistical test	**p-value**
Wilcoxon signed-rank test	0.0325
Fisher ratio test	0.283
Shapiro-Wilks test	0.784
Global adjusted p-value	0.0976

Abbreviations: *NPDE:* Normalised prediction distribution errors.

Table S5: Distribution of normalised prediction distribution errors.

Distribution of NPDEs	
Mean	0.2958 (se=0.14)
Variance	1.19 (se=0.21)
Skewness	-0.0491
Kurtosis	-0.4235

Abbreviations: *NPDE:* Normalised prediction distribution errors, se: Standard error.

Table S6: Probability to achieve predefined targets (98% $T_{>MIC}$ and $Cmin_{>MIC-<5xMIC}$) and distribution of predicted minimum concentrations based on the re-estimated meropenem PK model, a MIC value of 8 mg/L and for selected dosing regimens according to Table 3.8.

Creatinine clearance [mL/min] (Cockcroft-Gault)	1 g meropenem, 4 h infusion, 6 h dosing interval (Dosing regimen 1)					1 g meropenem, 4 h infusion, 8 h dosing interval (Dosing regimen 2)					1 g meropenem, 4 h infusion, 12 h dosing interval (Dosing regimen 3)				
	Probability of		Cmin [mg/L]			Probability of		Cmin [mg/L]			Probability of		Cmin [mg/L]		
	98% $T_{>MIC}$	$Cmin_{>MIC-<5xMIC}$	$P_{0.05}$	Median ($P_{0.5}$)	$P_{0.95}$	98% $T_{>MIC}$	$Cmin_{>MIC-<5xMIC}$	$P_{0.05}$	Median ($P_{0.5}$)	$P_{0.95}$	98% $T_{>MIC}$	$Cmin_{>MIC-<5xMIC}$	$P_{0.05}$	Median ($P_{0.5}$)	$P_{0.95}$
10	100.0	22.9	23.9	51.1	90.9	100.0	68.0	14.0	34.1	64.5	93.2	88.0	5.5	17.8	38.6
20	100.0	61.6	17.7	36.1	63.3	98.6	90.6	9.7	23.0	43.6	69.9	71.2	3.2	10.9	24.5
30	99.8	86.0	13.3	27.3	48.4	92.4	91.6	6.8	16.6	32.4	40.4	43.4	1.9	7.2	17.2
40	98.8	94.7	10.3	21.4	39.0	78.8	80.8	4.9	12.5	25.5	19.2	21.4	1.2	4.9	12.8
50	95.6	94.4	8.1	17.4	32.4	61.0	64.6	3.5	9.7	20.6	7.8	9.4	0.7	3.4	9.8
60	89.0	89.6	6.5	14.3	27.6	42.4	47.0	2.6	7.6	17.1	3.2	3.8	0.4	2.5	7.8
70	79.2	81.0	5.3	12.1	23.9	27.6	32.0	2.0	6.2	14.5	1.2	1.4	0.3	1.8	6.2
80	67.2	70.2	4.3	10.3	20.9	16.8	20.4	1.5	5.0	12.4	0.4	0.6	0.2	1.3	5.0
90	54.2	58.4	3.6	8.8	18.5	9.8	12.8	1.2	4.1	10.7	0.2	0.2	0.1	1.0	4.1
100	42.2	46.8	3.0	7.7	16.5	5.8	7.8	0.9	3.4	9.3	0.0	0.0	0.1	0.7	3.4
110	31.4	36.6	2.6	6.7	14.9	3.0	4.6	0.7	2.9	8.2	0.0	0.0	0.1	0.6	2.9
120	23.5	28.2	2.2	5.9	13.5	1.8	2.6	0.6	2.4	7.3	0.0	0.0	0.0	0.4	2.4
130	17.4	21.6	1.9	5.3	12.4	1.0	1.6	0.5	2.1	6.5	0.0	0.0	0.0	0.4	2.1
140	12.8	16.7	1.7	4.8	11.6	0.6	1.0	0.4	1.9	6.0	0.0	0.0	0.0	0.3	1.8
150	9.4	12.7	1.5	4.4	10.9	0.4	0.6	0.3	1.7	5.6	0.0	0.0	0.0	0.2	1.6
175	7.5	10.3	1.4	4.2	10.4	0.2	0.6	0.3	1.5	5.3	0.0	0.0	0.0	0.2	1.5
200	7.4	10.6	1.4	4.2	10.4	0.2	0.4	0.3	1.5	5.2	0.0	0.0	0.0	0.2	1.5
250	7.4	10.4	1.4	4.2	10.4	0.2	0.4	0.3	1.5	5.2	0.0	0.0	0.0	0.2	1.5
300	7.2	10.4	1.4	4.2	10.4	0.2	0.4	0.3	1.5	5.3	0.0	0.0	0.0	0.2	1.5

Colour coding probabilities: *Green:* ≥90 PTA, *Yellow:* ≥50-<90 PTA, *Red:* 0 - <50 PTA; Colour coding Cmin distribution: *Red:* ≥64 mg/L, *Light red:* ≥16-<64 mg/L, *White*:<16 mg/L .
Abbreviations: *MIC:* Minimum inhibitory concentration, $T_{>MIC}$: Time above the MIC, *Cmin:* Minimum meropenem concentration, $P_{0.05}$: 5th percentile, $P_{0.95}$: 95th percentile.

Table S7 (continued): Probability to achieve predefined targets (98% $T_{>MIC}$ and $Cmin_{>MIC-<5xMIC}$) and distribution of predicted minimum concentrations based on the re-estimated meropenem PK model, a MIC value of 8 mg/L and for selected dosing regimens according to Table 3.8.

Creatinine clearance [mL/min] (Cockcroft-Gault)	2 g meropenem, 4 h infusion, 6 h dosing interval (Dosing regimen 4)					2 g meropenem, 4 h infusion, 8 h dosing interval (Dosing regimen 5)					2 g meropenem, 4 h infusion, 12 h dosing interval (Dosing regimen 6)				
	Probability of		Cmin [mg/L]			Probability of		Cmin [mg/L]			Probability of		Cmin [mg/L]		
	98% $T_{>MIC}$	$Cmin_{>MIC-<5xMIC}$	$P_{0.05}$	Median ($P_{0.5}$)	$P_{0.95}$	98% $T_{>MIC}$	$Cmin_{>MIC-<5xMIC}$	$P_{0.05}$	Median ($P_{0.5}$)	$P_{0.95}$	98% $T_{>MIC}$	$Cmin_{>MIC-<5xMIC}$	$P_{0.05}$	Median ($P_{0.5}$)	$P_{0.95}$
10	100.0	0.0	47.6	101.9	179.8	100.0	0.0	28.1	68.0	127.1	100.0	0.0	11.0	35.5	75.1
20	100.0	0.0	35.3	72.2	125.9	100.0	0.0	19.3	46.1	86.6	100.0	1.4	6.4	21.8	48.2
30	100.0	0.0	26.7	54.5	96.6	100.0	0.0	13.6	33.2	64.5	100.0	6.8	3.8	14.3	34.1
40	100.0	0.0	20.6	42.8	77.9	100.0	0.4	9.7	25.0	50.8	99.4	17.6	2.3	9.7	25.5
50	100.0	0.0	16.2	34.7	64.9	100.0	1.4	7.1	19.4	41.3	97.6	31.4	1.4	6.8	19.7
60	100.0	0.0	13.0	28.7	55.2	100.0	4.0	5.2	15.3	34.2	94.2	44.8	0.9	4.9	15.5
70	100.0	0.2	10.6	24.1	47.7	100.0	8.4	3.9	12.3	28.9	88.6	53.8	0.6	3.6	12.4
80	100.0	0.4	8.7	20.5	41.8	99.8	14.6	3.0	10.0	24.7	81.2	58.2	0.4	2.6	10.1
90	100.0	1.2	7.2	17.6	37.1	99.6	22.6	2.3	8.3	21.4	72.2	57.6	0.2	2.0	8.3
100	100.0	2.4	6.0	15.3	33.0	99.0	31.2	1.8	6.9	18.6	62.4	53.2	0.2	1.5	6.8
110	100.0	4.4	5.1	13.4	29.7	98.0	39.6	1.4	5.7	16.4	53.2	47.6	0.1	1.1	5.7
120	100.0	6.8	4.4	11.9	27.0	96.8	46.7	1.2	4.9	14.5	44.2	41.8	0.1	0.9	4.9
130	100.0	10.0	3.9	10.6	24.7	95.0	53.4	1.0	4.2	13.0	36.8	36.2	0.1	0.7	4.2
140	100.0	13.2	3.4	9.7	23.1	93.2	57.6	0.8	3.7	12.0	30.6	31.0	0.0	0.6	3.7
150	100.0	17.4	3.0	8.9	21.7	90.6	60.4	0.7	3.3	11.1	25.4	26.2	0.0	0.5	3.3
175	100.0	20.8	2.8	8.4	20.7	88.2	61.9	0.6	3.1	10.5	21.8	22.9	0.0	0.4	3.0
200	100.0	20.8	2.8	8.4	20.8	88.2	62.0	0.6	3.1	10.4	22.0	23.0	0.0	0.4	3.0
250	100.0	20.8	2.8	8.4	20.8	88.4	61.8	0.6	3.1	10.5	21.7	22.9	0.0	0.4	3.0
300	100.0	21.0	2.8	8.4	20.8	88.5	62.0	0.6	3.1	10.5	22.0	23.0	0.0	0.4	3.0

Colour coding probabilities: *Green:* ≥90 PTA, *Yellow:* ≥50-<90 PTA, *Red:* 0 - <50 PTA, Colour coding Cmin distribution: *Red:* ≥64 mg/L, *Light red:* ≥16-<64 mg/L, *White*:<16 mg/L .
Abbreviations: *MIC:* Minimum inhibitory concentration, $T_{>MIC}$: Time above the MIC, *Cmin:* Minimum meropenem concentration, $P_{0.05}$: 5th percentile, $P_{0.95}$: 95th percentile.

Table S8 (continued): Probability to achieve predefined targets (98% $T_{>MIC}$ and $Cmin_{>MIC-<5xMIC}$) and distribution of predicted minimum concentrations based on the re-estimated meropenem PK model, a MIC value of 8 mg/L and for selected dosing regimens according to Table 3.8.

Creatinine clearance [mL/min] (Cockcroft-Gault)	3 g meropenem, 4 h infusion, 6 h dosing interval (Dosing regimen 7)					3 g meropenem, 4 h infusion, 8 h dosing interval (Dosing regimen 8)					3 g meropenem, 4 h infusion, 12 h dosing interval (Dosing regimen 9)				
	Probability of		Cmin [mg/L]			Probability of		Cmin [mg/L]			Probability of		Cmin [mg/L]		
	98% $T_{>MIC}$	$Cmin_{>MIC-<5xMIC}$	$P_{0.05}$	Median ($P_{0.5}$)	$P_{0.95}$	98% $T_{>MIC}$	$Cmin_{>MIC-<5xMIC}$	$P_{0.05}$	Median ($P_{0.5}$)	$P_{0.95}$	98% $T_{>MIC}$	$Cmin_{>MIC-<5xMIC}$	$P_{0.05}$	Median ($P_{0.5}$)	$P_{0.95}$
10	100.0	0.4	47.6	101.9	179.8	100.0	9.0	28.1	68.0	127.1	99.4	59.9	11.0	35.5	75.1
20	100.0	5.2	35.3	72.2	125.9	100.0	36.0	19.3	46.1	86.6	94.2	81.8	6.4	21.8	48.2
30	100.0	20.0	26.7	54.5	96.6	99.6	65.4	13.6	33.2	64.5	79.8	78.2	3.8	14.3	34.1
40	100.0	42.4	20.6	42.8	77.9	97.8	83.4	9.7	25.0	50.8	59.6	61.0	2.3	9.7	25.5
50	100.0	63.6	16.2	34.7	64.9	93.2	87.8	7.1	19.4	41.3	38.8	41.8	1.4	6.8	19.7
60	99.6	79.0	13.0	28.7	55.2	84.8	83.6	5.2	15.3	34.2	23.2	25.8	0.9	4.9	15.5
70	98.6	87.2	10.6	24.1	47.7	73.4	74.8	3.9	12.3	28.9	13.0	15.2	0.6	3.6	12.4
80	96.6	90.8	8.7	20.5	41.8	60.6	63.6	3.0	10.0	24.7	7.0	8.4	0.4	2.6	10.1
90	93.2	90.2	7.2	17.6	37.1	48.4	52.2	2.3	8.3	21.4	3.8	4.8	0.2	2.0	8.3
100	88.2	86.9	6.0	15.3	33.0	36.8	41.2	1.8	6.9	18.6	1.8	2.6	0.2	1.5	6.8
110	81.8	81.7	5.1	13.4	29.7	27.0	31.2	1.4	5.7	16.4	1.0	1.4	0.1	1.1	5.7
120	75.0	75.8	4.4	11.9	27.0	20.0	24.1	1.2	4.9	14.5	0.4	0.8	0.1	0.9	4.9
130	67.2	69.4	3.9	10.6	24.7	14.6	18.0	1.0	4.2	13.0	0.2	0.4	0.1	0.7	4.2
140	60.4	62.9	3.4	9.7	23.1	10.8	13.7	0.8	3.7	12.0	0.2	0.2	0.0	0.6	3.7
150	53.6	56.6	3.0	8.9	21.7	7.8	10.6	0.7	3.3	11.1	0.0	0.2	0.0	0.5	3.3
175	47.8	51.6	2.8	8.4	20.7	6.2	8.6	0.6	3.1	10.5	0.0	0.0	0.0	0.4	3.0
200	47.6	51.4	2.8	8.4	20.8	6.3	8.6	0.6	3.1	10.4	0.0	0.0	0.0	0.4	3.0
250	48.0	51.6	2.8	8.4	20.8	6.0	8.4	0.6	3.1	10.5	0.0	0.0	0.0	0.4	3.0
300	47.6	51.0	2.8	8.4	20.8	6.2	8.4	0.6	3.1	10.5	0.0	0.0	0.0	0.4	3.0

Colour coding probabilities: *Green:* ≥90 PTA, *Yellow:* ≥50-<90 PTA, *Red:* 0 - <50 PTA, Colour coding Cmin distribution: *Red:* ≥64 mg/L, *Light red:* ≥16-<64 mg/L, *White*:<16 mg/L .
Abbreviations: *MIC:* Minimum inhibitory concentration, $T_{>MIC}$: Time above the MIC, *Cmin:* Minimum meropenem concentration, $P_{0.05}$: 5th percentile, $P_{0.95}$: 95th percentile.

Table S9 (continued): Probability to achieve predefined targets (98% $T_{>MIC}$ and $Cmin_{>MIC-<5xMIC}$) and distribution of predicted minimum concentrations based on the re-estimated meropenem PK model, a MIC value of 8 mg/L and for selected dosing regimens according to Table 3.8.

Creatinine clearance [mL/min] (Cockcroft-Gault)	4 g meropenem, 4 h infusion, 6 h dosing interval (Dosing regimen 10)					4 g meropenem, 4 h infusion, 8 h dosing interval (Dosing regimen 11)					4 g meropenem, 4 h infusion, 12 h dosing interval (Dosing regimen 12)				
	Probability of		Cmin [mg/L]			Probability of		Cmin [mg/L]			Probability of		Cmin [mg/L]		
	98% $T_{>MIC}$	$Cmin_{>MIC-<5xMIC}$	$P_{0.05}$	Median ($P_{0.5}$)	$P_{0.95}$	98% $T_{>MIC}$	$Cmin_{>MIC-<5xMIC}$	$P_{0.05}$	Median ($P_{0.5}$)	$P_{0.95}$	98% $T_{>MIC}$	$Cmin_{>MIC-<5xMIC}$	$P_{0.05}$	Median ($P_{0.5}$)	$P_{0.95}$
10	100.0	0.0	71.5	152.7	269.1	100.0	1.2	42.1	101.8	189.5	99.8	27.0	16.5	53.1	111.8
20	100.0	0.4	52.8	108.2	188.8	100.0	10.4	29.0	69.1	129.7	98.2	62.5	9.7	32.7	72.2
30	100.0	3.6	39.9	81.7	144.7	100.0	30.8	20.3	49.8	96.6	91.4	78.0	5.7	21.4	51.1
40	100.0	12.1	31.0	64.4	116.7	99.6	54.4	14.5	37.5	76.3	78.0	74.8	3.5	14.6	38.1
50	100.0	25.6	24.4	52.1	97.2	98.2	72.6	10.7	29.1	61.8	60.8	61.4	2.1	10.3	29.4
60	100.0	42.6	19.5	43.1	82.8	95.0	81.6	7.9	23.0	51.5	43.2	45.4	1.3	7.3	23.2
70	99.8	58.7	15.9	36.2	71.5	89.4	83.0	5.9	18.4	43.4	28.8	31.4	0.9	5.3	18.6
80	99.4	71.0	13.0	30.8	62.8	81.6	79.2	4.5	15.0	37.1	18.4	20.8	0.6	4.0	15.1
90	98.6	80.0	10.7	26.5	55.5	72.0	71.9	3.5	12.4	32.0	11.6	13.4	0.4	3.0	12.4
100	97.2	85.0	9.1	23.0	49.7	61.6	63.4	2.7	10.3	27.9	6.8	8.4	0.2	2.2	10.2
110	94.8	87.2	7.7	20.1	44.5	51.0	53.8	2.2	8.6	24.6	4.0	5.0	0.2	1.7	8.5
120	91.7	86.4	6.6	17.8	40.5	41.6	45.4	1.8	7.3	21.8	2.4	3.0	0.1	1.3	7.3
130	88.0	84.4	5.7	16.0	37.2	33.8	37.6	1.4	6.3	19.6	1.4	2.0	0.1	1.1	6.2
140	83.6	81.2	5.1	14.5	34.6	27.6	31.4	1.2	5.6	18.0	0.8	1.2	0.1	0.9	5.5
150	79.1	77.6	4.5	13.4	32.7	22.4	26.2	1.0	5.0	16.7	0.6	0.8	0.1	0.7	4.9
175	74.8	74.2	4.2	12.6	31.3	18.7	22.6	0.9	4.6	15.8	0.4	0.6	0.0	0.6	4.5
200	74.9	74.4	4.1	12.6	31.2	18.7	22.4	0.9	4.6	15.7	0.4	0.6	0.0	0.6	4.6
250	75.2	74.6	4.1	12.6	31.2	18.8	22.3	0.9	4.6	15.7	0.4	0.6	0.0	0.6	4.5
300	75.0	74.3	4.1	12.6	31.2	18.6	22.2	0.9	4.6	15.8	0.4	0.6	0.0	0.6	4.5

Colour coding probabilities: *Green:* ≥90 PTA, *Yellow:* ≥50-<90 PTA, *Red:* 0 - <50 PTA, Colour coding Cmin distribution: *Red:* ≥64 mg/L, *Light red:* ≥16-<64 mg/L, *White*:<16 mg/L .
Abbreviations: *MIC:* Minimum inhibitory concentration, $T_{>MIC}$: Time above the MIC, *Cmin:* Minimum meropenem concentration, $P_{0.05}$: 5th percentile, $P_{0.95}$: 95th percentile.

Table S10 (continued): Probability to achieve predefined targets (98% $T_{>MIC}$ and $Cmin_{>MIC-<5xMIC}$) and distribution of predicted minimum concentrations based on the re-estimated meropenem PK model, a MIC value of 8 mg/L and for selected dosing regimens according to Table 3.8.

Creatinine clearance [mL/min] (Cockroft-Gault)	4 g meropenem, 24 h infusion, 24 h dosing interval (Dosing regimen 13)					6 g meropenem, 24 h infusion, 24 h dosing interval (Dosing regimen 14)					8 g meropenem, 24 h infusion, 24 h dosing interval (Dosing regimen 15)				
	Probability of		Cmin [mg/L]			Probability of		Cmin [mg/L]			Probability of		Cmin [mg/L]		
	98% $T_{>MIC}$	$Cmin_{>MIC-<5xMIC}$	$P_{0.05}$	Median ($P_{0.5}$)	$P_{0.95}$	98% $T_{>MIC}$	$Cmin_{>MIC-<5xMIC}$	$P_{0.05}$	Median ($P_{0.5}$)	$P_{0.95}$	98% $T_{>MIC}$	$Cmin_{>MIC-<5xMIC}$	$P_{0.05}$	Median ($P_{0.5}$)	$P_{0.95}$
10	91.2	56.0	32.2	60.1	102.1	97.8	11.9	48.3	90.1	152.3	97.8	8.8	50.0	99.1	174.5
20	75.1	73.6	25.8	45.0	74.2	95.2	41.6	38.8	67.5	111.0	95.2	34.2	39.4	72.1	124.6
30	50.0	63.1	21.4	36.0	59.0	88.2	66.8	32.0	53.9	88.3	88.2	60.3	32.3	56.3	97.0
40	27.2	41.2	18.1	30.0	49.0	75.3	75.8	27.2	44.9	73.5	75.4	72.4	27.3	46.3	79.4
50	12.4	22.2	15.7	25.7	42.1	57.8	69.0	23.5	38.5	63.2	58.5	68.0	23.6	39.3	67.1
60	5.4	11.0	13.8	22.5	36.9	40.4	55.4	20.7	33.7	55.4	41.1	56.0	20.8	34.2	58.1
70	2.2	5.2	12.3	20.0	33.0	26.2	41.0	18.5	30.0	49.5	26.4	41.8	18.5	30.3	51.3
80	1.0	2.4	11.1	18.0	29.8	16.2	28.0	16.7	27.0	44.7	16.4	29.2	16.7	27.2	46.0
90	0.4	1.0	10.1	16.4	27.2	9.3	18.2	15.2	24.6	40.7	9.8	19.6	15.2	24.7	41.7
100	0.2	0.4	9.3	15.0	25.0	5.4	11.6	13.9	22.6	37.4	5.6	12.4	13.9	22.6	38.2
110	0.0	0.2	8.6	13.9	23.2	3.0	7.2	12.9	20.9	34.7	3.2	8.0	12.9	20.9	35.3
120	0.0	0.0	8.0	13.0	21.6	1.8	4.4	12.0	19.5	32.5	1.8	4.8	12.0	19.5	32.9
130	0.0	0.0	7.6	12.2	20.4	1.0	2.8	11.3	18.3	30.6	1.0	3.0	11.3	18.3	30.9
140	0.0	0.0	7.2	11.6	19.5	0.6	1.8	10.7	17.4	29.2	0.6	2.0	10.8	17.4	29.5
150	0.0	0.0	6.8	11.1	18.7	0.4	1.2	10.2	16.6	28.0	0.4	1.2	10.2	16.7	28.3
175	0.0	0.0	6.6	10.8	18.2	0.2	0.8	9.8	16.1	27.3	0.2	1.0	9.8	16.1	27.4
200	0.0	0.0	6.6	10.7	18.1	0.2	0.8	9.8	16.1	27.3	0.2	1.0	9.8	16.1	27.4
250	0.0	0.0	6.5	10.7	18.2	0.2	0.8	9.8	16.1	27.2	0.2	1.0	9.8	16.1	27.4
300	0.0	0.0	6.6	10.7	18.2	0.2	0.8	9.8	16.1	27.2	0.2	1.0	9.8	16.1	27.4

Colour coding probabilities: *Green:* ≥90 PTA, *Yellow:* ≥50-<90 PTA, *Red:* 0 - <50 PTA, Colour coding Cmin distribution: *Red:* ≥64 mg/L, *Light red:* ≥16-<64 mg/L, *White*:<16 mg/L .
Abbreviations: *MIC:* Minimum inhibitory concentration, $T_{>MIC}$: Time above the MIC, *Cmin:* Minimum meropenem concentration, $P_{0.05}$: 5th percentile, $P_{0.95}$: 95th percentile.

Table S11: Terms included in the PubMed literature search (https://pubmed.ncbi.nlm.nih.gov/) for suitable pharmacokinetic models for piperacillin.

Main search term	In combination with one or multiple search terms (and/or)	Last access
Piperacillin	• population pharmacokinetics • population pharmacokinetic • pharmacokinetic models • pharmacokinetic model • individualization • individualizing • dosing software • dosing scheme • dosage optimization • dose optimization • pharmacometrics • pharmacometric • population model • precision dosing • NLME • nonmem • PK model • one-compartment • one compartment • two compartment • two-compartment • three compartment • three-compartment • Monte Carlo	19.08.2019

Table S12. Dosing regimens integrated in the model-informed dosing software DoseCalculator.

	Dose [mg]	Infusion duration [h]	Dosing interval [h]
	Meropenem		
Short-term infusion			
	1000	0.5	6
	1000	0.5	8
	1000	0.5	12
	2000	0.5	6
	2000	0.5	8
	2000	0.5	12
Prolonged infusion			
	1000	4	6
	1000	4	8
	1000	4	12
	2000	4	6
	2000	4	8
	2000	4	12
Continuous infusion			
	1000	24	24
	2000	24	24
	4000	24	24
	6000	24	24
	Piperacillin[1]		
Short-term infusion			
	4000	0.5	6
	4000	0.5	8
	4000	0.5	12
Prolonged infusion			
	4000	4	6
	4000	4	8
	4000	4	12
Continuous infusion			
	4000	24	24
	8000	24	24

[1]In combination with tazobactam in a ratio of 8:1.

Table S13: Additional dosing regimen integrated for piperacillin during the evaluation of the DoseCalculator .

	Dose [mg]	**Infusion duration [h]**	**Dosing interval [h]**
Short-term infusion			
	2000	0.5	6
	2000	0.5	8
	2000	0.5	12
Prolonged infusion			
	2000	4	6
	2000	4	8
	2000	4	12
Continuous infusion			
	2000	24	24

5.2 Supplementary figures

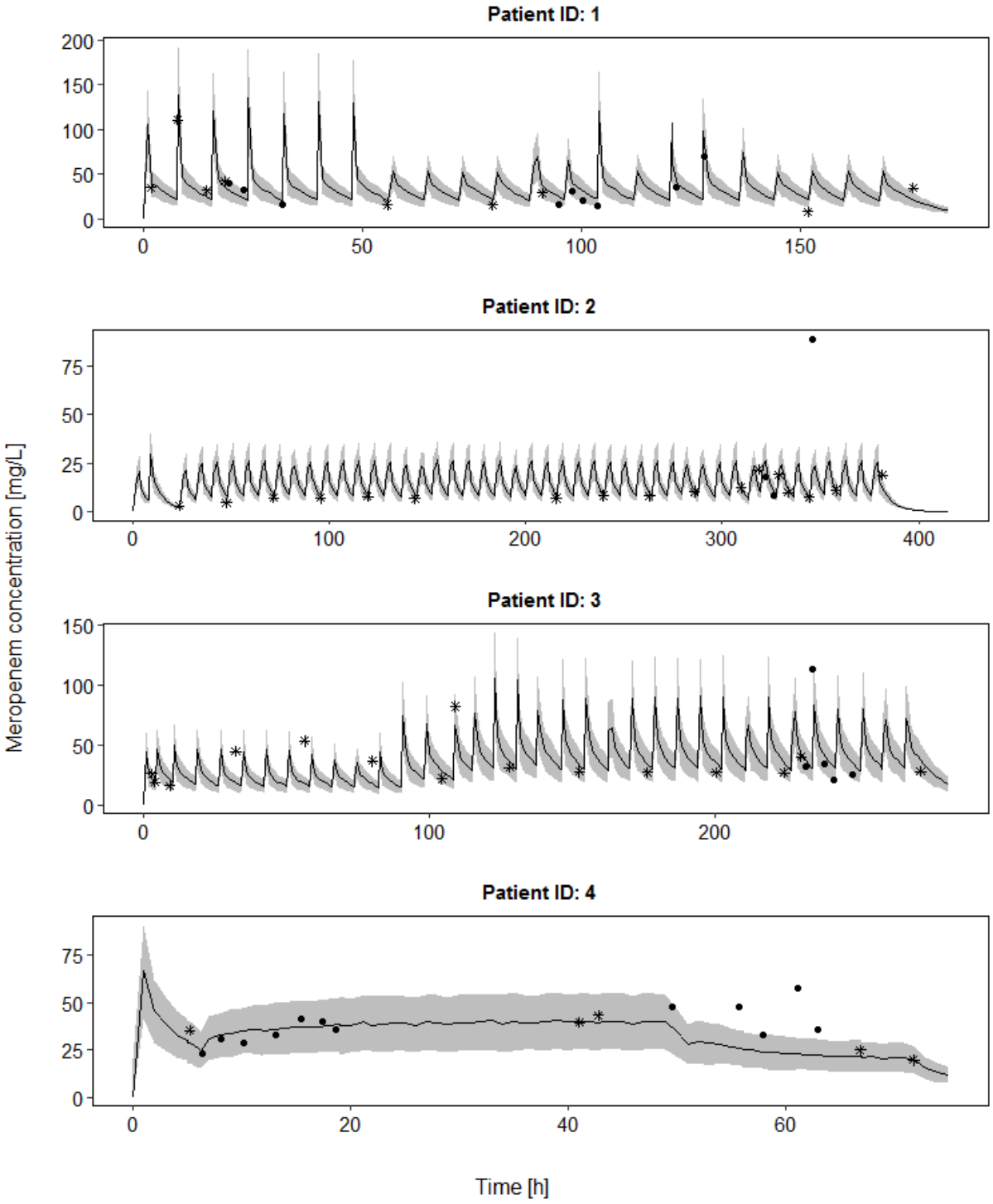

Figure S1: Observed meropenem concentrations and meropenem concentration-time profile predicted based on a pharmacokinetic model excluding CytoSorb® samples for patients 1 to 25. Black line: Median prediction, Grey shade: 50% prediction interval, Points: Meropenem samples with (points) and without (stars) CytoSorb®-treatment.

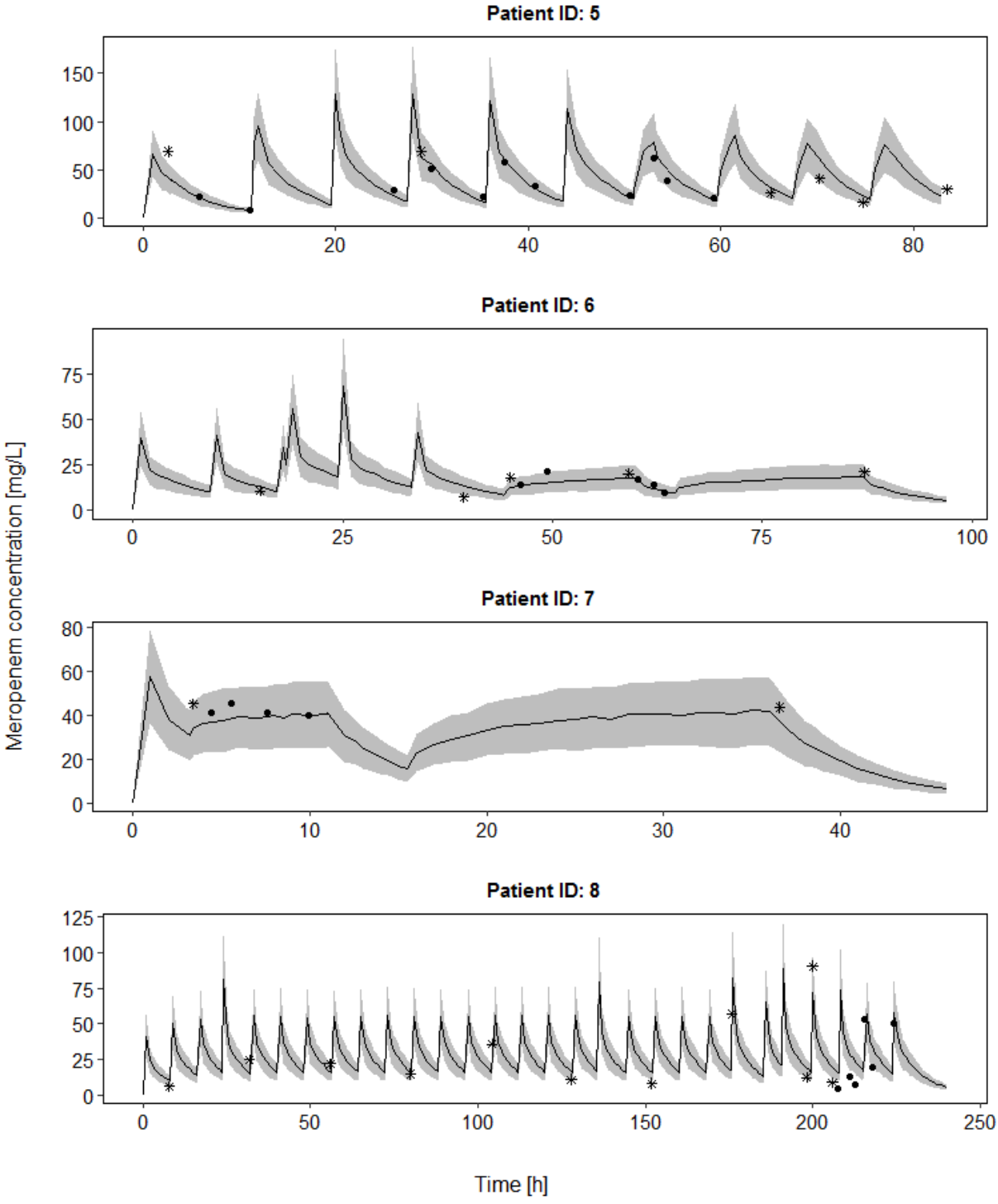

Figure S1 (continued): Observed meropenem concentrations and meropenem concentration-time profile predicted based on a pharmacokinetic model excluding CytoSorb® samples for patients 1 to 25. Black line: Median prediction, Grey shade: 50% prediction interval, Points: Meropenem samples with (points) and without (stars) CytoSorb®-treatment.

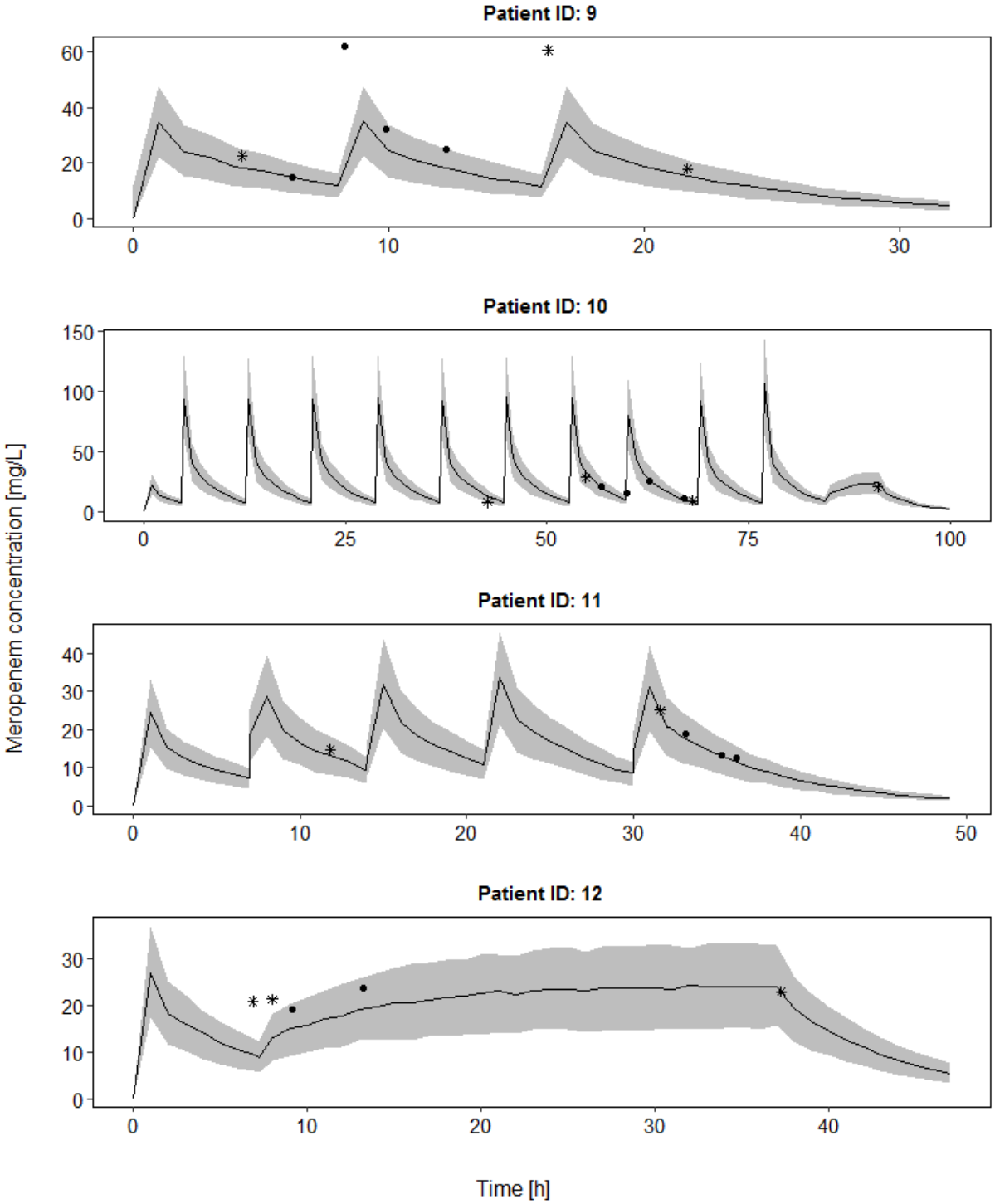

Figure S1 (continued): Observed meropenem concentrations and meropenem concentration-time profile predicted based on a pharmacokinetic model excluding CytoSorb® samples for patients 1 to 25. Black line: Median prediction, Grey shade: 50% prediction interval, Points: Meropenem samples with (points) and without (stars) CytoSorb®-treatment.

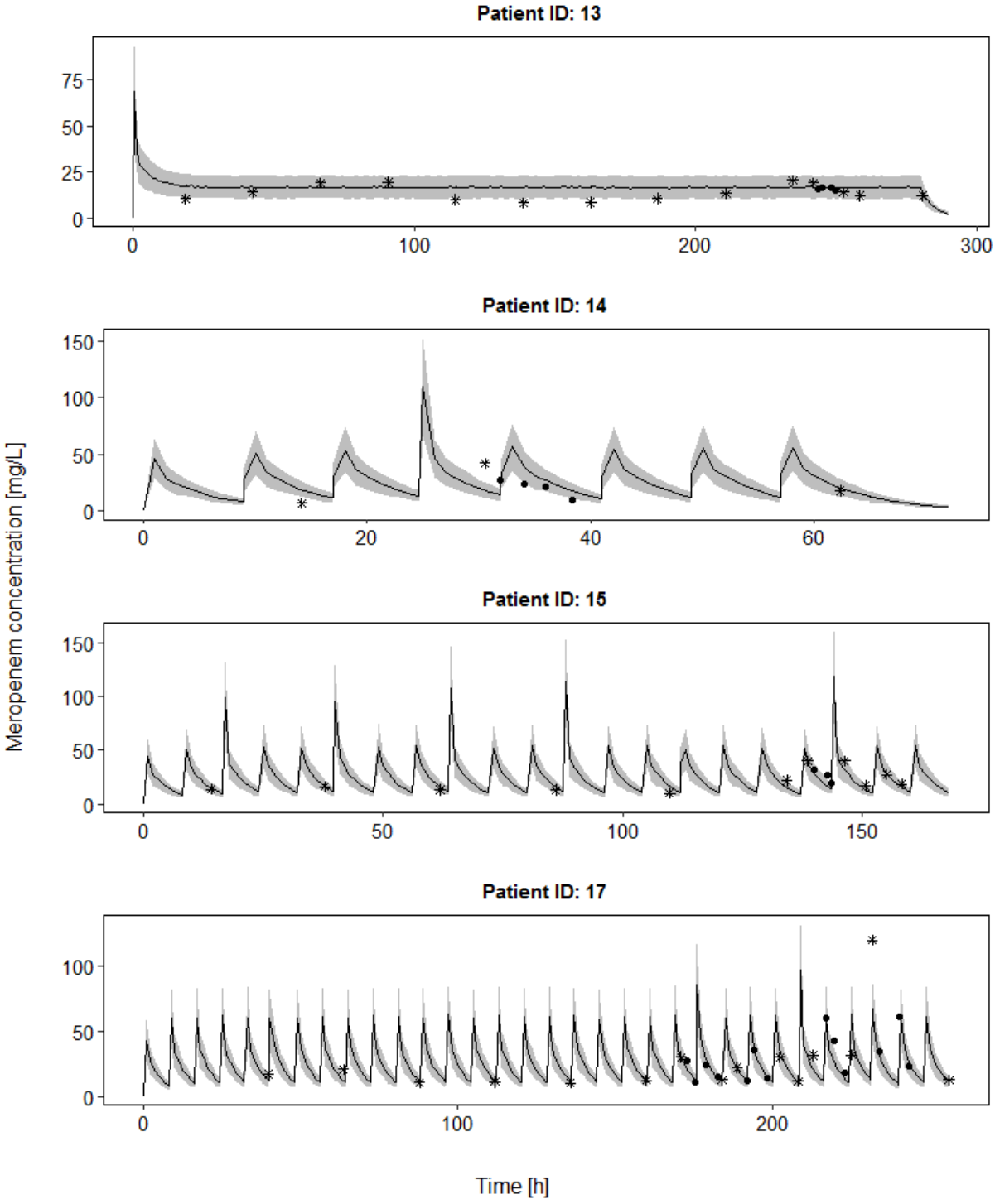

Figure S1 (continued): Observed meropenem concentrations and meropenem concentration-time profile predicted based on a pharmacokinetic model excluding CytoSorb® samples for patients 1 to 25. Black line: Median prediction, Grey shade: 50% prediction interval, Points: Meropenem samples with (points) and without (stars) CytoSorb®-treatment.

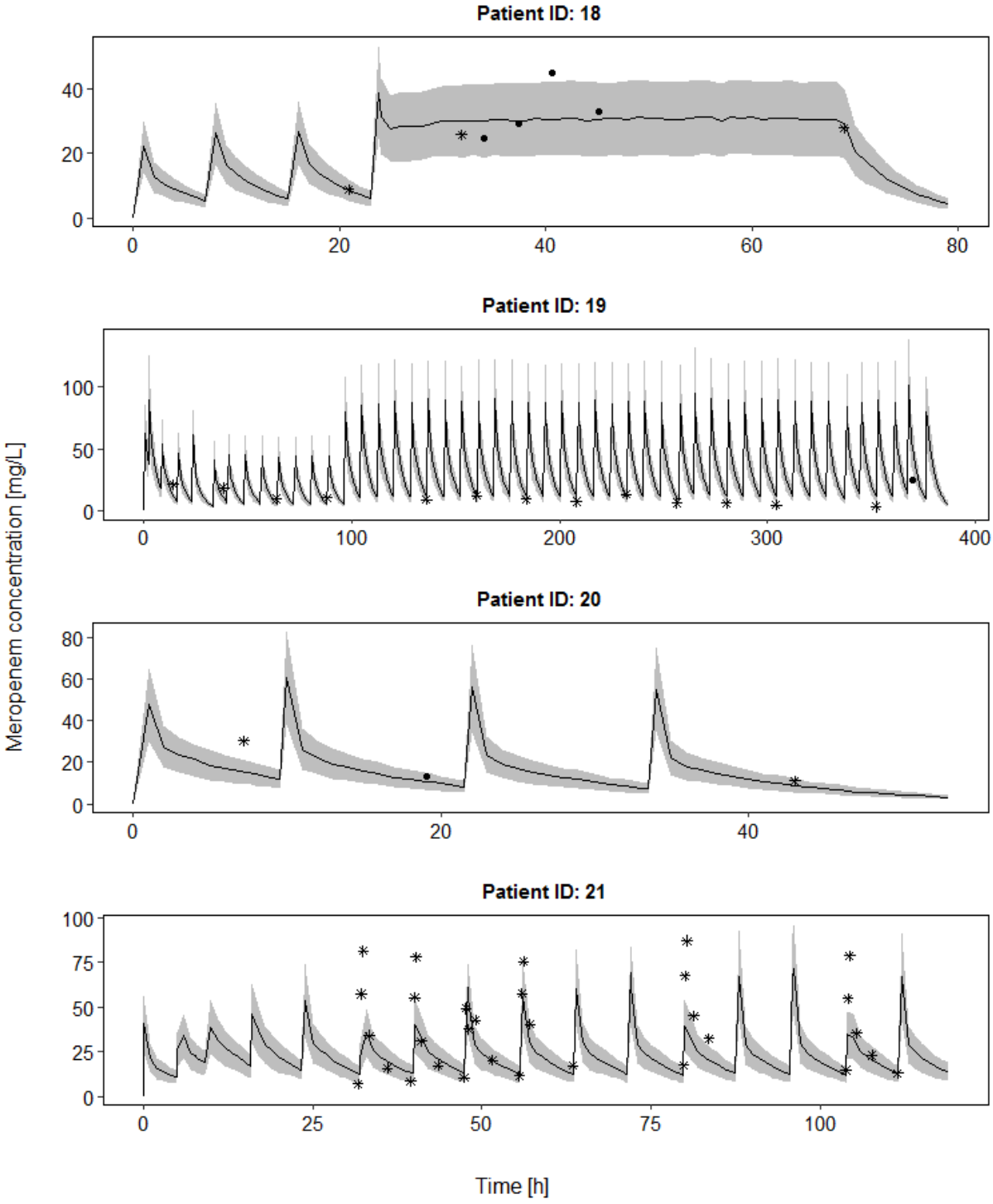

Figure S1 (continued): Observed meropenem concentrations and meropenem concentration-time profile predicted based on a pharmacokinetic model excluding CytoSorb® samples for patients 1 to 25. Black line: Median prediction, Grey shade: 50% prediction interval, Points: Meropenem samples with (points) and without (stars) CytoSorb®-treatment.

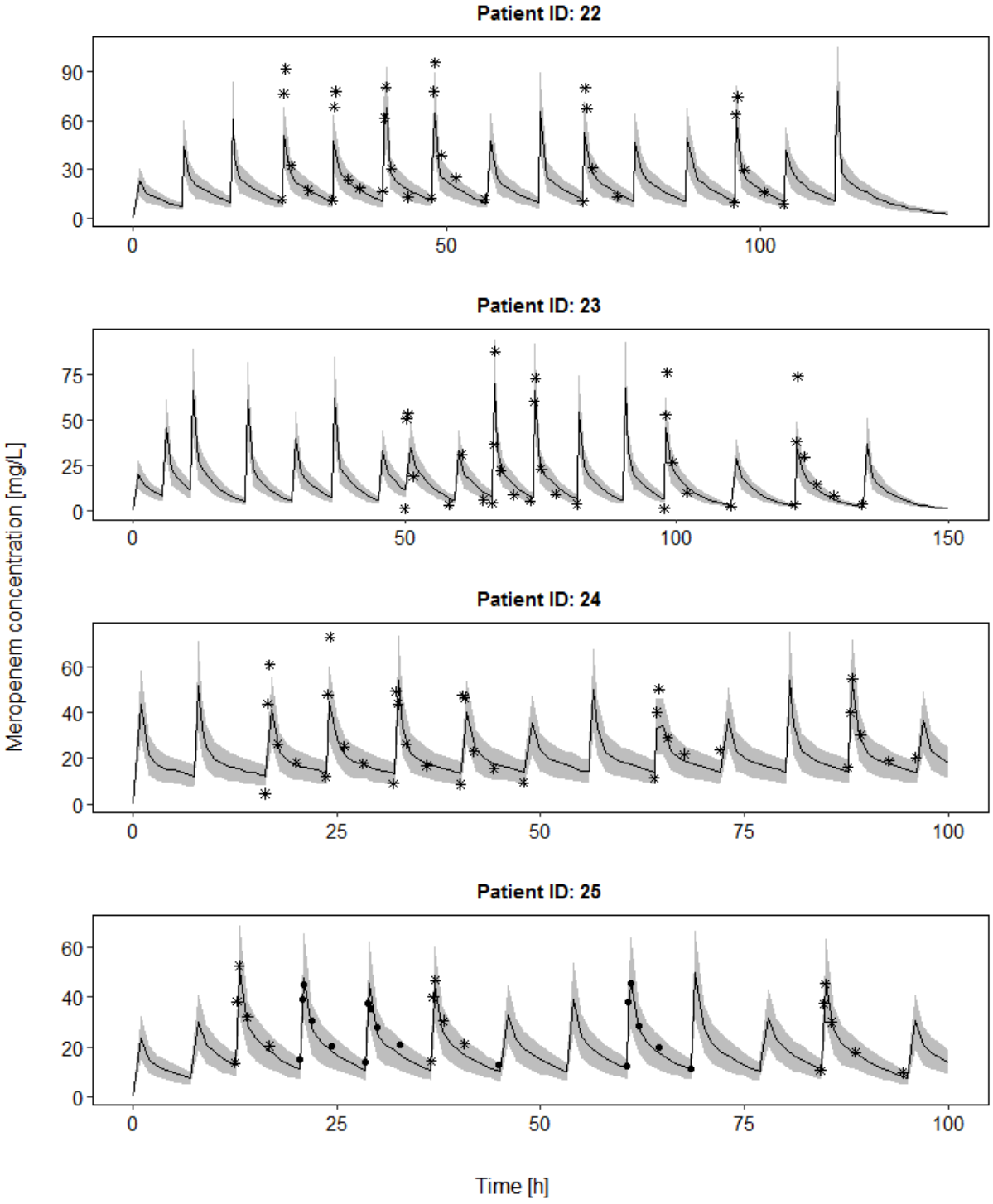

Figure S1 (continued): Observed meropenem concentrations and meropenem concentration-time profile predicted based on a pharmacokinetic model excluding CytoSorb® samples for patients 1 to 25. Black line: Median prediction, Grey shade: 50% prediction interval, Points: Meropenem samples with (points) and without (stars) CytoSorb®-treatment.

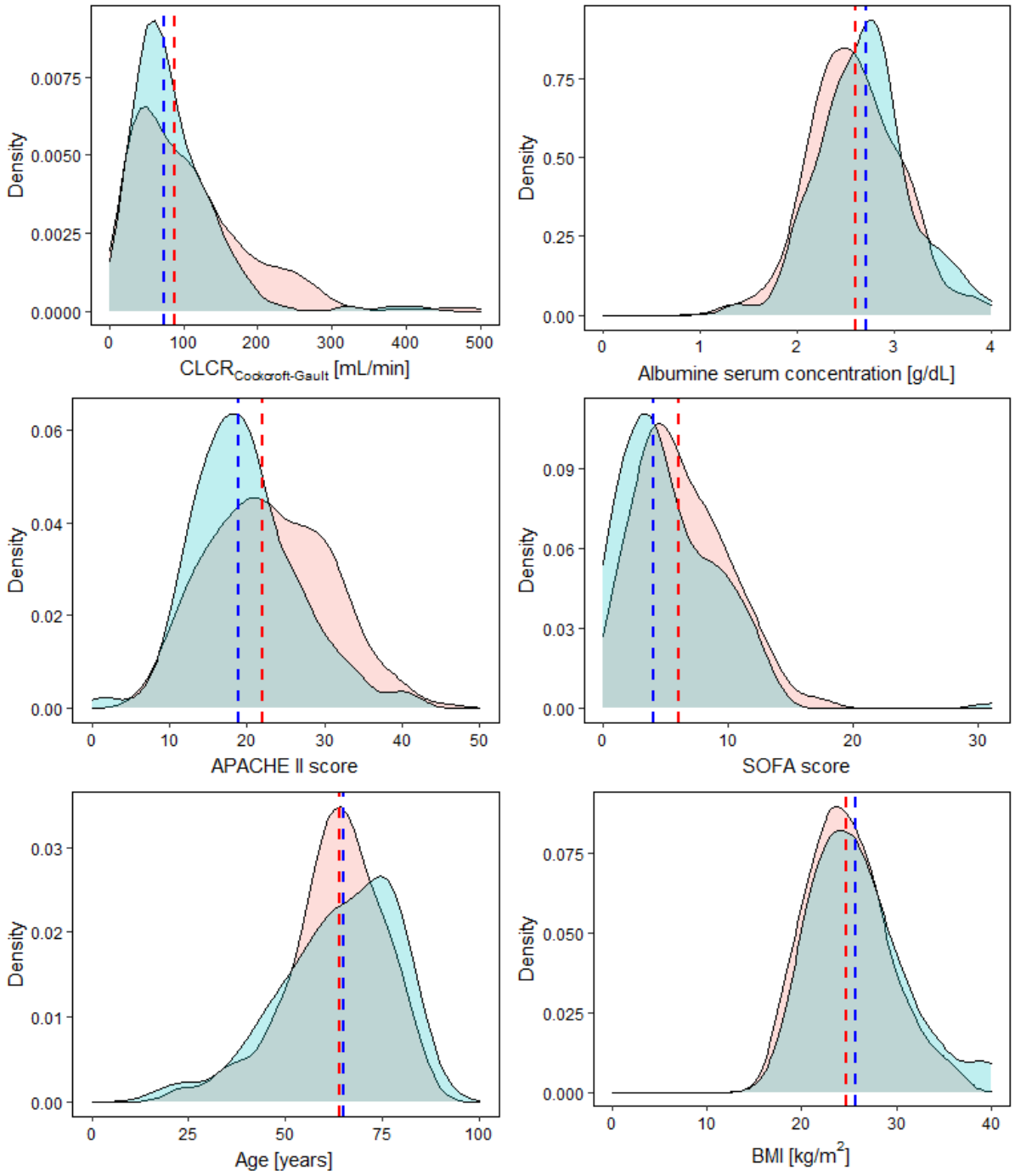

Figure S2: Density distributions for selected patient characteristics of the patients included in 'stage I' of the study separated by administered antibioitc.

Red: Patients receiving meropenem, *Blue:* Patients receiving piperacillin/tazobactam, *Shaded areas:* Density distribution, *Dotted lines:* Median of the patient characteristic in respective color.

Abbreviations: *$CLCR_{Cockroaf-Gault}$:* Creatinine clearance calculated based Cockcroft-Gault formula, *SOFA*: Sepsis-related Organ Failure Assessment, *APACHE II*: Acute Physiology And Chronic Health Evaluation II, *BMI:* Body mass index.

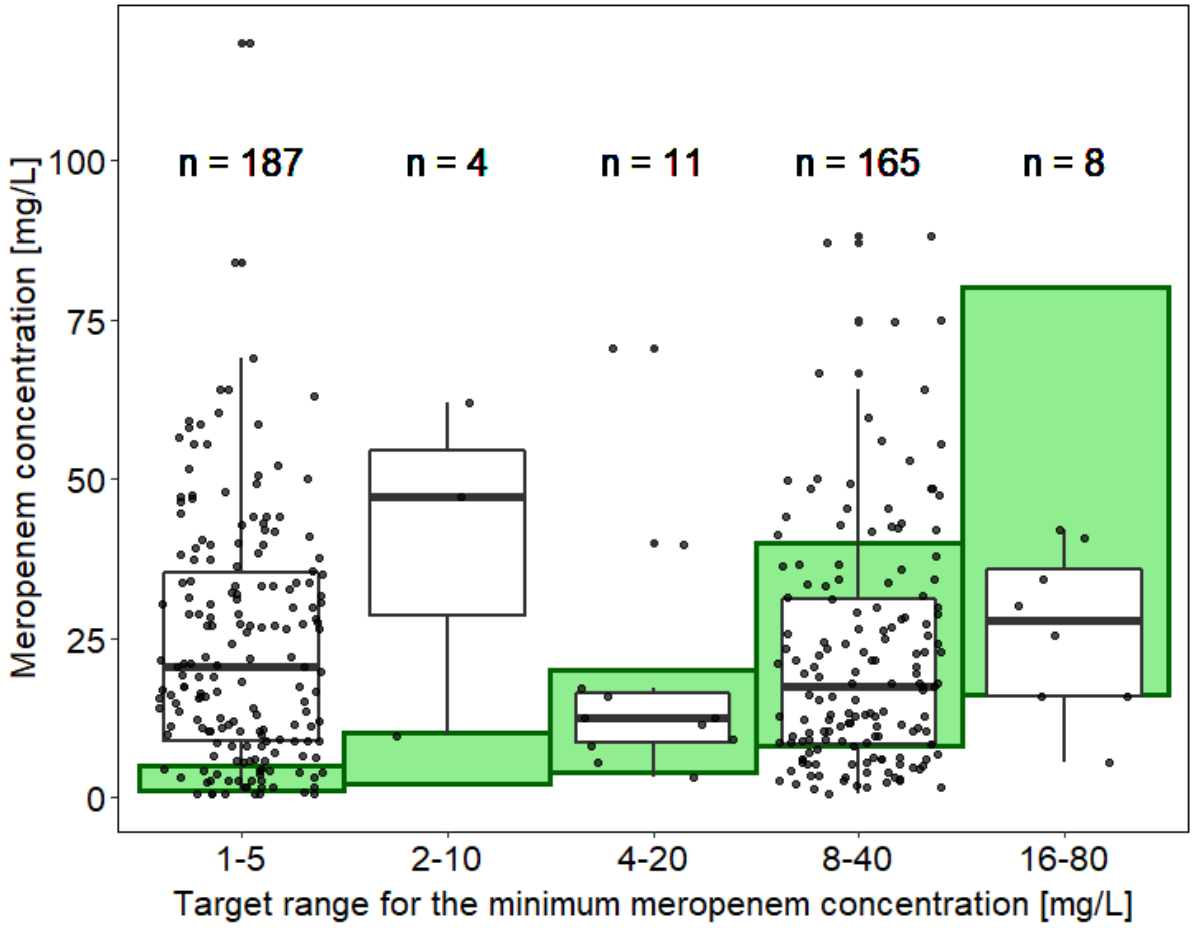

Figure S3: Boxplot of measured meropenem concentrations stratified by targeted drug concentration range.

Target range for the minimum drug concentration (C_{min}) defined as 1-5xMIC. If no MIC values could be determined an empirical target of 8-40 mg/L was used. *Points:* Measured meropenem concentrations*; Green shaded areas:* Targeted concentration range.

Abbreviations: *n*: Number, *MIC*: Minimum inhibitory concentration.

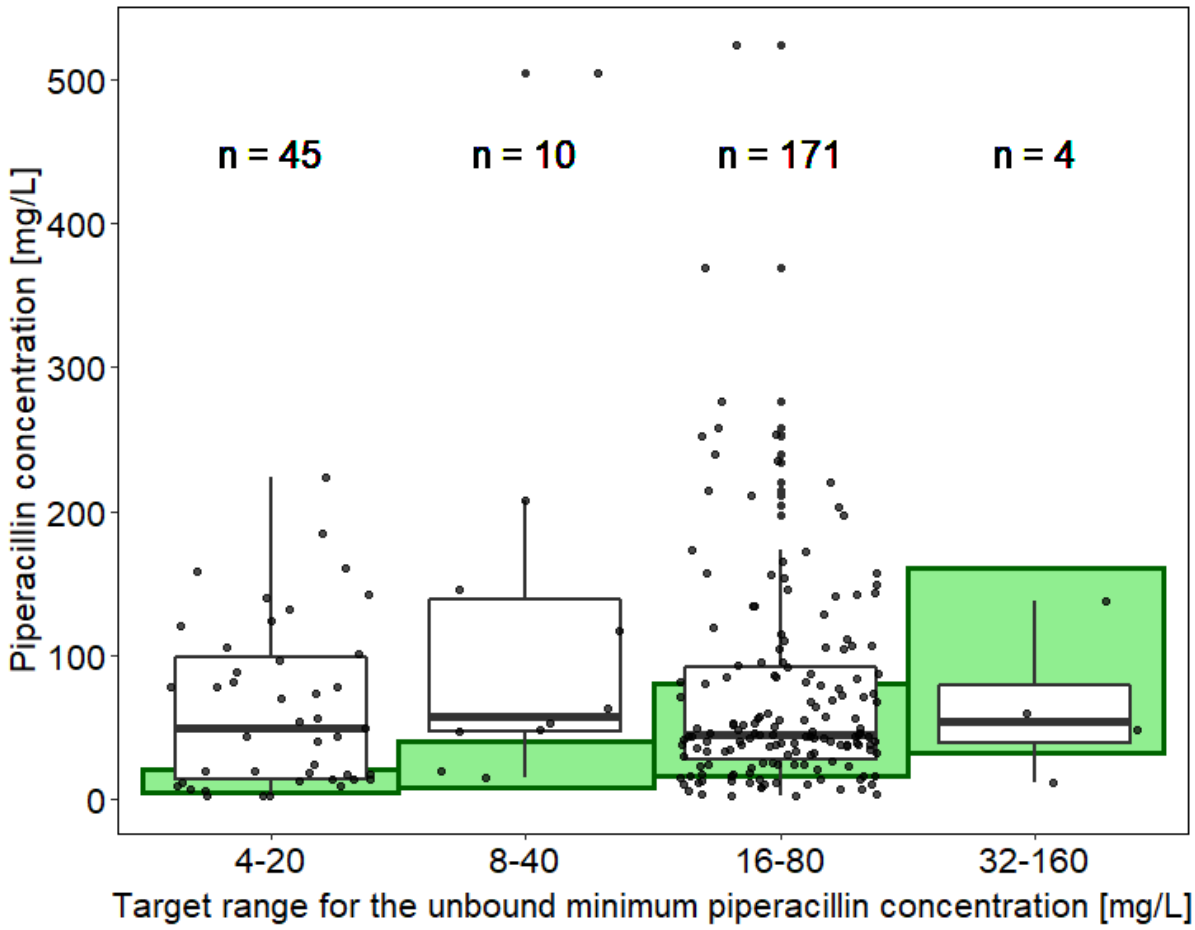

Figure S4: Boxplot of measured piperacillin concentrations stratified by targeted drug concentration range.

Target range for the minimum drug concentration (C_{min}) defined as 1-5xMIC. If no MIC values could be determined an empirical target of 16-80 mg/L was used. Unbound piperacillin concentrations were calculated based on a literature reported fraction unbound of 91% in critically ill patients [166]. *Points:* Measured piperacillin concentrations*; Green shaded areas:* Targeted concentration range.

Abbreviations: *n*: Number, *MIC*: Minimum inhibitory concentration.

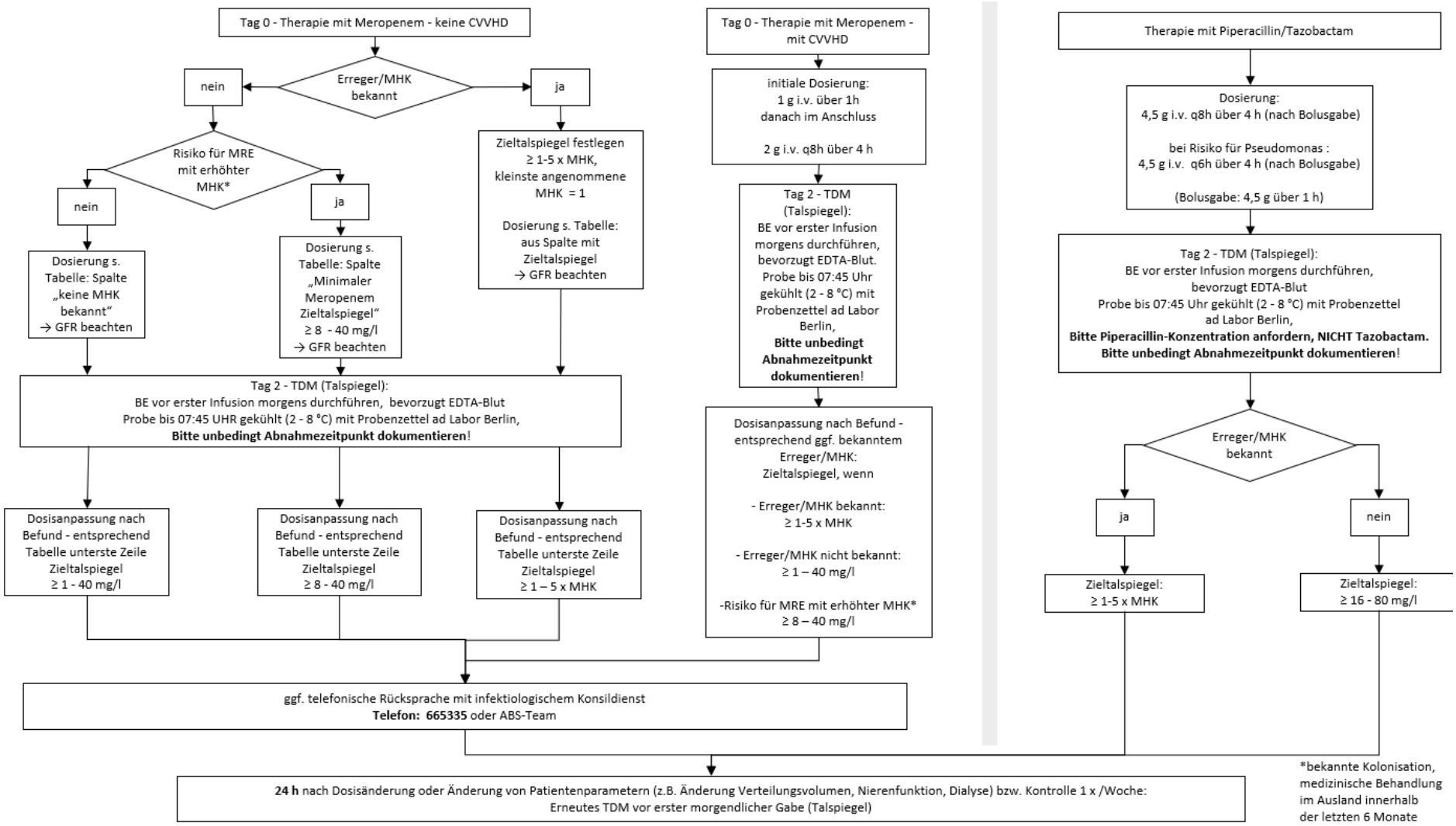

Figure S5: Simple step-by-step flowchart summarising the appropriate use of the tabular meropenem dosing tool developed for ‘stage II’ of the study.
The flowchart was provided to the healthcare professionals after detailed explanation of the tool and displayed in the participating wards.
Abbreviations: *CVVHD:* Continuous veno-venous haemodiafiltration; *MHK*: Minimale Hemmkonzentration; *MRE*: Multiresistenter Erreger; *TDM*: Therpeutisches Drug Monitoring.

Antibiotika-Proben → CCM,Toxikologie

Kühlpads bitte zurück an Station MID-144i - Zettel bitte z. Hd. Frau Kießling, Toxikologie Labor Berlin

Patienten-Aufkleber	**Abnahme-Datum, Abnahme-Uhrzeit** (bitte **genaue** Abnahmezeit eintragen)
Patienten-Aufkleber	☐ Talspiegel ☐ Spitzenspiegel ☐ Meropenem ☐ Piperacillin ☐ Dosierungstabelle angewendet ☐ angestrebter Zielspiegel: _______[mg/L] _______________ _______________ Datum Uhrzeit
Patienten-Aufkleber	☐ Talspiegel ☐ Spitzenspiegel ☐ Meropenem ☐ Piperacillin ☐ Dosierungstabelle angewendet ☐ angestrebter Zielspiegel: _______[mg/L] _______________ _______________ Datum Uhrzeit
Patienten-Aufkleber	☐ Talspiegel ☐ Spitzenspiegel ☐ Meropenem ☐ Piperacillin ☐ Dosierungstabelle angewendet ☐ angestrebter Zielspiegel: _______[mg/L] _______________ _______________ Datum Uhrzeit

Bitte beachten:

- Für die Probenentnahme **EDTA-Röhrchen** verwenden
- Nach der Probennahme können die Proben **maximal** 20 min im Kühlschrank aufbewahrt werden, spätestens dann müssen die Proben **gekühlt** in das Präsenzlabor (**CCM**). **WICHTIG: weiche KÜHLPADS** aus dem **KÜHLSCHRANK** verwenden (**nicht** aus dem Tiefkühler)
- **Talspiegel**: Bitte die Proben gesammelt **bis spätestens 7:45 Uhr verschicken**
- **Vor Verschicken der Probe bitte diesen Zettel kopieren**, Kopie in den TDM-Kasten. Danke.

Antibiotic Stewardship Charité

✉ miriam.stegemann@charite.de ☎ *665037* ✉ frieder.pfaefflin@charite.de ☎ *665287*

✉ anja.theloe@charite.de ☎ *561045*

Version 22.12.2020

Figure S6: Blood sample collection sheet used during ‘stage II’ of the study.

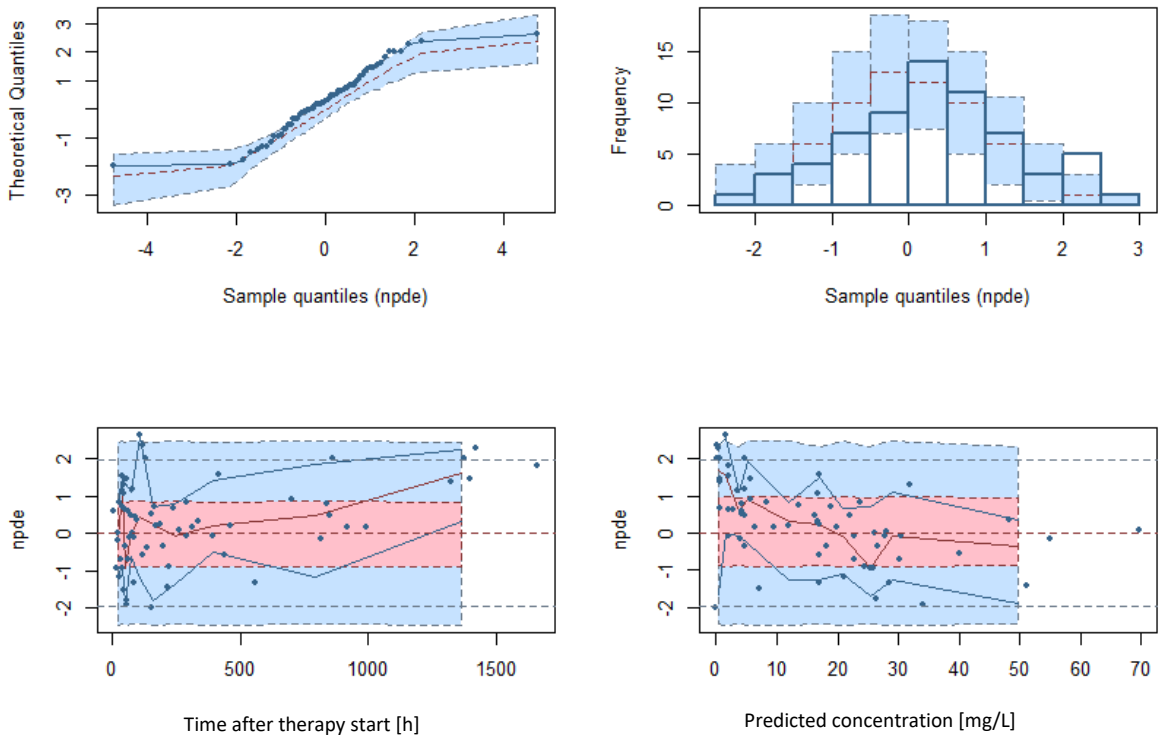

Figure S7: Graphical output of the normalized prediction distribution error (NPDE) analysis for meropenem.

Upper left: Quantile-quantile plot of NPDE versus the expected standard normal distribution. Upper right: Histogram of NPDE with the density of the standard normal distribution overlaid. Lower left: Scatterplot of NPDE versus time after therapy start. Lower right: Scatterplot of NPDE versus predicted concentration. *Pink area:* Prediction interval for the median, *Blue area:* 95% prediction interval.

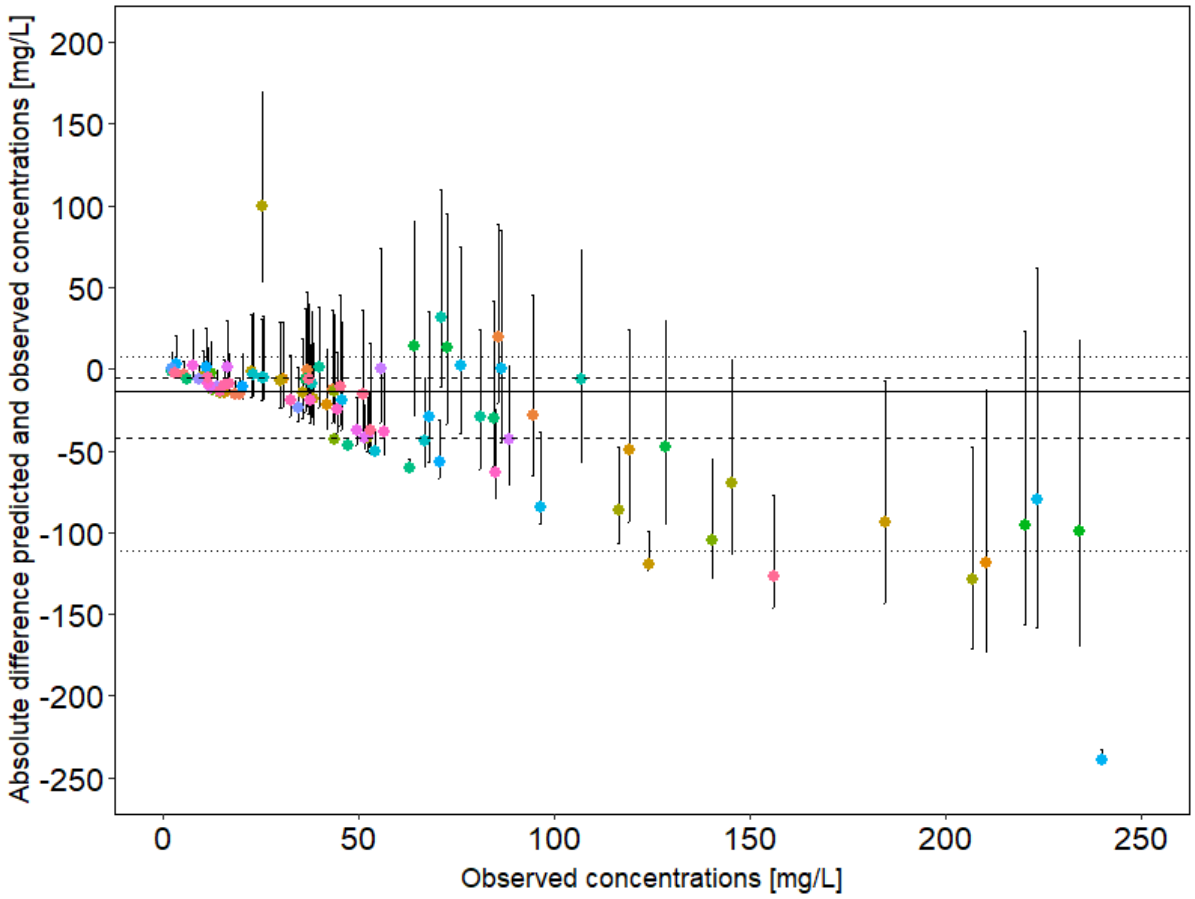

Figure S8: Absolute difference between predicted and observed concentrations (prediction error) (mg/L) plotted against observed piperacillin concentrations (n=90) when predicting concentration employing the pharmacokinetic model by Andersen et al. [178]
Points: median prediction error per observed concentration. *Colours:* individual patients (i=46). *Error bar:* 90% prediction interval of prediction error per sample. *Solid horizontal line:* median prediction error. *Dashed line:* 50% prediction interval of median prediction error. *Dotted line:* 90% prediction interval of median prediction error.

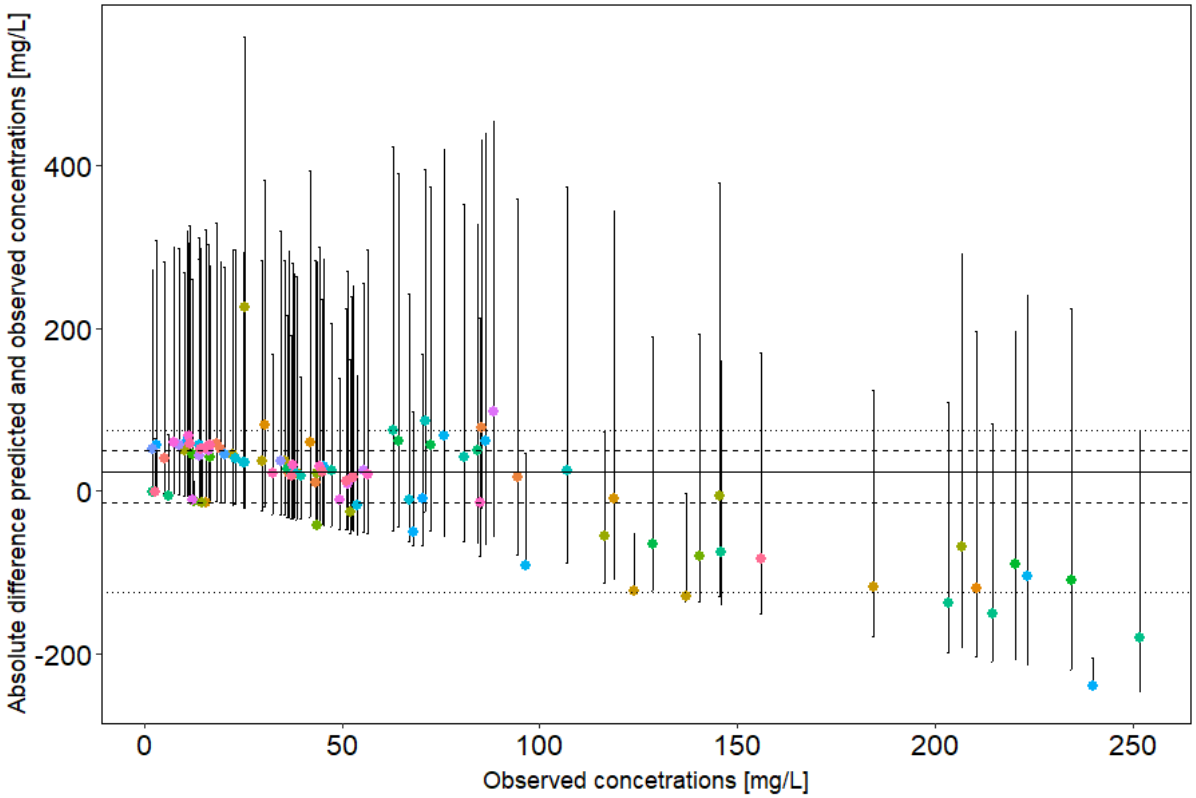

Figure S9: Absolute difference between predicted and observed concentrations (prediction error) (mg/L) plotted against observed piperacillin concentrations (n=90) when predicting concentration employing the pharmacokinetic model by Öbrink-Hansen et al. [176]
Points: median prediction error per observed concentration. *Colours:* individual patients (i=46). *Error bar:* 90% prediction interval of prediction error per sample. *Solid horizontal line:* median prediction error. *Dashed line:* 50% prediction interval of median prediction error. *Dotted line:* 90% prediction interval of median prediction error.

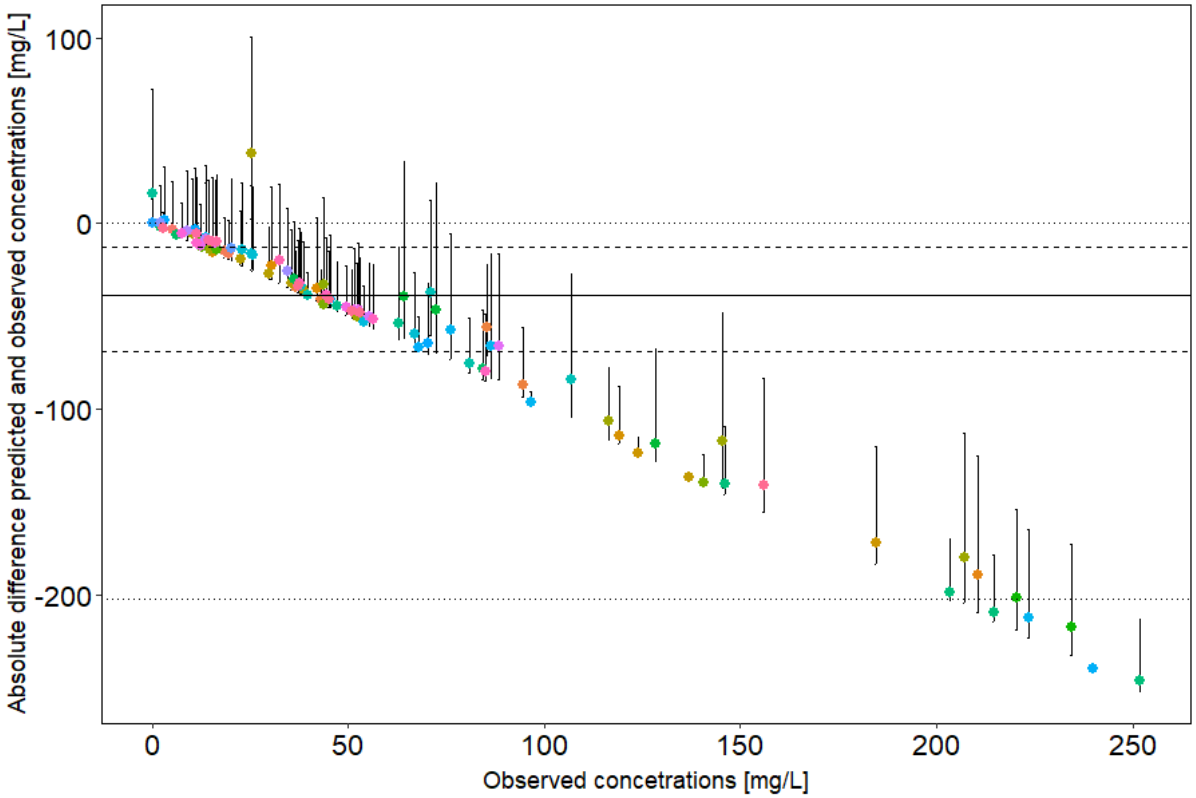

Figure S10: Absolute difference between predicted and observed concentrations (prediction error) (mg/L) plotted against observed piperacillin concentrations (n=90) when predicting concentration employing the pharmacokinetic model by Roberts et al. [175]
Points: median prediction error per observed concentration. *Colours:* individual patients (i=46). *Error bar:* 90% prediction interval of prediction error per sample. *Solid horizontal line:* median prediction error. *Dashed line:* 50% prediction interval of median prediction error. *Dotted line:* 90% prediction interval of median prediction error.

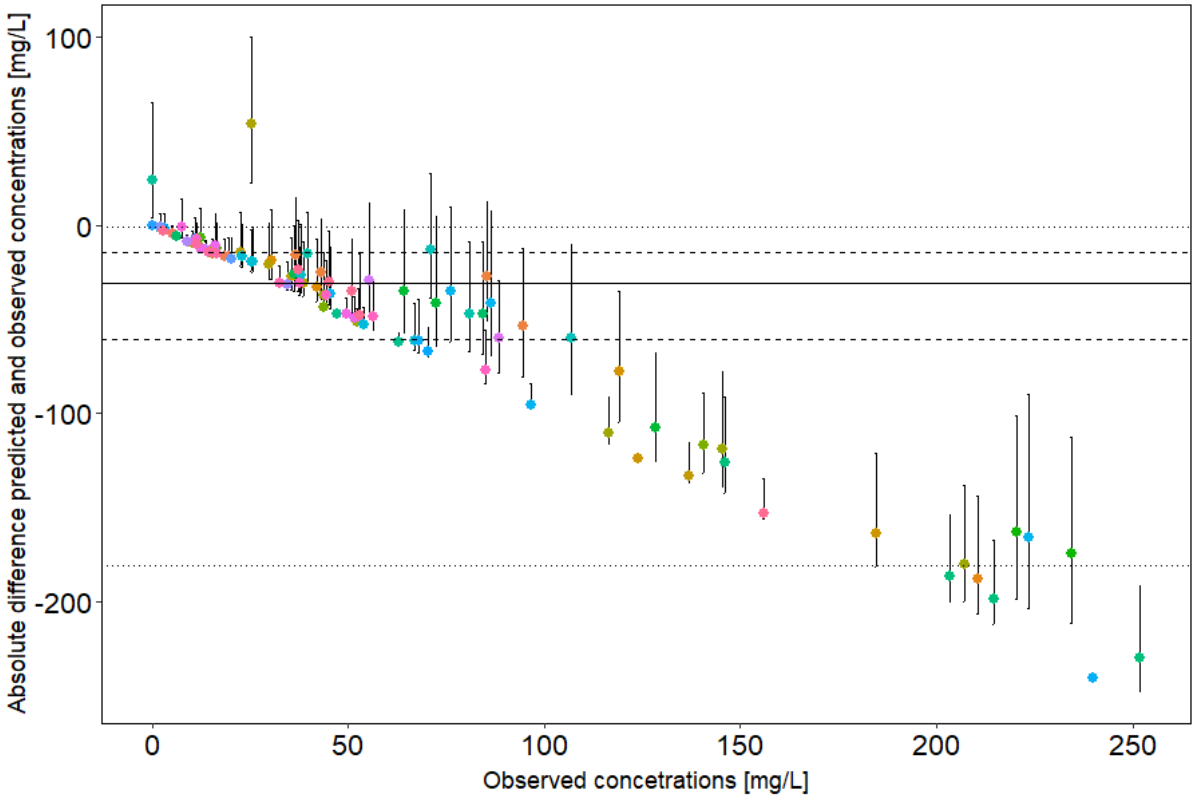

Figure S11: Absolute difference between predicted and observed concentrations (prediction error) (mg/L) plotted against observed piperacillin concentrations (n=90) when predicting concentration employing the pharmacokinetic model by Li et al. [177]
Points: median prediction error per observed concentration. *Colours:* individual patients (i=46). *Error bar:* 90% prediction interval of prediction error per sample. *Solid horizontal line:* median prediction error. *Dashed line:* 50% prediction interval of median prediction error. *Dotted line:* 90% prediction interval of median prediction error.

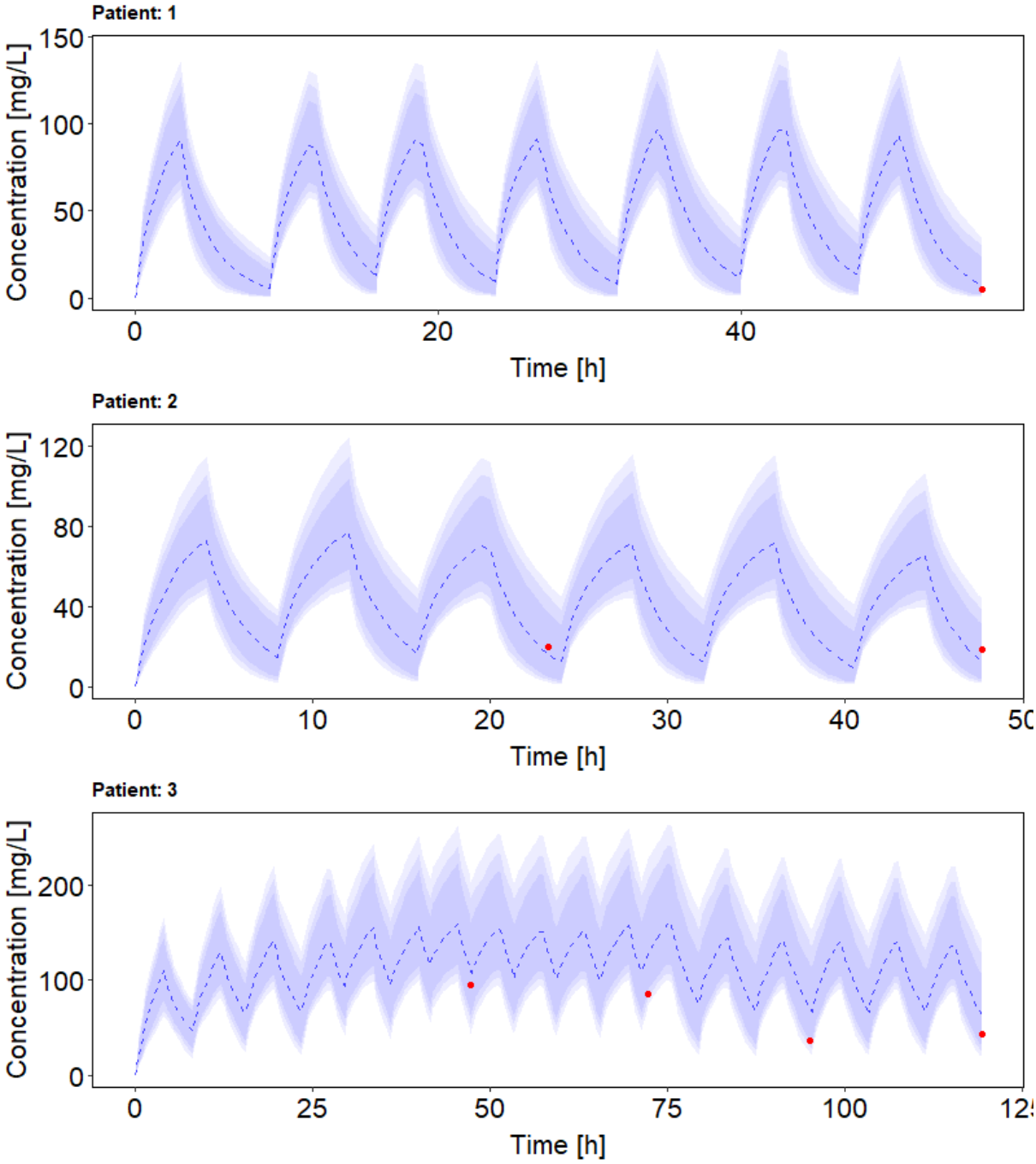

Figure S12: Model-predicted piperacillin concentration-time profiles employing the piperacillin pharmacokinetic model by Sukarnjanaset et al. [50] and observerd piperacillin concentrations. Blue dashed line: median piperacillin prediction; Blue shaded areas: 90%, 95% and 99% prediciton intervall; Red points: observerd piperacillin concentrations.

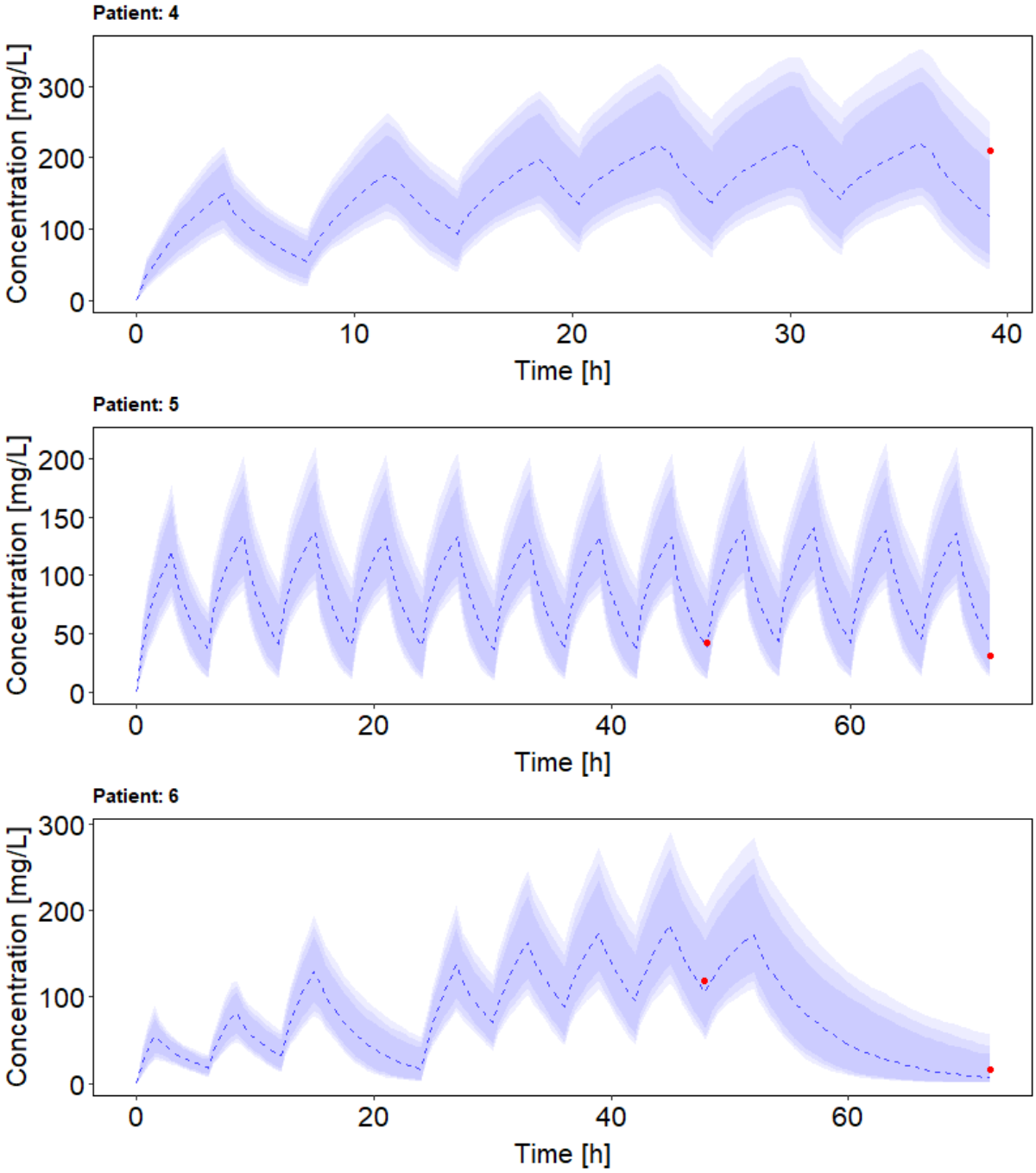

Figure S12 (continued): Model-predicted piperacillin concentration-time profiles employing the piperacillin pharmacokinetic model by Sukarnjanaset et al. [50] and observerd piperacillin concentrations.

Blue dashed line: median piperacillin prediction; Blue shaded areas: 90%, 95% and 99% prediciton intervall; Red points: observerd piperacillin concentrations.

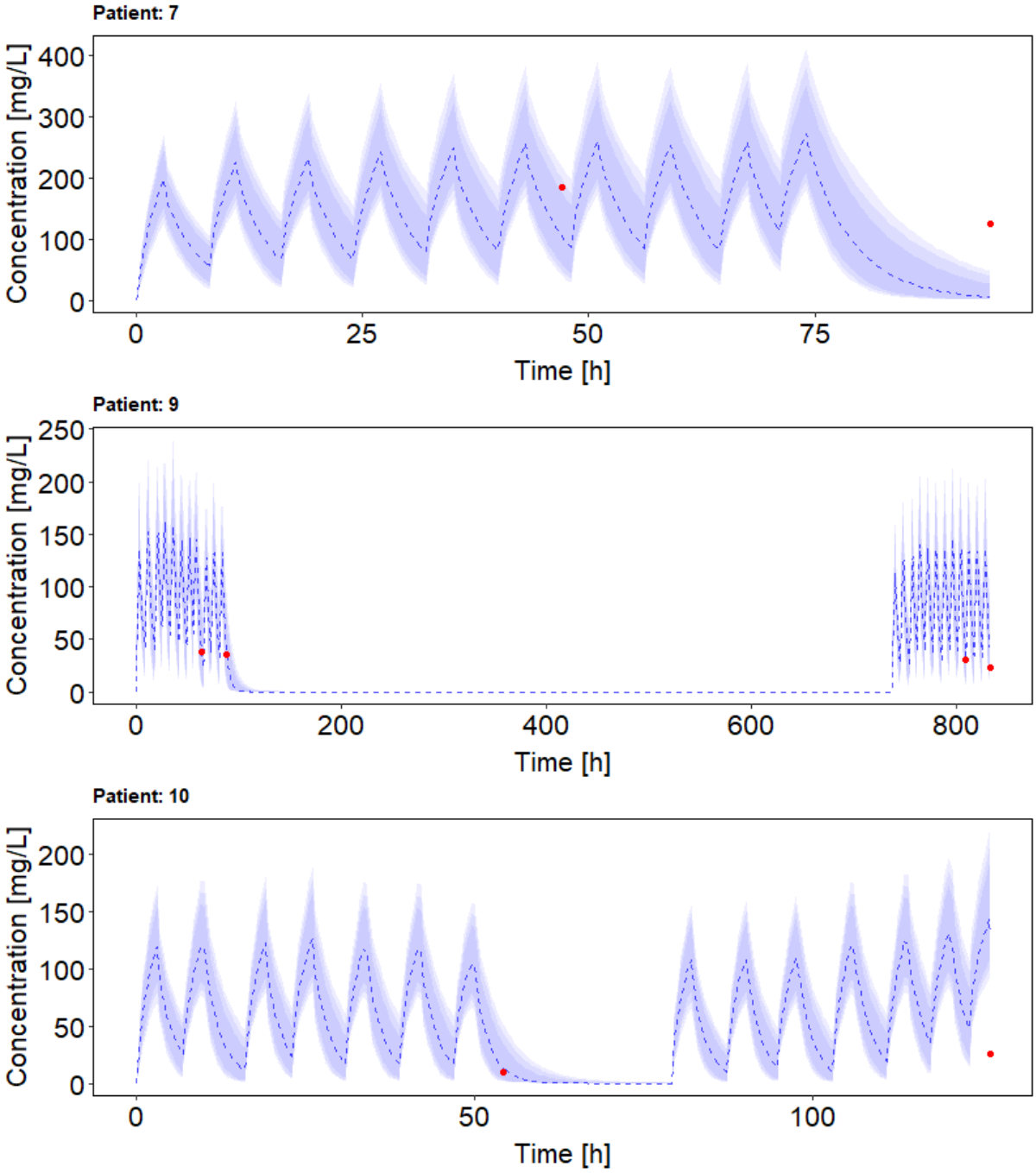

Figure S12 (continued): Model-predicted piperacillin concentration-time profiles employing the piperacillin pharmacokinetic model by Sukarnjanaset et al. [50] and observerd piperacillin concentrations.

Blue dashed line: median piperacillin prediction; Blue shaded areas: 90%, 95% and 99% prediciton intervall; Red points: observerd piperacillin concentrations.

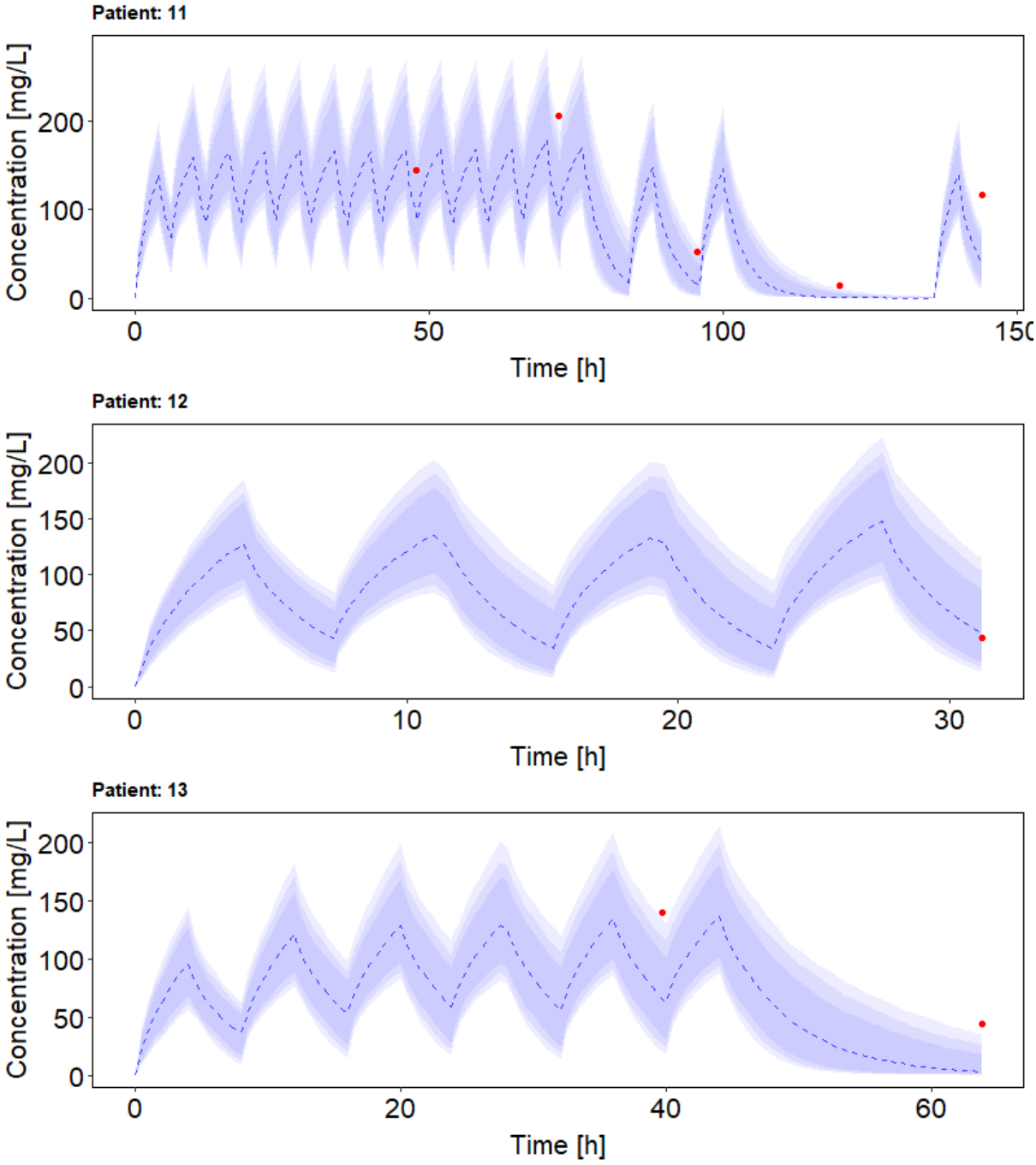

Figure S12 (continued): Model-predicted piperacillin concentration-time profiles employing the piperacillin pharmacokinetic model by Sukarnjanaset et al. [50] and observerd piperacillin concentrations.

Blue dashed line: median piperacillin prediction; Blue shaded areas: 90%, 95% and 99% prediciton intervall; Red points: observerd piperacillin concentrations.

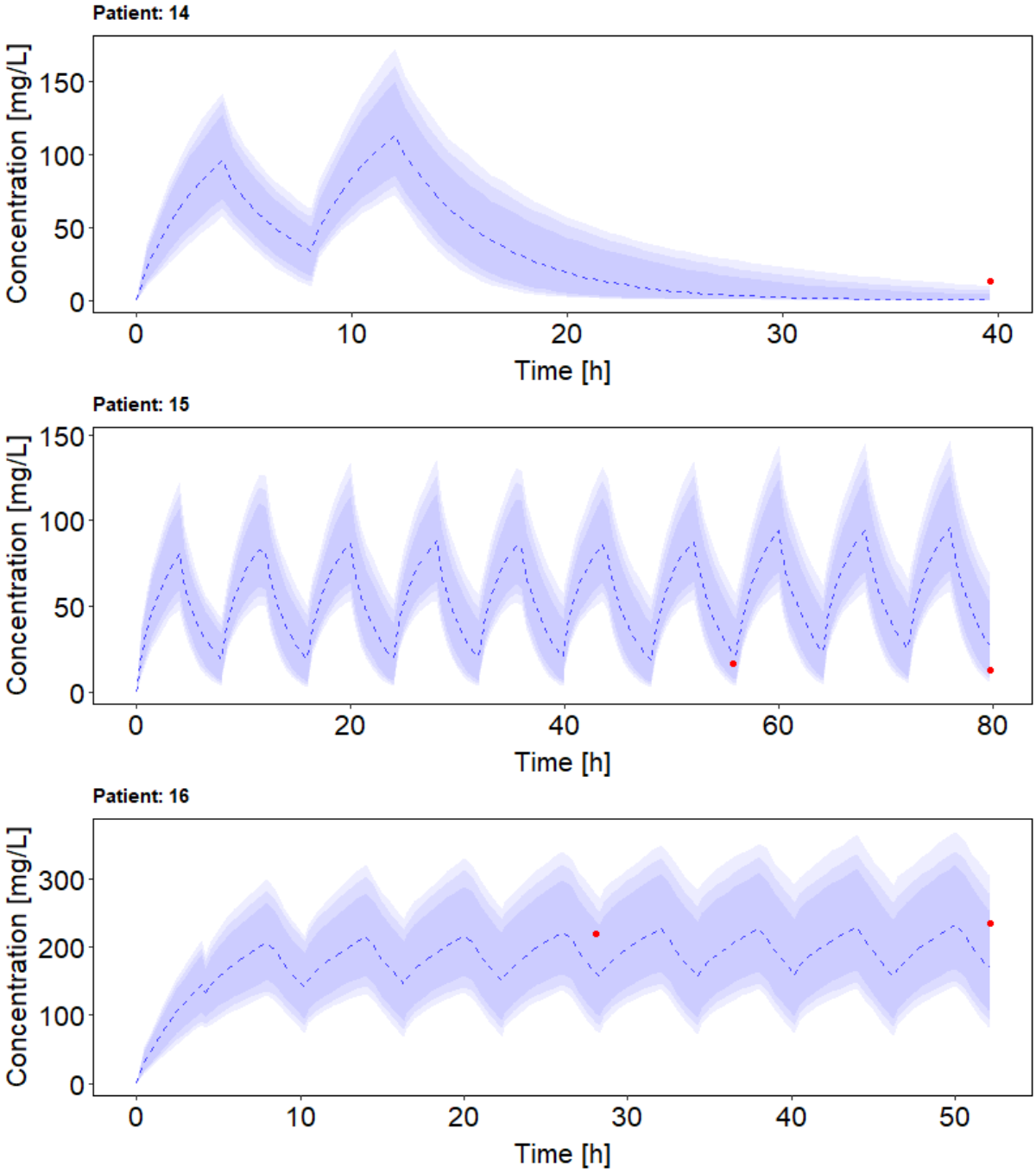

Figure S12 (continued): Model-predicted piperacillin concentration-time profiles employing the piperacillin pharmacokinetic model by Sukarnjanaset et al. [50] and observerd piperacillin concentrations.

Blue dashed line: median piperacillin prediction; Blue shaded areas: 90%, 95% and 99% prediciton intervall; Red points: observerd piperacillin concentrations.

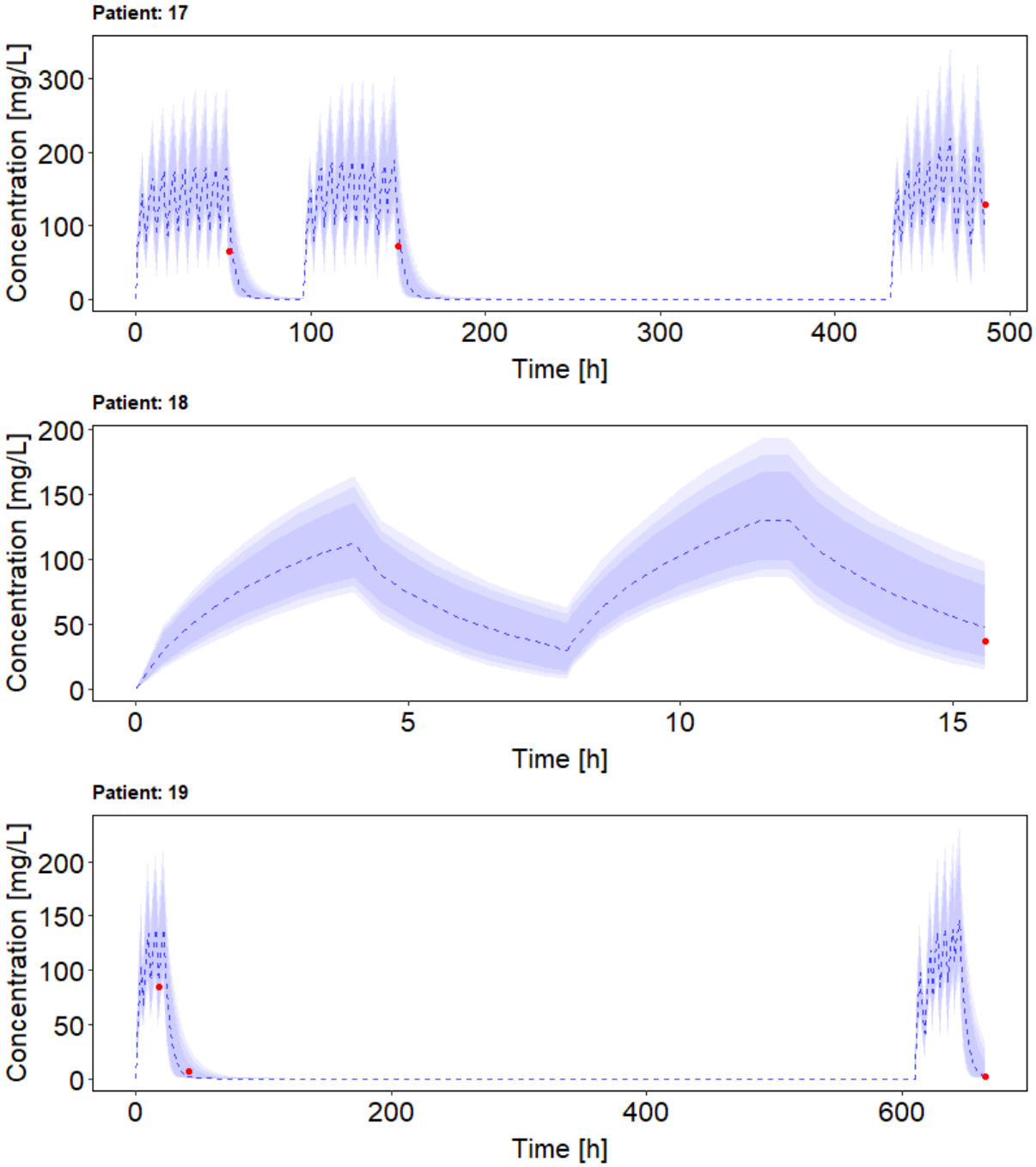

Figure S12 (continued): Model-predicted piperacillin concentration-time profiles employing the piperacillin pharmacokinetic model by Sukarnjanaset et al. [50] and observerd piperacillin concentrations.

Blue dashed line: median piperacillin prediction; Blue shaded areas: 90%, 95% and 99% prediciton intervall; Red points: observerd piperacillin concentrations.

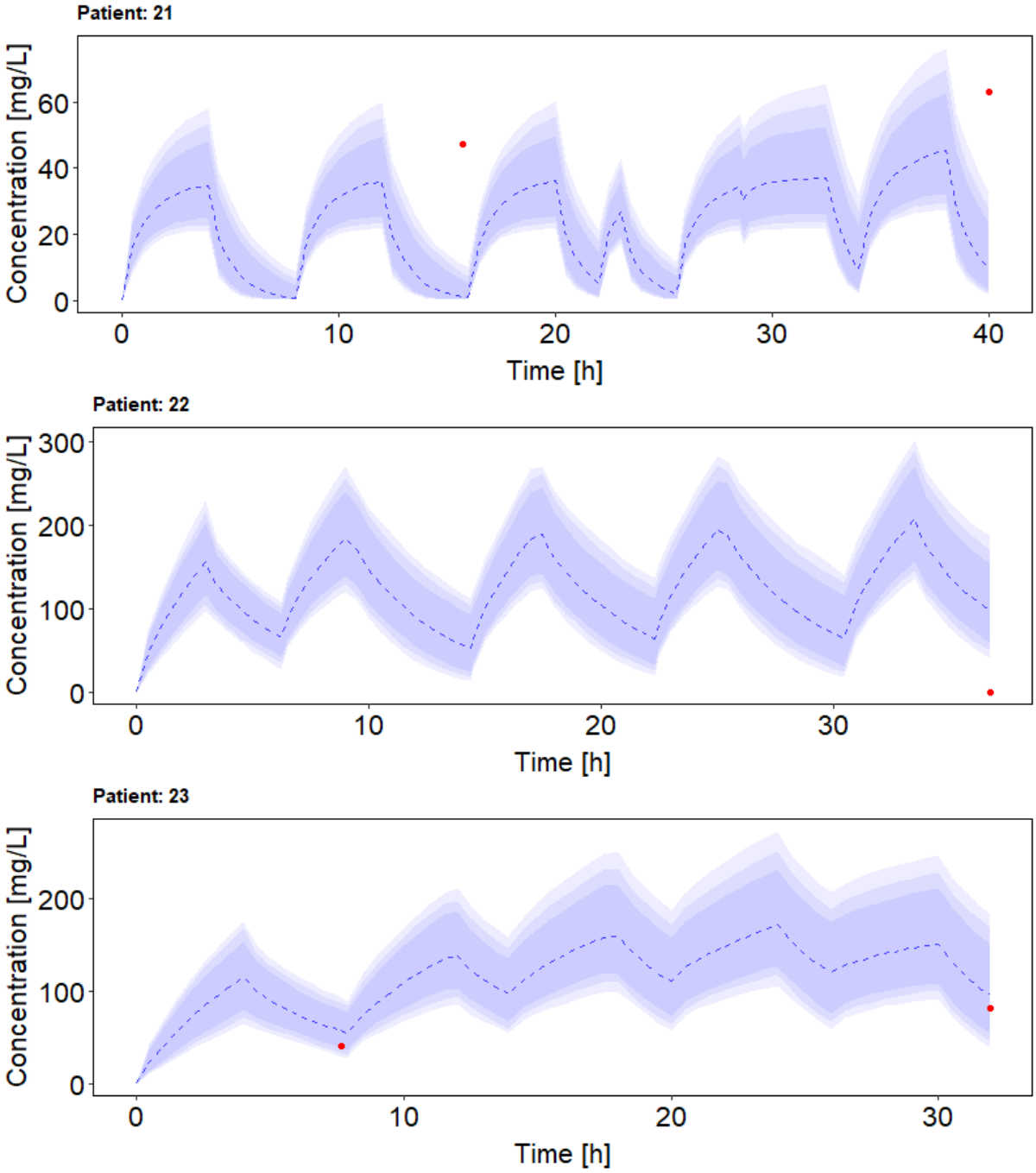

Figure S12 (continued): Model-predicted piperacillin concentration-time profiles employing the piperacillin pharmacokinetic model by Sukarnjanaset et al. [50] and observerd piperacillin concentrations.

Blue dashed line: median piperacillin prediction; Blue shaded areas: 90%, 95% and 99% prediciton intervall; Red points: observerd piperacillin concentration.

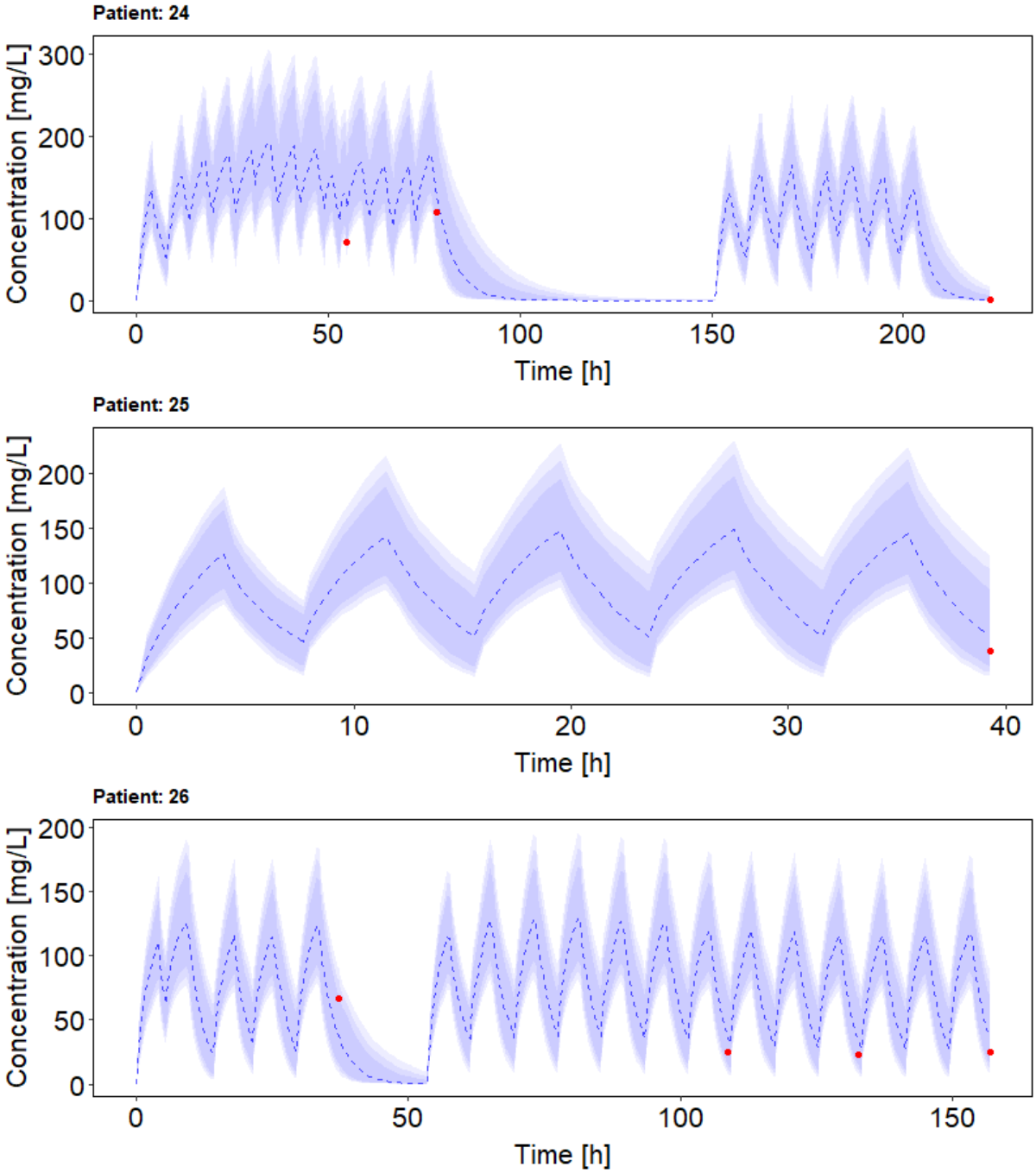

Figure S12 (continued): Model-predicted piperacillin concentration-time profiles employing the piperacillin pharmacokinetic model by Sukarnjanaset et al. [50] and observerd piperacillin concentrations.

Blue dashed line: median piperacillin prediction; Blue shaded areas: 90%, 95% and 99% prediciton intervall; Red points: observerd piperacillin concentration.

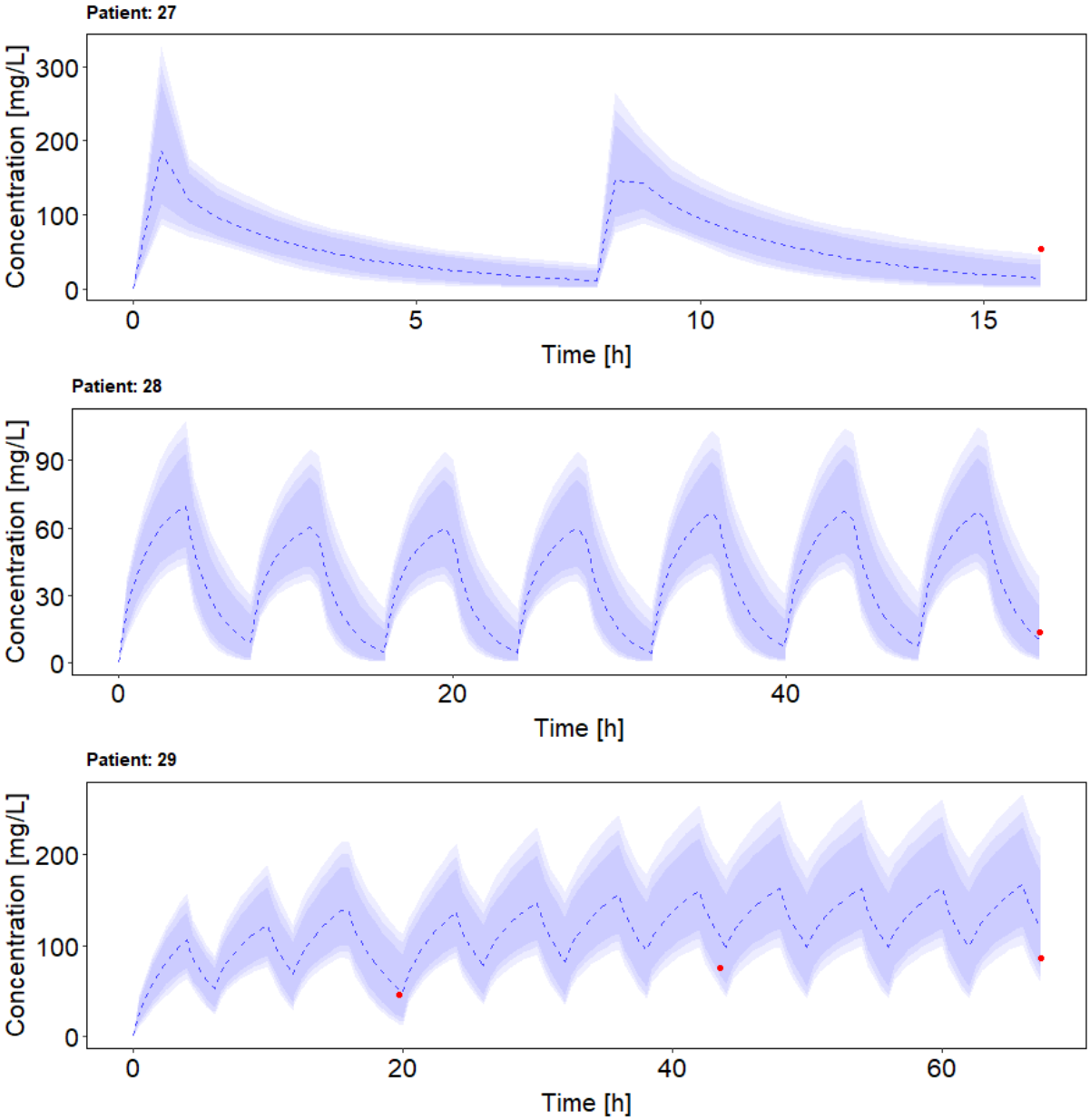

Figure S12 (continued): Model-predicted piperacillin concentration-time profiles employing the piperacillin pharmacokinetic model by Sukarnjanaset et al. [50] and observerd piperacillin concentrations.

Blue dashed line: median piperacillin prediction; Blue shaded areas: 90%, 95% and 99% prediciton intervall; Red points: observerd piperacillin concentration.

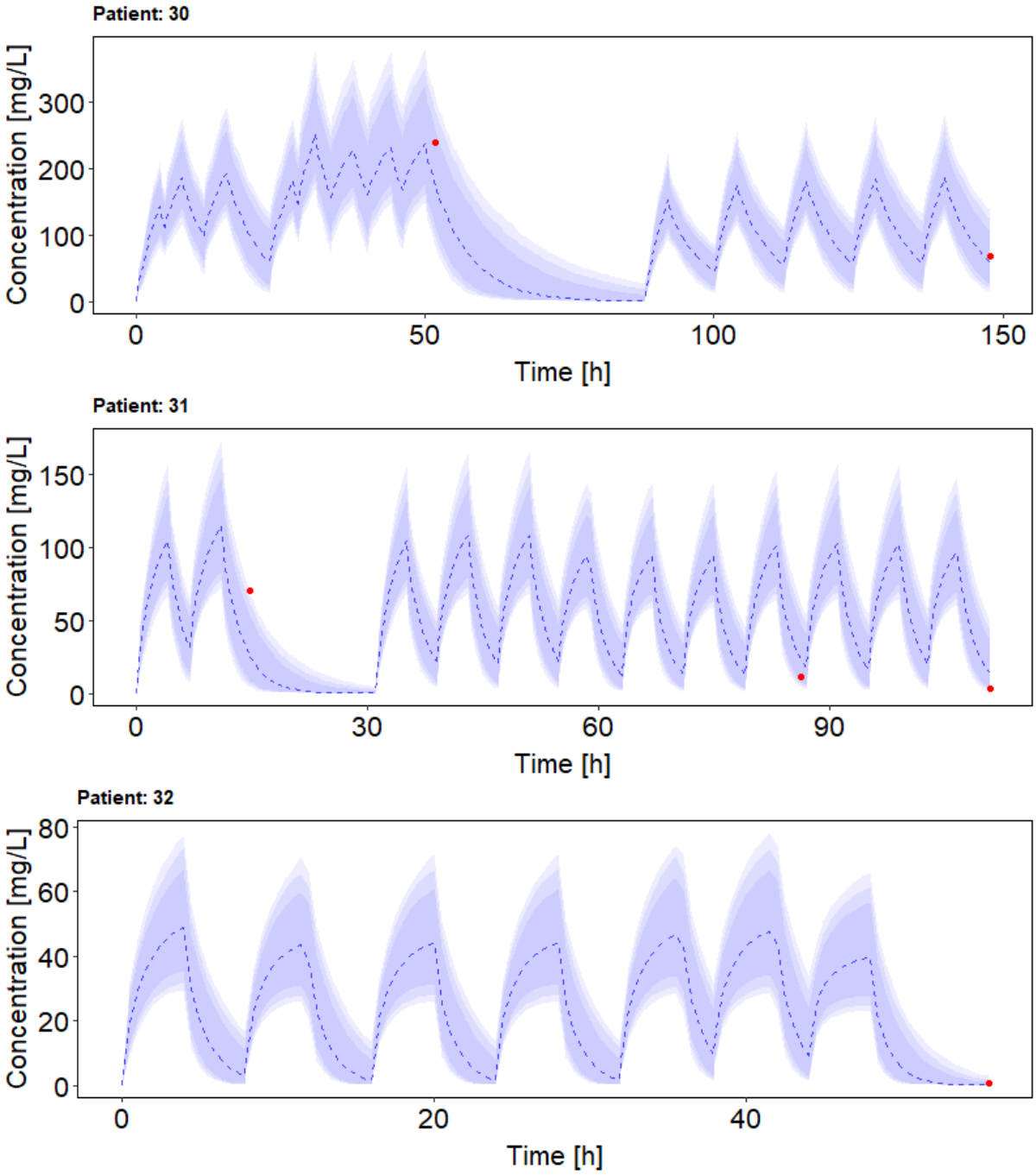

Figure S12 (continued): Model-predicted piperacillin concentration-time profiles employing the piperacillin pharmacokinetic model by Sukarnjanaset et al. [50] and observerd piperacillin concentrations.

Blue dashed line: median piperacillin prediction; Blue shaded areas: 90%, 95% and 99% prediciton intervall; Red points: observerd piperacillin concentration.

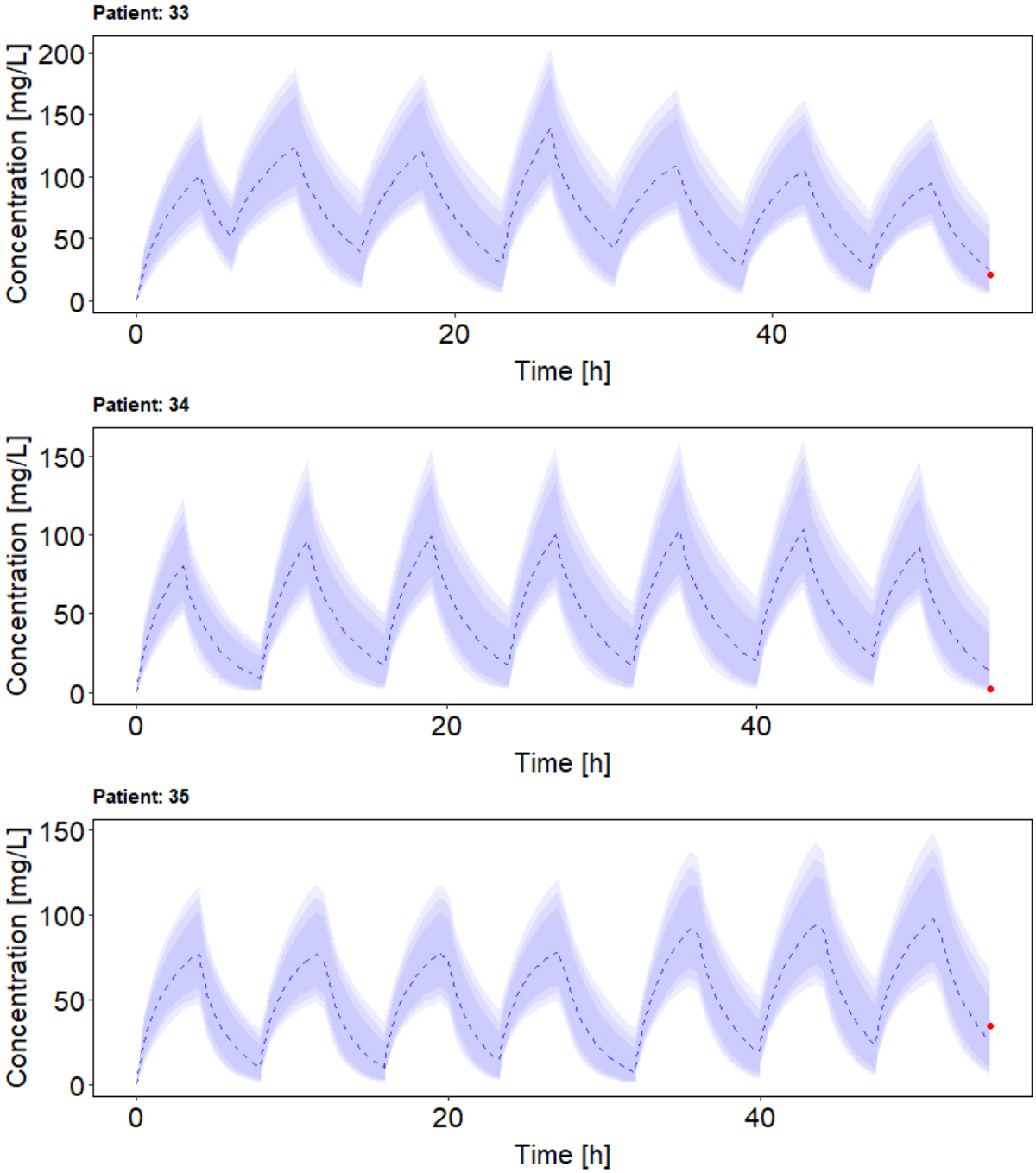

Figure S12 (continued): Model-predicted piperacillin concentration-time profiles employing the piperacillin pharmacokinetic model by Sukarnjanaset et al. [50] and observerd piperacillin concentrations.

Blue dashed line: median piperacillin prediction; Blue shaded areas: 90%, 95% and 99% prediciton intervall; Red points: observerd piperacillin concentration.

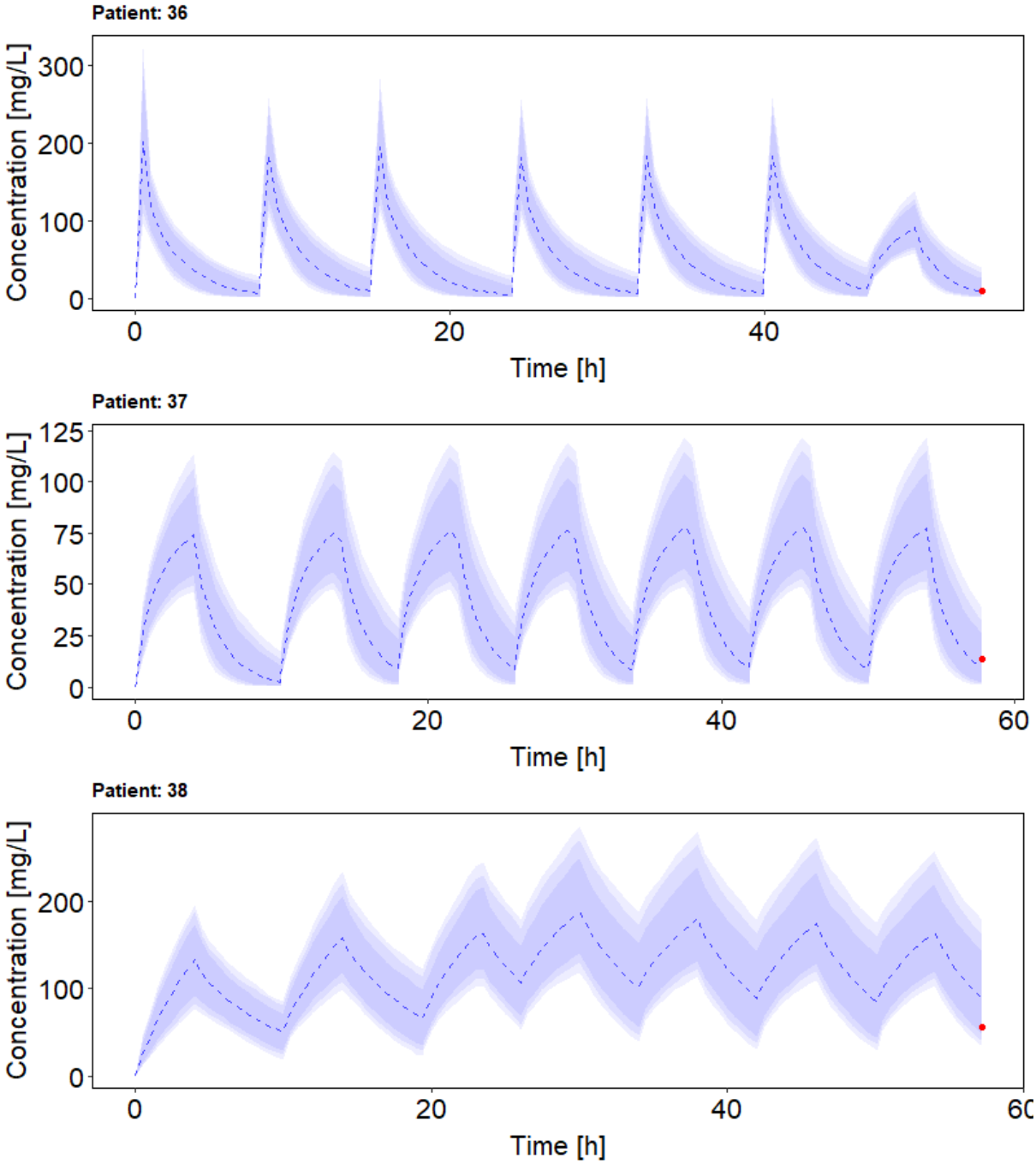

Figure S12 (continued): Model-predicted piperacillin concentration-time profiles employing the piperacillin pharmacokinetic model by Sukarnjanaset et al. [50] and observerd piperacillin concentrations.

Blue dashed line: median piperacillin prediction; Blue shaded areas: 90%, 95% and 99% prediciton intervall; Red points: observerd piperacillin concentration.

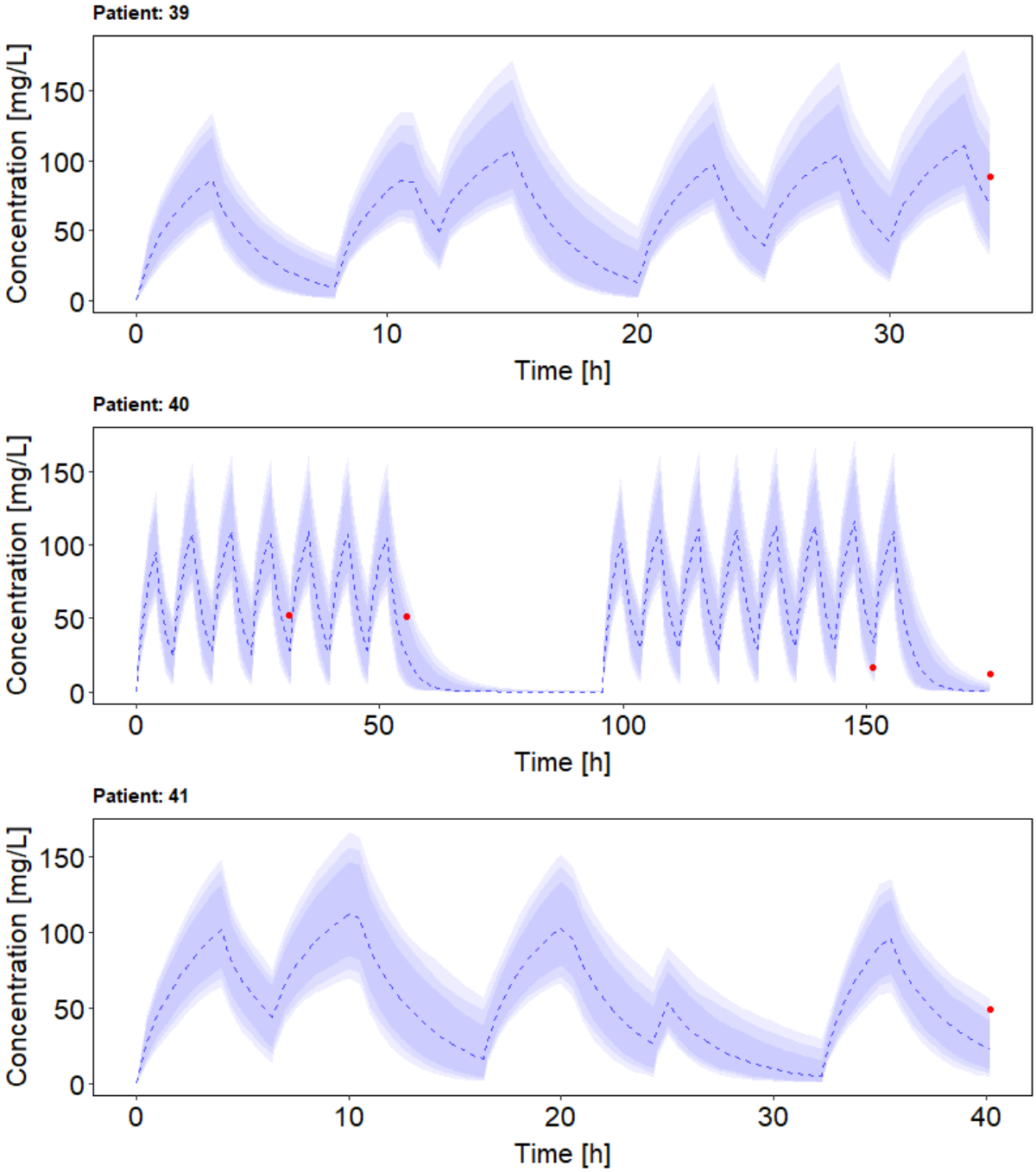

Figure S12 (continued): Model-predicted piperacillin concentration-time profiles employing the piperacillin pharmacokinetic model by Sukarnjanaset et al. [50] and observerd piperacillin concentrations.

Blue dashed line: median piperacillin prediction; Blue shaded areas: 90%, 95% and 99% prediciton intervall; Red points: observerd piperacillin concentration.

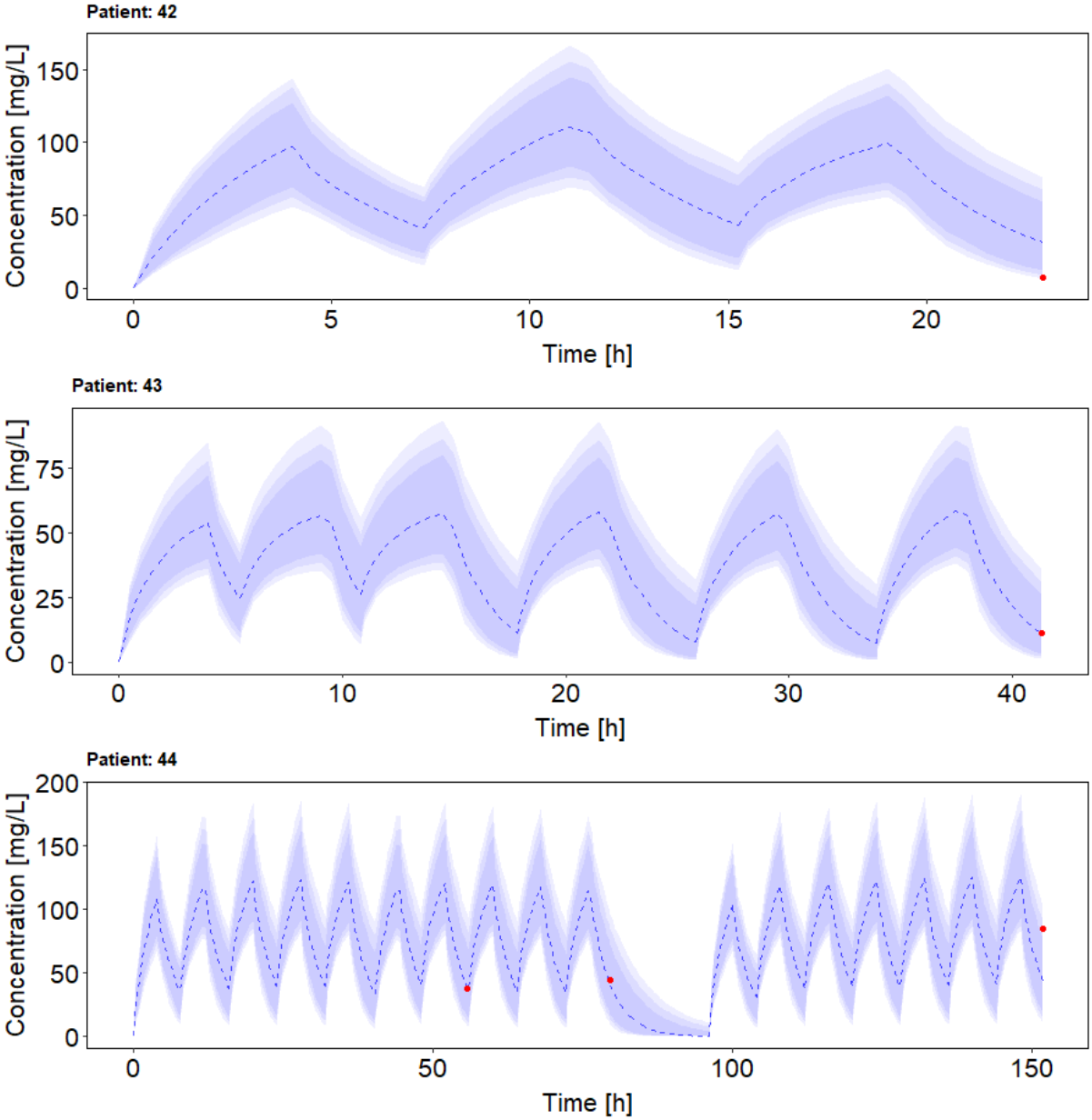

Figure S12 (continued): Model-predicted piperacillin concentration-time profiles employing the piperacillin pharmacokinetic model by Sukarnjanaset et al. [50] and observerd piperacillin concentrations.

Blue dashed line: median piperacillin prediction; Blue shaded areas: 90%, 95% and 99% prediciton intervall; Red points: observerd piperacillin concentration.

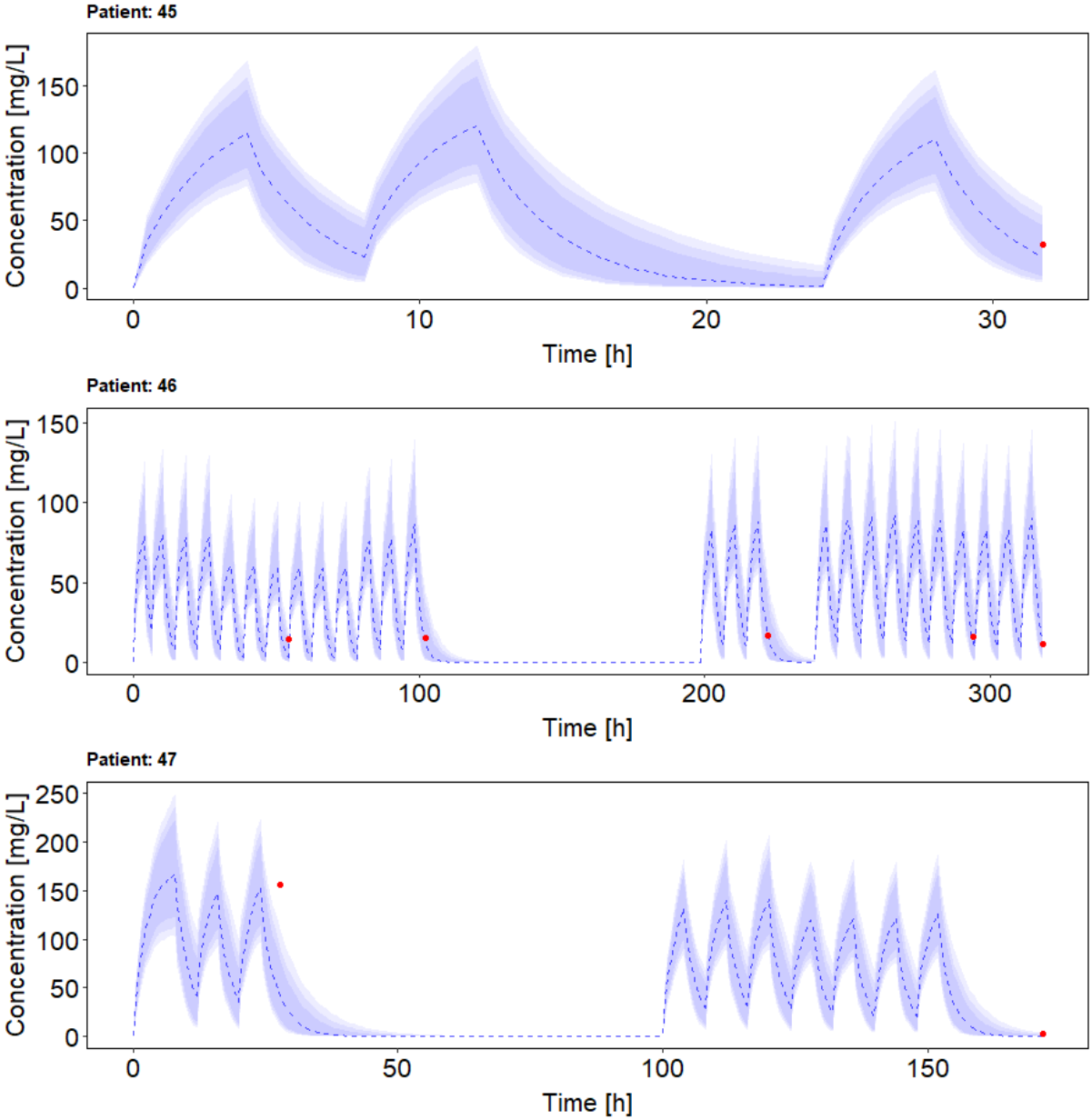

Figure S12 (continued): Model-predicted piperacillin concentration-time profiles employing the piperacillin pharmacokinetic model by Sukarnjanaset et al. [50] and observerd piperacillin concentrations.

Blue dashed line: median piperacillin prediction; Blue shaded areas: 90%, 95% and 99% prediciton intervall; Red points: observerd piperacillin concentration.

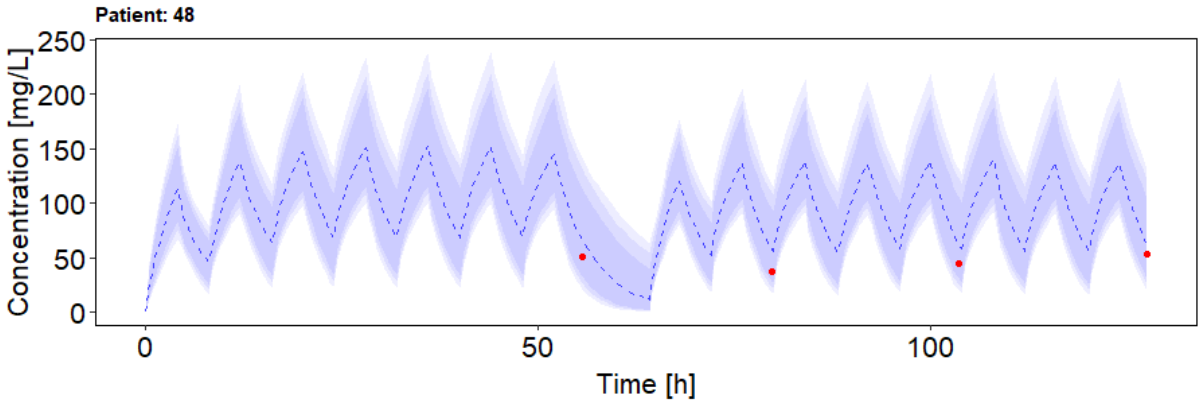

Figure S12 (continued): Model-predicted piperacillin concentration-time profiles employing the piperacillin pharmacokinetic model by Sukarnjanaset et al. [50] and observerd piperacillin concentrations.

Blue dashed line: median piperacillin prediction; Blue shaded areas: 90%, 95% and 99% prediciton intervall; Red points: observerd piperacillin concentration.

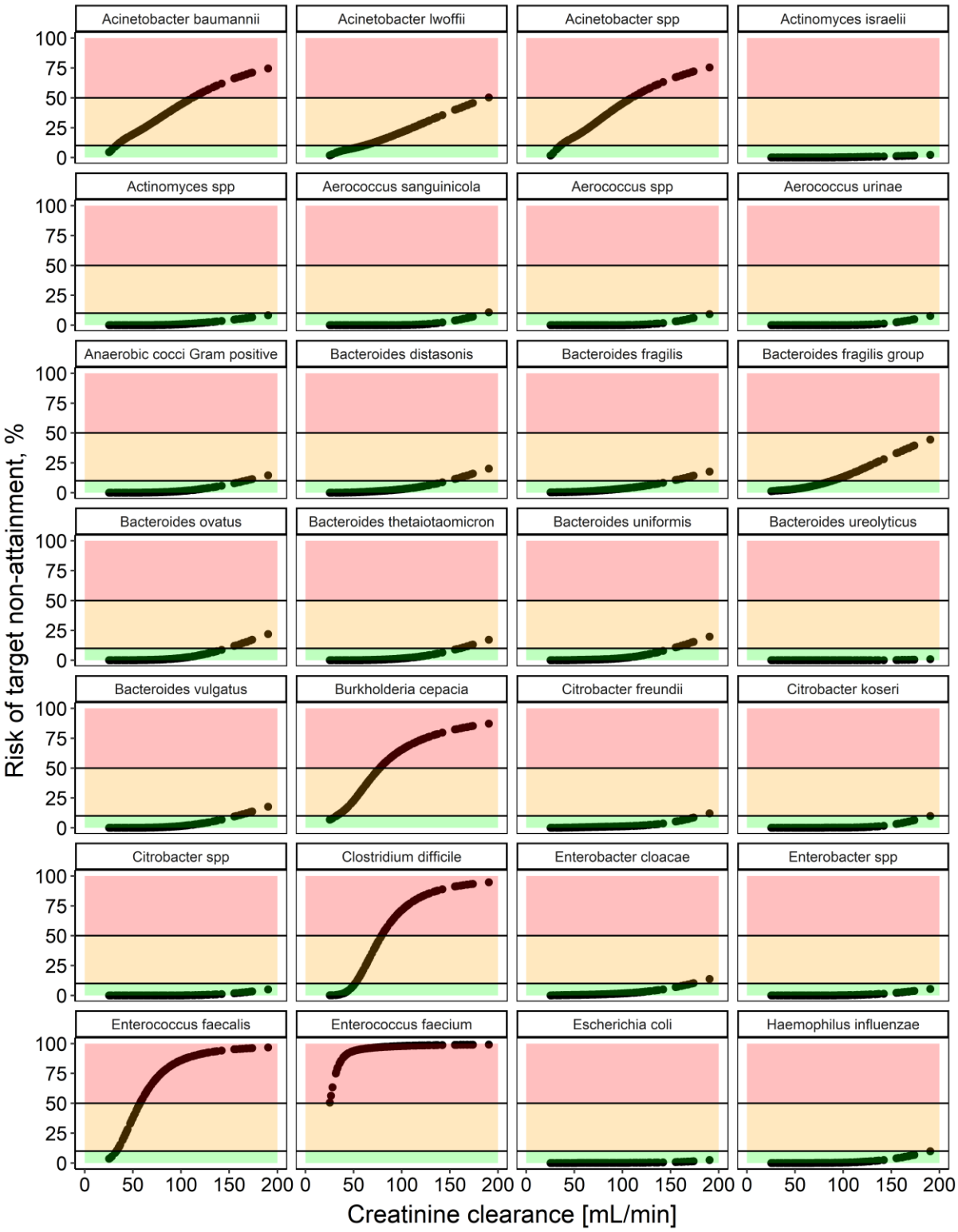

Figure S13: MeroRisk Calculator predicted risk of target non-attainment for critically ill patents (n = 155) and alphabetically ordered pathogens from *Acinetobacter baumannii* to *Haemophilus infuenzae* (modified from [173]).

The risk of target non-attainment (unbound drug concentration being above the minimum inhibitory concentration (MIC) for 100% of the time) was assessed using EUCAST MIC distributions of the investigated pathogens and cumulative fraction of response analysis. Risk predictions for patients with creatinine clearance calculated using Cockcroft-Gault equation ($CLCR_{CG}$) $\geq$ 50 mL/min (points) and for patients with $CLCR_{CG}$ < 50 mL/min (x). Risk predictions $\leq$10% (green), >10% to $\leq$ 50% (orange) and >50% (red).

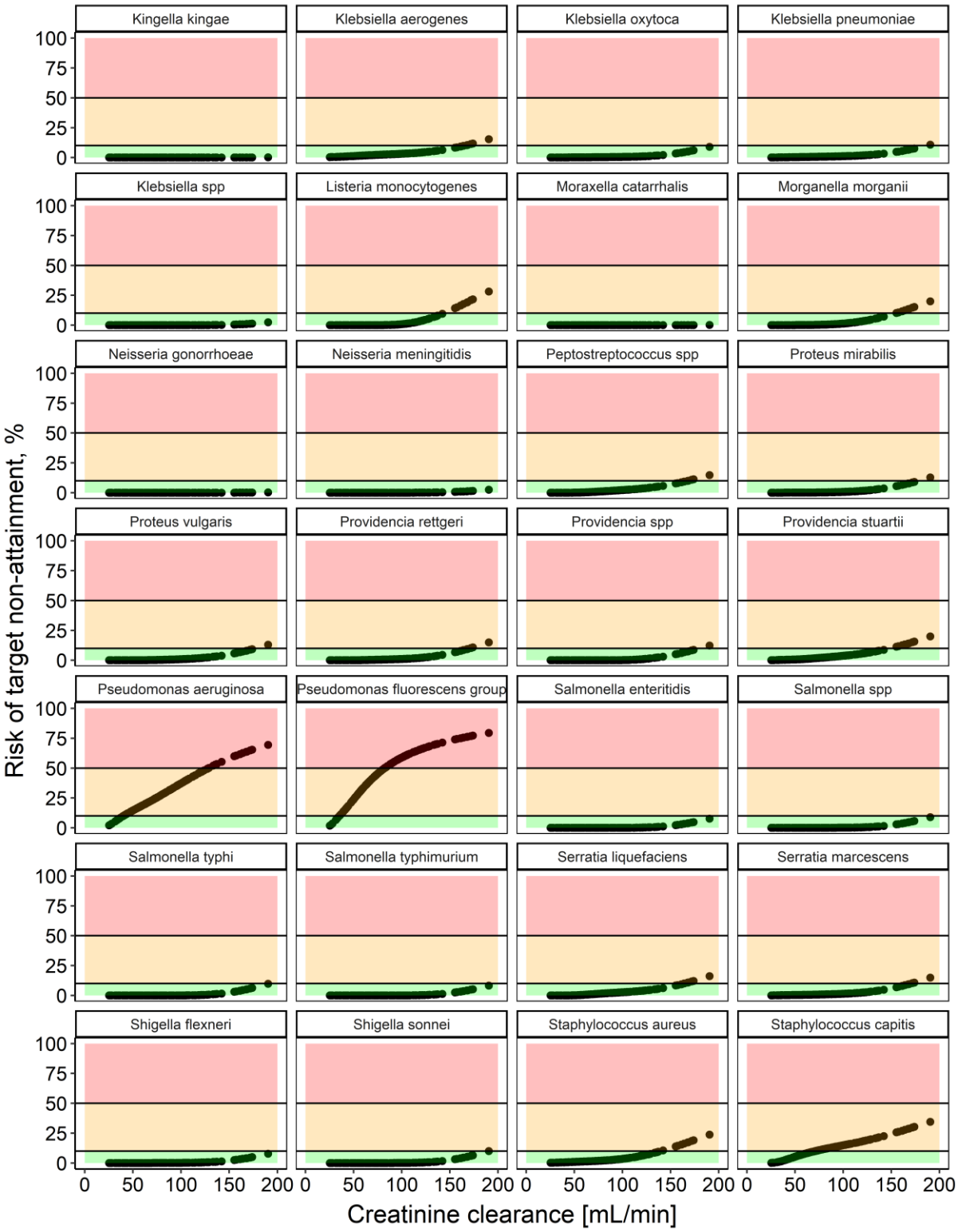

Figure S13 (continued): MeroRisk Calculator predicted risk of target non-attainment for critically ill patents (n = 155) and alphabetically ordered pathogens from *Kingella kingae* to *Staphylococcus capitis* (modified from [173]).

The risk of target non-attainment (unbound drug concentration being above the minimum inhibitory concentration (MIC) for 100% of the time) was assessed using EUCAST MIC distributions of the investigated pathogens and cumulative fraction of response analysis. Risk predictions for patients with creatinine clearance calculated using Cockcroft-Gault equation ($CLCR_{CG}$) $\geq$ 50 mL/min (points) and for patients with $CLCR_{CG}$ < 50 mL/min (x). Risk predictions $\leq$10% (green), >10% to $\leq$ 50% (orange) and >50% (red).

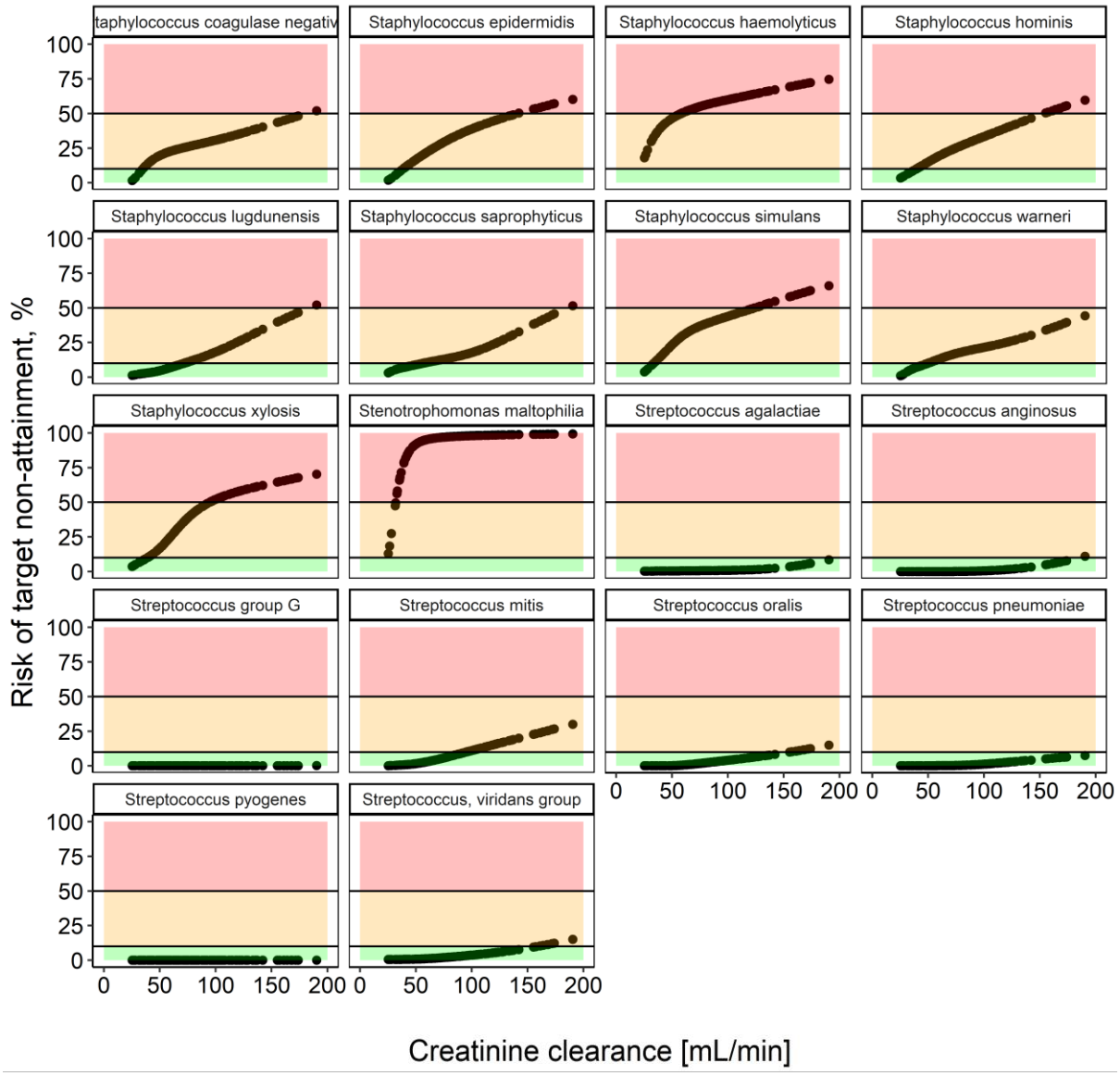

Figure S13 (continued): MeroRisk Calculator predicted risk of target non-attainment for critically ill patents (n = 155) and alphabetically ordered pathogens from *Staphylococcus coagulase negative* to *Streptococcus, viridans group* (modified from [173]).

The risk of target non-attainment (unbound drug concentration being above the minimum inhibitory concentration (MIC) for 100% of the time) was assessed using EUCAST MIC distributions of the investigated pathogens and cumulative fraction of response analysis. Risk predictions for patients with creatinine clearance calculated using Cockcroft-Gault equation ($CLCR_{CG}$) $\geq$ 50 mL/min (points) and for patients with $CLCR_{CG}$ < 50 mL/min (x). Risk predictions $\leq$10% (green), >10% to $\leq$ 50% (orange) and >50% (red).

5.3 Supplementary formulae

5.3.1 General statistics

General statistical measures used to characterise the central tendency and the dispersion of distributions are summarised in Table S14 and Table S15, respectively.

Table S14: Statistical measures describing the tendency of a distribution.

Mean		$\bar{x} = \frac{\sum_{i=1}^{n} x_i}{n}$	(Eq.5.1)
Median	If n is odd:	$\tilde{x} = x_{\frac{n+1}{2}}$	(Eq.5.2)
	If n is even:	$\tilde{x} = 0.5 * \left(x_{\frac{n}{2}} + x_{\frac{n+1}{2}}\right)$	
Geometric mean		$\bar{x}_{geom} = \sqrt[n]{\prod_{i=1}^{n} x_i}$	(Eq.5.3)

Table S15: Statistical measures describing the dispersion of a distribution.

Range		$R = x_{min} - x_{max}$	(Eq.5.4)
Percentile	If n is odd:	$P = x_{n*p}$	(Eq.5.5)
	If n is even:	$P = 0.5 * \left(x_{n*p} + x_{n*p+1}\right)$	
Variance		$\sigma^2 = \frac{1}{n-1} * \sum_{i=1}^{n} (x_i - \bar{x})^2$	(Eq.5.6)
Standard deviation		$\sigma = \sqrt{\sigma^2}$	(Eq.5.7)
Coefficient of variation		$CV, \% = \frac{\sigma}{\bar{x}} * 100$	(Eq.5.8)

Geometric standard deviation	$\sigma_{geom} = exp\left(\sqrt{\frac{1}{n} * \sum_{i=1}^{n}\left[ln\left(\frac{x_i}{\bar{x}_{geom}}\right)\right]^2}\right)$	(Eq.5.9)

5.3.2 Renal function markers

Creatinine clearance (CLCR) is a commonly used renal function marker. It can be determined in different ways. In this thesis CLCR determined by 24h urine collection and by estimation based on Cockcroft and Gault formula was used (Table S16).

Table S16: Methods used to calculate creatinine clearance.

$CLCR_{24h\text{-}urine}$	$CLCR_{UC}\left[\frac{mL}{min}\right] = \frac{C_{crea,urine}\left[\frac{mg}{dL}\right].V_{urine}[mL]}{C_{crea,serum}\left[\frac{mg}{dL}\right].\Delta t\ [min]}$	(Eq.5.10)
$CLCR_{CG}$	$CLCG_{CG} = \frac{(140 - age\ [years]) * weight\ [kg]}{72 *\ C_{crea,serum}\left[\frac{mg}{dL}\right]}$	(Eq.5.11)

Abbreviations: *$CLCR_{24h\text{-}urine}$*: Creatinine clearance calculated based on 24 h urine collection, *$CLCR_{CG}$*: Creatinine clearance calculated based on Cockcroft-Gault formula.

Publications

Original articles

- **F. Weinelt,** M. Stegemann, A. Theloe, F. Pfäfflin, S. Achterberg, F. Weber, L. Dübel, A. Mikolajewska, A. Uhrig, P. Kiesling, W. Husinga, R. Michelet, S. Hennig, C. Kloft
  Evaluation of a meropenem and piperacillin monitoring program in intensive care unit patients calls for the regular assessment of empirical targets and easy-to-use dosing decision tools.
  Antibiotics 11(6), 758 (2022)
- C. Scharf; **F. Weinelt;** I. Schroeder; M. Paal; M. Weigand; M. Zoller; M. Irlbeck; C. Kloft; J. Briegel; U. Liebchen
  Does the cytokine adsorber CytoSorb® reduce vancomycin exposure in critically ill patients with sepsis or septic shock? A prospective observational study
  Annals of Intenisve Care (2022)
- U. Liebchen, M. Klose, M. Paal, M. Vogeser, M. Zoller, I. Schroeder, L. Schmitt, W. Huisinga, R. Michelet, J. Zander, C. Scharf, **F. Weinelt***, C. Kloft*
  Evaluation of the MeroRisk Calculator, a user-friendly tool to predict the risk of meropenem target non-attainment in critically ill patients
  Antibiotics 10:468 (2021).
  *shared senior authorship
- U. Liebchen, C. Scharf, M. Zoller, **F. Weinelt***, C. Kloft*
  No clinically relevant removal of meropenem by cytokine adsorber CytoSorb® in critically ill patients with sepsis or septic shock
  Intensive Care Medicine 47, 1332–1333 (2021)
  *shared senior authorship
- M. Paal, C. Scharf, A. Denninger, L. Ilia, C. Kloft, N. Kneidinger, U. Liebchen, S. Michel, C. Schneider, S. Schröpf, C. Schuster, M. Vogeser, **F. Weinelt**, J. Zander, M. Zoller, I. Schroeder
  Target site pharmacokinetics of meropenem: Measurement in human explanted lung tissue by bronchoalveolar lavage, microdialysis, and homogenized lung tissue
  J. Antimicrob. Chemother. 65: 12 (2021).
- U. Liebchen[#], **F. Weinelt**[#], C. Scharf, I. Schroeder, M. Paal, M. Zoller, C. Kloft, J. Jung*, R. Michelet*
  Combination of pharmacokinetic and pathogen susceptibility information to optimize meropenem treatment of gram-negative infections in critically ill patients
  Antimicrobial Agents and Chemotherapy (2021)
  [#]shared first authorship, *shared senior authorship

- Mueller-Schoell, R. Michelet, **F. Weinelt**, C. Kloft, G. Mikus G
  CYP2D6 phenotype explains reported yohimbine concentrations in four severe acute intoxications.
  Archives of Toxicology (2021)
- **F. Weinelt**, M. Stegemann, A. Theloe, F. Pfäfflin, S. Achterberg, L. Schmitt, W. Husinga, R. Michelet, S. Hennig, C. Kloft
  Development of a model-informed dosing tool to optimise initial antibiotic dosing - a translational example for intensive care units.
  Pharmaceutics 13(12), 2128 (2021)

Oral presentations

- How to develop and implement interactive dosing software for intensive care unit patients? A case study in model-informed precision dosing
  10th PharMetrX Symposium, 18 May 2021

Conference abstracts

- **F. Weinelt**[#], F. Weber[#], M. Klose, M. Stegemann, A. Theloe, F. Pfäfflin, S. Achterberg, W. Huisinga, S. Wicha, R. Michelet, S. Hennig, C. Kloft
  Optimising meropenem dosing in the intensive care unit with a model-informed precision dosing tool: The TIAS study
  Annual Meeting of the Deutsche Pharmazeutische Gesellschaft (DPhG), Marburg, Germany, 13-16 September 2022
  [#]shared first authorship
- L. Schatz, G. Hempel, **F. Weinelt**, U. Liebchen
  Systematic evaluation of meropenem pharmacokinetic models for Bayesian forecasting in critically ill patients undergoing continuous renal replacement therapy
  Quantitative Systems Pharmacology Conference, Leiden, Netherlands, 20-22 April 2022
- R. Michelet, **F. Weinelt**, M. Klose, A. Mueller-Schoell, F. Kluwe, C. Montefusco-Pereira, M. Van Dyk, M. Vay, W. Huisinga, C. Kloft, G. Mikus
  Using microdose-based activity measurement to individualise dosing of cytochrome P450 metabolised drugs: a case study with yohimbine and tamoxifen
  29th Population Approach Group Europe (PAGE), Online, 2-3 and 6-7 September 2021.
- U. Liebchen, I. Schroeder, M. Paal, M. Zoller, M. Irlbeck, **F. Weinelt**, C. Kloft, J. Briegel, C. Scharf.
  Does the cytokine adsorber CytoSorb® increase vancomycin elimination in critically ill patients with sepsis or septic shock? A prospective observational study
  10th international congress „Sepsis & Multiorgan Dysfunction", Weimar, 8-10 September 2021

- **F. Weinelt**, M. Stegemann, A. Theloe, F. Pfäfflin, L. Dübel, A. Uhrig, S. Achterberg, R. Lorenz, HJ. Epple, L. Ehmann, W. Huisinga, S. Hennig, C. Kloft.
  Utilising the full potential of model-based dosing tables: an interprofessional collaboration to develop and integrate meropenem dosing tables into clinical routine.
  30th European Congress of Clinical Microbiology and Infectious Diseases (ECCMID), Paris, France, 18-21 April 2020 (accepted, conference cancelled due to COVID-19 pandemic)
- **F.A. Weinelt**, L. Ehmann, R. Michelet, W. Huisinga, J. Zander, M. Zoller, C. Kloft.
  A joint pharmacokinetic model for piperacillin/tazobactam including mechanistic renal clearance in critically ill patients.
  28th Population Approach Group Europe (PAGE), Stockholm, Sweden, 11-14 June 2019. PAGE 28: 9093 [https://www.page-meeting.org/default.asp?abstract=9093], (2019).
- **Weinelt, F. A.,** Ehmann, L, Marrek, R., Huisinga,W., Zander,J, Zoller, M., Kloft,C.
  Variability of piperacillin serum concentrations in intensive care patients.
  Annual Meeting of the Deutsche Pharmazeutische Gesellschaft (DPhG), Hamburg, Germany, 02-05 October 2018
- Kast J, **Weinelt FA**, Seubert C, Eisenschenk S, Derendorf H.
  Effect of Armodafinil on Simulated Driving, Electroencephalogram, and Cognitive Performance in Sleep Deprived Healthy Subjects.
  University of Florida CTSI Research Day, 5 June 2017, Gainesville, FL, USA
- Sorf A, Cihalova D, **Weinelt F**, Ceckova M, Staud F.
  A study of interactions of cyclin-dependent kinase inhibitors AZD5438 and R547 with ABC drug efflux transporters ABCB1, ABCG2 and ABCC1.
  Toxcon, 27. – 29. May 2015, Brno, Česká republika